RESONANCE ENERGY TRANSFER BASED DETECTION OF G-PROTEIN COUPLED RECEPTOR DIMERIZATION

BY

DOUGLAS FRANCIS RAMSAY

UNIVERSITY
of
GLASGOW

This thesis is presented for the degree of doctor of philosophy

May 2002

Institute of biomedical and life sciences

University of Glasgow

Abstract

Over the past decade there has been a growing body of evidence, obtained from studies employing a wide variety of pharmacological, biochemical and biophysical techniques, suggesting that G protein coupled receptors (GPCRs) exist not as monomeric entities but rather as dimers or other higher order oligomeric arrays. To further the accumulation of knowledge pertaining to this research area, the work presented in this thesis has made use of one such particular biophysical technique called bioluminescence resonance energy transfer (BRET). In order to utilise this system GPCRs were modified at their carboxyl terminal tail with either the *anthozoan* enzyme *Renilla* luciferase or the fluorescent protein eYFP. Through this expedient, if the differentially tagged GPCRs are in close proximity when co-expressed within mammalian cells, upon addition of the bioluminescent molecule coelenterazine, there is a non-radiative exchange of energy between the *Renilla* and eYFP, resulting in a fluorescent emission from eYFP. The technique can be used to monitor interactions in real time, in living cells and does not require any biochemical manipulations/treatments such as are associated with more traditional approaches to this line of enquiry (e.g. co-immunoprecipitation). Using this technique, it was demonstrated that the β2-AR was closely associated when expressed within HEK 293T cells, as were the δ-opioid and κ-opioid receptors since all gave robust signals in energy transfer experiments. Contrary to some previous reports however, it was not seen to be the case that the presence of ligand was capable of modulating the magnitude of the energy transfer signal. This indicated that for these GPCRs the binding of ligand did not result in any alteration in the dimerization status of the receptor. It was further shown, through monitoring the energy transfer at varying

levels of receptor expression, that energy transfer was favourable between homomers of the κ-opioid receptor. At similar receptor densities, energy transfer between co-expressed κ-opioid-receptor and TRHr was seen to be considerably less favourable, requiring far higher receptor expression levels to be achieved before meaningful levels of energy transfer could be detected. These results strongly indicated that closely related GPCR types had a greater propensity for mutual interaction than did more distantly related ones. Many of these results were confirmed using a modified version of BRET, designated $BRET_2$, which conferred an additional sensitivity to detection of protein-protein interactions. Using $BRET_2$ a previously ill-defined result obtained with traditional BRET, that suggested that the β2-AR might interact with the δ-opioid-receptor, was confirmed.

An additional purpose of the work described herein was to explore the potential of GPCR dimerization as a means of providing a novel ligand detection assay suitable for application to industrial high-throughput screening programmes. Since the experiments concentrating on GPCR oligomerization failed to provide such an assay, it was decided that the ability of GPCRs to recruit β-arrestin as part of the process of desensitisation should be evaluated as a possible alternative. Using a cell line stably expressing the GPCR CCR2 the ability of this receptor to recruit various fluorescent proteins conjugated to β-arrestin2 (β-arrestin-red NFP and β-arrestin-cyan NFP) from the cytosol in response to receptor activation was demonstrated. The β-arrestin2 was localized into endocytic vesicles and remained tightly associated with the internalised receptors after sequestration had occured. This behaviour was in accordance with other previous reports for GPCRs that, like CCR2, possessed serine and threonine clusters within their carboxyl terminal tails. If adapted to a FRET based format this particular protein-protein interaction could form the basis of a ligand screening

method for agonists that would be equally applicable to most GPCRs. It was further shown that β-arrestin2-red NFP had a higher affinity for CCR2 than did β-arrestin1-GFP through the monitoring of the respective kinetics and extent of translocation when the constructs were co-expressed within the same cells.

As an alternative strategy for the detection of ligands, a constitutively active mutant of β2-AR (CAM β2-AR) was modified C-terminally with the bioluminescent enzyme *Renilla* luciferase. This CAM β2-AR was structurally destabilized to a high degree so that only modest expression levels could be obtained upon expression of the *Renilla* modified receptor construct (CAM β2-AR-Rluc) in HEK 293T cells. Upon prolonged exposure to various antagonist ligands, a two to three fold upregulation of the receptor construct could be detected via light output from the luciferase. From parallel competition binding experiments it was also demonstrated that, for each of these ligands, the EC_{50} for upregulation highly correlated with the dissociation equilibrium constant (K_i). This strongly indicated that it was the presence of the ligand within the receptor binding pocket that alone accounted for the observed upregulation effects. In a similar manner, it was demonstrated that agonist compounds were also capable of mediating a similar degree of upregulation. The increase in receptor density of CAM β2-AR in response to the presence of ligand was subsequently shown to be dependent on the constitutively active nature of the receptor. In an additional experiment co-transfection of CAM β2-AR-Rluc along with a GFP conjugated version of the α_{1b}-adrenoceptor into HEK 293T cells and subsequent monitoring of the upregulation of either construct in response to selective ligands confirmed the necessity for pharmacological specificity in mediating the upregulatory effect. Finally, to show that this assay method would be suitable as a means of detecting ligands in a high-throughput screening format, the ability of β2-AR to be upregulated was assessed in

the presence of a wide variety of compounds, only a proportion of which possessed pharmacological specificity for the β2-AR. When tested in this manner it was seen that only compounds that were specific for β2-AR were capable of mediating an upregulatory effect.

Contents

List of Figures

List of Tables

Abbreviations

α_{1A}-AR α_{1A}-adrenoceptor

α_{1b}-AR α_{1b}- adrenoceptor

α_{2A}-AR α_{2A}- adrenoceptor

ADP adenosine diphosphate

AT1AR angiotensin II type 1 receptor

β2-AR β2 adrenoceptor

BHK baby hamster kidney

BRET bioluminescence resonance energy transfer

BSA bovine serum albumin

CAM constitutively active mutant

cAMP cyclic adenosine monophosphate

CCKr cholecytokinin receptor

CCR chemokine receptor

CFP cyan fluorescent protein

cGMP cyclic guanosine monophosphate

CHO Chinese hamster ovary

DAG diacylglycerol

DHA dihydroalprenololol

DOR δ-opioid receptor

EGF epidermal growth factor

eYFP enhanced yellow fluorescent protein

FACS fluorescence activated cell sorter

FRET fluorescence resonance energy transfer

FSH follicle stimulating hormone

G protein GTP-binding protein

GABA γ-amino butyric acid

GAP GTPase activating protein

GDP Guanosine diphosphate

GFP green fluorescent protein

GnRHR gonadotopin releasing hormone receptor

GPCR G protein coupled receptor

GRK G protein receptor kinase

GTP Guanosine triphosphate

HA heamaglutinin

HBS hepes buffered saline

HEK human embryonic kidney

IANBD (N, N'-dimethyl-N (iodoacetyl)-N'-(7-nitrobenz-2-oxa-1, 3-diazol-4-yl) ethylene diamide)

IP_3 inositol (1,4,5) trisphosphate

KOR κ-opioid receptor

LB medium Luria-Bertani medium

LH luteinizing hormone

MAPK mitogen activated protein kinase

MCH melanin concentrating hormone

MCP-1 monocyte chemoattractant protein 1

MOR μ-opioid receptor

NFP novel fluorescent protein

NMR nuclear magnetic resonance

PBP periplasmic binding protein

PBS phosphate buffered saline

PCR polymerase chain reaction

PIP_2 phosphatidyl inositol (4,5) bisphosphate

PKA protein kinase A

PKC protein kinase C

Pluc *Photinus* luciferase

PTH parathyroid hormone

RAMPs receptor activity-modifying proteins

RFP red fluorescent protein

RGS regulator of G protein signalling

Rluc *Renilla* luciferase

SDS sodium dodecyl sulphate

SDS-PAGE sodium dodecyl sulphate polyacrylamide gel electrophoresis

SSTR somatostatin receptor

T.A.E. Tris acetate EDTA

T.E. Tris EDTA

T.E.M. Tris EDTA $MgCl_2$

7 TM seven transmembrane

TM (I-VII) transmembrane helix (1-7)

TRAP thrombin receptor agonist peptide

TRHr thyrotropin releasing hormone receptor

TSH thyroid-stimulating hormone

VIP vasoactive intestinal peptide

Acknowledgements

I would like to extent warm thanks to the many people who have contributed, directly or otherwise, to the completion of this research project. Firstly to my supervisor Professor Graeme Milligan for providing a plentiful supply of ideas and suggestions throughout the whole course of my studies. I am also greatly indebted to my fellow colleagues at Glasgow University who worked in both Labs A10 and A3 for providing constant assistance and advice. For the extensive use of the spectofluorimeter, I would like to thank Professor Richard Cogdell and Niall Fraser both of whom also provided useful input concerning the resonance energy transfer studies. Aside from my co-workers at Glasgow University I should like to express my gratitude to those with whom I worked during my stay at the GSK research laboratories in Stevenage especially to Stephen Rees, my supervisor whilst working there, and also to Nicola Bevan whose patience in providing help with my experiments was much appreciated.

I thank BBSRC and GSK for providing me with funding for my studentship and last but by no means least, my parents for maintaining me throughout this time.

Author's statement

The author here declares that this volume presented for the degree of doctor of philosophy was written entirely by himself. All the results presented in chapters 3-5 are entirely the author's own work. At the back of the thesis there are two published journal papers that made use of some of the results presented in Chapters 3 and 5. In one of these papers (McVey *et al.*, 2000) are a number of experiments that were not performed by the author himself (Figures 1,2 and 5). Mary McVey, a colleague working within the same laboratory as the author, performed these experiments. All other Figures in this paper represent the author's own work and are also presented in Chapter 3. All of the experiments presented in the second paper (Ramsay *et al.*, 2001) are entirely the author's own work.

Chapter 1

Introduction

1.1. Some preliminaries.

The G-protein coupled receptors (GPCRs) are a family of integral membrane proteins that occur in a variety of organisms and which are capable of interacting with a wide range of ligands. More than 1000 types of GPCR have been identified since the first receptors were cloned more than a decade ago. The spectrum of ligands that are known to participate in interactions with these receptors include: ions (calcium ions acting on the parathyroid and kidney chemosensor); amino acids (glutamate and γ-amino butyric acid-GABA); monoamines (catacholamines, acetylcholine, serotonin, etc.); lipid messengers (prostaglandins, thromboxane, anandamide [endogenous cannabinoid], platelet activating factor, etc.); purines (adenosine and ATP), neuropeptides (tachykinins, neuropeptide Y, endogenous opioids, cholecytokinin, vasoactive intestinal peptide[VIP], etc.); peptide hormones (angiotensin, bradykinin, glucagon, calcitonin, parathyroid hormone [PTH], etc.); chemokines (interleukin-8, fMLP [formyl-Met-Leu-Phe], RANTES, etc.); glycoprotein hormones (TSH, LH/FSH, chorionganadotropin, etc.) and proteases such as thrombin. In addition to all of these, GPCRs are involved in both the light sensory pathway through rhodopsin and in olfactory sensation due to a wide range of distinct odorant receptors. All members of this receptor superfamily comprise a single polypeptide chain which characteristically contains seven stretches of mostly hydrophobic residues of 20 to 30 amino acids, linked by hydrophilic domains of variable length. The hydrophobic regions exhibit the secondary structural motif known as the alpha helix and it has been established that it is these hydrophobic regions that are embedded in the plasma

membrane with the hydrophilic regions exposed to the polar environment on the exterior or interior face of the cell surface (for this reason GPCRs are sometimes known as seven transmembrane or 7TM receptors). GPCRs have also been named through their ability to recruit and mediate signalling events through their interaction with heterotrimeric GTP-binding proteins (G proteins). These intracellular mediators of signalling events function as guanine nucleotide exchange factors where interaction with the GPCR acts as a molecular switch, inducing a conformational change in the α-subunit of the associated G-protein leading to the exchange of GDP for GTP. This activates the G protein causing dissociation of its α-subunit from the receptor and also from its associated $\beta\gamma$ subunits. Both the GTP bound α subunit and the free β/γ complex are capable of initiating cellular signalling events which include, among others, the activation or inhibition of adenylyl cyclase, the activation of phospholipases and also the regulation of calcium and potassium ion channel activity. It has further been shown in recent years that GPCRs are capable of activating signalling cascades normally associated with growth factor receptor activity, such as the mitogen activated pathways.

It is not surprising then that GPCRs have been the major target in industrially based drug discovery programmes over the past ten years, given the diversity of ligands that are capable of interacting with these proteins and the wide range of effector systems that they are capable of modulating. It is also probable that GPCRs will remain the principal targets for therapeutic intervention for quite some time to come, considering that there exists a growing number of GPCRs for which no natural ligand has yet been identified (known as orphan GPCRs). For this reason, many of the ensuing studies to be presented in the subsequent Chapters of this thesis focus upon the various phenomena associated with GPCRs in order to evaluate their potential in providing

the basis by which a novel screening assay designed to identify new ligands might be established. In this first Chapter the structure, function and signalling properties of GPCRs will be considered briefly before turning to the three main phenomena associated with GPCRs that form the core of the thesis, namely, receptor desensitisation, constitutive activation of GPCRs and dimerization of GPCRs.

1.2. Structural and functional features of GPCRs.

1.2.1. Structural features of the major GPCR families.

There has been considerable difficulty in resolving the three-dimensional structure of GPCRs through the use of X-ray crystallography or NMR. This is principally because the receptors are complicated transmembrane proteins that have proved difficult to purify in large quantities and even when this has been achieved they have proved almost impossible to crystallize. Much of what is known concerning the structure of GPCRs has been derived second hand from the structure of a light activated proton pump from *Halobacterium halobrium*, called bacteriorhodopsin. This molecule has substantial similarities to GPCRs in that it possesses seven-transmembrane α-helices and, like vertebrate rhodopsin, it uses retinal as its chromophore. However, this proton pump is not coupled to G protein, nor does it share sequence homology with any of the known GPCRs. The only GPCR that has had its three dimensional structure resolved to any degree of accuracy, is the vertebrate homologue of bacteriorhodopsin. A low resolution structure for both bovine and frog rhodopsin has been obtained (Unger *et al.*, 1995; Unger *et al.*, 1996), in addition to which a low resolution structure of squid rhodopsin has recently become available (Davies *et al.*, 1996). More recently still, the crystal structure of bovine rhodopsin has been determined in some detail down to a resolution of 2.8Å (Palczewski *et al.*, 2000). The projection

maps of these studies show that both bovine rhodopsin and bacteriorhodopsin are folded as seven helical bundles, with supporting evidence that transmembrane segment III is the central helix in the bundle and that the helices are placed in an anticlockwise fashion as viewed from outside the cell.

The GPCR superfamily does not display any overall sequence homology and the only structural feature that is common to all members is the presence of the seven transmembrane α-helix domains. GPCRs can be divided into three major subfamilies. The basis for this subdivision is the presence of highly conserved key residues and sequences of residues within the individual subfamilies; the presence of conserved structural motifs such as disulphide bridges and also the presence or absence of a palmitoylation site within the carboxyl terminal tail. The major subfamilies comprise of the rhodopsin and β2-adrenoceptor family (family A); the glucagon/VIP/calcitonin receptor family (family B) and the receptors related to the metabotropic neurotransmitter family of receptors (family C). In addition to this there are two other minor unrelated subfamilies of yeast pheromone GPCR, family D (STE2 receptors) and family E (STE3 receptors).

Family A is the largest and best characterized of these subfamilies. The overall homology between members of this subfamily is low but despite this, there are a number of "fingerprint" residues that are mainly located within the transmembrane segments and these are conserved within 95% to 98% of all family A receptors. Among all family A receptors there is only one single residue, identified here by its Schwartz numbering scheme nomenclature (Schwartz *et al.*, 1995), that is totally conserved and this is ArgIII:26 that forms part of a conserved D/E RY motif located at the bottom of TMIII. As shall be discussed later, it is thought that this residue is important in the activation of GPCRs. Among the most highly conserved residues

present in Family A GPCRs are several prolines present in TMIV, TMV, TMVI and TMVII. These are thought to introduce kinks into the α-helices and may be important in allowing flexibility about the ligand-binding pocket of the receptor. It is probable that such residues function in a dynamic role within the receptor, possibly allowing interchange between different conformational states that may be stabilized through the association/ dissociation of various ligands. Many Family A receptors also have a highly conserved disulphide bridge between a cysteine at the top of TMIII and a cysteine located somewhere in the middle of the second extracellular loop. The second extracellular loop is thereby subdivided into two smaller loops and this has the effect of tying up TMIII close to TMIV and TMV, forming a central column in the seven-helical cluster. The lengths of most of the transmembrane loops within this family of receptors are remarkably well preserved. The loops connecting TMI and TMII and TMII and TMIII are short and do not, to any significant degree, vary much in length. The disulphide bridge mentioned above creates two short loops that tether TMIV and especially TMV close together with the first three α-helical bundles. The intracellular loop connecting TMV with TMVI is not well conserved in length however and may vary from as little as 10 amino acids (rhodopsin) to several hundreds of amino acids long. It has been proposed that rhodopsin like receptors are structurally composed of two intra molecular domains, held together by a network of relatively short loops, an A-domain consisting of TMI through TMV and a B-domain consisting of TMVI and VII. This is a contention supported by experiments where the co-expression of two plasmids each coding for one of the receptor's domains were capable of reconstituting a fully functional split receptor (Schwartz, 1996).

Other prominent features of Family A receptors are the extracellular amino-terminal domain and an intracellular carboxyl terminal domain. The N-terminus is very

variable in both its length and sequence. In the subfamily of the glycoprotein hormone receptors for TSH, FSH/LH and choriongonadotropin this segment tends to be very long and contains a number of well-conserved cysteines that are expected to form a network of disulphide bridges and thus generate a well-defined globular domain. The N-terminus of family A receptors usually contain a number of Asn-X-Thr/Ser recognition motifs for N-linked glycosylation. It is not thought that these modifications are involved in ligand binding but as is the case for many cell surface proteins glycosylation seems to facilitate maturation and export of the receptor from the E.R./ Golgi-apparatus (Von Heijne, 1990). The length of the carboxyl terminal tail is also highly variable; it is usually rich in serine and threonine residues that are potential sites for kinases such as β-adrenergic receptor kinase (βARK). Both the C-terminal domain and the third intracellular loop contain potential sites for phosphorylation by cAMP dependent kinase (protein kinase A; PKA) or protein kinase C (PKC). These are of functional significance in the process of receptor desensitisation that follows on from receptor activation (detailed later). A further structural feature of the C-terminal domain of Family A GPCRs is the presence of a palmitoylation site represented on one or more cyctein residues located 15 to 20 amino acid residues C-terminal to TMVII. The presence of the modification with palmitic acid tethers the C-terminal tail to the cytoplasmic face of the cellular plasma membrane. This forms a small peptide region lying between the NPXXY motif immediately following TM VII and the point of palmitoylation. It has been shown that this short stretch of amino acids forms an eighth α-helix lying perpendicular to TM VII. From the crystal structure of rhodopsin it is thought that this short helix is located in a hydrophobic environment and that it is an important contact site for interaction with G-protein (Palczewski *et al.*, 2000). Like phosphorylation, the palmitoylation

process appears to be regulated by receptor activation and seems to be involved in the process of receptor desensitisation (Schwartz, 1996). The two processes of palmitoylation and phosphorylation can influence one another, for instance, conformational constraints induced by the modification with palmitic acid can restrict the access of certain molecules to the phosphorylation sites (Schwartz, 1996). The consequences of palmitoylation tend to vary between distinct receptor types.

The Family B receptors comprise approximately 20 different receptors for a variety of peptide hormones and neuropeptides such as VIP, calcitonin, PTH and glucagon. This family exhibits no sequence homology at all with family A except for the conservation of the disulphide bridge between cysteines at the top of TMIII and the middle of extracellular loop 2. There is no conservation of the DRY motif in family B receptors and although there are conserved proline residues present in the α-helical domains, the positions of these residues are distinct from the conserved positions observed in family A receptors. Aside from the seven transmembrane domains present in family B members, their most conspicuous feature is a large N-terminal domain (>100 amino acids). This contains a number of conserved cysteine residues which are presumably involved in the formation of disulphide bridges thus forming a globular domain that is thought to be involved in ligand binding.

The size of family A GPCR N-terminal domains are of modest magnitude compared to that of the family C receptors (500-600 amino acids). Family C GPCRs include the metabotropic glutamate and γ-amino-butyric acid (GABA) receptors, the calcium receptors, the mammalian pheromone receptors and recently identified putative taste receptors. Like family A and family B receptors there is a conserved disulphide bridge linking the second and third extracellular loops but aside from this they do not share any sequence homology with either of the other two main GPCR families. The large

N-terminal domains of the family C receptors bares considerable resemblance to a family of bacterial binding proteins that function as transporters for amino acids and other small molecules across the periplasmic space (Periplasmic binding proteins, PBPs). This extracellaular region of the metabotropic glutamate receptor (mGluR) can be divided into two separate regions: a ligand binding domain (LBR) and a cysteine rich region. The LBR has been demonstrated to be the ligand-binding domain through chimeric receptor analysis (Takahishi *et al.*, 1993) and also through homology model building (O'Hara *et al.*, 1993; Costantino *et al.*, 1999) based upon the crystal structure of the leucine/isoleucine/valine-binding protein (LIVBP), a PBP (Sack *et al.*, 1989). More directly, the extracellular regions of mGluR, when expressed in soluble form, have been shown to serve as ligand binding sites, conferring ligand-binding specificity (Han *et al.*, 1999). Recently, the LBR of mGluR1 has been crystallized and shown to be a homodimer consisting of two protomers, existing in a number of different conformational forms (Kunishima *et al.*, 2000). Each protomer consists of an amino and carboxyl terminal domain designated LB1 and LB2 respectively with the LB1 domain providing the dimer interface in all the identified conformational forms. These two domains form a "clamshell" like structure with the glutamate-binding site located within the interdomain crevice. Through analysis of the crystal structure, it was determined that the LBP dimer exists in a dynamic equilibrium between active and resting states where the active state is favoured through the presence of glutamate in the binding crevice. The switch to the active conformation was accompanied by a conformatial change involving a reorientation in the position of the dimer interfaces. As will be seen later on, this dimerization of GPCR domains is now thought to play a crucial role in certain aspects of GPCR regulation.

1.2.2. Ligand binding to GPCRs.

The interactions that occur between ligands and their cognate GPCRs have been best studied for the family A group of receptors. In rhodopsin the mechanism of receptor activation is unique in that the activating ligand, a photochromophore called 11-*cis*-retinal, is covalently attached to the receptor and is buried within a binding crevice located within the seven transmembrane domain bundle. Retinal is known to attach to the ϵ-amino group of a lysine residue located in the middle of transmembrane segment VII and to make a Schiff-base interaction with a glutamate residue located on the top of TMIII in rhodopsin. (Zhukovsky *et al.*, 1992). Upon absorption of a photon 11-cis-retinal undergoes an isomerization to all-*trans*-retinal, this leads to the formation of an overall conformation known as the metarhodopsin II state, allowing the receptor to be activated (Sakmar, 1998). In this case, all-*trans*-retinal can be seen as acting as an agonist whereas the 11-*cis*-retinal conformation can be viewed as an inverse agonist holding the receptor in an inactive conformation in the absence of light. Clearly, since photodetection requires such a rapid response to photons in mediating receptor signalling events, it is advantageous to have the activating ligand constitutively associated with the GPCR. Another family A receptor for which the mechanisms of receptor activation have been elucidated in some detail is the β2-AR whose natural ligands are adrenaline and noradrenaline (both catacholamines). These ligands belong to a class of small molecules known as biogenic amines, other members include serotonin, histamine, acetylcholine and dopamine. Docking of catecholamines to the β2-AR is facilitated through interaction of the ligand with a receptor binding crevice that is buried deeply within the seven transmembrane helical bundle. The specific and direct interaction of the amine group from the ligand with the carboxyl group from a highly conserved aspartic acid residue located in TMIII (AspIII:08) is thought to be

the most energetically important binding characteristic (Strader *et al.*, 1991). Other interactions that are thought to be crucial in the stabilization of ligand docking are the hydrogen bonds formed between the hydroxyls of the catechol ring in adrenaline and two serines in TMV that are separated by one α-helical turn (SerV:09 and SerV:12) (Strader *et al.*, 1989). Other key residues thought to play a role in the stabilization of the catachol ring within the receptor binding site are a phenolalanine residue in TMVI (PheVI:17) (Tota *et al.*, 1990) and an asparagine residue, also in TMVI (AsnVI:20), thought to form a hydrogen bond with the β-hydroxyl of adrenaline (Weiland *et al.*, 1996). Evidence suggests that antagonists that are related structurally to adrenaline share the characteristic of binding to the conserved (AspIII:08) in TMIII, however, the other key ionic interactions are thought to differ. Although the majority of ligands for β2-AR are thought to interact with this buried binding crevice, some antagonists that are structurally distinct from adrenaline seem to interact with other residues of β2-AR located outside of this binding pocket.

Other ligands, such as the large glycoprotein hormones, tend to gain most of their binding energy through interaction with the large globular N-terminal domain of the receptor. Similarly, medium and small neuropeptides and peptide hormones usually have their major points of interaction located in the N-terminal domain, although additional contact points located in the extracellular loops may be involved. The range of such interactions and the huge diversity of contact points employed by different receptor types means that it is not practical to discuss these in depth here. However, it should be mentioned here that an interesting mode of receptor activation is employed by the thrombin receptor. In this case the N-terminal segment of the receptor forms the activating agonist, where proteolytic cleavage of this domain removes most of the segment to reveal a small pentapeptide that is still covalently tethered to the receptor.

This peptide is then free to interact with other parts of the exterior receptor leading to receptor activation.

1.2.3. Conformational changes associated with GPCR activation.

GPCRs are thought to exist in a dynamic equilibrium between resting (R) and ligand activated (R*) states, with R* being capable of activating G-protein and initiating cellular signalling events. The structural changes that are thought to accompany the transition from R to R* upon ligand binding have been elucidated in some detail for the light activated photoreceptor rhodopsin. As mentioned previously, in rhodopsin the isomerization of 11-*cis*-retinal to all-*trans* retinal upon exposure to light induces a conformational change in the receptor that leads to the formation of the metarhodopsin II state that is though to represent the active form (R*) of rhodopsin. The receptor, having adopted the R* conformation, is then able to mediate signalling through the G-protein transducin. Biophysical and biochemical analyses of both native rhodopsin and metarhodopsin II have revealed that there are structural differences between the two conformations of the receptor. The studies suggested that the structural changes associated with the transition from R to R* were not drastic and that ligand isomerization induced changes in the relative orientation of the individual transmembrane helices and that this in turn affected the relative conformation of the intracellular receptor surface, facilitating G-protein activation. One such study has indicated that upon light activation of rhodopsin there is a small outward movement of the cytoplamic portion of TM III relative to the other TM α-helices in the receptor core (Lin and Sakmar, 1996). This movement was accompanied by an ill-defined structural change in the second intracellular loop. An activation mechanism involving a rearrangement in the orientation of certain α-helices present in the transmembrane

core was further substantiated by observations that disulphide crosslinking of the cytoplasmic ends of TM III and TM VI was capable of preventing activation of rhodopsin (Farrens *et al.*, 1996). Such results suggest that GPCR activation involves an opening of the intracellular face of the receptor and that this in turn allows the G-protein to have access to previously inaccessible amino acid sequences essential for its activation. Confirmatory evidence, implicating a role for TMs III and VI in receptor activation, has been provided by a study employing the cysteine-specific fluorescent marker molecule IANBD (N, N'-dimethyl-N (iodoacetyl)-N'-(7-nitrobenz-2-oxa-1, 3-diazol-4-yl) ethylene diamide) which is sensitive to changes in the polarity of its environment (Gether *et al.*, 1997b). This study showed that in the case of the β2-AR, the presence of the agonist isoprenaline in the receptor binding site led to a decrease in the fluorescence of two IANBD conjugated cysteine residues present in TMs III and IV, a finding consistent with a reorientation of these two transmembrane segments towards a more polar environment (i.e. away from the α-helical bundle).

1.2.4. Structural determinants important for G-protein coupling and activation.

The ability of a given GPCR to mediate signalling through a particular pathway is governed by its ability to interact with a limited set of structurally related G-proteins whose classification is defined through the nature of the α-subunit. Much information concerning the receptor regions implicated in mediating such interactions has been obtained through analysing hybrid receptors constructed between functionally distinct members of the GPCR family. Most of these studies suggest that amino acid residues located in intracellular loop 2 and in the amino and carboxyl-terminal portions of intracellular loop 3 are essential in conferring the selectivity of G-protein recognition

(Savarese *et al.*, 1992; Hedin *et al.*, 1993). The eighth helix, formed through palmitoylation of the carboxyl terminal tail may also contribute to receptor/G-protein interactions (Savarese *et al.*, 1992; Stader *et al.*, 1994), although it is unlikely to be essential for G-protein coupling since the fully functional mammalian gonadotropin releasing hormone receptor completely lacks a carboxyl-terminal tail (Tsutsumi *et al.*, 1992). These findings have been in close agreement with experiments that have made use of short peptides derived from receptors' intracellular domains. It has been demonstrated that such peptides corresponding to regions from intracellular loop 2 or the amino and carboxyl segments of intracellular loop 3 are capable of mimicking or inhibiting receptor interactions with G-proteins (König *et al.*, 1989; Münich *et al.*, 1991; Okamoto *et al.*, 1992). It is thought likely that the highly conserved D/E RY motif located at the junction between TM III and intracellular loop 2 is particularly critical in receptor activation. This has been clearly demonstrated in experiments where replacement of the conserved arginine residue with various amino acids was seen to abolish coupling to G-proteins (Zhu *et al.*, 1994; Scheer *et al.*,1996). Additional studies designed to monitor the effects on functional endpoint output of introducing amino-acid substitutions for this arginine into the M_1 muscarinic receptor has shown that the charge conserved Arg→ Lys substitution was the least effective in impairing G-protein coupling (Jones *et al.*, 1995). It is possible therefore that the conserved, charged arginine residue is capable of interacting with some anionic site present on the G-protein(s) and that by this expedient G-protein activation is achieved. Other mechanisms through which the D/E RY motif contributes to receptor activation involve the protonation of the acidic amino acid (glu or asp). Protonation of this residue results in a net neutral charge induced upon the residue and this is thought to be important in allowing the adjacent arginine side chain to interact with G protein.

Consistent with such a notion, it was shown in studies involving rhodopsin and the α_{1b}-adrenoceptor that substitution of the Glu/Asp residue with various neutral amino acids led to the generation of mutant receptors that were constitutively active, that is to say that they had an elevated basal signalling activity (Acharya *et al.*, 1996; Cohen *et al.*, 1993; Hill Eubanks *et al.*, 1996). A stretch of charged residues present in the carboxyl terminal portion of the third intracellular loop is also thought to be important in mediating efficient G-protein coupling, as has been revealed through several site directed mutagenesis studies (Franke *et al.*, 1992; Kundel *et al.*, 1993; Högger *et al.*, 1995). It may therefore be speculated that these residues, in conjunction with the conserved D/E RY motif at the interface of TM III and intracellular loop 3, represent, at least in the case of family A receptors, the essential components in facilitating GPCR activation.

1.3. Signalling and desensitisation of G protein coupled receptors.

1.3.1. Signalling through G protein coupled receptors.

GPCRs transduce signals from the extracellular environment to the inside of the cell. This is achieved through the binding of the receptor to a ligand on the external face of the plasma membrane which induces or stabilizes an active conformation of the receptor allowing activation of an associated heterotrimeric G protein. Through interaction with G proteins a receptor can influence a variety of effector systems. Heterotrimeric G proteins consist of α and $\beta\gamma$ subunits and are classified according to the larger α subunit which contains the GDP binding cleft which, upon exchange of GDP for GTP, triggers activation of the G-protein. This consequently leads to dissociation of the α subunit from the $\beta\gamma$ subunits with both types of subunit (α and $\beta\gamma$) being capable of stimulating/inhibiting cellular effector systems.

A brief description of the molecular architecture of heterotrimeric G-proteins is as follows. The α subunit, has located at its centre binding sites for two or three phosphates, ribose and a magnesium ion as well as containing the GDP/GTP binding domain. The presence of magnesium is essential for the binding of the guanine nucleotide. The protein possesses an intrinsic GTPase activity so as to limit the activation time of the protein and limit its ability to interact with downstream effectors following receptor activation. The carboxyl terminus of the α subunit contains the receptor binding region important for its interaction with seven transmembrane domain type receptors. Certain G- protein α subunits can also be specifically ADP- ribosylated by bacterial toxins. For example the G protein $G\alpha_s$ can be specifically ADP- ribosylated on an arginine residue, via cholera toxin, near the GTP binding domain. The action of cholera toxin on $G\alpha_s$ is manifest in constitutive activation and a decrease in its intrinsic GTPase activity. In contrast, the G protein $G\alpha_i$ is ADP- ribosylated by pertusis toxin at a cysteine residue that is located four amino acids from the COOH terminal of the protein and this is known to cause G protein uncoupling and inhibit signalling responses through GPCRs utilizing this G protein subtype.

There are four major families of G proteins, G_s, G_i, G_q and G_{12} all of which have a number of variant subtypes and there is also considerable diversity among the $\beta\gamma$ subunits with 5 known β, and 11 known γ subunits. Such diversity means that there are over 1000 possible G protein heterotrimer combinations. The different types of $G\alpha$ subunit target different effector systems in order to mediate their second messenger response. For instance α_s protein is known to increase levels of cAMP in response to activation by GPCRs and it does so by directly interacting with and stimulating the enzyme adenylyl cyclase.

The activation of adenylyl cyclase is the most well established paradigm for the generation of second messenger molecules in response to G protein activation via GPCRs. Cyclic AMP is formed from adenosine triphosphate (ATP) by the enzymic action of adenylyl cyclase; termination of the signal is achieved by a phosphodiesterase enzyme which converts cAMP into 5'- adenosine monophosphate (5'-AMP). The target molecule upon which cAMP acts is a cAMP-dependent protein kinase known as protein kinase A (PKA). PKA is a serine/threonine kinase which exists as a tetramer with two regulatory and two catalytic subunits. The regulatory subunits each contain two binding sites for cAMP. Once cAMP has occupied both of these binding sites the catalytic subunits dissociate and become active.

The pathway from binding of extracellular ligand to physiological response has been well characterized for the action of β2-AR on skeletal muscle cells and will serve here as a single example of a functional response mediated through the action of $G\alpha_s$. It should be stressed however that this is merely one pathway in a particular cell type stimulated through the elevation of intracellular cAMP levels. This example is as follows. *In vivo*, adrenaline binds to the β2-AR on the extracellular face of the plasma membrane and adenylyl cyclase is rapidly activated (within seconds) through $G\alpha_s$ resulting in elevated cellular levels of cAMP. The cAMP thus generated binds to the regulatory subunits of PKA and activates it through the release of the catalytic subunits. These then phosphorylate the enzyme phosphorylase kinase at serine residues on its α and β subunits at the phosphate acceptor recognition sequence RRXSX; phosphorylation of the β subunit converts the phosphorylase kinase to its active form. The activated phosphorylase kinase then in turn phosphorylates and activates another molecule called phosphorylase b converting it to phosphorylase a, this then splits glucose-1-phosphate molecules from glycogen. Other targets for the

catalytic subunits of PKA in this signalling system are glycogen synthase and a phosphorylase phosphatase inhibitor protein. These additional targets for PKA play complementary roles in the signalling pathway in that phosphorylation of glycogen synthase inhibits activity and prevents further synthesis of glycogen from glucose. The phosphorylase inhibitor, once activated by PKA inhibits phosphorylase phosphatase whose target substrate is phosphorylase A, this has the effect of prolonging the dephosphorylation of phosphorylase A and consequently attenuating the breakdown of glycogen.

Other downstream targets for cAMP include cyclic nucleotide gated ion (CNG) channels, where the binding of cAMP (or cGMP) drives a conformational change that leads to the opening of an ion-conducting pore. CNG channels are important mediators in the visual and olfactory transduction pathways and are also present in many other tissues where they facilitate in regulating intracellular calcium levels (Richard and Gordon 2000; Zagotta and Siegelbaum, 1996). Another PKA independent pathway is that mediated through cAMP-guanine nucleotide exchange factors (cAMP-GEFs) or exchange protein activated by cAMP (Epac). For the cAMP GEF Epac1, binding of cAMP to Epac stimulates guanine nucleotide exchange activity thereby activating the monomeric G-protein Rap-1. GTP bound Rap-1 activates the kinase Raf-1 leading to the phosphorylation of the MAPK kinase MEK which then in turn phosphorylates and activates ERK (de Rooji *et al.*, 1998; Kawasaki *et al.*, 1998). ERK then translocates to the nucleus where it activates transcription factors through direct phosphorylation. ERKs are also thought to be involved in exocytosis and this particular pathway may therefore be important for cAMP mediated enhancement of cellular secretion in certain cell types (Ozaki *et al.*, 2000). Other targets for cAMP GEFs include the monomeric G-proteins Rap2 (Vanessa *et*

al., 1999) and possibly Ras (Pharm *et al.*, 2000). Through the latter cAMP would be able to activate additional kinase cascades such as the PI3-K/PDK1 pathway. It can be seen that there are many pathways that can be stimulated through the elevation of cAMP levels within a cell. The ultimate physiological response may be mediated through any one of these and indeed may be a result of complex regulation via the crosstalk between interdependent cascades.

The α_i subunit is known to mediate the opposite effect to α_s by inhibiting adenylyl cyclase. It was identified through the ability of certain hormones to decrease levels of intracellular cAMP in a S49 lymphoma cell line lacking α_s, known as cyc$^-$. Other α subunits are capable of mediating signalling through the activation of phospholipid signalling pathways, for instance α_q and α_{11} subunits activate phospholipase C. This causes hydrolysis of phosphatidyl inositol (4,5) bisphosphate (PIP_2) and leads to the generation of two second messengers, a water soluble product called inositol (1,4,5) trisphosphate (IP_3) and a membrane associated product called diacylglycerol (DAG). IP_3 mobilizes the release of Ca^{2+} from intracellular stores localized in the endoplasmic reticulum. DAG activates the enzyme protein kinase C (PKC) which then phosphorylates various target proteins.

Another notable signal transduction system is that which is coupled to the activation of rhodopsin, the cGMP signalling system. In this case the generation of the signal is accompanied by a decrease rather than an increase in the intracellular levels of the signalling molecule. As mentioned previously, capture of a photon by retinal covalently bound to the rhodopsin receptor present in the rod cells of the retina results in receptor activation and adoption of the metarhodopsin II receptor conformation. This leads to activation of the G protein G_t (known as transducin): $G\alpha_t$ interacts with a specific cGMP phosphodiesterase and this in turn becomes activated leading to an

increase in the rate of cGMP breakdown in the rod cell. These retinal cells contain cGMP dependent Na^+ channels that remain open due to a cGMP binding site. Upon light activation of rhodopsin the levels of cGMP in the cell fall causing dissociation of cGMP from the ion channel, consequently closing it. The rod cells then hyperpolarize; this provides a signal for the release of a neurotranmitter which leads in turn to the propagation of a nerve impulse.

1.3.2. Attenuation of the signalling process.

An important aspect of the signal transduction mechanisms detailed above is that since a receptor in its activated conformation is capable of interacting with and hence activating many G protein molecules, a rapid amplification of the signal generated in response to agonist can be expected to ensue. It is clearly necessary that some form of regulation must be employed in order to attenuate such responses to agonist stimulation. On one level, control of second messenger generation is exerted through the G protein itself. Inactivation of the G protein requires hydrolysis of GTP to GDP in the binding cleft of $G\alpha$ and this causes $G\alpha$ to reassociate with $\beta\gamma$ subunits, preventing further signalling. G protein α subunits possess an intrinsic GTPase activity that can be measured *in vitro*, however, this cannot usually account for the rapid termination of signalling observed in most systems. Interaction with effector systems can lead to an enhancement in this rate of GTP hydrolysis, such proteins are called GAPs (GTPase activating proteins). There are a number of downstream effectors that can function as GAPs: phospholipase Cβ stimulates the GTPase activity of $G\alpha_q$ *in vitro* (Biddlecome *et al.*, 1996) and the γ subunit of cGMP phosphodiesterase stimulates GTP hydrolysis by $G\alpha_t$ (Arshavsky *et al.*, 1992). Other proteins capable of functioning as GAPs are the RGS (regulators of G protein

signalling) family of proteins. These are a superfamily of signal regulating proteins first isolated from yeast. From yeast two hybrid studies, a human protein, GAIP was identified possessing the 130 amino acid residue core that defines members of the RGS superfamily. Other mammalian RGS proteins have since been identified and these have been designated RGS1, RGS2, RGS3 and RGS4 etc. It has been shown in experiments using purified extracts of GAIP and RGS4 along with purified extacts of $G\alpha_{i1}$, $G\alpha_{i2}$, $G\alpha_{i3}$, $G\alpha_{o}$ and $G\alpha_{s}$ that for all the $G\alpha$ subtypes tested, except $G\alpha_{s}$, RGS4 and GAIP were capable of stimulating the rate of GTP hydrolysis by more than 40 fold (Berman *et al.*, 1996).

The other level at which the extent of signalling through agonist activation of a GPCR may be modulated, is at the receptor itself (a phenomenon known as desensitisation). Desensitisation of GPCRs is a multistep process that begins by the receptor being functionally uncoupled from G protein and thereby terminating any further signalling events. The receptor is then internalised into intracellular compartments where through dephosphorylation by specific phosphatases the receptor can be resensitised. The receptor may then be recycled back to the plasma membrane where it is free to interact with more ligands and participate in further signalling events. Otherwise, when stimulation is chronically persistent, receptor downregulation occurs where the receptor density at the plasma membrane is decreased. The mechanisms by which this is achieved are thought to include redirection of internalised receptors to the lysosome where proteolytic degradation of the receptor leads to a concomitant loss in receptor number and destabilization of the mRNA transcripts for the GPCR causing a reduction in the receptor protein expression levels. It is these specific processes that shall now be described in more detail.

1.3.3. Homologous and heterologous desensitisation.

1) Homologous desensitisation. This involves a specific attenuation of signalling through a receptor that has been exposed to an activating agonist. It is mediated primarily through the concerted action of two proteins: G protein receptor kinases (GRKs) which phosphorylate the activated receptor and arrestins that act to functionally uncouple G proteins from further interaction with the receptor (Figure 1.1). Upon agonist activation of the GPCR conformational changes occur in the receptor allowing it to adopt a state that is capable of activating G protein. This active conformation also becomes a target for certain GRKs, a protein family that comprises seven different members that all share significant sequence homology. GRKs have been directly implicated in mediating the desensitisation of GPCRs. In cells transfected with GRK cDNAs, resulting in the overexpression of these kinase molecules, it was found that second messenger production by various GPCRs (β1, β2 and α_{1B}-adrenoceptors, dopamine D1 receptor and thyroid stimulating hormone receptor) could be substantially attenuated (Pippig *et al.*, 1993; Freedman *et al.*, 1995; Diviani et al., 1996). Furthermore, it was found that through the expression of antisense mRNA for GRK2 and 3 the degree to which the β2- adrenoceptor desensitised in response to agonist could be significantly decreased (Shihi and Malbon, 1994).

GRKs contain a central catalytic domain, an amino terminal domain implicated in substrate recognition (that also contains an RGS-like domain) and a carboxyl terminal domain thought to be involved in targeting the kinase to the plasma membrane. For GRKs 1-3 membrane targeting takes place only after stimulation of cellular receptors occurs, being localized in the cytosol in unstimulated cells. GRK-1 responds to light activation of rhodopsin in retinal cells to translocate to the plasma membrane and this

Figure 1.1. The processes that underlie the desensitisation and internalisation of GPCRs in response to agonist activation.

Firstly ligand docking to the receptor binding site causes a conformational change that triggers exchange of GDP for GTP on the alpha subunit of a receptor associated heterotrimeric G protein. This then diffuses across the membrane laterally where it can interact with downstream targets and initiate signalling events. In response to receptor activation there is a rapid initial activation of PKA as intracellular cAMP levels are elevated. This leads to phosphorylation of the receptor on regions of its third intracellular loop and carboxyl terminal tail. Subsequent recruitment of GRKs to the plasma membrane leads to further phosphorylation events which promote the association of β-arrestin molecules. These facilitate in the process of clatherin mediated receptor endocytosis into vesicles. A subsequent drop in pH within the lumin of the vesicle results in ligand dissociation and dephosphorylation of the receptor by GPCR specific phosphatases. This returns the receptor to its native state, the resensitised receptor can now recycle back to the plasma membrane where it can participate in further signalling events.

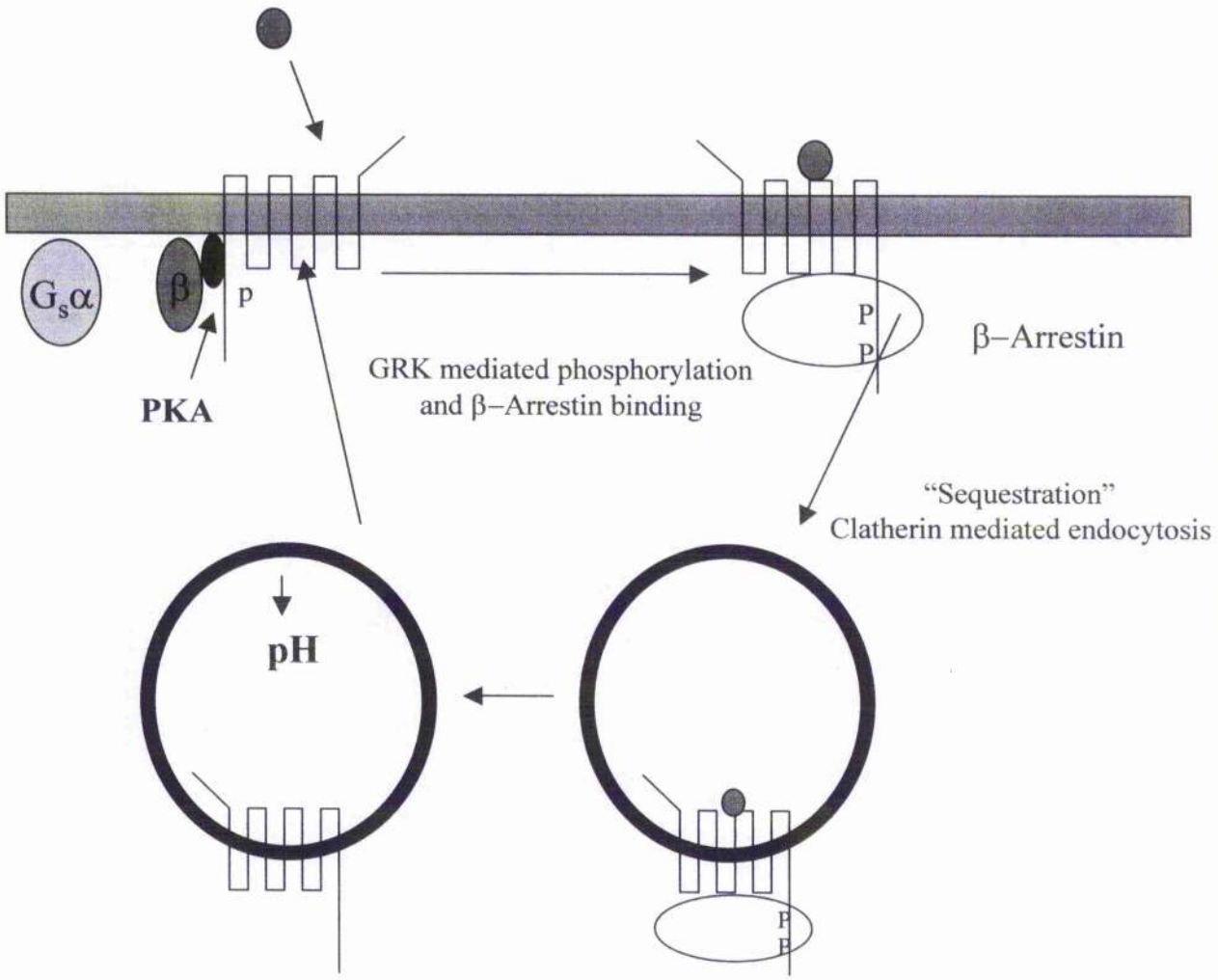
$G_s\alpha$
β
P
PKA
GRK mediated phosphorylation
and β–Arrestin binding
P
P
β–Arrestin
"Sequestration"
Clatherin mediated endocytosis
pH
P
P

Figure 1.1.

is thought to be aided by a post-translational farnesylation of the kinase's carboxyl terminal CAAX motif. GRK2 and GRK3 are both kinases that have been implicated in the desensitisation of the β2-AR. Their translocation to the plasma membrane seems to be mediated through their association with G protein βγ subunits. It has been shown through *in vitro* experiments that incubation of purified GRK2 with a peptide corresponding to the sequence of the third intacellular loop of the M_3- muscarinic receptor along with purified Gβγ resulted in the formation of a functional ternary complex in which Gβγ acted as an adaptor protein (Guangyu *et al.*, 1997). Gβγ acts in this case not only by facilitating the spatial translocation of GRK2 from the cytosol but also in positioning the enzyme directly on its substrate allowing phosphorylation to occur. Another factor that can influence the targeting of GRK2 and GRK3 to the plasma membrane is the binding of IP_3 to a carboxyl terminal plekstrin homology domain (Pitcher *et al.*, 1995). Also, mitogen activated kinase (MAPK) phosphorylation of the carboxyl terminal of GRK2 which has been shown to decrease the kinase's activity in response to activating ligands (Pitcher *et al.*, 1999). Translocation of GRK4 and GRK6 to the plasma membrane seems rather to be mediated by palmitoylation of cysteine residues present in the carboxyl terminal tail. This modification seem to be essential in facilitating translocation since the non-palmitoylated kinase is present only in the cytosol of the cell (Stoffel *et al.*, 1998). Upon interaction with their substrate receptors GRKs are thought to bring about phosphorylation of serine and threonine residues present in the third intracellular loop and carboxyl terminal tail. In support of this, it was seen through site directed mutagenesis of all the serine and threonine residues present in carboxyl terminal tail of the β2-AR or through similar mutagenisis of the third intracellular loop of the M_2

muscarinic acetylcholine receptor that GRK mediated phosphorylation was completely abolished (Bouvier *et al.*, 1998; Nakata *et al.*, 1994).

It is not the phosphorylation of the activated receptor alone that causes its uncoupling from G-protein however. The abrogation of further signalling events is due instead to the interaction of the activated receptor with other types of cellular proteins known as arrestins. It is thought that the close interaction of arrestins with the phosphorylated receptor prevents access of further G proteins to the receptor's intracellular loops and COOH tail domain thus "arresting" the signalling process. There have been identified four different members of the arrestin family and these can be subdivided into two main groups based on sequence homology, tissue distribution and function: 1) visual arrestin and cone arrestin (X-arrestin or C-arrestin) and 2) β-arrestins (β-arrestin1 and β-arrestin2). Visual arrestin is primarily expressed in the rod cells of the retina with low expression in the pineal gland (Smith *et al.*, 1994), C-arrestin is present in both the retina and the pineal gland (Craft *et al.*, 1994) whereas the β-arrestins are ubiquitously expressed in tissues other than the retina and are primarily located in neuronal tissues and the spleen (Attramadal *et al.*, 1992). A number of splice variants are known to exist for visual arrestin, β-arrestin1 and β-arrestin2 increasing the number of arrestins which may be functionally distinct (see Ferguson, 2001 for review). Arrestins have been shown to bind preferentially to agonist activated and GRK phosphorylated GPCRs and *in vitro* it has been shown that β-arrestin binding for the β2-AR is increased 10 to 30 fold by GRK phosphorylation (Lohse *et al.*, 1992). The enhanced affinity of β-arrestins for GPCRs due to phosphophorylation on serine and threonine residues present on the carboxyl terminal tail and third intracellular loop seems to be specific for the action of GRKs since phosphorylation by other second messenger dependent kinases does not seem to enhance the affinity of β-

arrestin for GPCRs. Clearly, since GRKs phosphorylate receptors on a number of different sites, arrestins must be able to recognize and interact with multiple receptor domains and conformations. The molecular structure of visual arrestin has been characterized in some detail and can be divided into three functional and two regulatory domains (Guervich *et al.*, 1995). The functional domains comprise a receptor activation domain located in the amino terminal portion of the molecule, a phosphate sensor domain also located in the amino terminus and a secondary receptor binding domain located in the carboxyl terminal portion of the protein. The two regulatory domains reside in either the carboxyl or amino terminal halves of the arrestin protein respectively. The molecular architecture of visual arrestin is arranged in such a way as to allow the phosphate sensor domain to form a polar core along with the amino-terminal and carboxyl-terminal regulatory domains (Gurevich *et al.*, 1995; Hirch *et al.*, 1999). From data obtained through both mutagenesis studies and from the crystal structure of visual arrestin it is thought that the arrestin carboxyl terminal tail interacts with this polar core in order to stabilize the resting state of the protein. Interaction with the phosphorylated carboxyl terminal tail of the agonist activated receptor leads to disruption of the interaction between the arrestin carboxyl terminus and the polar core. This conformational rearrangement of the amino and carboxyl terminal domains about the polar core of the arrestin molecule facilitates its interaction with the activated receptor (Hirch *et al.*, 1999).

2) Heterologous desensitisation. In heterologous desensitisation of GPCRs a distinct mechanism from that of the homologous pathway is employed in dampening the response of a receptor to activating ligand. It is achieved through phosphorylation of receptors via the enzymic action of the second messenger dependent kinases PKA and PKC both of which catalyse the transfer of a γ- phosphate group to serine and

threonine residues present in specific amino acid consensus recognition sequences. PKA is activated in response to elevated intracellular levels of cAMP. The β2-AR contains two PKA consensus sequences, one in the third intracellular loop the other in the proximal region of the receptor's carboxyl terminal tail. Many other GPCRs also contain PKA consensus sites in these regions. PKC is activated by receptors that couple to phospholipase signalling pathways and leads to the phosphorylation and desensitisation of many G_q and G_i linked GPCRs. Any receptor that couples to these pathways can cause activation of these second messenger dependent kinases which are then capable of phosphorylating and hence desensitising a wide variety of GPCRs present in the cell. This is because agonist occupancy of and activation of potential substrate receptors does not seem to significantly enhance the phosphorylation kinetics of these kinases. In this manner many GPCR types may therefore be desensitised non-specifically in response to activation of a single GPCR type within the cell. This form of heterologous desensitisation is quite efficient with phosphorylation by PKA and PKC leading to a 40%-50% loss of receptor function.

Interactions may occur between the two different desensitisation pathways, for instance GRK2 can be directly phosphorylated by PKC (Chuang *et al.*, 1995). This phosphorylation has been shown to increase both the affinity of GRK2 for its substrate and the V_{max} of its enzymic activity as well as increasing the desensitising potency of the kinase. It is probable that PKC interacts with GRK2 through directly binding to its pleckstrin homology domain, since PKC has been shown to bind to this domain in a number of different protein types. These interactions may have major implications for the manner in which heterologous desensitisation is brought about.

1.3.4. Internalisation and resensitisation of G protein coupled receptors

Following on from the phosphorylation and desensitisation of many GPCRs there is often an associated sequestration of the receptors from the plasma membrane into small endocytic vesicles. This is a rapidly occurring process and usually takes place within a few minutes of receptor activation. Initially it was thought that the removal of receptors from the plasma membrane was part of the desensitisation process designed to attenuate signalling by spatially separating the receptors from G protein at the plasma membrane. However desensitisation is known to occur far more rapidly (less than 1 minute) than sequestration does and it is now thought that the role of receptor internalisation is more important in facilitating the dephosphorylation of the activated receptors and then returning them in a resensitised state back to the plasma membrane. Other roles for receptor internalisation are thought to include targeting of receptors to the lyzosome in response to a sustained treatment with agonist where degradation ultimately leads to a downregulation in receptor density. Also, it is now becoming clear that receptor sequestration is important for the activation of signalling pathways that are not mediated through the action of heterotrimeric G proteins but instead involve the activation of tyrosine kinase pathways that have classically been identified with growth factor receptor signalling.

The events that trigger receptor endocytosis have been somewhat obscure until recent years. Phosphorylation of GPCRs following their activation seemed a likely candidate for such a trigger mechanism and a number of studies have focused on trying to determine the role that phosphorylation plays in receptor internalisation. Many such experiments made use of dominant negative mutants of GRK in order to inhibit receptor phosphorylation. It was shown that a dominant negative mutant of GRK2 could inhibit the phosphorylation and internalisation of the M_2 muscarinic

acetylcholine receptor in COS7 cells (Tsuga *et al.*, 1994). Moreover, it was shown that overexpression of wild type GRK2 in the same cell type could enhance both the rate and extent of internalisation. However it was observed that similar experiments could not be repeated in either BHK-21 or HEK 293 cells (Pals-Rylaarsdam *et al.*, 1995). It is likely that the discrepancies between these sets of experiments were due to higher expression levels of GRK2 present in the HEK293 and BHK-21 cells preventing effective inhibition of phosphorylation with the dominant negative mutant since it has been determined that GRK2 expression levels vary greatly from cell type to cell type (Aramori *et al.*, 1997) with the lowest GRK expression levels being found in COS7 cells (COS7< HEK 293 cells< RBL-2H3 cells). It has been confirmed that phosphorylation is an essential step for the internalisation of a number of receptors including the β2-AR (Ferguson *et al.*, 1995), the AT1AR (Smith *et al.*, 1998), the D2 dopamine receptor (Itokawa *et al.*, 1996) and numerous others. Despite an obvious role for phosphorylation in mediating receptor internalisation it seems that it is not absolutely indispensable for endocytosis to occur. This was shown by an experiment where an internalisation/phosphorylation defective mutant of the β2-AR was rescued by overexpression of either β-arrestin1 or β-arrestin2 within the same cells (Ferguson *et al.*, 1996). For most receptors then, it seems that internalisation is mediated through the concerted actions of both arrestin and GRK on the activated receptor target. In support of this contention it has been observed that the extent to which the β2-AR can be internalised in different cell lines correlates well with the levels of GRK and β-arrestin present (Menard *et al.*, 1997). It is probable that different receptor types have evolved so as to internalise according to the conditions within the cell in which they are naturally expressed. This is demonstrated by the fact that CXCR1 is effectively internalised in response to agonist when expressed within the neutrophil-like RBL-

2H3 cells in contrast to which, no internalisation can be observed in similar experiments carried out on HEK 293 cells (Barlic *et al.*, 1999). It is of note that RBL-2H3 cells express GRK2 and β-arrestin2 at substantially higher levels than HEK 293 cells and thus CXCR1 may only internalise in the presence of high levels of these proteins.

The role of β-arrestin in mediating receptor endocytosis has recently been elucidated in more detail. It is believed that β-arrestin can specifically target receptors for endocytosis through the clathrin mediated endocytosis pathway. The involvement of clathrin in the internalisation of GPCRs was demonstrated through the use of a dominant negative mutant of dynamin, lacking in GTPase activity, to block internalisation of β2-AR (Zhang *et al.*, 1996). It has also been demonstrated that the β2-AR and β-arrestins are colocalized with clathrin in clathrin-coated pits (Goodman *et al.*, 1996). β-arrestin is thought to serve as an adaptor molecule directly linking the receptor with components of the clathrin internalisation machinery. For example, it has been shown that β-arrestins can bind to both the heavy chain of the clathrin triskelion molecule and to the heterotetrameric AP-2 adapter complex. AP-2 is thought to be essential in linking the arrestin bound receptor to clathrin since the interaction of β-arrestin with the β2-adaptin subunit of AP-2 is essential for β2-AR internalisation (Laport *et al.*, 2000). For some GPCRs the clathrin-mediated pathway does not seem to be strictly necessary for endocytosis to occur since it has been observed that the AT1AR and the M_2 muscarinic acetylcholine receptor are capable of undergoing normal rates of internalisation in the presence of dominant negative mutants of β-arrestin and dynamin (Zhang *et al.*, 1996; Volger *et al.*, 1999). However internalisation of these receptors is enhanced by the overexpression of GRK and β-arrestin molecules suggesting that these two receptor types are both capable of

utilizing the clathrin route to endocytosis but that they exhibit redundancy in their choice of internalisation pathway. In the presence of negative inhibitors of clathrin-mediated endocytosis these receptors must be capable of utilizing other internalisation routes. As yet these alternative endocytic pathways have not been identified.

If it were the case that the desensitisation of GPCRs was an irreversible process, cellular signalling would soon be so perturbed as to prevent appropriate responses to external stimuli from occurring. As a possible mechanism for the prevention of such an occurrence, it has been suggested that the internalisation of GPCRs is essential for the dephosphorylation, resensitisation and return of these same receptors back to the plasma membrane of the cell where they can participate in further signalling events. It is thought that the intracellular compartments used to internalise GPCRs are enriched in specific GPCR phosphatases that allow an endocytosed GPCR to be dephosphorylated and then returned to the cell surface in a pre-ligand exposed state. In this model arrestins would play an important role in not only mediating receptor desensitisation but also in resensitisation of the receptor. Evidence for this is seen in experiments where the β2-AR is not resensitised in COS7 cells unless co-expressed with high levels of β-arrestin (Zhang *et al.*, 1997). The effective resensitisation of receptors seems to require the dissociation of β-arrestin from the endocytic complex before interaction with the GPCR-specific dephosphorylases can occur, as is seen to be the case for the β2-AR (Anborgh *et al.*, 2000). It has recently been suggested that the ability of β-arrestins to dissociate with the internalised GPCR complex is determined by the presence of clusters of serine and threonine residues present on the GPCR's carboxyl terminal tail. It has been shown through confocal microscopy studies that with respect to the strength and duration of the interaction between a given GPCR and arrestin molecules, the GPCR superfamily can be divided into two

broad groups depending on whether or not they possess these serine/threonine clusters (Oakley et al., 2000). Receptors that lack such clusters tend not to internalise into an endocytic complex with arrestin molecules and leave the arrestin localized in a diffuse distribution at the plasma membrane (β2-AR, μ-opioid receptor, endothelin type A receptor, dopamine D1A receptor and the α_{1b}-AR). This was in contrast to receptors that did posses these serine/threonine clusters on the carboxyl terminal tail, where the arrestin was observed to remain associated with the receptor even after it had internalised (angiotensin II type1A receptor, neurotensin receptor 1, vassopressin V2 receptor, TRH receptor and substance P receptor). It has also been shown that for the V2 vassopressin receptor a serine cluster present on the carboxyl terminal tail was responsible for preventing the recycling of the receptor (Innamorati *et al.*, 1998) and it is likely that this will also be the case for other such receptors possessing serine/threonine clusters within the carboxyl terminal tail.

1.4. Constitutive activation of G protein coupled receptors.

It has become apparent over the last decade that GPCRs are capable of exhibiting constitutive activity and that they are capable of activating downstream effectors even in the absence of any activating ligand. This behaviour was first brought to light in experiments where the carboxyl terminal portions of the third intracellular loops of the α_{1b}-AR and the β2-AR were swapped. From these experiments it was anticipated that the specificity of G protein coupling with respect to the α_{1b}-AR (G_q-coupled) and β2-AR (G_s-coupled) would be reversed. This however was not seen to be the case. Instead the mutant β2-AR was seen to produce elevated levels of cAMP production in the absence of any activating ligand when compared to the wild type β2-AR expressed at similar levels (Samama *et al.*, 1993). Similar results were obtained with

the α_{1b}-AR: the mutant receptor again exhibited a constitutively active phenotype with elevated levels of inositol phosphate production and downstream signalling even in the absence of agonists (Cottechia *et al.*, 1990; Allen *et al.*, 1991).

The mutant β2-AR had just four point mutations located at the distal end of the third intracellular loop (Figure 1.2). As well as exhibiting enhanced levels of basal second messenger production, the mutations were also seen to impart a number of characteristic properties that distinguished it from the wild type receptor (Samama *et al.*, 1993). For instance, it was observed that cAMP generation via both the CAM and the wild type β2-AR increased as a function of receptor expression levels. However the CAM β2-AR produced basal levels of cAMP that were comparable to those produced by the wild type receptor in the presence of isoprenaline. In addition to this it was seen that the mutant had an increased affinity for full agonists such as isoprenaline and adrenaline that was about 25-fold in excess of that seen at the wild type receptor. Furthermore, by determining the intrinsic activities of a range of partial agonists and comparing these values with the affinities of the same ligands for the CAM β2-AR, it could be seen that agonist affinity correlated well with the intrinsic activity. When the affinities of the various agonist compounds for both wild type and CAM β2-AR were compared in the presence of Gpp(NH)p which causes uncoupling of the receptor from G protein, it was shown that the preference in affinity for mutant over wild type receptor was greatest for full agonists, intermediate for partial agonists and undetectable for very weak agonists and antagonists.

Through the consideration of these experimental results, Samama and co-workers were able to show that the established model proposed to explain the mechanism of interaction between ligand, receptor and G protein was not adequate to explain their new findings. This model, known as the ternary complex model, is composed of four

Figure 1.2. Diagrammatic representation of the β2-AR, showing its seven transmembrane domain helices, its extracellular and intracellular loops as well as its amino and carboxyl terminal domains.

Highlighted (in grey) are the 4 amino acid residues present in the carboxyl terminal portion of the third intracellular loop that were altered upon exchanging this portion of the receptor with that of the analogous region derived from the α_{1b}-AR. The phenotypic attributes of this CAM β2-AR are described in the main text. This receptor was used extensively in the studies presented herein.

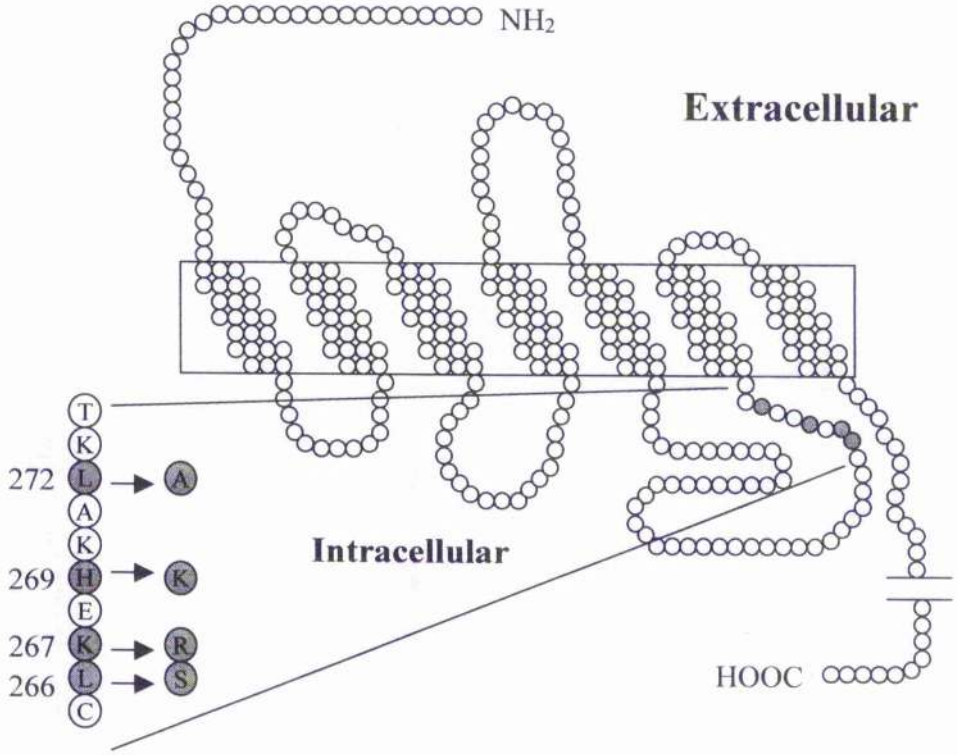
NH2
Extracellular
Intracellular
HOOC
272
269
267
266
T
K
L
A
K
H
E
K
L
C
A
K
R
S

Figure 1.2.

equilibrium reactions governed by the law of mass action and described by affinity constants (Figure 1.3a). There are three species involved in the dynamic equilibrium, hormone (H), receptor (R) and G protein (G). The two equilibrium constants K and M are independent of one another since the binding of R to H does not effect the binding of R to G and vice versa. The other two constants αK and αM are interdependent however, since the binding of H depends upon the quantity of RG and similarly the binding of G depends upon the abundance of HR. In this manner, the α factor describes to what extent the binding of H to R effects the binding of G to R and vice versa. This model has three intrinsic properties: 1) an agonist-independent formation of an active complex is predicted by the model, the magnitude of which is governed by the constant M; 2) the ratio between the affinities of H for the two forms of the receptor R and RG is defined by the dimensionless factor α and therefore reflects the ability of H to promote the formation of the HRG complex, α is consequently a factor that defines a ligand's molecular efficacy; 3) the affinity of H for R in the absence of G protein is described by K and is not therefore related to the α factor describing molecular efficacy and from this it is expected that ligand affinity and molecular efficacy are not correlated. Upon application of this model to the CAM β2-AR it was possible to explain a number of their experimental observations, for example, the increased basal activity of the mutant could be explained through an increase in the value of the M constant. However, an increase in the M constant could not by itself account for the increased affinity of the mutant receptor for agonists even in the absence of G-protein coupling. Such behaviour would require an additional increase in the value of the K constant. However, the model does not predict any correlation for affinity (K) of an agonist for the G-protein uncoupled receptor (R) and the molecular efficacy (α) as was observed in the experimental results. The ternary

Figure 1.3. Theoretical models describing the mechanisms of interaction between GPCR, hormone and G-protien.

A) The ternary complex model describing the interaction of a receptor (R) with G protein (G) and hormone (H). The model is more fully described in the main text. **B)** The extended ternary complex model where the receptor can exist in two forms, inactive R and active R*. The capacity of the receptor to undergo this isomerisation is determined by the constant J. **C)** The cubic ternary complex model, where both active R_a and inactive R_i states of the receptor are allowed to interact with G protein but only HR_aG mediates a response.

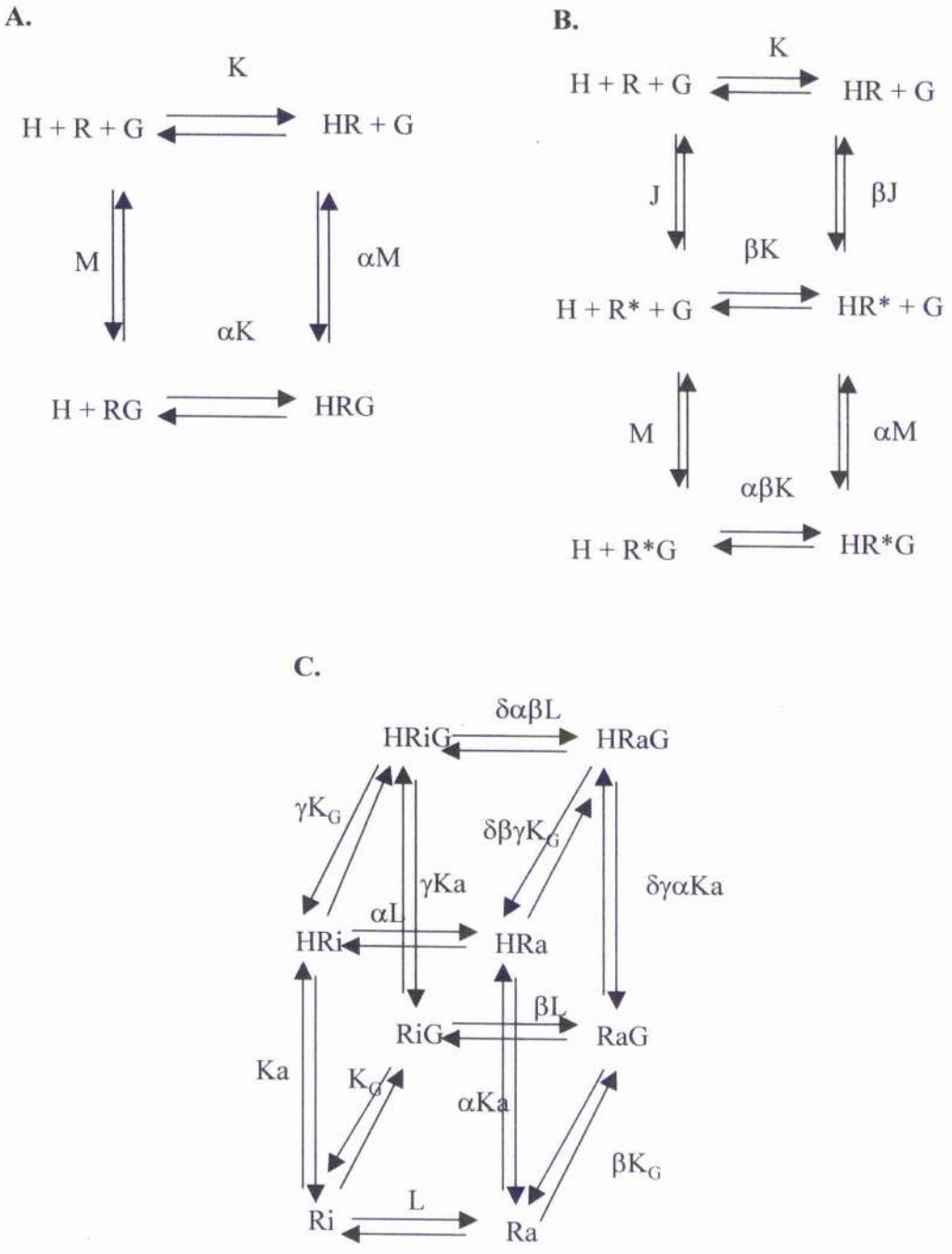
A.
K
H + R + G
HR + G
M
αM
αK
H + RG
HRG
B.
K
H + R + G
HR + G
J
βJ
βK
H + R* + G
HR* + G
M
αM
αβK
H + R*G
HR*G
C.
δαβL
HRiG
HRaG
γK_G
δβγK_G
γKa
δγαKa
αL
HRi
HRa
βL
RiG
RaG
Ka
K_G
αKa
βK_G
L
Ri
Ra

Figure 1.3.

complex model was then deemed inadequate in explaining the observed results with CAM β2-AR. The researchers then proposed a new model called the extended ternary complex model (Figure 1.3b) to better explain their findings. In this model, the assumption is made that the receptor exists in equilibrium between two conformations designated R and R*. In this new model it is assumed that only the active conformation of the receptor is capable of coupling to the G protein hence HR*G is the only ternary complex that can be formed. This model also introduces two new dimensionless constants, J, which describes the extent of the spontaneous isomerization between R and R*, and β which describes the extent to which the binding of ligand influences the R↔R* equilibrium. In the model the capability of ligand to bring about the formation of the ternary complex depends on two factors: 1) the ability of H to facilitate the transition from R to R* as described by the constant β; 2) the capacity of H to bring about stabilization of the ternary complex, as determined by the constant α. It was shown that this model was adequate in accounting for the observed correlation between the intrinsic activity of a ligand in the G protein uncoupled state and its affinity for the receptor.

To demonstrate, consider the fractional occupancy of the receptor H, given by $[H]/([H] + K_{app})$ where $K_{app} = (1/K).\ (1+J.(1+M[G])/(1+ \beta J.(1+\alpha M[G])$. From this equation it can be seen that J affects the apparent dissociation constant of a ligand for the receptor and that the extent to which this occurs is dependent upon both the constants α and β. For neutral antagonists α and β are equal to 1 and therefore K_{app} is equal to 1/K, the true K_d for the compound. For an agonist α and β are greater than 1 and this will lead to a decrease in K_{app}, the extent of which depends on the size of α and β ($J \neq 0$). When α and β are greater than 1 increasing values of J result in a decrease in K_{app}, enhancing the apparent affinity of the agonist for the receptor. Thus

the extended ternary complex model explained what the simple ternary complex could not, namely, that increased constitutive activity of a receptor leads to an enhanced affinity of that receptor for agonists, the extent of which is determined by the efficacy of the ligand. In addition for this, a shift in the R↔R* equilibrium towards the right, represented by an increase in J, along with the constant M, promotes the formation of the ligand independent complex [R*G]. Thus an increase in the value of J results in an enhanced basal activity as is observed with constitutively active receptors.

Since this initial work identifying two constitutively active GPCRs with point mutations present in their third intracellular loops, many more CAM GPCRs have been identified with mutations in a wide range of structural domains. One important ramification of these efforts has been the discovery that many antagonists are capable of suppressing the basal second messenger production of these CAM receptors. Such antagonists have the opposite effect to agonists and have therefore become known as inverse agonists and it is now believed that most antagonists possess at least some degree of inverse efficacy and that only a few antagonists may be classed as being truly neutral. The mechanism of action of inverse agonists has generally been interpreted within the context of the extended ternary complex model described above. From this model, given that the R* conformation is favoured by CAM receptors, if inverse agonists favour the R conformation of the receptor it might be expected that inverse agonists would have a decreased affinity for CAM GPCRs in a manner contrary to agonists. Consistent with such a theory are experiments that have been carried out on a CAM α_{2A}-AR where the efficacious inverse agonists yohimbine and rauwolscine were observed to be 1.7 and 2.1 fold weaker for the CAM α_{2A}-AR as compared to wild type (Wade *et al.*, 2001). These results were consistent with approximately 50% of the CAM α_{2A}-AR being in the R* state as compared to the wild

type receptor where there was no detectable constitutive activity in the absence of agonist. Other evidence that suggests that inverse agonists are capable of stabilizing the R state of the receptor comes from analysis of desensitisation-associated events at CAM GPCRs. It has been demonstrated that CAM GPCRs are not only capable of producing increased basal levels of second messenger molecules but they are also constitutively phosphorylated and desensitised. This was first demonstrated for the CAM β2-AR possessing four point mutations in its third intracellular loop, where the receptor was purified and then reconstituted into phospholipid vesicles. It was found that in such preparations this CAM β2-AR was phosphorylated by GRK in a manner comparable to the agonist occupied wild type receptor (Pei *et al.*, 1994) lending support to the contention that the mutated receptor was equivalent to the active R* conformation which stimulates G_s and is a substrate for GRKs. In further studies it was shown that this constitutive phosphorylation could be suppressed 50% by the inverse agonist ICI 118 551 and it was also shown that the affinity of this compound for CAM β2-AR was reduced when compared with the wild type receptor (Samama *et al.*, 1994). These findings all suggest that inverse agonists are capable of binding to and stabilizing the R conformation of the receptor in preference to the R* conformation. Another method that has provided evidence that inverse agonists stabilize a distinct conformation of the GPCR to agonists comes from studies that monitor the fluorescence of a reporter group incorporated into the native β2-AR (Gether *et al.*, 1996). Here, it was seen that inverse agonists were capable of inducing fluorescence changes that were opposite to those induced by agonist compounds. One interpretation of these results is that the native receptor is isomerising between the R and R* states and that inverse agonists and agonists are capable of enriching these

respective conformations. Such observations are all consistent with the extended ternary complex model.

From consideration of the various models put forward for the purpose of shedding light upon the possible mechanisms of receptor activation, it has been proposed that inverse agonists can suppress receptor signalling by three possible methods (Strange, 2002). 1) Inverse agonists bind to and stabilize the R state of the receptor in preference to R* (α<1). 2) Inverse agonists bind to either of the G protein uncoupled states of the receptor R and R* in preference to the G protein coupled state, R*G (β<1). 3) Inverse agonists do not redistribute different states of the receptor but instead switch the receptor to an inactive conformation that can exist in both G protein coupled and uncoupled forms but is, in both cases, inactive. An extended model, called the cubic ternary complex model (Figure 1.3c), predicts this final postulate and suggests that there will be an inactive conformation of the receptor that can nonetheless couple to G protein (Weiss *et al.*, 1996). Experiments that have attempted to discriminate between these possibilities have mainly employed radioligand binding techniques. From the extended ternary complex model, it should be the case that agonists will label the R*G state with high affinity whereas radiolabelled inverse agonists will label the R and/or R* states with higher affinity. Given this, it might be expected that the affinity for an inverse agonist when measured through competition binding with a radiolabelled agonist would be different to that determined in competition binding studies with a radiolabelled inverse agonist. This is provided that there is an excess of R to G in the experimental system such that there are substantial subpopulations of R*G and R/R* respectively. Such studies have been carried out using the 5-HT_{1A} receptor where the inverse agonist spiperone shows a clear difference in affinity for the receptor in the presence of a radiolabelled inverse agonist

than it does in the presence of radiolabelled agonist (McLoughlin and Strange, 2000). This is consistent with an enrichment of the G-protein uncoupled form of the receptor as predicted by the extended ternary complex model (postulates 1 and 2). However, the inverse agonist methiothepin does not show any difference in affinity for the $5HT_{1A}$ receptor, whether in the presence of radiolabelled agonist or inverse agonist. This finding supports the view that upon binding of the inverse agonist to the receptor there is a switch to an inactive conformation that can still couple to G proteins but which is incapable of activating them (postulate 3). Taken together these experimental observations suggest that inverse agonists may be capable of inactivating receptors by more than one distinct mechanism.

Another phenomenon that has been associated with constitutively active receptors is that of receptor upregulation upon prolonged exposure to ligands. This was initially noted in studies with the CAM β2-AR. With this mutant receptor it was observed that typical expression levels in mammalian cells were markedly lower than those seen with wild type receptors. It was found that the expression levels of CAM β2-AR could be increased upon exposing the cells expressing the CAM receptor to sustained treatment with betaxolol (Samama *et al.*, 1994). It was further observed in studies where expression levels of CAM β2-AR in NG108-15 cells were monitored in both the presence and absence of betaxolol that these upregulation events took place in the absence of any alteration in the levels of mRNA encoding the receptor protein (MacEwan and Milligan, 1996). It was at first thought that this upregulatory effect was a consequence of the inverse efficacy of the antagonist ligand. In experiments focusing on the β2-AR it was observed that betaxolol, an inverse agonist of high efficacy, was capable of upregulating both wild type and CAM versions of the receptor with the upregulatory effect being far more pronounced for the CAM

receptor (MacEwan and Milligan, 1996). Similarly another β2-AR inverse agonist called sotolol was able to produce a marked upregulation of the CAM receptor as well as a modest increase in the number of ligand binding sites for the wild type receptor. In contrast to this a neutral antagonist called alprenolol was incapable of inducing an upregulation of either wild type or CAM β2-AR. Subsequent studies on this receptor type have since indicated that these observed increases in receptor number following prolonged exposure to ligands were not dependent on the inverse efficacy of the ligand. It was shown that the CAM β2-AR, when expressed in insect Sf9 cells was capable of being effectively upregulated by either betaxolol or the agonist isoprenaline (Gether *et al.*, 1997a). It was further demonstrated that this upregulatory effect was the result of an extension in the half-life of the CAM β2-AR molecule in the presence of either agonist or antagonist, as demonstrated on purified extracts of the receptor protein. Also, from the results of Chapter 5 presented herein, it can be seen that a range of agonists were capable of inducing upregulation of CAM β2-AR when receptor number was monitored as a function of light output from a luciferase tagged β2-AR fusion construct. Viewed in retrospect, it may have been the case that in the experiments with alprenolol, where no upregulation was observed, not all of the ligand was effectively washed out of the membrane extracts and this consequently lead to an inhibition in binding of the [^{3}H]-radioligand to the receptor and an underestimation of the receptor number. This hypothesis is strengthened through observations that alprenolol was capable of upregulating a β2-AR-GFP fusion protein using confocal analysis (McLean *et al.*, 1999). In addition to the CAM β2-AR, a wide variety of GPCRs have been shown to be upregulated in response to a sustained treatment with ligands and these are detailed in the discussion section of Chapter 5, as

are the mechanisms and structural determinants believed to underlie the upregulation process.

The upregulation of receptors, especially wild type receptors, in response to inverse agonists may have important physiological implications pertaining to the therapeutic administration of drugs. This stems from the fact that long-term drug therapies with antagonists may cause receptor upregulation and hence lead to increased tolerance of the patient to that particular drug therapy. This has been observed in patients after prolonged treatment with the histamine H_2 receptor inverse agonist cimetidine where drug tolerance and increased H_2 receptor sensitivity occur following withdrawal (Smit *et al.*, 1996; Alewijnse *et al.*, 1998).

1.5. Dimerization of G protein coupled receptors.

1.5.1. Dimerization of opioid receptors.

The function of GPCRs and their mechanisms of activation have been described above under the assumption that the stoichiometry of interaction between ligand, receptor and G protein is 1:1:1. Concerning the mechanisms by which GPCRs functionally couple to G protein and traffic to the plasma membrane of the cell, there is now substantial evidence that this may be an oversimplification. It is now believed, through a diverse array of studies that have employed a wide variety of techniques, that GPCRs exists as dimers or higher order oligomeric arrays when expressed within mammalian cells. In this respect GPCRs are not atypical of other transmembrane receptor proteins. For example, single transmembrane domain growth factor receptors such as epidermal growth factor receptor (EGF) are known to dimerize in response to ligands. The direct association of the two proteins is essential for the initiation of the signalling events that eventually result in cell proliferation and growth. Although

traditional models depict GPCRs as being monomeric entities there has been in existence, for some quite considerable length of time, evidence suggestive of the contrary. For no other type of GPCR is this better exemplified than for the opioid receptors. Opioids have a wide range of biological effects including analgesia, miosis, bradycardia, sedation, hypothermia and depression of nerve reflexes. Principally however, they have been the focus of intense research interest in the pharmaceutical industry due to their ability to relieve pain by inhibiting neurotransmitter release from dorsal root ganglion projections in the dorsal horn of the spinal cord. Three subtypes of opioid receptor, μ, δ and κ, have been identified based upon their specificity of binding to different ligands. These have been subsequently shown also to differ in their distribution and function. A large number of opioid receptor subtypes have been identified through their differential ability to bind specific radiolabelled ligands. For example, the δ-opioid specific compounds naltrindole, naltriben and BNTX were used to identify two distinct δ-opioid subtypes (Jiang *et al.*, 1991; Mattia *et al.*, 1991). The number of subtypes identified for the opioid receptors exceeded the number of opioid genes discovered (only three) corresponding to the original μ, δ and κ receptor types. The question that then naturally arose was this: if there only exist, in total, three cDNAs for the opioid receptor family of proteins, why were there so many different subtypes distinguishable through ligand binding experimental procedures? It was unlikely that the answer to this question was that there existed many splice variants of the opioid receptors and that these same splice variants exhibited distinct pharmological properties. This was an inference derived from the following observation: that although a splice variant of the μ-opioid receptor was identified (MOR1b) that differed from the original in the length and amino acid sequence of the

carboxyl terminal tail (Zimprich *et al.*, 1995), it presented a pharmacological profile that was essentially similar to the previously cloned μ-opioid receptor.

Functional evidence seemed to indicate that opioid receptors were capable of interacting, and that the ability of the different opioid receptor types to interact might form the basis of subtype specificity. Evidence that the μ-opioid receptor and δ-opioid receptor could interact was obtained from the observation that delta selective agonists could modulate morphine-induced analgesia (Vaught and Takemori, 1979). This was backed up by pharmacological evidence, where it was observed that the moderately delta selective ligand leucine enkephalin (Leu-Enk) functioned as a non-competitive inhibitor of the slightly μ selective ligand naloxone. Leu-Enk was observed to decrease the maximum binding of radiolabeled naloxone in saturation binding experiments without an apparent decrease in affinity of the compounds (Rothman and Westfall, 1981, 1982). The researchers postulated that a population of the δ-opioid receptors complexed to μ-opioid receptors caused this, where, through an allosteric inhibition mechanism, binding of naloxone to the complexed μ-receptors was inhibited. Early biochemical evidence supporting the existence of opioid receptor interactions were provided by studies that made use of Rhodamine conjugated enkephalin analogues to label δ-opioid receptors at the cell surface (Hazum *et al.*, 1979). These studies revealed that the receptors tended to cluster at the cell surface and that this clustering could be abolished through the application of low concentrations of DDT, leading to the formation of a uniformly diffuse pattern instead. This suggested that disulphide bonds might be important in mediating these associations.

Despite these early indications that opioid receptors were capable of interacting it was not until relatively recently that the phenomenon was given serious attention. Over the

past decade, with the development of molecular genetic cloning and advancements in biochemical techniques, evidence supporting dimerization of opioid receptors has accumulated rapidly. Some examples follow:

A study making use of sodium dodecyl- sulphate polyacrylamide gel electrophoresis (SDS-PAGE) showed that the δ-opioid receptor expressed in mammalian cells produced a band of about twice the molecular weight that was expected for the δ-opioid receptor, indicative of a dimeric species. Through the co-expression of differentially tagged receptors it could be shown via precipitation with an antibody directed against one of the epitopes and detection with an antibody directed against the other epitope, that this band was indeed a dimeric species and not a complex consisting of the δ-opioid receptor and another protein of similar size (Cvejic and Devi, 1997). These dimers were shown to be unstable in the presence of SDS and required a crosslinking molecule to strengthen the complex, suggesting that the interactions were ionic in nature. It was also shown that pre-incubation with certain, although not all, types of agonist were capable of destabilising the strength of the dimeric complex and that this preceded receptor sequestration. These results contrasted with those obtained from similar experiments carried out on the κ-opioid receptor where the dimer complex, as detected via SDS-PAGE, was unaffected by the presence of selective ligands (Jordan and Devi, 1999). The molecular weight band representing the dimeric species was also resistant to SDS and was sensitive to reducing agents suggesting that κ-opioid receptor interactions were mediated through disulphide bonds. It was subsequently shown that the κ-opioid receptor and δ-opioid receptor could heterodimerize using the differential tagging co-immunoprecipitation technique, although no interaction between the κ-opioid receptor and the μ-opioid receptor could be demonstrated (Jordan and Devi, 1999). Like the κ-opioid receptor

homodimers these were found to be SDS resistant and sensitive to reducing agents. It was also observed that the κ-δ homodimer exhibited a pharmacology that was distinct from either κ-opioid or δ-opioid receptors alone. It was observed that the κ-δ homodimer lost its affinity for selective agonists (DPDPE and U-69593) as determined through competition binding studies with [^{3}H]-diprenorphine, whereas non-selective ligands retained their ability to displace the radioligand. It was further shown that in the presence of both selective ligands together, the ability to displace [^{3}H]-diprenorphine was restored (Jordan and Devi, 1999). Complexing of the δ-opioid receptor with the κ-opioid receptor was also seen to have effects on the internalisation properties of the receptors. Specifically, the δ-opioid receptor, which normally internalises in response to the agonist etorphine was unable to internalise in response to this ligand when co-expressed with the κ-opioid receptor. Another observed effect of κ-δ co-expression included a leftward shift in the dose dependent inhibition of adenylyl cyclase in response to simultaneous stimulation with both selective κ and δ-opioid agonists when compared to treatment with either agonist alone. Again using SDS-PAGE techniques, interactions between the δ-opioid receptor and the μ-opioid receptor have been demonstrated (George *et al.*, 2000). It was shown that, as was the case for κ-δ interactions, μ-δ heterodimers exhibited a pharmacological profile that was distinct from that seen by expressing δ-opioid receptor or μ-opioid receptor alone. When μ and δ-opioid receptors were co-expressed, highly selective agonists for either receptor were seen to have reduced potency and altered rank order for affinity whereas less selective ligands such as leucine enkephalin and endomorphine-1 had an enhanced affinity. The researchers attributed this alteration in the pharmacological profile to the generation of a novel ligand binding site generated through the interaction of the two receptor types. In their study, George and co-workers also

showed that co-expressed μ and δ-opioid receptors were insensitive to pertussis toxin treatment, suggesting that the μ-δ heterodimer was capable of coupling to a G protein distinct from G_i. These interactions between μ and δ- opioid receptors are likely to be of physiological relevance since studies on the dorsal root ganglia and measurement of the frequency of action potential firing in single neurones has shown that both μ and δ- opioid receptors co-localize in the same cells (Egan and North, 1981; Fields *et al.*, 1980; Zieglgansberger *et al.*, 1982). It is probable then, that the large number of opioid receptor subtypes observed *in vivo* result from the direct interaction of different opioid receptor types. In support of this hypothesis, it should be noted that κ-δ receptor complexes which were seen to bind non-selective ligands such as bremazocine and ethylketocyclazocine with high affinity but were unable to bind the highly selective κ-agonist U69593 resemble, with regards to their pharmacological profile, previously described kappa2 receptor subtypes found in guinea pig brain (Audiger *et al.*, 1982; Nock *et al.*, 1988; Zukin *et al.*, 1988).

1.5.2. Dimerization of the β2-adrenoceptor.

The well-characterized β2-AR has also been the focus of many investigations concerning the dimerization of GPCRs. Initial studies again made use of epitope tagged versions of the wt β2-AR to perform co-immunoprecipitation experiments. β2-AR was shown to be consistutively dimerized in an interaction that was resistant to SDS treatment (Herbert *et al.*, 1996). It was found, in contrast to studies focusing on the δ-opioid receptor that pre-incubation with agonist compounds led to a stabilization of the dimeric complex and that the reverse was the case when exposed to inverse agonist prior to SDS-PAGE analysis. The researchers were also able to implicate one of the transmembrane domains as being important in mediating these interactions.

When the β2-AR was expressed in the presence of a peptide mimicking the sequence of transmembrane domain VI of the receptor it was found that both dimerization and agonist-induced activation of cAMP were inhibited. Together these results suggested that for the β2-AR, dimerization was an important event in receptor activation and that biological activity of the receptor might be conferred through conversion of the receptor from a monomeric to a dimeric state.

One of the main detractions of the above-described experiments involving the peptide derived from TM VI was that it was not clear exactly how the peptide brought about adenylyl cyclase inhibition. It may have been due to the peptide inhibiting the dimerization of β2-AR or alternatively it could have been a result of the inactivation of the monomeric form of the β2-AR through formation of a "pseudodimer" with the peptide. The dimeric form was subsequently shown to be the active receptor conformation in studies where the wild type β2-AR was shown to be capable of functionally rescuing a non-palmitoylated and constitutively desensitised mutant of the β2-AR (Herbert *et al.*, 1998). This functional rescue was most likely to be attributable to the direct interaction between the wild type and mutant β2-AR since it was possible to co-immunoprecipitate these two receptor types from cell extracts where they had been co-expressed.

1.5.3. Heterodimerization of the $GABA_B$ receptor: how GPCRs can function as mutual chaperones in facilitating cell surface delivery.

The δ-opioid receptor and the β2-AR are both class A receptors. A class C receptor for which the evidence for dimerization is unequivocal is the $GABA_B$ receptor, which plays a major role in neurotransmission. In native tissues $GABA_B$ receptors modulate the activity of specific ion channels including inwardly rectifying K^+ channels

(GIRKS) and N- and P/Q type Ca^{2+} channels. The $GABA_BR1$ receptor was eventually identified and cloned through the use of a high affinity antagonist and was shown to be a member of the GPCR superfamily. However, $GABA_BR1$ was found to exhibit poor coupling to both GIRK channels and adenylyl cyclase. Publication of the sequence for this receptor led to an intensive search for other receptors that shared sequence homology with the originally isolated cDNA for $GABA_BR1$. This resulted in the identification of a receptor sequence called $GABA_BR2$ that exhibited 35% sequence homology with $GABA_BR1$ and was also a member of the GPCR superfamily. A number of lines of evidence seemed to indicate that the fully functional form of the $GABA_B$ receptor consisted of a heterodimer between these two identified 7TM proteins. It was determined that the mRNA for $GABA_BR1$ and $GABA_BR2$, in rat tissue, were present in the same neuronal cells (Jones *et al.*, 1998; Kaupman *et al.*, 1998). It was also observed that upon co-expression of $GABA_BR1$ and $GABA_BR2$ there was an up to tenfold increase in agonist potency as compared to expression of $GABA_BR2$ alone (Kaupman *et al.*, 1998). Direct evidence for the interaction of these two receptor types was provided by yeast two hybrid cross experiments, where screening of the carboxyl terminal tail of $GABA_BR1$ using a human brain cDNA library identified $GABA_BR2$ as a protein that had a high affinity for this region of $GABA_BR1$ (White *et al.*, 1998; Kuner *et al.*, 1999). In addition to this, co-expression of $GABA_BR1$ and $GABA_BR2$ allowed a robust coupling to GIRKs, stimulation of $[^{35}S]GTP\gamma S$ binding and inhibition of forskolin-stimulated cAMP accumulation. In short, through the co-expression of $GABA_BR1$ and $GABA_BR2$ a receptor with a pharmacological profile that was similar to that reported for native $GABA_B$ receptors present in rat brain was engendered. This restoration of $GABA_B$ functional activity appears to be linked to the peculiar trafficking properties

of the two GABA receptor types. Previous reports had attributed the poor functional activity of $GABA_BR1$ to its inability to target efficiently to the plasma membrane, the receptor being retained as an immature glycoprotein within the cell (White *et al.*, 1998). It is believed that association of $GABA_BR1$ with $GABA_BR2$ allows successful cell surface expression of the $GABA_B$ receptor to occur. Evidence for this was obtained from studies using FACs analysis to determine proportions of $GABA_BR1$ present on the cell surface when expressed alone or co-expressed with $GABA_BR2$ (White *et al.*, 1998). From all of this corroborative data, it seems almost certain that the $GABA_B$ heterodimers are pre-formed in the endoplasmic reticulum and that they are tightly associated upon their transit to the plasma membrane. As yet there has been no evidence to suggest that this association is in any way influenced by the presence of agonists/antagonists. The mechanism by which $GABA_B$ receptors dimerize appears to be unique in that it involves the interaction of coiled-coil α-helical domains within the carboxyl terminal tails of the receptors (Mitrovic *et al.*, 2000). It has been demonstrated that the intracellular retention of $GABA_BR1$ was mediated through an RXR(R) retention motif present on the carboxyl terminal tail (Margreta-Mitrovic *et al.*, 2000). The researchers further showed that the masking of this retention motif led to the successful cell surface delivery of the heterodimeric unit. This view of $GABA_B$ receptors acting as mutual chaperones is not unique within the field of GPCR pharmacology. A similar role has been attributed to a group of single transmembrane domain proteins called RAMPs. These have been implicated in facilitating the maturation of the calcitonin receptor and the calcitonin receptor like receptor, both members of the class B category of GPCRs. It has been demonstrated that the pharmacological profile, and the pattern of glycosylation of these receptors can be modified according to the type of RAMP that they are co-expressed with and

that this is due to a direct association within the endoplasmic reticulum (McLatchie *et al.*, 1998). Other evidence that GPCRs can function as mutual chaperones in facilitating the correct delivery of the receptor complex to the surface of the cell comes from studies which used several N-terminus truncation mutants of the V2 vasopressin receptor, to analyse the effect of co-expressing such mutants with the wild type receptor in COS-7 cells (Zhu and Wess, 1998). It was found the mutants were capable of inhibiting the function, ligand binding and cell surface expression of the wild type V2 receptor. Furthermore, these truncation mutants did not interfere with the function and trafficking of other receptors such as the β2-AR and the D1 dopamine receptor. These observations strongly indicate that the specific interaction of GPCRs occurs in the endoplasmic reticulum and that this facilitates the correct folding of the receptor, an essential pre-requisite for receptor export.

The intracellular retention of GPCRs within the endoplasmic reticulum may have important physiological consequences *in vivo*. For instance, it has been determined that there are eight splice variants of the α_{1A}-AR present in the human liver (Cogé *et al.*, 1999). Three of these give rise to receptors that possess all seven transmembrane domains, the other five are truncated receptors that lack TM VII. When transiently expressed in COS-7 cells the truncation mutants are seen to be impaired in both regards to their capacity to bind ligands and their ability to induce signal transduction and were exclusively localised intracellularly. This was in contrast to the full length receptors that were unimpaired in their capacity to bind ligands or mediate signal transduction and which were seen to be present both at the cell surface and also inside the cell. Co-expression of each of the α_{1A}-AR truncation isoforms with the original 7TM α_{1A}-AR led to an inhibition in receptor signalling, ligand binding and cell surface expression of this original, presumably through interaction of the isoforms

prior to export from the endoplasmic reticulum (Cogé *et al.*, 1999). The selective co-expression of truncated receptors along with full length GPCRs in different body tissues may therefore represent a novel pathway whereby the biological properties of a GPCR can be regulated.

Recent experiments have shown that the constitutive interaction between the $GABA_BR1$ with $GABA_BR2$ receptors is essential not only in facilitating correct trafficking to the plasma membrane, it is also a prerequisite for maintaining the receptor in an appropriate functional state. Co-expression of $GABA_BR1$ with a mutant of $GABA_BR2$ where the N-terminal domain was substituted for that of $GABA_BR1$ was seen to result in a receptor that responded to ligands in an aberrant way. Exposure to GABA led to an inhibition, rather than an activation of GIRK channels and the complex between $GABA_BR1$ and the mutant receptor exhibited an elevated constitutive activity (Margreta-Mitrovich *et al.*, 2001). It was proposed that the N-terminus of $GABA_BR2$ may normally suppress the signalling of $GABA_B$ and that binding of GABA to the N-terminal PBP domain of $GABA_BR1$ relieves this inhibition. It was also proposed that the inhibition of $GABA_BR1$ signalling via the mutant $GABA_BR2$ could be a reflection of the fact that the PBP domain of $GABA_BR1$ can provide an inefficient inhibitory effect upon its partner only when in the GABA bound state.

1.5.4. Various GPCRs: their ability to dimerize as determined via SDS-PAGE and the pharmacological/physiological consequences thereof.

Through the differential tagging of GPCRs, subsequent co-immunoprecipitation and SDS-PAGE analysis has (in addition to the $GABA_B$ receptor, opioid receptors and β2-AR) been used to demonstrate a variety of interactions, both homomeric and

heteromeric, between GPCRs. Such studies are usually accompanied by binding and functional data to provide additional information concerning the nature of the interactions. There are numerous examples of these, a selection of which shall now be presented.

Among the class A receptors the dopamine D2 receptor has been shown to exist both as a monomer and a dimer when expressed within mammalian cells. In experiments similar to those performed for the β2-AR, it was demonstrated that peptide sequences derived from the TM regions VI and VII of the dopamine D2 receptor were capable of disrupting the strength of the dimeric complex as revealed by SDS-PAGE (Gordon *et al.*, 1996). Similarly, by co-immunoprecipitation, oligomerization of the dopamine D3 receptor has also been demonstrated with bands appearing on SDS-PAGE that were indicative of both dimerization and tetramerization (Nimchinsky *et al.*, 1997). This was obtained from the analysis of endogenously expressed receptor present in rodent and primate brain tissue. The dopamine D3 receptor was also shown to oligomerize with a naturally occurring truncated D3-like protein termed D3nf. It is thought that D3nf could be responsible for targeting the dopamine D3 receptor to specific locations within the dentritic tree. Also, since D3nf seems to influence the assembly of the D3 receptor it is probable that alterations in D3nf would have important consequences for neurotransmission. Numerous other GPCRs have been demonstrated to dimerize in this manner e.g. homo-oligomerization of the histamine H_2 receptor (Fukushima et al., 1997), homodimerization of the metabotropic Glutamate receptor-1 (class C family receptor) (Ray and Hauschild, 2000; Tsuji *et al.*, 2000), homodimerization of CCR2 (Rodriguez-frade *et al.*, 1999), heterodimerization between CCR2 and CCR5 (Mellado *et al.*, 2001) as well as homodimerization of CCR5 (Vila-Coro *et al.*, 2000).

As well as heterodimerization between receptors that are fairly closely related GPCRs, more distantly related receptor types have been shown to exhibit interactions, of which the association that occurs between the AT1AR and the bradykinin B2 receptor shall serve as an example. These two GPCRs are known to couple to distinct types of G protein, $G\alpha_i$ (AT1AR) and $G\alpha_q$ (bradykinin B_2 receptor) respectively. They are also known to be functional antagonists: angiotensin II is a vassopressor (increasing vascular contractility and blood pressure) whereas bradykinin is a vasodepressor (decreasing vascular contractility and blood pressure). It was found that upon co-transfection of AT1AR with the bradykinin B_2 receptor that the potency and efficacy of angiotensin II was increased and that the potency and efficacy of bradykinin was decreased (Pfieffer *et al.*, 2001). The physiological relevance of these interactions was tested by reducing the levels of bradykinin B_2 receptor expression in smooth muscle cells that endogenously expressed both types of receptor through the use of anti-sense oligonucleotides (Abdalla *et al.*, 2000). This caused a significant decrease in the levels of angiotensin II stimulated increase in intracellular Ca^{2+} without any alteration in the levels of AT1AR expression. These results show that the interaction of distantly related GPCR types could have an important role in mediating signalling events *in vivo*. Other interactions between distantly related GPCRs include reported interactions between the β2-AR and both the δ-opioid and κ-opioid receptors (Jordan *et al.*, 2000). An interaction has even been reported between the adenosine A1 receptor (class A) and the metabotropic glutamate receptor (class C), where the heteromeric complex was isolated from cerebellar neuronal cultures and from cells co-transfected with differentially epitope tagged receptors (Ciruela *et al.*, 2001).

1.5.5. Evidence for dimerization of GPCRs obtained from functional rescue/complementation experiments.

Another line of enquiry that has contributed to our knowledge of GPCR dimerization is that of functional rescue/complementation experiments. These are of a similar sort to those described previously for the β2-AR, where upon co-expression of a wild type and a mutant receptor the wild type was seen to rescue the aberrant phenotype of the mutant. In such studies the interaction is inferred from the functional rescue rather than being directly demonstrated. These types of experiment have recently been applied to the lutcinizing hormone receptor. This is a GPCR that essentially consists of two halves, an N-terminal extracellular domain (exodomain) and a C-terminal membrane associated portion (endodomain). Binding of the hormone to the exodomain causes receptor activation through interaction with the endodomain. It was demonstrated that co-expression of a binding defective mutant (mutation in the exodomain) with a signal defective mutant (mutation in the endodomain) resulted in restoration of ligand binding and signalling of the receptors whereas this was not observed when either receptor was expressed alone (Lee *et al.*, 2002). This observation suggested that the exodomain of one receptor was capable of interacting with the endodomain of another receptor, implying a very close interaction between the two. Similar types of experiments have been used to provide evidence that the somatostatin receptor subtypes sst_1 and sst_5 interact. The wild type sst_1 receptor, which is incapable of binding the ligand SMS- (201-995) was co-expressed with a carboxyl terminal tail deletion mutant of the sst_5 receptor, which was capable of binding to SMS- (201-995) but was defective in its ability to signal. Exposure of the co-transfected cells to SMS- (201-995) lead to a dose dependent inhibition of forskolin stimulated cAMP production (Rochville *et al.*, 2000).

Touching upon this issue of functional complementation, a certain study of interest focusing upon chimeras between the α_{2C}- adrenoceptor and the M_3 muscarinc acetylcholine receptor should not be omitted. In this study the TM domains I-V and VI-VII were swapped to generate the chimeric receptors [α_{2c}(TM I-V)-M_3(TMVI-VII) and M_3(TMI-V)- α_{2c}(TMVI-VII)]. When transfected alone neither chimera was able to bind to selective muscarinic or adrenergic ligands. However upon co-expression the ability of these receptors to bind ligand and mediate signalling events was restored (Maggio *et al.*, 1993).

1.5.6. Detection of GPCR dimerization using biophysical techniques.

The biophysical technique known as resonance energy transfer has been in use for quite a considerable time in the field of biochemical research. This involves monitoring of the non-radiative transmission of energy from one fluorescent molecule (a donor) to another (an acceptor) and is characterised by a loss of fluorescence (quenching) at the donor fluorophore and a resultant emission peak emitted via excitation of the acceptor fluorophore (see Chapter 3 for in depth discussion). These non-radiative events only occur when the donor and acceptor fluorophores are in very close proximity to one another (typically 50-100Å) and the technique has been used in the past to accurately determine intermolecular distances and to elucidate whether or not protein molecules are capable of interacting with one another. In recent years, with the advent of molecular cloning technology, it has become possible to apply these techniques to receptor protein molecules being expressed in living cells. This can be achieved by in-frame ligation of mutant versions of the GFP molecule derived from the jellyfish *Aequorea victoria* to provide appropriately donor and acceptor tagged receptor chimeras. Alternatively, antibodies that have been conjugated to

fluorescent dyes can be used to label the extracellular face of GPCRs that have been genetically modified to incorporate specific epitope tags. These techniques have now been applied to a number of GPCRs in order to provide evidence for dimerization. Homodimerization of the dopamine D2 receptor has been demonstrated through the in frame ligation of cyan fluorescent protein (CFP) and yellow fluorescent protein (YFP) to the carboxyl terminal tails of both the long and short isoforms of the receptor. Co-expression of the respectively tagged receptor types revealed significant levels of energy transfer between both long and short isoforms of the receptor which suggested that this GPCR existed at least in a partly dimerized state when expressed in mammalian cells (Wurch *et al.*, 2001). The extent of dimerization could be increased through the presence of the agonist compound (-)-NPA, an effect that was seen to be dose dependent. These findings would seem to lend their support to the notion of dimerization playing a role in receptor activation as has been suggested for the β2-AR. It should here be noted however that these agonist induced increases in the extent of energy transfer may not necessarily imply that the ligand has increased the dimerization status of the receptor. This is because the efficiency of energy transfer is not only related to the distance between the donor and acceptor fluorophores but is also determined by the relative orientation between these two molecules. As a consequence of this, it may be the case that ligand binding to the receptor induces a conformational change that results in a receptor orientation that is more conducive to the non-radiative transfer of energy and hence this results in a greater observed magnitude of energy transfer. In further experiments it was shown that by introducing an untagged version of the dopamine D2 receptor into the transfection mixture with the CFP and YFP tagged chimeric constructs, energy transfer between the chimeras could be effectively abolished (Wurch *et al.*, 2001). In this experiment both the long

and short isoforms of the dopamine D2 receptor were seen to reduce energy transfer between short form CFP and YFP tagged versions of dopamine D2 receptor, suggesting that heterodimerization between splice variants could occur. It was further demonstrated, as a control, that no reduction in energy transfer occurred when an unmodified β2-AR was introduced into the co-transfection mixture in a similar manner as before. Evidence that the thyrotropin receptor exists as a dimer has been provided through the construction of receptors differentially tagged with the GFP variants RFP and YFP (Latif *et al.*, 2001). Although the close spatial proximity of the receptors was demonstrated in this study, no ligand induced increases in energy transfer were reported. Photobleaching FRET has been used to demonstrate that homodimerization of the somatostatin receptor SSTR5 occurs (Rochville *et al.*, 2000). Photobleaching is the loss of fluorescence that is observed when a fluorescent molecule is exposed to an excitatory wavelength of light over a prolonged period of time. If there is energy transfer between the excited fluorophore and an acceptor molecule the photobleaching process will occur less rapidly because there has been introduced into the system a new non-radiative pathway directing energy away from radiative photoemission. To take advantage of this system the donor acceptor pairing of fluorescein and rhodamine were used to label hemagglutinin (HA) specific antibodies. HA tagged SSTR5 was then expressed in CHO-K1 cells and then incubated in the presence of either fluorescein-conjugated mAB or both fluorescein and rhodamine conjugated mAB together in order to label the cell surface receptors. The decay in photobleaching in single cells was then measured through imaging via confocal microscopy. There was a significant slowdown in the rate of photobleaching observed in the cells where SSTR5 had been labelled with both donor and acceptor fluorophores, in comparison to cells where the receptor was labelled with just the

fluorescein molecule alone (Rochville *et al.*, 2000). The researchers took this observation to indicate that the SSTR5 receptors were in sufficiently close proximity to allow energy transfer to occur between the fluorophores. It was further demonstrated that addition of agonist to the system resulted in significant increases in the observed FRET efficiencies between donor and acceptor fluorophores.

An alternative, but related, system to FRET has recently been developed, called bioluminescence resonance energy transfer (BRET), which was the system of choice for the studies presented herein. The BRET system is described fully in Chapter 3. Briefly, in this system the fluorescent donor molecule is substituted with a bioluminescent one, called coelenterazine. In this case the excitation energy for the donor molecule is provided not through absorbance of a photon of light, but instead through the oxidation of the coelenterazine molecule that is achieved through its interaction with a luciferase enzyme derived from the marine organism *Renilla reniformis*. The acceptor in this system is a red shifted mutant version of the GFP from *A. victoria* (eYFP). In-frame ligation of *Renilla* luciferase to the carboxyl terminal tail of one GPCR and similar ligation of eYFP to the carboxyl terminal tail of another receptor allows the close proximity of such tagged receptors to be detected when co-expressed within mammalian cells through monitoring of the energy transfer that occurs between *Renilla* luciferase and eYFP. Other researchers have also adopted this system and used it successfully to detect protein-protein interactions between GPCR molecules. Of note are studies carried out on the β2-AR where this receptor was shown, through analysis of the light emission spectrum obtained from cells expressing both *Renilla* and eYFP tagged forms of the β2-AR, to be constitutively dimerized (Angers *et al.*, 2000). It was also shown that the presence of the agonist isoprenaline was capable of increasing these levels of energy transfer, an effect that

could be blocked by the presence of the antagonist propranolol. Similarly this technique has been applied to the thyrotropin releasing hormone receptor (TRHr). Again, it was demonstrated using BRET that these receptors are consitutively homo-oligomerized and that the extent of this oligomerization could be increased through exposure to TRH (Kroeger *et al.*, 2001). Furthermore it was established that inclusion of untagged TRHr in the transfection mix could abolish energy transfer in a manner similar to the experiment described for the dopamine D2 receptor (above). The self-self interactions observed with the TRHr seemed to be specific since no energy transfer was observed when the eYFP conjugated TRHr was co-expressed with *Renilla* conjugated gonadotropin releasing hormone receptor (GnRHR). Also, inhibition of BRET was not observed upon inclusion of untagged GnRHR into a transfection mixture of TRHr-Rluc and TRHr-eYFP. One concern with these types of biophysical studies is that increases in energy transfer could be due to clustering of receptors into vesicles as sequestration proceeds in response to receptor activation by agonists. It was shown that this was not the case for TRHr since the increases in the BRET signal in response to ligand were maintained, even in the presence of a dominant negative version of dynamin, named Dyn K44A that inhibits sequestration. Another receptor for which dimerization has been investigated using BRET is the cholecytokinin receptor (CCKr). This is a class A GPCR that binds to the small peptide hormone CCK and has numerous actions that effect nutrient homeostasis. BRET was used to show that this receptor existed in a homo-oligomerized state by co-expressing CCKr-Rluc and CCKr-eYFP chimeric constructs in COS cells (Cheng and Miller, 2001). Interestingly, in this study it was observed that upon addition of the peptide CCK there was a loss of energy transfer observed, an effect that was dose dependent. These results indicate that for this GPCR the presence of ligand in the

receptor binding pocket favours the monomeric species of the receptor. Cheng and Miller also attempted to address the question of whether the changes in energy transfer observed were due to alterations in the conformation the receptor homodimers or whether they were truly due to monomerization (Cheng and Miller, 2001). Their strategy was to not only position the donor and acceptor molecules on the carboxyl terminal tails of the receptors, but also to generate a construct where eYFP was placed on the amino terminal of the CCKr (eYFP-CCKr). When eYFP-CCKr was co-expressed with CCKr-Rluc (C-terminal modification) the same agonist induced changes in BRET were observed as before and this was also the case for two Rluc and eYFP tagged truncation mutants of the CCKr. Thus, since the loss of BRET was preserved upon co-expressing modified CCKr with the position of the donor and acceptor moieties varied, this seemed to lend credence to the presupposition that the loss in BRET was a consequence of ligand induced monomerization.

Chapter 2

Materials and Methods

2.1. Materials

2.1.1. General reagents, enzymes and kits

Restriction enzymes-Roche molecular biochemicals and Promega.

Fast-link DNA ligation kit (Epicentre)- Contents: Fast-link DNA-ligase@ 2U/ul, 10X fast-link buffer (330mM Tris acetate {pH 7.8}, 660mM potassium acetate, 100mM magnesium acetate, 5mM DTT), ATP 10mM.

Wizard Plus SV Minipreps DNA purification system - (Promega).

QIAGEN Plasmid Maxi Kit (Qiagen).

Contents: Buffer P1 (Resuspension buffer), 50mM Tris.Cl, pH 8.0; 10mM EDTA; 100ug/ml RNase A.

Buffer P2 (lysis buffer), 200mM NaOH, 1% SDS

Buffer P3 (neutralization buffer) (3.0M potassium acetate, pH 5.5)

Buffer QBT (equilibration buffer) (750mM NaCl; 50mM MOPS, pH 7.0; 15% isopropanol)

Buffer QC (wash buffer) (1.0M NaCl; 50mM MOPS, pH 7.0; 15% isopropanol).

Buffer QN (elution buffer) (1.25M NaCl; 50mM Tris.CL, pH 8.5; 15% isopropanol).

RNaseA (100mg/ml),

10x QIAGEN-tip 500

QIAquick Gel Extraction Kit-Qiagen

Contents: Buffer QG (2 X 50ml)

Buffer PE 10ml plus 40ml ethanol

QIAquick spin columns

Collection tubes 2ml

***Pfu* DNA Polymerase** –(Promega) plus 10X Reaction Buffer with $MgSO_4$: (200mM Tris-HCl (pH 8.8 at 25°C), 100mM KCl, 100mM $(NH_4)_2SO_4$, 20mM $MgSO_4$, 1.0% Triton® X-100 and 1mg/ml nuclease-free BSA.)

dNTP's (deoxynucleotide triphosphate set) (Roche)- 100mM lithium salt solutions of dATP, dCTP, dGTP, dTTP.

Antibiotics (Sigma)

Kanamycin A ($C_{18}H_{36}N_4O_{11}$), Stock solution 10mg/ml in distilled H_2O.

Ampicillin ($C_{16}H_{19}N_3O_4S$), Stock solution 100mg/ml in distilled H_2O.

Geneticin ($C_{20}H_{40}N_4O_{10}.2H_2SO_4$), Stock solution 10mg/ml in distilled H_2O.

Coelenterazine – Nanolight technologies (Prolume).

Deep blue C - Packard.

Luclite Luciferase gene reporter kit (Packard)- Contents: Luclite buffer 10ml (10 aliquotes), lyophilized substrate (10 aliquotes).

Dual luciferase Reporter assay system (Promega)- Contents: 10x10ml Luciferase assay buffer II; 10x1 vial Luciferase assay substrate (lyophilized product); 10x11ml Stop and Glo buffer; 10x1 vial stop and Glo substrate; 10x250ul stop and Glo solvent; 30ml passive lysis buffer (5X).

2.1.2. Pharmacological compounds

5-HT 5-hydroxytryptamine hydrogen maleate (Sigma).

8-OH-DPAT (±) 8-Hydroxy-2-dipropylamino tetraline (Tocris).

Angiotensin II Asp-Arg-Val-Tyr-Ile-His-Pro-Phe, $C_{49}H_{69}N_{13}O_{12}$ (Sigma).

ATP 2'Monophosphoadenosine 5'-diphosphoribose sodium salt, $C_{15}H_{24}N_5O_{17}P_3$ (Sigma)

Betaxolol hydrochloride-1-[4-[2-(Cyclopropylmethoxy)ethyl] phenoxy] –3-isopropylamino-2-propanol (Tocris).

Calcitonin (human) peptide, $C_{151}H_{226}N_{40}O_{45}S_3$ (Sigma).

Carbachol Carboamoylcholine chloride, $C_6H_{15}ClN_2O_2$ (Sigma)

CGP 12177 hydrochloride 4-[3-[(1,1-Dimethylethyl)amino]2-hydroxypropoxy]-1,3-dihydro-2H benzimidazol-2-one (Tocris).

Clenbuterol hydrochloride 4-Amino-α-(t-butylaminomethyl)-3,5,-dichlorobenzyl alchohol (Tocris).

CPA –N^6-Cyclopentyladenosine (Sigma).

DADLE-[D-Ala^2, D-Leu^5] Enkephalin (Sigma).

DPCPX - 1,3, - Dipropyl-8-cyclopentylxanthine (Sigma).

Formoterol (hemisulfate salt) (±) –(R*,R*)-N-[2-Hydroxy-5-[1-hydroxy-2-[[2-(4 methoxyphenol)-1- methylethylene]amino]ethyl]phenyl]formamide (Tocris).

GNTI dihydrochloride 5′-Guanidinyl-17-(cyclopropylmethyl)-6,7-dehydro-4,5a-epoxy-3,14-dihydroxy-6,7-2′,3′-indolomorphinan (Tocris).

GW590623X CCR2 antagonist (Astra-Zenecca Ltd).

ICI 118,551 hydrochloride (±)-(-1-[2,3-(Dihydro-7-methyl-1H-inden-4-yl)oxy]-3-[(1-methylethyl)amino] 2-butanol (Tocris).

ICI 174 864 – N,N, dialyl- Tyr-Aib-Aib-Phe-Leu (Tocris)

ICI-199, 441 hydrochloride 2-(3,4-Dichlorophenyl)-N-methyl-N-[(1S)-1-phenyl-2-(1-pyrrolidinyl) ethyl]acetamide (Tocris).

IL-8 (Interleukin 8) C-X-C family chemokine, 72 amino acids (Sigma).

Isoproteronol (hemisulfate salt) (1-[3',4'-Dihydroxyphhenyl] -2-Isopropyl aminoethanol (Sigma).

MCH (Melanin concentrating hormone) peptide, $C_{105}H_{160}N_{30}O_{26}S_4$ (Sigma).

Naloxone hydrochloride (5a)-4,5-Epoxy-3, 14-dihydro-17- (2-propenyl) morphinan-6-one (Tocris).

NECA 5'-(N-Ethylcarboxamido) adenosine (Sigma).

Oxytosin α Hypophamine, Cys-Tyr-Ile-Glu-Asn-Cys-Pro-Leu-Gly-NH_2 (Sigma)

PGE2 Protaglandin E_2, $C_{20}H_{32}O_5$ (Sigma)

Phentolamine 2- [N-(3-Hydroxyphenyl) -p-toluidinomethyl] -2- imidazoline hydrochloride (Sigma).

Procaterol hydrochloride (±)-erythro-8-Hydroxy-5- [1-hydroxy -2-(isopropylamino) butyl] carbostynil (Tocris).

Propranolol hydrochloride (RS)-1-[(1-Methylethyl)amino]-3-(1-naphthalenyloxy)-2-propanol (Tocris).

PYY -$C_{194}H_{295}N_{55}O_{57}$ (gut hormone peptide) (Sigma).

Salbutamol sulphate α1-[[(1,1-Dimethylethyl)amino]methyl]-4-hydroxy-1,3 benzenedimethanol (Tocris).

SLGRL Ser-Leu-Ile-Gly-Arg-Arg-Leu-NH_2 (Tocris).

Sotalol hydrochloride N-[4-[1-Hydroxy-2-[(1-methylethyl) amino]ethyl]phenyl] methanesulphonamide (Tocris).

TRAP (thrombin receptor agonist peptide) Ser-Phe-Leu-Leu-Arg-Asn-Pro-Asn-Asp-Lys-Tyr-Glu-Pro-Phe (Tocris).

2.1.3. Tissue culture

DMEM- Dulbecco's modified Eagle's medium (Cell culture Labfax, BIOS scientific publishers, 1992), with 4500mg glucose/L, sodium bicarbonate and pyroxidine hydrochloride (Sigma).

DMEM-F12 Ham- Dulbecco's modified Eagle's medium F-12 Ham (Cell culture Labfax, BIOS scientific publishers, 1992), with 15mM HEPES, sodium bicarbonate and pyroxidine hydrochloride (Sigma).

0.25% Trypsin-EDTA Solution- Contains 2.5g porcine trypsin and 0.2g EDTA in 250ml (Sigma).

Optimem-1- A modification of Eagle's minimal essential medium (Cell culture Labfax, BIOS scientific publishers, 1992), buffered with HEPES and sodium bicarbonate, and supplemented with hypoxanthine, thymidine, sodium pyruvate, L-glutamine, trace elements and growth factors. Protein level is minimal (15ug/ml) with insulin and transferrin being the only protein supplements. Contains phenol red at a reduced level as a pH indicator (Gibco/Invitrogen).

L-Glutamine-100mM sterile filtered solution (100X concentrated) (Gibco/Invitrogen).

Freezing solution- 70% DMEM, 20% New born calf serum (NBCS) (Sigma), 10% Dimethyl sulfoxide (DMSO).

Flasks, dishes and pipettes-75cm^2 tissue culture flask with vent cap (polystyrene/sterile) (Iwaki), 150cm^2 tissue culture flask (polystyrene/sterile) (Iwaki). 100mm tissue culture dish (polystyrene), sterile (Iwaki). 60mm tissue culture dish (polystyrene), sterile (Iwaki). 6 well dish with lid, flat bottom, well diameter 35mm (Tissue culture treated/sterile) (Iwaki). 24 well dish with lid, flat bottom, well diameter 16mm (tissue culture treated/sterile) (Iwaki).

Cryovials, sterile, non-pyrogenic, DNAse and RNAse free (Cellstar).

15ml and 50 ml polypropylene plastic tubes with lid (Sterilin).

25ml disposable serological pipette (Corning). 10ml disposable serological pipette (Corning). 5ml disposable serological pipette (Corning).

2.1.4. Radiochemicals

[^{3}H]-Diprenorphine-66Ci/mmol in ethanol solution (Amersham).

[^{3}H]-Dihydroalprenolol-40Ci/mmol in ethanol solution (Perkin-elmer lifesciences)

[^{3}H]-Naltrindole-33Ci/mmol in ethanol solution (Perkin-elmer life sciences)

[^{3}H]-Adenine- 1 μCi/μl in ethanol solution (Perkin-elmer life sciences)

2.1.5. Oligonucleotides (Interactiva)

Primer melting temperature (T_m) was determined by the following equation:

T_m =[(number of G plus C) X 4°C + (number of A + T) X 2°C] (M.J. McPherson and S.G. Moller, PCR, BIOS scientific publishers, 2000).

The T_m, is the temperature at which half the primers are annealed to their target region. When calculating T_m only the part of the primer which would anneal to the template was considered.

(1) (B2AR FWD) 5'-AAA AAG CTT GCC ACC ATG GGG CAA CCC GGG AA-3' (Tm=56°C/ length=32 nucleotides)

(2) (B2AR REV) 5'-CCT CTC GAG CAG TGA GTC ATT-3' (Tm=50°C/length=21 nucleotides)

(3) (RLUC FWD) 5'-TCG CTC GAG ACT TCG AAA GTT TAT G-3' (Tm=54°C/ length=25 nucleotides)

(4) (RLUC REV) 5'-GCG TCT AGA TTA TTG TTC ATT TT-3' (Tm=56°C/ length=23 nucleotides)

(5) (PLUC FWD) 5'-GCC CTC GAG GAC GCC AAA AAC-3' (Tm=46°C/ length=21 nucleotides)

(6) (PLUC REV) 5'-TGC TCT AGA TTA CAC GGC GAT CTT-3' (Tm=44°C/ length=24 nucleotides)

(7) (EYFP FWD B2) 5'-AGA CTC GAG ATG GTG AGC AAG GGC GA-3' (Tm=54°C/ length=26 nucleotides)

(8) (EYFP REV B2) 5'-TGA TCT AGA TTA CTT GTA CAG CTC GTC-3' (Tm=52°C/ length=27 nucleotides

(9) (BRET1+RF) 5'-GCC AAG CTT GCC ACC ATG ACT TCG AAA GTT TAT GAT-3' (Tm=54°C/ length=36 nucleotides)

(10) (BRET1+RR) 5'-CGC CGG ATC CCG GGC CCG TTG TTC ATT TTT GAG AAC TCG-3' (Tm=54°C/ length=39 nucleotides)

(11) (BRET1+EF) 5'-G CCG GAT CCC CGG GTA CCG GTC GCC ACC ATG GTG AGC AAG GGC-3' (Tm=54°C/ length=43 nucleotides)

(12) (EYFPTr) 5'-AGA AAG CTT ATG GTG AGC AAG GGC GA-3' (Tm=54°C/ length=26 nucleotides)

(13) (DOR-1 FWD) 5'-AAA GCT AGC GCC ACC ATG GAG CAA AAG CTC AAT TCT GAA GAG GAC TTG GAA CCG GCC CCC TCC G-3' (Tm=58°C/ length=64 nucleotides)

(14) (DOR-1 REV) 5'-ATA GGA TCC GGC GGC AGC GCC AC-3' (Tm=52°C/ length=23 nucleotides)

(15) (BARR2 FWD) 5'-AAA G CTA GCA GCC ACC ATG GGG GAG AAA CCC GG-3' (Tm=56°C/ length=33 nucleotides)

(16) (BARR2 REV) 5'-AAA ATG GGG CCC ACA GAA CTG GTC GTC ATA GT-3' (Tm=58°C/ length=32 nucleotides)

(17) (CCR2 FWD) 5'-AAA G CTA GCA GCC ACC ATG CTG TCC ACA TCT CGT T-3' (Tm=56°C/ length=35 nucleotides)

(18) (CCR2 REV) 5'-AAA TGG ATC CGC TAA ACC AGC CGA GAC TTC C-3' (Tm=58°C/ length=31 nucleotides)

2.2. Buffers and Reagents

2.2.1. Buffers and reagents for molecular biology

LB Medium (Luria-Bertani Medium)

Bacto-tryptone 10g

Bacto-yeast extract 5g

NaCl 10g

Dissolved in 950ml of distilled H_2O, pH adjusted to 7.0 with 5M NaOH. Volume adjusted to 1L with distilled H_2O. Sterilized by autoclaving for 20mins at 15lb/sq. in on liquid cycle.

LB Media (Luria-Bertani Medium) containing agar

Was made as above except for the addition of 15g/L of bacto-agar prior to autoclaving.

50mM Calcium chloride

17.5g of $CaCl_2.6H_2O$ was dissolved in 1L of distilled H_2O and sterilized by autoclaving for 20mins at 15lb/sq. in on liquid cycle.

Ethidium bromide (10mg/ml)

1g of ethidium bromide was added to 100ml of H_2O and left stirring for several hours. Container was wrapped in magnesium foil and stored at room temperature.

Tris acetate (TAE) (50X)

242g Tris base, 57.1ml glacial acetic acid, 100mL 0.5M EDTA (pH 8.0). Made up to one litre with distilled H_2O. 10ml of this stock was diluted in 450ml of H_2O as required to make 1X buffer.

Gel loading buffer (6X)

0.25% bromophenol blue, 40% sucrose (w/v) dissolved in distilled H_2O.

2.2.2. Buffers and reagents for biochemical assays

Tris-EDTA buffer (T.E.1)

10mM Tris Base 0.1mM EDTA dissolved in distilled H_2O, pH 7.4.

Tris-EDTA buffer (T.E.2)

50mM Tris Base 1mM EDTA dissolved in distilled H_2O, pH 7.4.

Tris-EDTA-Magnesium chloride buffer (T.E.M.)

50mM Tris Base, 1mM EDTA, 12.5mM $MgCl_2$ dissolved in distilled H_2O, pH 7.4.

Adenylyl cyclase assay medium

This consisted of DMEM minus serum buffered with HEPES (20mM pH 7.4) and containing the phosphodiesterase inhibitor 1mM 3-isobutyl-1-methylxanthine (IBMX).

Adenylyl cyclase stop solution

5% trichloroacetic acid, 1mM cAMP, 1mM ATP made up in dH_2O.

Phosphate buffered saline (PBS)

8g of NaCl, 0.2g of KCl, 1.44g of Na_2HPO4 and 0.24 of KH_2PO_4, dissolved in 800ml of distilled H_2O. The pH was adjusted to 7.4 with HCl, and the volume to one litre with distilled H_2O. This was then sterilized by autoclaving for 20mins at 15lb/sq. in on liquid cycle.

Hepes buffered saline (HBS)

0.95g of HEPES, 1.75g of NaCl was adjusted to a volume of 200ml with dH_2O, pH was adjusted to 7.4 with HCl. This was then sterilized by passage through a 0.22 micron filter.

P.B.S. supplemented with magnesium and glucose

P.B.S was prepared as above to which was made the following additions: magnesium (0.1 g/l), glucose (1 g/l) and 2 µg/ml aprotinin (Sigma).

Extracellular buffer

125mM NaCl, 5mM KCl, 2mM $CaCl_2$, 2mM $MgCl_2$, 0.5mM NaH_2PO_4, 5mM $NaHCO_3$, 10mM HEPES, 10mM Glucose, 0.1% BSA. Chemicals were dissolved in distilled water, the pH was adjusted to 7.4 and this was then sterilized by passage through a 0.22 micron filter.

BCA protein assay buffer A

1% (w/v) Na_2-BCA (4,4,- dicarboxy- 2,2, - Biquinoline), 2% (w/v) Na_2CO_3, 0.16% (w/v) K.Na tartate, 0.4% (w/v) NaOH, 0.95% (w/v) $NaHCO_3$, dissolved in dH_2O and pH was adjusted to 11.25 with 50% NaOH.

BCA protein assay buffer B

4% (w/v) $CuSO_4$ dissolved in dH_2O.

2.3. Molecular biology

2.3.1. LB plates

LBA was made as detailed above. After autoclaving, medium was swirled gently to distribute melted agar evenly throughout the solution. Medium was allowed to cool to 50°C before addition of a thermolabile antibiotic. The final concentration depended on the type of antibiotic used, ampicilin (100µg/ml), kanamycin (50µg/ml) or geneticin (25µg/ml). Media was mixed by swirling to avoid generating air bubbles. Plates (10cm petri dishes) could then be poured directly from the flask, using about 25ml of liquid per dish. Any air bubbles were removed by flaming the surface of the

medium with a Bunsen burner before the agar had hardened, which normally took about 30 minutes. Once hardened, plates were inverted and stored at 4°C.

2.3.2. Preparation of competent bacteria

E. Coli, strain DH5α was used for all transformation procedures. A sample of DH5α was taken from glycerol stock via stabbing with a sterile pipette tip. This was used to inoculate a 3ml LB culture, which was grown for 16-20 hours at 37°C in a rotary shaker. Next day 1ml was used to inoculate 50ml (1 in 50 dilution) of LB and subsequently incubated for 2-3 hours at 37°C in a rotary shaker. A sample was then removed to a clear plastic cuvette and the O.D. at 600nm was determined using a spectrophotometer. Incubation of the 50ml culture continued until the O.D. was between 0.4 and 0.6 measured against a LB blank. Bacteria were then pelleted at 3000rpm for 10 minutes in a swinging bucket rotor and then resuspended in 10ml (1/5 volume) of ice-cold 50mM $CaCl_2$. Bacterial cells were left for 30 minutes, then pelleted as before at 4°C, then resuspended in 4ml (1/12 volume) of ice cold 50mM $CaCl_2$ and left overnight at 4°C.

Next day glycerol stocks were prepared by adding 160μl of the resuspension to 40μl of glycerol (20% glycerol stock) in a sterile 1.5ml plastic microcentrifuge tube (Eppindorf). This was vortexed briefly to ensure complete mixing and then stored at -80°C until required.

2.3.3. Transformation of competent cells with bacteria

1) 200ul aliquots of competent DH5α were taken from -80°C storage and thawed on ice.

2) Using a sterile pipette tip 50-500ng of plasmid DNA in a volume of 15ul or less was added to each tube and the contents then mixed by swirling gently. Tubes were left on ice for 30 minutes.

3) The tubes were then transferred to a water bath, which had been preheated to 42°C and heat shocked for 60 seconds.

4) Tubes were immediately transferred to ice and allowed to chill for 5 minutes.

5) 1ml of LB was added to each tube. Cultures were incubated for 60 minutes at 37°C in a rotary shaker.

6) 330ul of each culture was transferred to a 100mm plate with LBA containing an appropriate antibiotic. A sterile bent glass rod was used to spread the bacteria.

7) Plates were left at room temperature for 20 minutes or until all the liquid had been absorbed.

8) Plates were inverted and left to incubate at 37°C. Colonies appeared after 12-16 hours.

2.3.4. Preparation of plasmid DNA

This was performed according to the manufacturer's instructions, a brief outline is provided below. For a more detailed explanation of the principal see Qiagen purification handbook (Qiagen, 1999).

1) A single colony was picked from a plate of transformed bacteria and used to inoculate a starter culture of 3ml LB containing appropriate selective antibiotic. This was incubated for 8-9 hours in a rotary shaker at 37°C.

2) The entire starter culture was used to inoculate a 400ml LB culture in a conical flask containing appropriate antibiotics. This was grown at 37°C for 12-16 hours with vigorous shaking.

3) Bacterial cells were harvested by centrifugation at 6000rpm using a Beckman JA-14 rotor for 15 minutes at 4°C.

4) The bacterial pellet was resuspended in buffer P1.

5) 10ml of buffer P2 was added and mixed by inversion 4-6 times then left for 5 minutes at room temperature. This allowed lysis of the bacteria.

6) 10ml of chilled buffer P3 was added and again mixed by inversion and then left on ice for 20 minutes.

7) The sample was then centrifuged at 10000rpm using a Beckman JA-14 rotor for 30 minutes at 4°C. The supernatant containing plasmid DNA was then filtered via pouring through mira-cloth.

8) A Qiagen-tip 500 was then equilibrated by applying 10ml of buffer QBT.

9) Supernatant from step 7 was then poured into the Qiagen tip and allowed to enter the resin by gravity flow.

10) The Qiagen tip was washed with 60ml of buffer QC.

11) DNA was eluted with 15ml of buffer QF.

12) The DNA was precipitated, by adding 10.5ml (0.7 volumes) of room temperature isopropanol to the eluate. This was mixed and centrifuged immediately at 17000 rpm in a Beckman JA-20 rotor for 30 minutes at 4°C. The supernatant was carefully poured off.

13) The DNA pellet was washed with with 5ml of room temperature 70% ethanol and then centrifuged immediately at 17000 rpm in a Beckman JA-20 rotor for 10 minutes at 4°C.

14) The pellet was allowed to air dry for 10 minutes and then re-dissolved in 1ml of sterile distilled water. The quantity of DNA obtained was determined by measuring the absorbance at 260nm.

2.3.5. Quantification of DNA

This was determined by spectrophotometric measurement of the amount of ultraviolet irradiation absorbed by the DNA bases.

In routine DNA measurements the stock DNA was diluted by a factor of 200 in sterile distilled H_2O. The absorbance of this sample at 260nm was determined: one absorbance unit being equal to 50ug/ml of double stranded DNA (Maniatis, second edition). The sample concentration could then be determined using the following formula.

Sample concentration = OD_{260} x dilution factor (200) x 50ug/ml

The purity of the sample was then determined by measuring the absorbance at 280nm, the ratio (OD_{260}/OD_{280}) provided an estimate of purity with a value of 1.8 representing a pure preparation. Typically, DNA samples gave a ratio in the range 1.6-2.0. This was adequate for all the procedures for which their use was required.

Otherwise, the amount of DNA in the sample could be determined using ethidium bromide fluorescent quantitation. Since the amount of fluorescence is equal to the total mass of the DNA, the quantity of DNA in the sample could be estimated by comparing the fluorescent yield of the sample with that of a series of known standards (1Kb ladder DNA markers, Promega).

2.3.6. Digestion of DNA with restriction endonucleases

All DNA restriction endonucleases were obtaind from either Roche Molecular biochemicals or from Promega. One unit of restriction endonuclease activity was capable of completely digesting 1μg of DNA in 60 minutes at the appropriate temperature. Volume activity of the enzymes (units/ul) ranged from 5-40. A typical reaction mixture is outlined below.

1μl of 1ug/ul plasmid DNA.

2μl of restriction enzyme (determined by restriction site to be cut).

2μl 10X buffer (choice determined by enzyme used, according to manufacturers instructions).

15μl of sterile distilled H_2O.

The reaction was then incubated at 37°C in a water bath for 3-24 hours. Most enzymes required an incubation temperature of 37°C unless otherwise stated by the manufacturer.

2.3.7. Electrophoresis of agrose gels

A horizontal slab gel apparatus (Life technologies) was used for electrophoresis of agrose gels. This apparatus was so designed as to allow pouring of the gel directly on the electrophoresis platform.

1) The plastic tray was cleaned with distilled water and placed on the platform, where the open ends were sealed with two plastic wedges. A plastic comb was cleaned and placed in position above the tray.
2) 50ml of 1X TAE buffer was prepared, to which was added 0.5g (1%) of electrophoresis grade agrose in a conical glass pyrex flask. The slurry was heated in a microwave oven until all the agrose had dissolved.
3) The solution was allowed to cool to about 60°C; 2μl of ethidium bromide (10mg/ml) solution was then added to give a final concentration of 0.4μg/ml.
4) All of the agrose solution was poured into the mould to give a gel thickness of about 5mm.

5) The gel was allowed to set completely which took 20-30 minutes, the comb and the plastic wedges were then removed. Enough TAE buffer was then added to cover the gel to a depth of about 1mm (250ml approximately).

6) DNA samples were mixed with a one sixth volume of gel loading buffer. The samples were then carefully loaded into the slots of the submerged gel using a sterile disposable micropipette tip.

7) The lid of the gel tank was then closed and leads attached so that the DNA would migrate towards the anode (red lead). A voltage of 100V was applied across the electrodes.

8) After about 40 minutes when the gel loading buffer dye was about three-quarters of the way down the gel the electic current was turned off and leads removed from the gel tank. DNA bands stained with ethidium bromide could then be veiwed by ultraviolet light, and photographed using an UV transilluminator.

2.3.8. Purification of DNA from agrose gels

DNA bands of interest were located using an UV transilluminator and were excised from the agrose gel with a sterile disposable scalpel blade. Excised gel fragments were transferred to a sterile Eppindorf tube. Recovery and purification of the fragment was achieved by using the QIAquick gel extraction kit, according to the manufacturors instruction, a brief out line of which is provided below.

1) The weight of the gel fragment was determined using a tabletop balance, where 100mg ~ 100μl.

2) 3 Gel volumes of buffer QG were added to the tube. This solubilizes the gel and provides appropriate conditions for binding of DNA fragments to the silica

membrane of the QIAquick columns. This was then incubated at 50°C in a water bath for 10 minutes or until all of the gel-slice had dissolved.

3) 1 Gel volume of isopropanol was added and the solution mixed.
4) A QIAquick spin column was placed in a 2ml collection tube and the sample applied to the top of the column. This was then centrifuged for one minute at 13000rpm in a tabletop microcentrifuge, the DNA absorbes to the silica membrane in high salt while contaminants pass through the column.
5) The flow through was discarded and the column was washed with 0.75ml of buffer and then centrifuged for 1 minute at 13000rpm, to remove salts.
6) The flow through was discarded and the column centrifuged for an additional minute at 13000rpm to remove any residual buffer PE.
7) The flow through was discarded and the column transferred to a sterile 1.5ml microcentrifuge tube. 30-50ul of sterile distilled H_2O was then added and then centrifuged for 1 minute at 13000rpm. The low salt concentration allowed elution of the DNA.

2.3.9. Ligation of DNA fragments

Once plasmid DNA and PCR gel fragments had been digested and purified via the methods described above, the amount of DNA present in the samples was determined by ethidium bromide fluorescent quantitation. Ligation of digested PCR fragments to the digested DNA backbone was achieved using a Fast-link ligation kit (Epicenter).

For ligations of DNA with cohesive ends the following reaction volumes were used:

1.5μl 10X Fast-link ligation buffer

1.5μl 10mM ATP

x μl vector DNA

x μl insert DNA

x μl sterile dH2O to a volume of 14μl

1μl Fast-link DNA ligase

Approximately 0.5μg of vector DNA was used per reaction. A vector to insert ratio of about 2 or 3 to one was typically aimed for, and multiple insert fragments could be used in a given ligation reaction. The reaction mix was left for 10-15 minutes at room temperature and then transformed into competent DH5α bacterial cells.

2.3.10. PCR

All reactions were carried out using Mastercycler gradient (Eppindorf), in 0.2ml PCR test tubes (Eppindorf). The particular conditions used in generating the PCR fragments depended on the gene fragment required (Table 2.1). All reactions had an initial stage where the sample was heated to 98°C for 2 minutes to ensure that the plasmid was completely denatured, and a final extension stage of 72°C for 2 minutes to ensure that all molecules were completely synthesised. The DNA polymerase pfu from the hyperthermophilic archaebacterium *pyrococcus furiosus*, which has both 3'-5' exonuclease proofreading activity and 5'-3' exonuclease activity, was used for the synthesis of DNA strands.

The template DNA was always used at 30ng/μl. All reactions were made up to 50μl in a 0.2ml PCR tube as follows.

(a) 5μl of 10X PCR buffer

(b) 5μl of 10mM dNTPs

(c) 5μl of primer 1 (10pmol/μl)

Table 2.1. The conditions employed in PCR amplification of various cDNA fragments used in ligation reactions.

Gene fragment	Forward Primer	Reverse Primer	Template DNA	DMSO	Melting stage	Annealing stage	Extension stage	Number of cycles
β2-adrenoceptor	(1) β2-AR fwd	(2) β2-AR Rev	β2-AR in pcDNA3	without	95°C/50 seconds	42°C/60 seconds	72°C /70 seconds	20
β2-adrenoceptor (CAM)	(1) β2-AR fwd	(2) β2-AR Rev	(CAM) β2-AR in pcDNA3	without	95°C/50 seconds	42°C/60 seconds	72°C /70 seconds	20
Rluc.1	(3) Rluc fwd	(4) Rluc Rev	pRLCMV	without	95°C/50 seconds	42°C/60 seconds	72°C /50 seconds	20
Pluc	(5) Pluc fwd	(6) Pluc Rev	pGL3-basic vector	without	95°C/50 seconds	42°C/60 seconds	72°C /60 seconds	20
eYFP. 1	(7)eYFP fwd B2	(8) eYFP rev B2	pEYFP	without	95°C/50 seconds	42°C/60 seconds	72°C /50 seconds	20
Rluc. 2	(9) (BRET1+ RF)	(10) (BRET1+RR)	pRLCMV	without	95°C/50 seconds	42°C/60 seconds	72°C /50 seconds	20
eYFP. 2	(11) (BRET1+ EF)	(8) eYFP rev B2	pEYFP	without	95°C/50 seconds	42°C/60 seconds	72°C /50 seconds	20
eYFP. 3	(12) (EYFPTr)	(8) eYFP rev B2	pEYFP	without	95°C/50 seconds	42°C/60 seconds	72°C /60 seconds	20
hDOR-1	(13) DOR-1 fwd	(14) DOR-1 Rev	hDOR-1 in pcDNA 4	without	95°C/50 seconds	56°C/60 seconds	72°C /60 seconds	20
β-arrestin 2	(15) BARR2 FWD	(16) BARR2 REV	Bovine β-arrestin 2 in pcDNA3	added	95°C/60 seconds	56°C/60 seconds	72°C /80 seconds	28
CCR2	(17) CCR2 fwd	(18) CCR2 Rev	hCCR2 in pcDNA3	added	95°C/60 seconds	42°C/60 seconds	72°C /80 seconds	35

Table 2.1.

(d) 5μl of primer 2 (10pmol/μl)

(c) 1μl of template DNA (30ng/μl of plasmid)

(d) 1μl pfu polymerase

(e) 5μl DMSO (optional)

(f) dH_2O (sterile) up to 50μl

2.4. Construction of fusion proteins

Structures and restriction sites used in cloning of all the constructs listed here are shown in Figure 1 (A-K). Any constructs mentioned in succeeding chapters, the construction of which is not detailed below, were made by other colleagues working within the same group as this author. The nucleotide sequence of all fragments generated via PCR amplification were verified to be correct via dideoxy-nucleotide sequencing (Leicester University).

2.4.1. Construction of wild-type and CAM ß$_2$-adrenoceptor/luciferase fusion proteins

Both human wild-type and CAM ß$_2$-adrenoceptor-*Renilla* luciferase fusion proteins were generated. A ß$_2$-adrenoceptor fragment was generated *via* PCR amplification of an existing ß$_2$-adrenoceptor DNA in pcDNA3. Generation of the CAM ß$_2$-adrenoceptor-fragment was also *via* the same PCR amplification of the CAM ß$_2$-adrenoceptor in pcDNA3. The mutations, which comprise the CAM sequence consist of four amino acid substitutions in intracellular loop 3 of the receptor. The primers used were as follows: (1) β2-AR fwd, which incorporates both a 5' *Hind*III cloning site and Kozak sequence. The reverse (2)β2-AR rev which incorporates an *Xho*I cloning site to allow linkage to the *Renilla* luciferase gene. Introducing the *Xho*I site

Figure 2.1. The arrangement of genes coding for various chimeric proteins plus the cloning sites used to facilitate their construction.

Constructs shown are **(A)** β2-AR gene sequence fused to that of *Renilla* luciferase and cloned into pcDNA3, **(B)** the gene sequence for a constitutively active mutant of the β2-AR (β2-AR(CAM)) fused to that of *Renilla* luciferase and cloned into pcDNA3, **(C)** the β2-AR sequence fused to that of enhanced yellow fluorescent protein (eYFP) and cloned into pcDNA3, **(D)** the thyrotropin releasing hormone receptor (TRHr) gene sequence fused to the eYFP gene and cloned into pcDNA3.1+, **(E)** the *Renilla* luciferase gene fused to the gene encoding cYFP cloned into pcDNA3 (IS=intergenic sequence), **(F)** The gene sequence for *Renilla* luciferase fused to that of a variant of green fluorescent protein (GFP_2) and cloned into pGFPN3. **(G)** β-arrestin2 fused to that of cyan NFP and cloned into the vector pAM-Cyan, **(H)** the gene encoding β-arrestin2 fused to that encoding red NFP and cloned into pAS-Red, **(I)** the gene encoding CCR2 fused to the cyan NFP gene sequence and cloned into pAM-cyan, **(J)** the gene sequence for CCR2 fused to that of yellow NFP and cloned into the vector pZS-Yellow, **(K)** the gene sequence for the δ-opioid receptor fused to GFP_2 and cloned into the vector pGFPN2, **(L)** the gene sequence for the β2-AR fused to the firefly luciferase from *Photinus pyralis* and cloned into the vector pcDNA3.

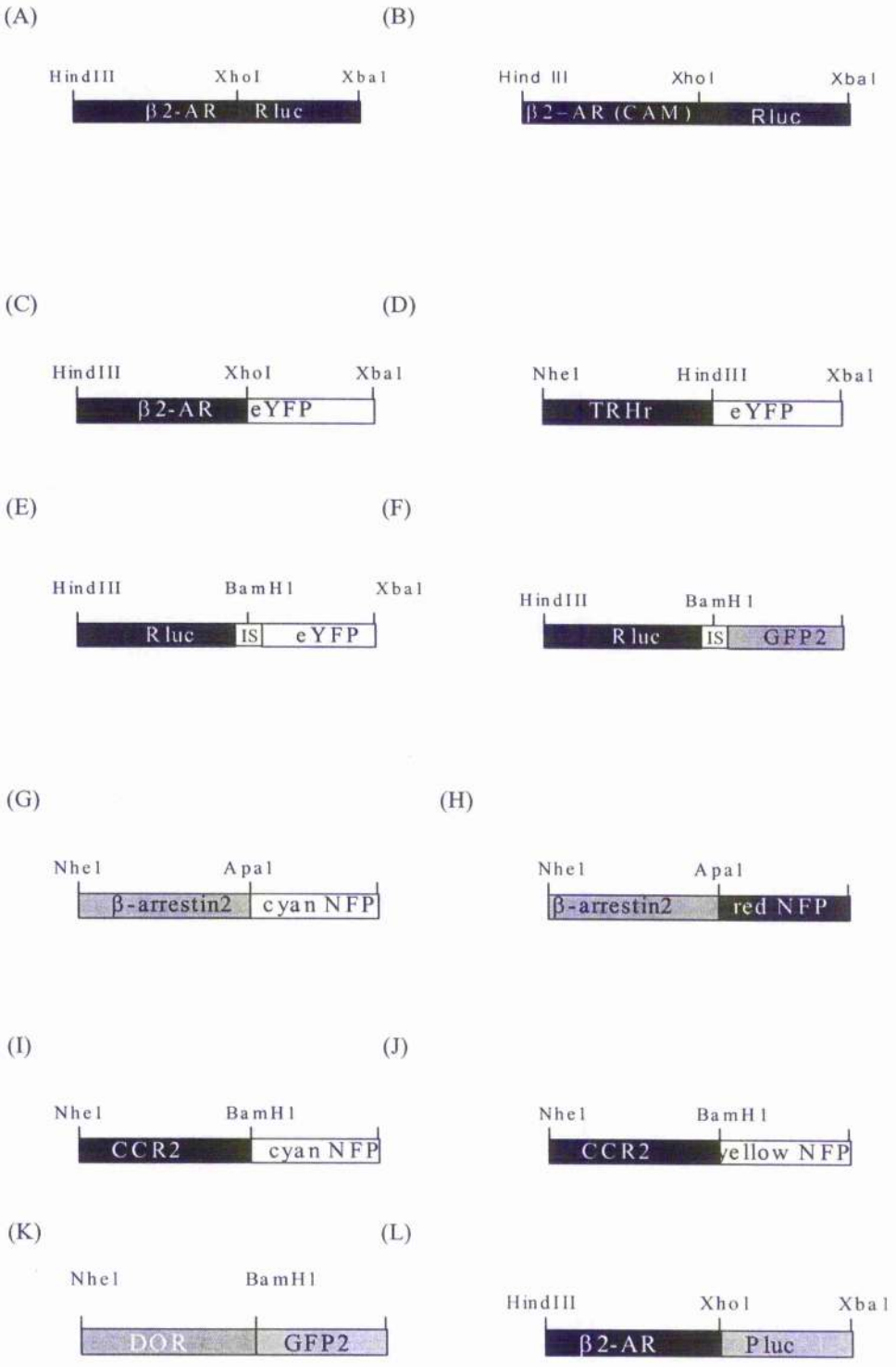
(A)
HindIII
XhoI
XbaI
β2-AR
Rluc
(B)
Hind III
XhoI
XbaI
β2-AR (CAM)
Rluc
(C)
HindIII
XhoI
XbaI
β2-AR
eYFP
(D)
NheI
HindIII
XbaI
TRHr
eYFP
(E)
HindIII
BamHI
XbaI
Rluc
IS
eYFP
(F)
HindIII
BamHI
Rluc
IS
GFP2
(G)
NheI
ApaI
β-arrestin2
cyan NFP
(H)
NheI
ApaI
β-arrestin2
red NFP
(I)
NheI
BamHI
CCR2
cyan NFP
(J)
NheI
BamHI
CCR2
yellow NFP
(K)
NheI
BamHI
DOR
GFP2
(L)
HindIII
XhoI
XbaI
β2-AR
Pluc

Figure 2.1.

results in an insertion of a glutamate residue between the $ß_2$-adrenoceptor DNA and the *Renilla* luciferase. It also resulted in alteration of the last nucleotide in the amino acid coding sequence of $ß_2$-adrenoceptor (G→C). This did not alter the amino acid sequence as the new codon CTC still encodes leucine. *Renilla* luciferase (Rluc.1) was similarly generated *via* PCR amplification of a *Renilla* luciferase DNA cloned into plasmid pRL.CMV (Promega). The primers used for amplification were (3) Rluc fwd, which incorporates an *Xho*I site at the 5' end of the gene to allow linkage to either the $ß_2$-adrenoceptor or the CAM $ß_2$-adrenoceptor fragment. The reverse primer, (4) Rluc rev, incorporates an *Xba*I site into the 3' end of the gene immediately downstream of the stop codon. Following PCR reactions the resultant fragments were digested with the appropriate enzymes and subsequently gel purified. The plasmid pcDNA3 was digested with *Hind*III and *Xba*I to provide a recipient vector for the ligated fragments. Ligations were performed using Fast-link DNA ligation kit (CAMBIO) in which digested pcDNA3, $ß_2$-adrenoceptor (or CAM $ß_2$-adrenoceptor fragment) and *Renilla* luciferase fragments were mixed and ligated together.

2.4.2. Construction of β2-adrenoceptor-eYFP

PCR of the β2-AR gene fragment was achieved as for the β2-AR-Rluc construct. PCR of eYFP (eYFP.1) used forward primer, (7) eYFP fwd B2, which incorporated a *Hind* III site and Kozac sequence, upstream of the gene sequence. The reverse primer, eYFP rev B2, incorporated an *Xba* 1 site immediately downstream of the gene sequence. Digestion and ligation of the fragments into pcDNA3 was performed as above. The β2-adrenoceptor in this construct had a cysteine to glutamate substitution in the last amino acid of the receptor sequence to facilitate cloning.

2.4.3. Construction of TRHr-eYFP

TRHr-eYFP was constructed as follows. TRHr-GFP the construction of which has been described previously (Drmota *et al.*, 1998), was digested with *Hind* III and *Xba* I to excise the GFP fragment. PCR amplification of the eYFP DNA fragment (eYFP.3) was achieved using pEYFP (Clontech) as a template. The primer (12) eYFPTr, included a *Hind* III site immediately upstream of the eYFP gene. The primer (8) eYFP rev B2 was used to place an *Xba*1 site immediately downstream of the stop codon at the end of eYFP.

2.4.4. Construction of $BRET_1$ and $BRET_2$ positive controls

For BRET1+, PCR of *Renilla* luciferase (Rluc.2) used the primer (9) BRET1+RF to incorporate a *Hind* III site and a Kozac sequence upstream of the Rluc gene sequence. The reverse primer (10) BRET1+RR placed part of the intergenic sequence and a *Bam* H1 site downstream of the Rluc coding sequence, also removing the Rluc stop codon to allow in frame ligation with eYFP. PCR of the eYFP gene sequence (eYYP.2) used the forward primer (11) BRET1+EF, which placed a *Bam* H1 site and part of the intergenic sequence upstream of the eYFP gene. The reverse primer (8) eYFP rev B2 was used to place an *Xba* 1 site immediately downstream of the eYFP stop codon.

The PCR fragments thus generated were digested and ligated to form an in frame fusion construct with a 13 codon intergenic sequence (5'-CGG GCC CGG GAT CCG GAT CCC CGG GTA CCG GTC GCC ACC-3') linking the Rluc and eYFP gene sequences. This chimeric protein was cloned into pcDNA 3.

For construction of the BRET2 +, the Rluc fragment from the above construct was excised using *Hind* III and *Bam* H1, the vector $pGFP_2$-N3 was similarly digested. This generated an inframe fusion protein between Rluc and GFP_2 with an 11 codon

intergenic, linking sequence (5'- CGG GCC CGG GAT CCG GAT CCA CCG GTC GCC ACC-3').

2.4.5. Construction of β-arrestin2-cyan NFP and β-arrestin2-Red NFP

PCR of the bovine beta-arrestin2 gene fragment used forward primer (15) BARR2 fwd to introduce an *Nhe*1 site and Kozac sequence immediately upstream of β-arrestin-2 gene sequence. The reverse primer (16) BARR2 Rev was used to introduce an *Apa*1 site immediately downstream of the β-arrestin-2 gene sequence. Primers were also designed to remove the stop codon from C-terminal tail of receptor. The plasmid pAM-Cyan-N1 (Clontech) was digested with the same restriction enzymes. Ligation of plasmid and the PCR fragment resulted in a chimeric protein, with cyan NFP attached to and in frame with the C-terminal tail of β-arrestin-2.

β-arrestin-2 red NFP was made using the above primers for PCR of bovine β-arrestin-2. The fragment was digested and then ligated into similarly digested pAS-Red (Clontech) plasmid vector.

2.4.6. Construction of CCR2-cyan NFP and CCR2-yellow NFP

PCR of the human receptor for MCP-1 (CCR2R) used forward primer (17) CCR2 fwd, which placed an Nhe1 site and Kozac sequence immediately upstream of the CCR2 gene sequence. The reverse primer (18) CCR2 rev, removed the stop codon from the C-terminal tail of the receptor and placed a *Bam* H1 site immediately downstream of the CCR2 gene sequence. The vector pAM-Cyan-N1 was digested using the same restriction enzymes and the CCR2 gene fragment was ligated, immediately upstream of, and in frame with the cyan NFP gene.

CCR2-yellow NFP was constructed using the same CCR2 PCR fragment as above. The fragment was digested and ligated into a similarly digested pZN-Yellow (Clontech) vector.

2.4.7. Construction of δ-opioid-GFP_2

The human δ-opioid receptor in pcDNA4 was used as a template for PCR amplification. The primer, (13) hDOR-1 fwd, was used to incorporate a c-Myc epitope tag, a Kozac sequence and an *Nhe*1 site immediately upstream of the human -δ-opioid receptor.

The reverse primer (14) hDOR-1 rev, incorporated a BamH1 site immediately downstream of the hDOR-1 sequence, also removing the receptor stop codon thus allowing in frame ligation with GFP_2. The plasmid $pGFPN_2$ (Green fluorescent protein, Packard) was digested with *Nhe*1 and *Bam*H1 to allow in frame ligation of the human -δ-opioid receptor with GFP_2.

2.4.8. Construction of β_2-adrenoceptor-Pluc

Construction of the $ß_2$-adrenoceptor fused to the luciferase from the firefly *Photinus pyralis* (Pluc) was achieved as follows. PCR of the $ß_2$-adrenoceptor was achieved as described above for $ß_2$-AR-Rluc. PCR of Pluc utilized the forward primer (5) Pluc fwd which incorporated an *Xho*1 site immediately upstream of the Pluc coding sequence and (6) Pluc rev which incorporated an *Xba*1 site immediately downstream of the Pluc coding sequence. This arrangement of restriction sites allowed direct in frame ligation of the $ß_2$-adrenoceptor with Pluc within the plasmid vector pcDNA3.

2.5. Cell culture

2.5.1. Routine cell culture

For cell growth (maintainance of cells in non-selective media), sterile pipettes and flasks were used for all manipulations, and all tissue culture work was carried out in a sterile flow cabinet. To initiate growth of a specific cell line, cells were brought up from liquid nitrogen storage and the aliquot was thawed rapidly at 37°C. The entire aliquot (1ml) was then added to a 75cm^2 tissue culture flask where 10ml of an appropriate media (Table 2.2), pre-warmed to 37°C in a water bath was added.

Cells were left at 37°C in an incubator overnight to allow cells to attach to the bottom of the flask. Next day, the media was removed and fresh media applied.

Typically cells were grown to a confluency of approximately 80-100% before being subcultured into new flasks.

2.5.2. Cell subculture

Once cells growing in 75cm^2 flasks had approximately reached confluency, they were cubcultured into new flasks. The following procedure was adopted.

Media was completely removed and the cells, while still adhered to the bottom of the flask were washed with 2ml of trypsin solution. This was then removed and a further 2ml of new trypsin was added and the flasks were placed in a 37°C incubator for 2 to 3 minutes. Any cells, which remained adhered, were detached by administering a sharp slap to the side of the flask. Once all the cells had been detached, 8ml of appropriate media containing serum was added to stop the enzymatic action of the trypsin. Cells were then spun at 1000rpm at room temperature in a swinging bucket rotor for 10 minutes to pellet the cells. Media containing the trypsin was then poured off and 1ml of fresh media was added. Cells were gently pipetted up and down to

Table 2.2. Growth media used for sustenance of different mammalian cell types.

Cell type	Media
HEK 293T	DMEM/10%NBCS/1mM L-Glutamine
CHO-K1	DMEM-12/10%FCS/1mM L-Glutamine

Table 2.2.

resuspend and to eliminate any cell clumping. The cells were then diluted as desired for further subculturing into 75cm^2 flasks.

2.5.3. Coating of coverslips and 24 well plates with poly-D-lysine

50mg of poly-D-lysine was dissolved in 50ml of sterile dH_2O (1mg/ml stock solution). Coverslips were prepared by soaking overnight in concentrated hydrochloric acid, washing several times with dH_2O and then autoclaving in a sealed container.

Coverslips were placed into the wells of a six well dish using sterile forceps, working in a flow cabinet. The stock solution of poly-D-lysine was then diluted 1 in 10 in sterile dH_2O and 2ml of this was added to each well containing a coverslip. Plates were then left in the sterile hood at room temperature for 30 minutes. The poly-D-lysine was removed and the wells washed three times with sterile dH_2O to remove any unadhered traces of the poly-D-lysine. The prepared dishes were sealed and allowed to dry overnight before seeding the cells next day. The same coating procedure was used for 24 well dishes, minus coverslips

2.5.4. Transient transfection

Cells were grown in an appropriately sized dish and allowed to reach approximately 90% confluency. All transfections on HEK 293T and CHO-K1 cells used lipofectamine. The amounts of DNA and lipofectamine used, was largly dependent on the dish size and the experimental requirements (see Table 2.3).

The DNA was first dissolved in optimem. A quantity of lipofectamine was also dissolved in an equal volume of optimem. These were combined and allowed to incubate for 30 minutes, before being made up to a final volume in optimem.

Table 2.3. Different transfection conditions employed corresponding to dish size used in transfection procedure.

	DNA (μg)	Lipofectamine (μl)	Incubation time	Final volume
10cm Dish	7-12μg in 500μl optimem	25μl in 500μl of optimem	30 minutes	5.0ml
6cm Dish	3-10μg in 250μl optimem	12.5μl in 250μl of optimem	30 minutes	2.5ml
6 well plate +/- coverslip	0.5-2μg in 100μl of optimem	8μl in 100μl of optimem	30 minutes	1.0ml

Table 2.3.

Cells to be transfected had growth media removed and an appropriate volume of optimem was added to the dish. The dish was gently swirled and the optimem was pipetted off, removing any traces of serum which tends to inhibit the action of the lipofectamine. The DNA/lipofectamine/optimem mixture was then added to the nearly confluent monolayer of cells and returned to the 37°C incubator for 4-7 hours. At the close of this period, an equal volume of growth medium containing 20% NBCS was added onto the transfection medium. The cells were then returned to the incubator for 18-20 hours, before the medium was replaced with growth medium containing 10%NBCS. The cells were then allowed a further 24 hours of growth before harvesting for assays. Cells growing on coverslips were transfected as for a normal 6 well dish transfection.

2.5.5. Generation and maintainance of β2-AR(CAM)-Rluc stable cell line

The following procedure was adopted.

(1) Naïve HEK 293 cells were split into three 10cm dishes and grown to approximately 50% confluency.

(2) The dishes were then transfected with 5ug DNA of either β2-AR(CAM)-Rluc or pcDNA3 (positive control), using DOTAP (Roche) transfection reagent. A third dish was left untransfected as a negative control. DNA was added to 40ul of DOTAP reagent along with 200ul of HBS buffer. This was left at room temperature for 10-15 minutes before being added dropwise to the dish containing cells in ordinary growth medium.

(3) Cells were left for 2-3 days until they had almost reached 100% confluency.

(4) Cells were then subcultured into duplicate 10cm^2 dishes by splitting the cells 1→ 10 in fresh growth medium, containing geneticin at a concentration of 1mg/ml.

(5) The cells were then maintained in these dishes for two to three weeks by renewing the selective medium every two to three days.

(6) After three weeks had passed, and all the cells in the untransfected dishes had died, individual antibiotic resistant colonies could be seen growing in the pcDNA3 and β2-AR(CAM)-Rluc transfected dishes. Colonies were removed from the β2-AR(CAM)-Rluc dishes by carefully sucking up the colony using a sterile pipette tip. About 40 colonies were selected and transferred to individual wells of 24 well tissue culture plates.

(7) Clones growing in 24 well dishes were then allowed to reach confluency before being subcultured into 6 well dishes and then into 75cm^2 flasks. Clones were maintained in selective medium.

(8) Clones were then screened for expression of the β2-AR(CAM)-Rluc chimeric construct, via the luciferase assay. Once clones producing readily detectable levels of luciferase activity had been identified a single clone was selected for further analysis.

2.5.6. Preservation of cell lines

Aliquots of both stably transfected and naïve cells were routinely frozen down to maintain stocks of frozen cells.

Cells were grown to approximately 70% confluency and then trypsinized and pelleted in the manner described for media subculture. Cells were then resuspended in 1ml of freezing solution and pipetted up and down in order to ensure a homogeneous

suspension of cells. The entire aliquot was then transferred to a cryo-vial and placed at -20°C for 1-2 hours until the aliquot was frozen. This was then transferred to a -80°C freezer and left overnight. Next day the aliquots were quickly transferred to dry ice and then stored in liquid nitrogen until required.

2.5.7.Cell harvesting

(1) The medium was removed from transfected dishes. 5ml of PBS was gently applied to wash away any remaining medium. This wash process was then repeated twice. Cells were kept on ice throughout all stages of the harvesting procedure.

(2) If cells were required for the BRET assay, a final volume of 5ml of PBS was added to a 10cm dish (2.5ml if using a 6cm dish). The cells were then gently resuspended using a 1ml Gilson pipette. The number of cells per 1ml of the suspension could then be determined using a haemocytometer and diluted if necessary.

(3) Otherwise, the cells were required for a membrane preparation and were pelleted at 3000rpm in a swinging bucket rotor at 4°C. The supernatant was discarded and the cell pellets were transferred to an -80°C freezer where they could be stored until required.

2.5.8. Counting cells using haemocytometer

Cell samples to be counted were diluted 1 in 20 in PBS. The cytometer and coverslip were then cleaned with ethanol and dH_2O and the coverslip put in place. Using a Gilson pipette, a small amount of the sample containing the cells was then applied to the chamber, which had a depth of 0.1mm. Using a light microscope the cells could

then be counted on the grid. The area of each grid is $1mm^2$ and therefore the volume is $0.1mm^3$.

The number of cells in $1cm^3$=N X 20(dilution factor) X 10^4

N= number of cells in $0.1mm^3$

The number of cells under 4 grids was counted and an average value was taken in each case to determine the number of cells per 1ml.

2.6. Biochemical assays and other methods of analysis

2.6.1. FACS analysis of HEK 293T cells for eYFP expression

Cells harvested and resuspended in PBS as described above were subject to FACS with machine settings optimised for HEK 293T cells expressing GFP protein from *Aequoria victoria*. The overlap between absorbance spectra for GFP and eYFP was sufficient for these settings to be adapted to the detection of eYFP. FACS readings were taken for both HEK 293T cells expressing eYFP and for untransfected HEK 293T cells. Dot plots showing forward scatter and side scatter of light were obtained and from this a population of cells were selected (gated) for fluorescence analysis. Histograms of the same cells plotting fluorescence intensity against number of events was also obtained, from which, using the untransfected sample, background fluorescence was defined. It was then possible to determine the mean fluorescence of cells in a given population for the remaining transfected samples.

2.6.2. BCA protein quantification assay

A standard curve of protein extracts made through the serial dilution of a stock solution containing bovine serum albumin (BSA) was established. 10μl of each concentration point were then applied to duplicate wells in a clear 96 well plate.

Similarly for the test samples, serial dilutions in dH_2O were established and 10μl were applied to duplicate wells of the same 96 well plate. To prepare the BCA working solution, 49 parts of BCA protein assay buffer A were combined with 1 part of BCA protein assay buffer B and then mixed. 200μl of this working solution was then applied to each of the wells containing protein samples and then the plate was left to incubate for 30 minutes at 37°C. After this period had elapsed the plate was removed to a spectrophotometer where the absorbance of the samples at 492nm was determined. The protein concentration of the unknown samples could then be determined through constuction of a calibration graph using the known BSA standards.

2.6.3. Radioligand binding

Cells were grown in 10 cm dishes. Following a 48 hour period post transfection cells were washed three times with ice-cold phosphate-buffered saline (PBS). Cells were then detached from plates with PBS/0.5 mM EDTA, pelleted and resuspended in ice-cold TE buffer (10 mM Tris HCl, 0.1 mM EDTA pH 7.5) and lysed with 2x10 second bursts of a polytron. The homogenate was centrifuged at 500xg to remove unbroken cells and nuclei. The supernatant fraction was then centrifuged at 48,000xg for 30 min and the pellet resuspended in TE buffer and stored at -80°C until use. Serial dilutions of the membrane samples were evaluated for their protein content using the BCA protein assay described above.

Specific binding at the kappa-opioid receptor was determined using the following conditions; [^{3}H]-Diprenorphine (5nM) was incubated with membrane preps expressing the kappa-opioid receptor at 30°C for 60 minutes in T.E. (50mM Tris, 5mM EDTA, pH 7.4) buffer. Naloxone at a concentration of 300μM was used to

determine non-specific binding. For the delta-opioid receptor, [^{3}H]-Naltrindole (5nM) was incubated with membrane preps expressing the delta-opioid receptor at 30°C for 60 minutes in T.E. (50mM Tris, 5mM EDTA, pH 7.4) buffer. Naloxone at a concentration of 300μM was used to determine non-specific binding. Specific binding at the β_2-adrenoceptor, was determined by incubating [^{3}H]-Dihydroalprenolol (2nM) with membrane preps expressing the β_2-adrenoceptor at 30°C for 60 minutes in T.E.M. (75mM Tris, 1mM EDTA, 12mM, $MgCl_2$, pH 7.4) buffer. Propranolol at a concentration of 10μM was used to determine non-specific binding.

All assays used triplicate tubes to obtain average d.p.m readings for each assay point. Counts on the scintillation counter in d.p.m., could be converted to molar concentrations of radioligand using the following formula.

$RL^* = 10^{-9} \times B/(V \times SA \times 2220)M$

Where B is the amount of bound ligand in d.p.m., V is the sample volume, used in the assay, and SA is the specific activity of the radioligand used.

In some instances, varying concentrations of compound were used to compete for binding with the tritiated radioligand, in order to determine the K_i of that particular compound at the receptor binding site. In this case the following formula was used in the determination of K_i.

$K_i = IC_{50}/(1+[L]/K_L)$

Where IC_{50} is the concentration of competitor which reduces the specific binding by 50%, [L] is the concentration of radioligand and K_L is the dissociation equilibrium constant of the radioligand (Haylett, 1996).

For the β2-AR, in some instances, filtration radioligand binding was performed using intact cells. In this case the cells were harvested in extracellular buffer and then counted using a heamocytometer. Approximately 400,000 cells were then applied to

each assay point using extracellular buffer as the assay medium. Specific binding was determined using [^{3}H]-Dihydroalprenolol (2nM) which was capable of permeating the cell membrane. Non-specific binding was determined using the antagonist propranolol (10μM). Replicates were incubated at 30°C for one hour. The d.p.m. per fmol for [^{3}H]-dihydroalprenolol was determined from the corresponding molarity of the standards. The number of fmol present for each cell sample and subsequently the number of receptors/cell were determined using the following formulae:

fmol= (specific d.p.m.)/d.p.m./fmol

fmol/cell= fmol/Number of cells

moles/cell= (fmols/cell)/10^{15}

receptors/cell= (moles/cell) x $6x10^{23}$

2.6.4. Adenylyl cyclase assay

Was performed essentially as described by (Wong, 1994)

(1) Cells were grown to 80% confluency in 24 well plates, to which was added 1uCi/ml of [^{3}H]-adenine. Cells were then incubated for 16-20 hours.

(2) Extacellular [^{3}H]-adenine was washed off with 1ml of adenylyl cyclase assay media, without detaching the cells.

(3) To each well was added 0.5ml of adenylyl cyclase assay medium containing test reagents. This was then incubated for 30 minutes at 37°C.

(4) The reaction was terminated by aspiration and addition of 1ml of ice cold stop solution to each well and incubated for 30 minutes at 4°C. Entire extract was then removed without disturbing the cells.

(5) Dowex columns were washed with 2ml of 1M HCl followed by 10ml of H_2O. The entire 0.5ml of TCA extract was applied to the Dowex column. This was

allowed to drain through the column and was collected in 25ml scintillation vials.

(6) A further 3ml of H_2O was applied to the column and eluate was collected in the same scintillation vial. This eluate contained the [^{3}H]-ADP and [^{3}H]-ATP. 9ml of scintillation fluid was added to the vial and then assayed on a scintillation counter to determine radioactivity (d.p.m).

(7) Alumina columns were washed with 10ml of 1M imidazole (pH 5.0) before use. Dowex columns were then placed over an equal number of the alumina columns. 10ml of H_2O was then applied to the columns and allowed to drip directly onto the alumina.

(8) [^{3}H]-cAMP was eluted from the alumina columns with 6ml of 0.1M imidazole (pH 7.5) and collected in a 25ml scintillation tube. 12.5ml of scintillation fluid was added to each vial and transferred to a counter.

(9) Results were expressed as the ratio of [^{3}H-]cAMP to total [^{3}H]-adenine nucleotides, i.e. [^{3}H]-cAMP / [^{3}H]-ATP + [^{3}H]-ADP + [^{3}H]-cAMP.

2.6.5. Correlation of receptor number with fluorescence for δ-opioid-GFP$_2$

Membrane preparations were first serially diluted in T.E. buffer. An arbitrary fluorescence value for 100µl of each concentration point was then determined using a Victor^2 (Wallac) multi-label counter. An equivalent concentration of membranes from untransfected HEK 293T cells was assayed for each point, to determine background fluorescence. Excitation of GFP$_2$ was at 405 nm, emission from the GFP was determined using a 500nm cutoff filter. The same membrane concentrations were then used to determine the receptor number (fmol) for each concentration point using radioligand binding (as detailed above), the two values were then correlated to

determine fmol/100µl. In routine $BRET_2$ experiments cells were counted using a haemocytometer and approximately 700,000 cells in a 100µl volume were seeded per well and untransfected cells were used to determine background fluorescence. It was therefore possible by use of Avagadro's number to estimate the number of acceptor tagged receptors/cell in each sample.

2.6.6. Correlation of receptor number with fluorescence for κ-opioid-eYFP

Membranes were prepared and receptor number was correlated with arbitrary fluorescence in the manner described for the delta-opioid-GFP_2 construct above with the following exceptions: excitation wavelength filter 485nm, emission wavelength filter 535nM.

2.6.7. Correlation of receptor number with luminescence

Membrane preps of HEK293T cells expressing β_2-AR-Rluc were serially diluted in PBS. To determine the luminescence in counts per second (C.P.S.), 1.5ml of diluted membranes were assayed in a Spex fluorolog spectrofluorimeter with the excitation lamp turned off (slit width=10nm, 2 seconds/increment) following addition of an equal volume of PBS containing 10µM coelenterazine (Prolume). An average value of the peak region centred at 480nm was determined for each of the concentration points. Similarly diluted membranes from the same preparation were assayed for specific binding of [^{3}H]-Dihydroalprenolol to determine receptor concentration (fmol), these two values were then correlated. Since approximately 3000000 cells (counted with a haemocytometer) were added during routine BRET experiments, it was possible to estimate the number of donor tagged receptors present by use of Avogadro's number.

2.6.8. Correlation of mean fluorescence (FACS) with acceptor concentration

In routine BRET experiments, transfected cells were analysed using a fluorescence activated cell sorter (FACS) to determine the mean fluorescence per cell (mean of 10,000 cells) of the transfected sample. This value was taken to represent the acceptor concentration. This method of counting cells was favoured over the use of a haemocytometer as being almost certainly a more accurate means of quantification and would therefore make results from different experiments more directly comparable.

To convert the mean fluorescence values on the FACS into concentration of receptors/cell, the following method was adopted. Cells expressing different levels of kappa-opioid-eYFP tagged receptor were grown to the same level of confluency in 6cm dishes. The number of cells per 100µl was then estimated using a haemocytometer and determined to be approximately 200,000 cells/100ul. The arbitrary fluorescence of a 100µl sample was then measured using the Victor^2 multi-label counter. These values could be converted to fmol, using the graph shown in Figure 3.17a which could then be further converted to receptors/cell using the following formula.

Recetors/cell= (Nmol x A)/200,000

Where Nmol is the number of moles as determined from the graph in figure 3.17a and A, is Avogadro's number.

The mean fluorescence was determined using FACS for the same cells as above. Mean fluorescence (FACS) could then be directly correlated with an approximation of receptor number.

2.6.9. BRET

Cells were harvested 48 h after transfection. Medium was removed from cell culture dishes and cells were washed twice with PBS before being detached to form a suspension. In samples where a time course addition of drug was required, cells were incubated at 37°C in PBS supplemented with 0.1% glucose and an appropriate volume was removed from the cell suspension at the indicated time intervals. Approximately 3,000,000 cells in 1.5 ml of PBS buffer were then added to a glass cuvette; an equal volume of PBS containing 10μM coelenterazine was added and the contents of the cuvette mixed. The emission spectrum (400-600nm) was immediately acquired using a Spex fluorolog spectrofluorimeter with the excitation lamp turned off (slit width=10nm, 2 seconds/increment). For comparisons between experiments, emission spectra were normalized with the peak emission from *Renilla* luciferase in the region of 480nm being defined as an intensity of 1.00. Energy transfer signal was calculated by measuring the area under the curve between 500nm and 550nm. Background was taken as the area of this region of the spectrum when examining emission from the isolated *Renilla* luciferase. The energy transfer signal was then expressed as a percentage above the background using the formula:

$((E_{AD}-E_D)/E_D)x100)$

Where E_D is the integrated emission spectrum between 500nm and 550nm for the isolated *Renilla* luciferase expressed alone and E_{AD} is the integrated emission spectrum between 500nm and 550nm for an Rluc-receptor construct expressed in the presence of an eYFP-receptor construct.

In some instances the victor^2 multilabel counter was used in determining energy transfer in BRET experiment, using a white-walled, culturplate (Packard). Cells resuspended in PBS were dispensed into wells of a 96-well plate, to a final volume of

90μl, to which was added either a further 10μl of PBS or 10μl of PBS containing a test compound at a suitable concentration. The Victor^2 was set up with 2 emission filters, capable of capturing light emitted from *Renilla* luciferase (using a 450nm bandpass 80nm filter) and from eYFP (using 500nm cutoff filter). A ten-minute incubation period was provided for the compound before addition of 100μl of coelenterazine (10μM). The intensity of light emitted by both *Renilla* luciferase and eYFP was then immediately determined using the Victor^2, by alternating between each filter, with 1 second well reading times. The amount of energy transfer was then expressed as a ratio of the value of light intensity emitted from eYFP compared to that of *Renilla* luciferase (light emitted 450nm/light emitted 500nm).

2.6.10. BRET$_2$

Cells were washed three times in PBS and then harvested in PBS supplemented with magnesium (0.1g/L) and glucose (1g/L). Cells were then counted on a haemocytometer and approximately 700,000 cells were dispensed/well into a 96 well, white-walled, culturplate (Packard). DeepBlueC (Packard) reagent was prepared as in accordance with the manufacturer's directions. Any compounds to be tested were dissolved in the same buffer as that used for the resuspension of the cells and then dispensed into the appropriate wells of a 96 well plate, to achieve a final concentration of 10µM. The plate was then left standing for 15 minutes at room temperature to allow time for the ligands to come to equilibrium with the expressed receptors. DeepBlueC was then added to a final concentration of 10µM before being assayed immediately either on a Victor^2 (wallac) or a Fusion universal microplate analyser (Packard), using 410nm (bandpass 80nm) to measure light emitted from DeepBlueC and a 515nm (bandpass 30nm) filter to measure light emitted from GFP$_2$.

The extent of energy transfer was defined as the ratio of light intensity (515nm)/light intensity (410nm) with the ratio obtained from cells expressing *Renilla* luciferase alone defined as zero energy transfer.

2.6.11. Confocal Laser Scanning Microscopy

Cells were observed using a laser scanning confocal microscope (Zeiss Axiovert 100) using a Zeiss Plan-Apo 63 × 1.40 NA oil immersion objective, pinhole of 25, and variable electronic zoom. The eYFP or GFP_2 was exited using a 488 nm argon/krypton laser and detected with 515-540 nm band pass filter. Excitation of cyan NFP was achieved using an argon laser (450nm), excitation of red NFP was achieved using a krypton laser (568nm). The images were manipulated with MetaMorph software.

Live cells were used in all experiments; cells were grown on glass coverslips and mounted on the imaging chamber. Cells were immersed in extracellular buffer, and temperature was maintained at 37 °C.

2.6.12. Luciferase activity assay

A stably transfected cell line of HEK 293 cells expressing the CAM β2-adrenoceptor C-terminally tagged with *Renilla* luciferase was used to seed 96 well microtiter plates to a volume of 90μl/well. The 96 well plates were then incubated overnight and on the following day, the cells were usually about 80% confluent. Compound additions were then prepared in phenol red free medium and 10μl from each of 10 stock solutions, of different concentrations, were added to the wells of the 96 well plates and then incubated for 24 hours. After this period had elapsed, the medium was pipetted off from each well.

50μl of phenol red free medium was then added to each well, plus 50μl of LucLite luciferase assay solution (Packard). Fifty microlitres of 15μM coelenterazine in phenol red free medium was then added to produce a final concentration of 5μM. The plates were then assayed immediately using a topcount luminometer (Packard) using two second well readings, to determine the light intensity in relative light units.

2.6.13. Dual luciferase assay

40μl of a sample of known protein concentration was added to the wells of a 96 well white plastic plate (Packard). Luciferase assay reagent II (LARII) and stop and glow reagent were prepared as according to the manufacturer's instructions.

100ul of LAR II reagent was added to the sample to be assayed in 96 well plates and this was assayed immediately on a topcount luminometer, using 2 second reading times to determine light intensity from Photinus luciferase in counts per second. The reaction was then quenched by addition of stop and glow reagent. This was then assayed similarly in the topcount and the light intensity from *Renilla* luciferase determined in counts per second.

CHAPTER 3

First results chapter

3.1. Introduction

3.1.1 Dimerization of GPCRs

Historically, models that depict the interaction between GPCRs and their respective G-proteins have assumed that the receptor units were monomeric and that they would couple to G-protein with a 1:1 ratio of interaction. Recent advances have provided compelling evidence that such models will soon have to be adjusted to take account of both interactions between identical receptor units (homomers) and between distinct receptor units (heteromers). Although in this chapter such interactions will be referred to as being dimeric, it is possible that the receptor complexes may comprise multiple subunits. However, since existing techniques are not capable of distinguishing between dimers and higher order oligomers and to simplify the discussion of these interactions, only the dimer scenario will be considered. Dimerization of GPCRs has been investigated using predominantly three different types of technique.

(1) Co-immunoprecipitation studies, where co-expressed receptors are precipitated with an antibody directed against one receptor type and then detected using SDS-PAGE with a separate antibody directed against the other expressed receptor type. This biochemical technique has been used to detect dimerization between members of both closely and more distantly related families of GPCRs.

(2) Functional complementation techniques as exemplified by Maggio *et al.*, 1993. Here chimeric receptors between elements of the α_{2c}-adrenoceptor and the M3 muscarinic acetylcholine receptor were generated via exchange of

TMs VI and VII, [α_{2c}(TM I-V)-M_3(TMVI-VII) and M_3(TMI-V)- α_{2c}(TMVI-VII)]. Both these chimeric constructs were incapable of binding selective ligands when expressed singly in mammalian cells whereas co-expression of the two mutated constructs resulted in a restoration of ligand binding and signalling properties. These results imply that the two receptors can interact.

(3) Most recently, biophysical techniques have been employed which generally rely on resonance energy transfer between closely associated, modified receptor molecules.

3.1.2 Bioluminescence resonance energy transfer (BRET)

In order to investigate dimerization of G-protein coupled receptors, one such biophysical approach for detecting the close proximity of two protein molecules was adopted, namely bioluminescence resonance energy transfer (BRET). This is a naturally occurring phenomenon similar to fluorescence resonance energy transfer (FRET). Bioluminescent coelenterates from the classes *Anthozoa* and *Hydrozoa* can produce green light via the intracellular oxidation of a coelenterate type luciferin, known as coelenterazine (Ward and Cormier, 1978). In *Anthozoans*, calcium initiates release of luciferin from a specific binding protein; the luciferin is then converted via molecular oxygen to oxyluciferin producing carbon dioxide in the presence of the enzyme luciferase.

Light emitted from Anthozoans is green, whereas, *in vitro* reactions involving the purified form of the luciferase produces blue light. The green fluorescence in *Renilla sp.* is due to energy transfer to a fluorescent protein (GFP), which is often carried along during purification of *Renilla* luciferase from whole organisms (Cormier *et al.*, 1974). Energy transfer in *Renilla* bioluminescence is a radiationless process such as

that described by Förster (Förster, 1966): energy from the electronic excited state of the oxycoelenterazine mono-anion is transferred to the fluorescent protein, resulting in green light emission (Figure 3.1). Electronic excitation, such as that generated by the oxyluciferin mono-anion can be efficiently transferred to a suitable energy acceptor (i.e. GFP) over distances as large as 70Å, in which case the oxyluciferin monoanion is said to be acting as a donor.

Several preconditions have to be met before such Förster type energy transfer events can occur. Firstly, there must be significant overlap between the donor emission and the acceptor absorbance spectra. The donor is raised to an excited state either by absorption of a photon (FRET) or via a chemical reaction (BRET), which induces a dipole upon it. If an acceptor is in close proximity, an oppositely charged dipole is induced, and it is consequently raised to an excited electronic state. These dipole-induced-dipole interactions fall off inversely with the sixth power of distance (Figure 3.2.). Such energy transfer is an all or none event: all of the energy must be transferred and this can only occur when the energy levels (i.e. spectra) overlap. FRET (or BRET) manifests itself as a decrease in donor fluorescence, called quenching and an increase in acceptor fluorescence.

The presence of acceptor also results in a decrease in the excited state lifetime of the donor molecule. In FRET, this lifetime is normally equilibrated between the rate at which the fluorophore is being driven towards the excited state via the intensity of the incident light upon it and the sum of the rates deactivating this state (i.e. fluorescence and non-radiative processes such as intersystem crossing and internal conversion). The presence of acceptor adds a new non-radiative process to the system, hence decreasing the excited state lifetime of the donor fluorophore (Alberty and Silby, 1997).

The FRET technique has been extensively developed over the past fifty years by a number of groups, (e.g. Baird and Holowka 1988; Cardullo et al., 1988; Fung and Stryer, 1978; Koppel et al., 1979; Kleinfeld, 1988). This discussion and the following formalisms are based on this preceeding work. The efficiency of energy transfer is, according to Försters theory, given by:

1) $F=R^{-6}/(R^{-6}+R_o^{-6})$

Where R is the distance between the centers of the donor and acceptor fluorophores. R_o is the distance at which energy transfer is 50% efficient.

The rate of energy transfer between any isolated donor-acceptor pair is given by:

2) $k_t= (1/\tau_o)(R_o/R)^6$

Where τ_o is the excited state lifetime of the donor in the absence of acceptor.

Here R_o is given by:

3) $R_o=(J\kappa^2 Q_o \eta^{-4})^{1/6} x 9.76 x 10^3$

Where J is the overlap between the donor emission and acceptor absorption spectra, η is the refraction index of the media between donor and acceptor flurophores, κ^2 is the dipole-dipole orientation factor and Q_o is the quantum yield of the donor in the absence of acceptor.

3.1.3 Use of BRET to detect protein-protein interactions in living cells

A modified version of the naturally occurring BRET system was chosen to investigate both homo-dimerization and hetero-dimerization between G-protein coupled receptor (GPCR) molecules. This system involves using *Renilla* luciferase (Rluc) catalysed oxidation of coelenterazine as a donor molecule and an enhanced yellow fluorescent protein (eYFP) as an energy acceptor. The eYFP is a red shifted mutant variant of the

GFP from the hydrozoan coelenterate, *Aequorea victoria*. This system has been successfully used to investigate interactions between circadian clock proteins from cyano-bacteria (Xu *et al.*, 1999). In their study, the cDNA for *Renilla* luciferase was fused in frame with the cDNA for the KiaB circadian clock protein, and similarly the gene coding eYFP was fused, in frame with the cDNA for either KiaB or KiaA circadian clock proteins. Co-expression of the Kia-B/Rluc and the KiaB-eYFP fusion proteins in *E. coli* cells led to a change in the emission spectrum of light upon addition of colenterazine, compared to the emission spectrum of light emitted from cells expressing KiaB/Rluc fusion protein alone. The alteration in the light emission spectrum was due to energy transfer between the donor and acceptor tagged pairs of molecules. No spectral shift was observed in bacterial cells co-expressing the KiaA-eYFP and the KiaB-Rluc constructs. Thus they were able to detect specific interactions between molecules by monitoring changes in the light emission spectrum due to energy transfer.

Particularly attractive features of this system are that the interactions can be monitored between proteins being expressed in living cells. The assay procedure avoids rupture of the cells because coelenterazine is a hydrophobic molecule that can readily permeate both eukaryotic and prokaryotic cell membranes/walls. BRET also avoids external manipulations and treatments with certain crosslinking reagents that are often necessary in co-immunoprecipitation based studies. There is also very little chance of the enzyme *Renilla* luciferase and eYFP having a natural affinity for one another since these two proteins are derived from different biological organisms: eYFP is a modified form of the GFP found in the hydrozoan coelenterate *Aequorea Victoria*. This GFP does not interact directly with the *Renilla* luciferase but with a

photo-protein called aequorin, which becomes activated on binding to calcium (Cormier *et al.*, 1974).

Further, since the system relies on a chemoluminescent reaction there is no need for light excitation of the donor. This has a number of advantages. There will be no photobleaching of the donor, which occurs in FRET systems when the fluorescent donor is exposed to repeated excitation with light of a suitable wavelength. Also, there will be no indirect excitation of the acceptor molecule with the external light source, which can often occur if there is only a poor separation between the absorbance spectra of the donor and acceptor pair.

The spectral overlap between coelenterazine and eYFP is similar to the spectral overlap between the *Aquorea victoria* mutant fluorescent proteins eYFP and enhanced cyan fluorescent protein. This donor and acceptor pairing has an R^0 value of approximately 50Å (Mahajan, 1998). We would therefore expect a significant degree of energy transfer between these two molecules provided they were separated by no greater a distance than 50Å.

Adoption of this BRET strategy would provide a useful method for investigating dimerization of GPCRs in living cells. Of particular interest was whether addition of agonist or antagonist ligands would alter the extent of dimerization in GPCRs. If so, addition of a pharmacological compound might then be expected to result in an increase or decrease in the amount of energy transfer measured. If such alterations in dimerization could be detected using BRET it is reasonable to assume that this might form the basis of a fast and effective screening assay for these pharmacological compounds. Such an assay would be of considerable interest to the pharmaceutical industry. Figure 3.3 demonstrates how such an assay might work in principle, considering three possible outcomes of adding a compound which has binding affinity

at that receptor type. If addition of agonist produces a conformational change which favours the active (R*) form of the receptor (Figure 3.3A) and consequently drives the receptors towards dimerization, this will cause an increase in the energy transfer signal. Alternatively, the receptors may have a high affinity for each other in the absence of bound ligand and are already associated with each other at the plasma membrane (Figure 3.3B). Addition of agonist might not affect this mutual affinity and the amount of energy transfer would remain the same. In a third scenario (Figure 3.3C), again, the receptors have high affinity for each other and are already associated at the plasma membrane. Addition of agonist favours the R* form of the receptor which has a destabilizing effect on the dimer complex. Receptors then dissociate into monomers with a concomitant loss of energy transfer.

If addition of pharmacological ligands was found to produce no alteration in energy transfer signals detected, BRET based detection of dimerization would not provide us with a method of screening for pharmacological compounds. However it would still further our understanding of how GPCRs are associated in living cells.

3.2 Results

The well-characterized β2-adrenoceptor (β2-AR) was chosen as a starting point in this investigation. Chimeric constructs with the β2-AR fused to either *Renilla* luciferase or to eYFP were made as described in section 2.4.1 and 2.4.2. To ensure that the fusion of these proteins to the carboxyl-terminal end of the receptor did not abolish the interaction of pharmacological compounds with the ligand binding site, radioligand binding using a single concentration of [^{3}H]-dihydroalprenolol was performed on membrane preparations of HEK 293T cells, transiently transfected with the modified constructs.

Figure 3.1. The pathway to both blue and green light emission in *Renilla reniformis*.

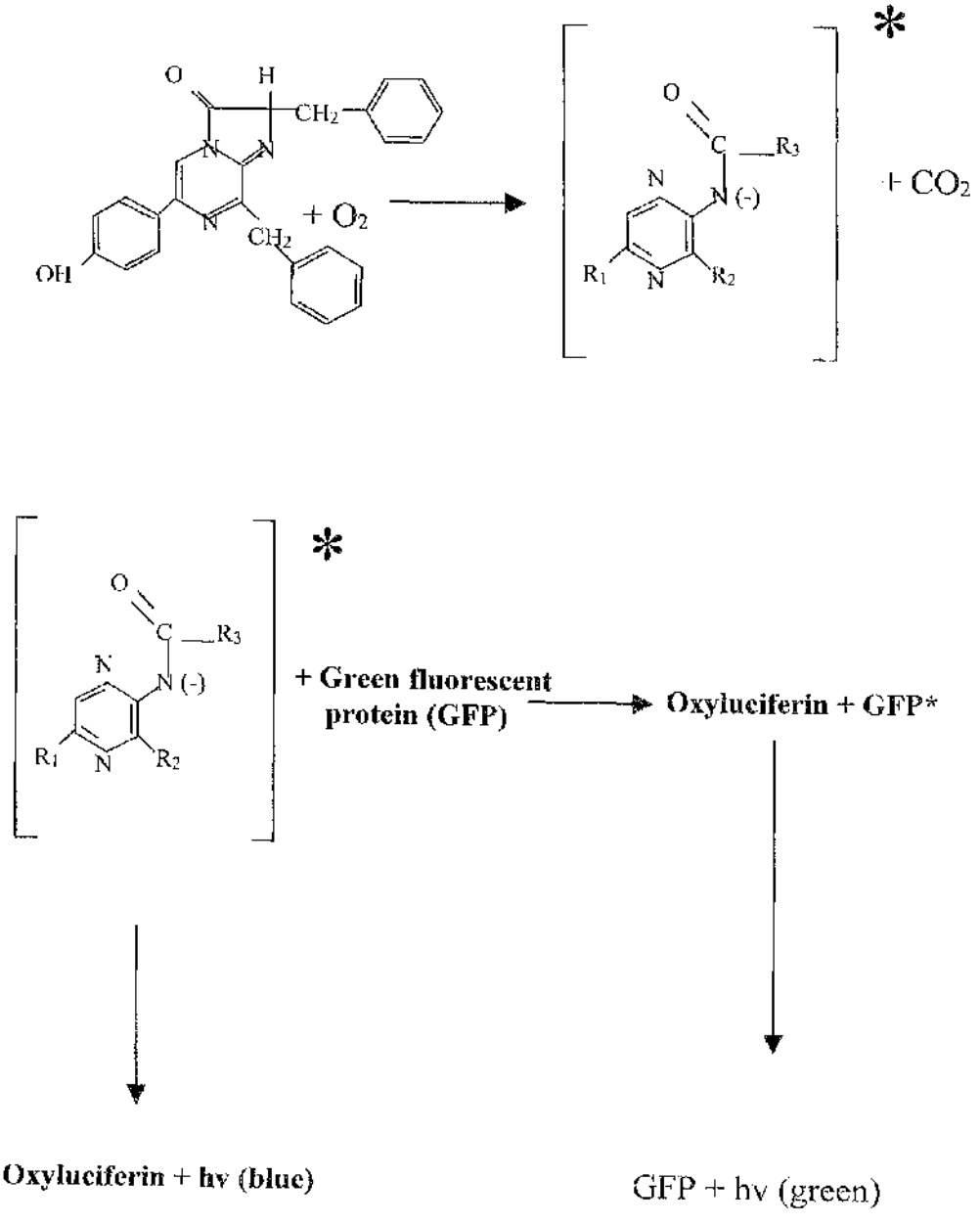
O
H
CH2
N
N
N
CH2
OH
+ O2
O
C
R3
N
N (-)
R1
N
R2
*
+ CO2
*
+ Green fluorescent protein (GFP)
Oxyluciferin + GFP*
Oxyluciferin + hv (blue)
GFP + hv (green)

Figure 3.1

Figure 3.2. The dipole-induced dipole interactions that occur between two fluorescent molecules that result in FRET.

(A) An incident photon of frequency ν_1 is absorbed by the donor.

(B) This induces a dipole on the donor molecule.

(C) Instead of emitting a photon, the excited donor induces a dipole on the acceptor molecule.

(D) The acceptor emits a photon of frequency ν_2.

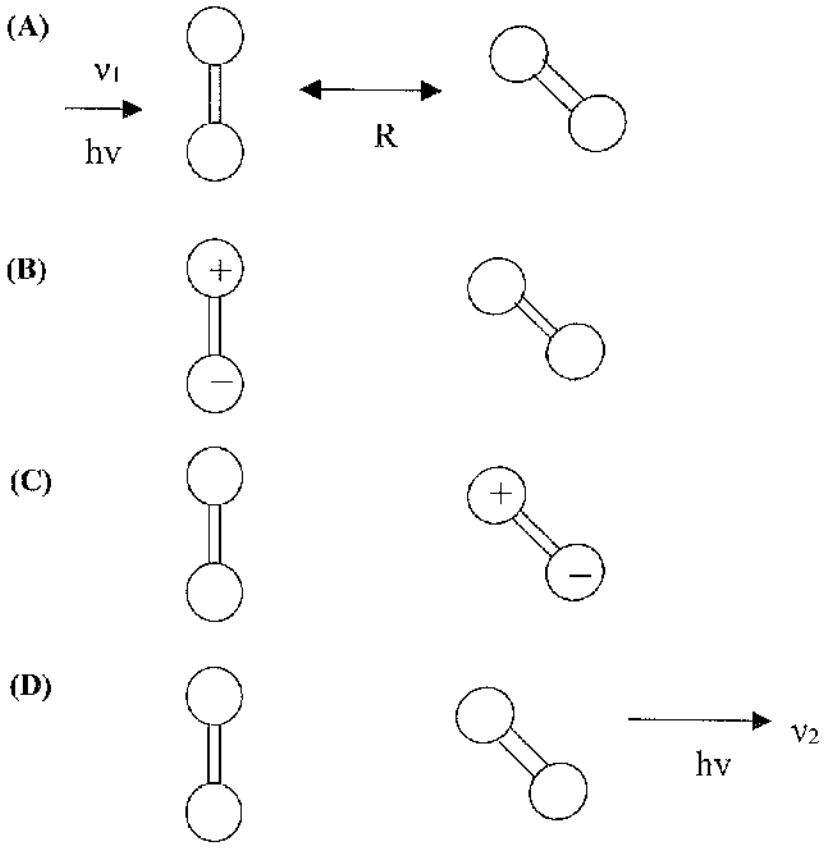

Figure 3.2.

Figure 3.3. The three possible outcomes of the BRET assay as applied to GPCRs.

(A) In the absence of ligand receptors are monomeric. Addition of compound drives the receptors towards dimerization.

(B) The receptors are constitutively dimerized and remain so in the absence, or presence of external ligands.

(C) The receptors are constitutively dimerized but become monomeric upon addition of external ligands.

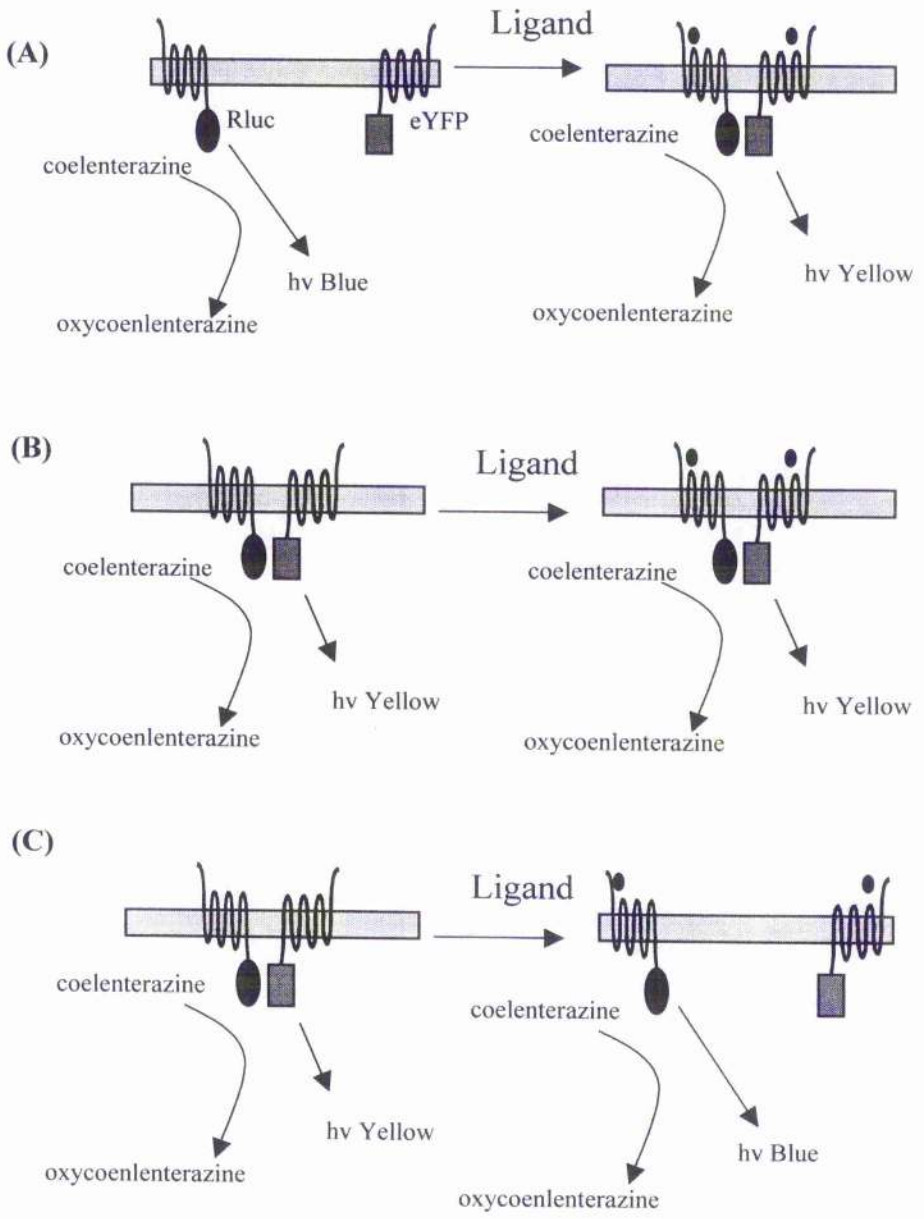
(A)
Ligand
Rluc
eYFP
coelenterazine
hv Blue
oxycoenlenterazine
coelenterazine
hv Yellow
oxycoenlenterazine
(B)
Ligand
coelenterazine
hv Yellow
oxycoenlenterazine
coelenterazine
hv Yellow
oxycoenlenterazine
(C)
Ligand
coelenterazine
hv Yellow
oxycoenlenterazine
coelenterazine
hv Blue
oxycoenlenterazine

Figure 3.3.

The β2-AR fused to *Renilla* luciferase (β2-AR-Rluc) was capable of binding to [^{3}H]-dihydroalprenolol (Figure 3.4) (1232±64fmol/mg). It was further observed that this construct was also capable of functionally coupling to endogenously expressed G-protein, since it was capable of generating cAMP in response to agonist (Figure 3.5). In intact cell adenylyl cyclase assays performed in HEK 293 cells the β2-AR-Rluc construct produced a three to four fold increase in intracellular cAMP when exposed for thirty-minutes to isoprenaline. This was comparable to the wild type β2-AR which produced a four to five fold increase of intracellular cAMP levels following a similar challenge. The level of constitutive signalling activity imparted by the Rluc modified version of the receptor appeared to be slightly elevated in comparison with its wild type counterpart. However, this was not markedly so.

To verify that the β2-AR fused to eYFP (β2-AR-eYFP) was similarly capable of binding agonist and antagonist ligands, competition binding was performed, using 5nM [^{3}H]-dihydroalprenaolol and varying concentrations of either isoprenaline (Figure 3.6A), or the inverse agonist betaxolol (Figure 3.6B). To determine the binding affinity of these ligands for the receptor, the dissociation equilibrium constant (K_i), was then determined. In both cases competition with [^{3}H]- dihydroalprenolol at the receptor was successful, yielding K_i values of $5.6x10^{-7}$M and $4.8x10^{-8}$M for isoprenaline and betaxolol respectively. It was thus confirmed that the eYFP tagged form of the β2-AR was correctly folded and capable of binding to appropriate ligands. In the case of isoprenaline, the K_i value obtained was indicative of a somewhat lower affinity than what might have been expected. Previous studies showed the K_i for isoprenaline at the wild type β2-AR to be $3.6x10^{-9}$M (MacEwan *et al.*, 1995). The reasons for this discrepancy were not experimentally determined.

Before determining the degree of energy transfer observed between β2-AR-Rluc and β2-AR-eYFP constructs when expressed in mammalian cells it was first necessary to establish what sort of energy transfer signal would be observed between Rluc and eYFP if all the donor and acceptor molecules present were forced into close proximity. To this end, a positive control vector was constructed in pcDNA3 where Rluc and eYFP were fused together with a short linking intergenic sequence separating the two sequences (Figure 2.1). The light emission spectrum between 400nm and 600nm was obtained from transiently transfected HEK 293T cells following the addition of coelenterazine. The emission spectrum thus generated displayed two distinct peak regions, one centred on 460nm, corresponding to the blue light emitted via the enzymic action of *Renilla* luciferase and another peak centred on 530nm, corresponding to yellow light emitted from eYFP (Figure 3.7A). This was in contrast to cells expressing only β2-AR-Rluc, where in the absence of acceptor, there is only one peak region, which is centred on 460nm (Figure 3.7B). It should be noted that there is a significant shoulder on the trace obtained from *Renilla* luciferase alone. There is thus a substantial overlap between the emission spectrum of *Renilla* luciferase and that of eYFP. Such overlap can make it difficult to resolve small amounts of energy transfer (see later, Figure 3.21).

Energy transfer between β2-AR-Rluc and β2-AR-eYFP was next investigated. An emission spectrum was obtained from co-transfected HEK 293T cells following addition of coelenterazine (Figure 3.8A). Overlayed for comparisons are the traces obtained from the positive control vector and from β2-AR-Rluc alone, with the emission spectra normalized at the peak region centred on 460nm. The co-transfected sample produced a clear energy transfer signal. To quantify the energy transfer, the area under the normalized light emission spectra between 500nm and 550nm were

determined. The mean energy transfer values between three separate experiments were taken for the positive control, the co-transfection of β2-AR-Rluc and β2-AR-eYFP and also for a mixture of cells expressing either β2-AR-Rluc or β2-AR-eYFP where the differentially tagged receptors are expressed in separate cells (Figure 3.8B). The positive control gave a robust energy transfer signal whereas the mixed cell population gave no discernable signal. Cells co-transfected with β2-AR-Rluc and β2-AR-eYFP gave a value intermediate between the positive control and mixed cells. This showed that the β2-AR-Rluc and β2-AR-eYFP constructs were in close enough proximity to produce a degree of energy transfer which was approximately 50% of that observed with the positive control construct, presumably due to some degree of constitutive homo-dimerization. The amount of energy transfer was considerably less for cells co-transfected with donor and acceptor tagged β2-AR fusion proteins than for the positive control vector. This is explainable in view of the fact that not all β2-AR dimers present in the cells will be donor acceptor pairs, since it is possible that donor-donor and acceptor-acceptor tagged receptor pairs may form. Considering that the donor-donor tagged receptor pairs contribute nothing to energy transfer and further considering that, due to the overlap in the Rluc and eYFP emission spectra, such donor-donor receptor pairs will have a masking effect on any emission from eYFP, the result is as expected. It was encouraging that no energy transfer could be observed between the Rluc and eYFP tagged constructs when they were expressed in separate cell populations and then mixed. This result underlines the fact that a very close spatial proximity between tagged receptor molecules is essential in enabling energy transfer events, such as those described by Förster (Förster, 1966), to occur. Energy transfer events of this kind are most likely to be caused by the close contact between specifically interacting receptor molecules which posses a high affinity for

one another provided that the levels of receptor expression are not excessively high (as will be demonstrated later in the chapter).

To see if this constitutive homo-dimerisation could be influenced by the addition of agonist or antagonist ligands, energy transfer was measured before and ten minutes after addition of isoprenaline (10^{-5}M) (Figure 3.9). The isoprenaline pre-treatment did not effect the basal level of constitutive energy transfer observed in co-transfected cells, the level of which remained intermediate between that of the positive control and a mixed population of cells expressing either the donor or acceptor tagged forms of the β2-AR. The ratio (Rluc/eYFP) was 0.853±0.015 for the untreated, co-transfected cells and 0.870±0.006 for co-transfected cells exposed to pre-treatment with isoprenaline. This was found not to be a statistically significant increase ($p > 0.05$). These experiments were carried out using a fixed filter multiwell plate reader as described in section 2.6.9 and in this case, the ratio (eYFP/Rluc) is given without a subtraction for background, to demonstrate the magnitude of the signal relative to noise in the system.

The δ-opioid receptor was chosen next for the continuation of the study. Previous reports based on co-immunoprecipitation experiments showed that the receptors were preformed as dimers at the plasma membrane and that addition of certain agonist ligands could decrease the extent of this dimerization (Cvejic and Devi, 1997). Additional evidence for constitutive homodimerization comes from time resolved FRET assays performed on living cells (McVey *et al.*, 2001). Chimeric constructs of the δ-opioid receptor were made with either Rluc or eYFP fused to the carboxy terminal end of its amino acid sequence. As with the β2-AR, a single concentration point radioligand binding assay was performed on cells transiently transfected with either of the δ-opioid chimeric constructs, this time using [^{3}H]-diprenorphine. The

eYFP tagged form of the receptor was seen to express at higher levels than its Rluc modified counterpart (248 +88fmol/mg for δ-opioid-Rluc and 892 ±122 fmol/mg for δ-opioid-eYFP) (Figure 3.10). No expression of endogenous receptor was detected in untransfected HEK 293T cells.

Energy transfer experiments between δ-opioid-Rluc and δ-opioid-eYFP co-transfected into HEK 293T cells revealed a robust energy transfer signal, with a clearly defined peak at 530nm indicative of energy transfer (Figure 3.11A). The magnitude of this signal was comparable in size to that observed for the positive control (Figure 3.11B) Neither the addition of the agonist peptide DADLE, nor the inverse agonist ICI 174 864 (each 10μM) was seen to induce a statistically significant alteration ($p<0.05$) in the strength of this signal given a ten minute pre-incubation period at room temperature with ligand, prior to assay (Figure 3.11C). As a control, energy transfer between β2-AR-Rluc and δ-opioid-eYFP was monitored in co-transfected cells. It was reasoned that these two receptor types should have little affinity for one another given the small degree of sequence homology present in their respective gene sequences. Very little energy transfer was observed between the β2-AR and δ-opioid receptors (Figures 3.11B and 3.11C). A possible explanation for this difference is that in the β2-AR/ δ-opioid receptor heterodimer the donor and acceptor moieties are further apart than is the case with the δ-opioid receptor homodimer. Since the efficiency of energy transfer is proportional to the inverse sixth power of distance (Equation 1) even a small increase in the distance between the centres of reaction of the two fluorophores would result in a dramatic drop in energy transfer efficiency. Alternatively the distances between the reaction centres of the donor and acceptor molecules could be similar for both homo and heterodimers but with the affinity of β2-AR for the δ-opioid receptor low compared to the mutual affinity of δ-opioid receptors. In this

scenario, the majority of Rluc tagged receptors would not be associated with eYFP tagged receptors when β2-AR-Rluc and δ-opioid-eYFP were co-expressed. This would limit the amount of energy transfer so that only a small signal at 530nm relative to the peak at 470nm would be observed. It is impossible to distinguish between these two hypotheses without recourse to a more quantitative analysis (see later).

Interestingly, a ten-minute pre-incubation with either the δ-opioid agonist DADLE or the β2-AR agonist isoprenaline resulted in a statistically significant ($p<0.05$), although somewhat modest, increase in energy transfer levels (Figure 3.11C). FACS analysis of the cells in the experiments described above revealed that similar levels of acceptor tagged receptor were present in cells co-transfected with either β2-AR-Rluc and δ-opioid-eYFP (mean fluorescence= 224.5 ± 19.0 (arbitrary units)) (n=4) or with and δ-opioid-Rluc and δ-opioid-eYFP (mean fluorescence= 228.5 ± 10.5 (arbitrary units)) (n=4). An example of a FACS reading from each of the co-transfected cells is shown (Figure 3.12). It was further verified that similar receptor expression levels were maintained in these experiments via single concentration point radioligand binding on membrane preparations of each of the co-transfected cell types. Table 3.1 shows the receptor expression levels determined in each case. Expression of β2-AR-Rluc was found to be considerably lower than that of the acceptor tagged δ-opioid receptor.

To further elucidate whether or not the energy transfer events observed were truly due to receptor oligomerization the ability of an untagged wild type version of the δ-opioid receptor to compete with its donor and acceptor chimeric counterparts was assessed. HEK 293T cells were co-transfected with optimal levels (2.5μg δ-opioid-Rluc and 5μg δ-opioid-eYFP, transfected in 6cm dishes) of DNA encoding donor and

Table 3.1. The expression levels of *Renilla* luciferase and eYFP-tagged forms of the human δ-opioid receptor and β2-AR in BRET studies.

Following transient expression of HEK 293T cells with combinations of *Renilla* luciferase and eYFP tagged forms of the δ-opioid receptor and β2-AR, levels of expression of receptor binding sites were estimated from the specific binding of single concentrations of the agonists [^{3}H]-dihydroalprenalol (DHA) (β2-AR) and [^{3}H]-diprenorphine (δ-opioid receptor), which are sufficient to occupy more than 90% of the receptors. Parallel FACS analysis of the cell populations demonstrated transfection efficiency to vary between 33% and 40%. These values were then combined to calculate the number of receptors per transfected cell. HEK 293T cells do not endogenously express the human δ-opioid receptor and although many clones of HEK 293T cells endogenously express a low level of the β2-AR this was not detectable in these studies. Data represents means ± S.E.M. from three independent experiments. ND, not detected.

Study	[^{3}H]-DHA binding receptors/cell	[^{3}H]-diprenorphine receptors/cell
δ-opioid receptor homo- oligomer	ND	200,000 ± 10,000
β_2-δ receptor hetero-oligomer	76,000 ± 14,000	243,000 ± 23000

Table 3.1.

acceptor tagged forms of the δ-opioid receptor, along with varying quantities of DNA encoding the wild type (unmodified) δ-opioid receptor. It was reasoned that introducing the untagged receptor would abolish the energy transfer signal by sequestering the donor and acceptor tagged forms of the δ-opioid receptor. Indeed this was found to be the case (Figure 3.13). Introducing larger quantities of the wild type δ-opioid cDNA caused a decrease in the strength of the energy transfer signal. This was approximately halved for the highest quantity of δ-opioid (wt) cDNA. To ensure that the loss of the signal was not simply due to decreasing levels of expression of δ-opioid-Rluc and δ-opioid-eYFP, the experiments were repeated substituting pcDNA3 vector for wild type δ-opioid cDNA as a competitor. Introducing large quantities of this pcDNA3 vector to the optimal δ-opioid-Rluc and δ-opioid-eYFP ratios in the transfection mix did not result in the same 50% loss of energy transfer as observed previously with wild type δ-opioid cDNA. As shown in both of the representitive experiments (Figure 3.14), introducing up to 4μg of pcDNA3 had little or no effect on the strength of the signal. It remains possible however that the blank pcDNA3 vector did not challenge the expression levels of δ-opioid-Rluc and δ-opioid-eYFP quite as effectively as did wild type δ-opioid cDNA.

Homo-dimerization of the κ-opioid receptor was next investigated. Previous studies on this receptor involving co-immunoprecipitation techniques suggested that this receptor type was constitutively homo-dimerized and that this was unaffected by the presence of agonist ligands (Jordan and Devi, 1999). To apply the BRET assay to this receptor type the κ-opioid receptor was modified at the carboxy terminal tail via fusion with either Rluc or eYFP in a manner analogous to the β2-AR and δ-opioid receptors. Single concentration point radioligand binding with [^{3}H]-diprenorphine, revealed that both of these chimeric constructs had been successfully expressed and

yielded a correctly folded receptor which was capable of binding to appropriate ligands (Figure 3.15). Again it was observed that the eYFP tagged form of the receptor expressed at significantly higher levels than the Rluc tagged chimera (528±14 fmol/mg for κ-opioid-Rluc and 2427±213 fmol/mg for κ-opioid-eYFP). Since the binding studies were performed on membrane preparations that comprised of all the cellular compartments, the differences could not have been brought about through any discrepancies in the trafficking properties of the differentially modified κ-opioid receptors. The differences in expression levels observed could have been due to an alteration in affinity of the receptor for ligand brought about by the presence of the carboxyl tail modification with Rluc or eYFP. However for these constructs this was not the case since both κ-opioid-Rluc and κ-opioid-eYFP have been shown to have K_d values that are indistinguishable from the wild type unmodified receptor in saturation binding studies with [^{3}H]-diprenorphine (Ramsay *et al.*, 2002). It is more likely therefore that the differences in expression levels were due to the relative stabilities of the constructs. However, the turnover numbers of the constructs were not experimentally determined in the course of these studies.

HEK 293T cells co-transfected with κ-opioid-Rluc and κ-opioid-eYFP cDNA produced a detectable energy transfer signal upon addition of coelenterazine with a distinct peak in the 530nm region. No change in the extent of energy transfer was observed upon addition of either the κ-opioid agonist ICI 199 441 or the κ-opioid antagonist GNTI when assayed over a time course of 30 minutes where the cells were maintained at 37°C throughout the time course. The subtle variations in energy transfer levels measured at the various time points following the initial reading for t=0 were not found, in both cases, to be statistically significant ($p > 0.05$) (Figure 3.16).

Having observed that a number of GPCRs types, when modified on their carboxyl terminus with either *Renilla* luciferase or cYFP, could give rise to levels of energy transfer which suggested that the molecules were in a close proximity with one another, the question of whether all GPCRs were equally capable of interaction, or whether different types of GPCRs would have differing affinities for one another naturally arose. In order to address this issue in a rigorous manner it was deemed necessary to analyse the increases in energy transfer as a function of increasing levels of acceptor tagged receptors (acceptors) against a relatively fixed concentration of donor tagged receptors (donors). It was reasoned that if the tagged receptors interact, then by maintaining the concentration of donors at a consistently low level in cells that are also co-expressing the acceptors at a variety of concentrations, it would be possible to correlate the increase in energy transfer signal with increased concentration of acceptors. If there were no high affinity interactions occurring between the donor and acceptor tagged receptors then over a wide range of acceptor concentrations, no increase in energy transfer would be expected, provided the surface density of the acceptors at the plasma membrane was not so great as to elicit energy transfer events from random molecular collisions. Also, if the tagged receptors were capable of interacting, then when the concentration of acceptors was elevated to a sufficiently high level, it would be expected that some saturation point would eventually be reached where all the donors were partnered with acceptors. The level of energy transfer at this saturation point would be determined by the efficiency of energy transfer between the donor and acceptor tagged receptor partners. Using this method it might be possible to determine whether the affinity of interaction between a given donor/acceptor pairing is greater or less than other donor/acceptor pairings subject to a similar analysis by noting the concentration of acceptor tagged receptors

at the point where saturation is achieved. To implement this analysis some method of rapidly quantifying the relative amounts of both donor and acceptor tagged receptor molecules present in co-transfected cells was first necessary.

To achieve this, κ-opioid-eYFP expression was correlated with fluorescence signal using a multiplate fixed filter fluorimeter (r^2=0.973) (Figure 3.17A). Mean fluorescence of cells expressing κ-opioid-eYFP, as determined using FACS, was also correlated with fluorescence from the fixed filter fluorimeter. Conversion of the x-axis to receptors/cell (see section 2.6.8) yielded the correlation graph of mean fluorescence against receptor number (receptors/cell) (Figure 16B). The two variables were found to correlate linearly (r^2 = 0.960). This method provided a convenient way of quantifying levels of eYFP tagged receptor expression in HEK 293T cells. Similarly, to determine expression levels of receptors tagged with Rluc, receptor expression from ligand binding was correlated with light intensity (c.p.s.) using a spectrofluorimeter. Similarly light intensity was found to correlate well with receptor number (r^2 – 0.994) and provided a convenient conversion of spectrofluorimeter readings into receptor numbers during routine BRET experiments (Figure 3.18).

To more thoroughly investigate interactions occurring between the donor and acceptor tagged versions of the κ-opioid receptor, using this quantitative method, HEK 293T cells were co transfected with the cDNAs for both κ-opioid-Rluc and κ-opioid-eYFP at various ratios in the transfection mixture, in such a way as to always maintain κ-opioid-Rluc expression at as low a level as possible. Prior to performing the BRET assay, the cells were subject to FACs analysis to determine the expression levels of acceptor tagged receptors within the cell. The emission spectrum emitted by the cells following addition of coelenterazine (5μM) was then obtained, with the value of energy transfer determined as described in section 2.6.9 From this trace, the number

of donor tagged receptors/cell was also determined from the intensity of luminescence emitted via *Renilla* luciferase in the manner described in section 2.6.7 Taking the data thus obtained, energy transfer was plotted against the concentration both of acceptor and donor tagged receptors/cell (Figure 3.19). It can be seen that when energy transfer is considered as a function of the acceptor concentration, a linear relationship is observed to exist between the two variables (Figure 3.19A) (r^2=0.90). It is also noted that although a wide range of κ-opioid-eYFP expression levels were achieved, it was not possible to saturate the system; this was despite the widest range of transfection ratios possible. Through plotting the same levels of energy transfer against the concentration of donor tagged receptors it could be seen that a narrow band of expression levels had been achieved, mostly ranging from about 25,000 to 100,000 receptors/cell (Figure 3.19B). The expression levels of κ-opioid-Rluc were consistently lower than those of κ-opioid-eYFP and no correlation could be determined between the expression levels of κ-opioid-Rluc and energy transfer (r^2=0.10), indicating that under these conditions the extent of energy transfer was predominantly dictated by the expression levels of the acceptor tagged receptor.

For the purpose of a comparison, similar experiments were performed through the co-transfection of the cDNA for κ-opioid-Rluc and TRHr-eYFP into HEK 293T cells at varying ratios in the transfection mixture. When expression levels of TRHr-eYFP are plotted against energy transfer levels, some degree of correlation could be obtained (r^2=0.68), however, as was the case for the κ-opioid-Rluc/ κ-opioid-eYFP pairing, no clear saturation of the system could be perceived even when TRHr-eYFP was expressed as highly as 400,000 copies/cell (Figure 3.20). Again, in this experiment, expression levels of κ-opioid-Rluc were maintained within a narrow range of expression (predominantly between 50,000 and 150,000 receptors/cell) and these

were expression levels which were considerably lower than the acceptor tagged receptor expression levels within the same cells. Since in neither case were saturating concentrations of acceptor tagged receptor achieved it is difficult to draw strong conclusions concerning the relative affinities of these two receptor pairings. It can however be shown that the levels of energy transfer achieved with the κ-opioid-Rluc/ TRHr-eYFP pairing were at the periphery of what might be considered meaningful levels of energy transfer, even at the highest levels of TRHr-eYFP expression achieved. This is clearly demonstrated by considering traces obtained from BRET experiments where different quantities of energy transfer were obtained (Figure 3.21). It can be seen that energy transfer readings of up to about 10 units are virtually impossible to resolve from background and the majority of energy transfer readings obtained in the κ-opioid-Rluc/ TRHr-eYFP pairing were of this order of magnitude. This casts doubt on whether these two GPCR types are in close enough proximity to produce any meaningful levels of energy transfer even when high levels of TRHr-eYFP are expressed within mammalian cells.

To show that the observed differences between the two different pairings subject to quantitative analysis, as detailed above, were not simply due to the different acceptor tagged receptors being predominantly localized to different cellular compartments, confocal pictures of both κ-opioid-eYFP and TRHr-eYFP were obtained following transient transfection of the cDNA encoding the respective constructs into HEK 293T cells. Pictures subsequently obtained revealed that both constructs had a predominantly plasma membrane localized cellular distribution (Figure 3.22) and given this, it would be expected that κ-opioid-Rluc would be equally accessible to both κ-opioid-eYFP and TRHr-eYFP when co-transfected with either into HEK 293T cells.

Figure 3.4. Expression levels of the wild type β2-adrenoceptor and *Renilla* tagged β2-adrenoceptor when expressed in HEK 293T cells.

Expression levels were determined for membrane preparations of untransfected HEK 293T cells, HEK 293T cells expressing the wild type β2-AR and HEK 293T cells expressing the β2-AR-Rluc chimeric protein using [^{3}H]-DHA (2nM) in a single concentration point, radioligand binding assay. Results are from a single transfection, representative of three such performed, standard errors were determined for triplicate well assay points.

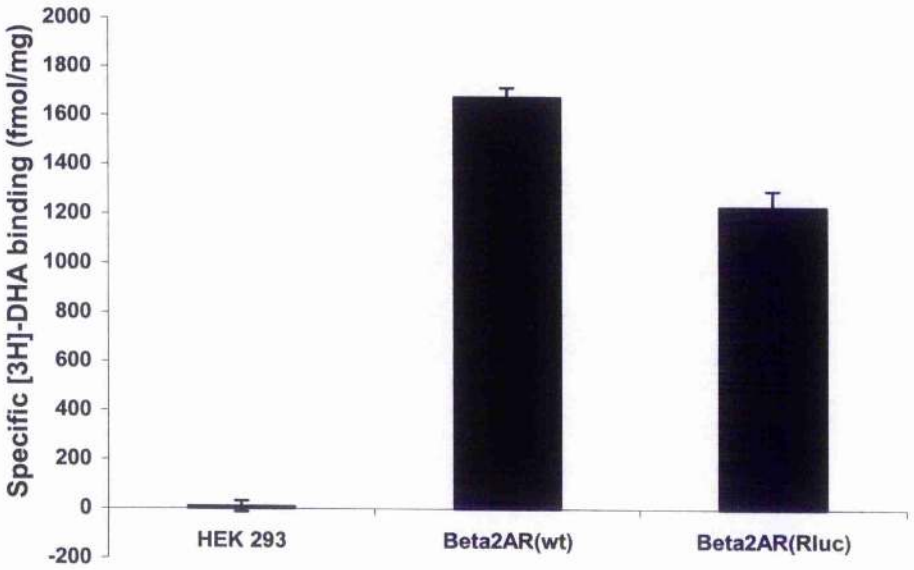
Specific [3H]-DHA binding (fmol/mg)
2000
1800
1600
1400
1200
1000
800
600
400
200
0
-200
HEK 293
Beta2AR(wt)
Beta2AR(Rluc)

Figure 3.4.

Figure 3.5. Functional coupling of wild type β2-adrenoceptor and *Renilla* tagged β2-adrenoceptor to adenylyl cyclase in HEK 293T cells.

HEK 293T cells were mock transfected or transiently transfected with cDNAs encoding wild type β2-AR or β2-AR-Rluc. Twenty-four hours later cells were labelled with [^{3}H]-adenine and a further twenty-four hours later cAMP generation was measured as described in section 2.6.4 in the presence or absence of a 30 minute pretreatment at 37°C with the β2-AR agonist isoprenaline (10μM). Results are taken from a representative experiment of three performed.

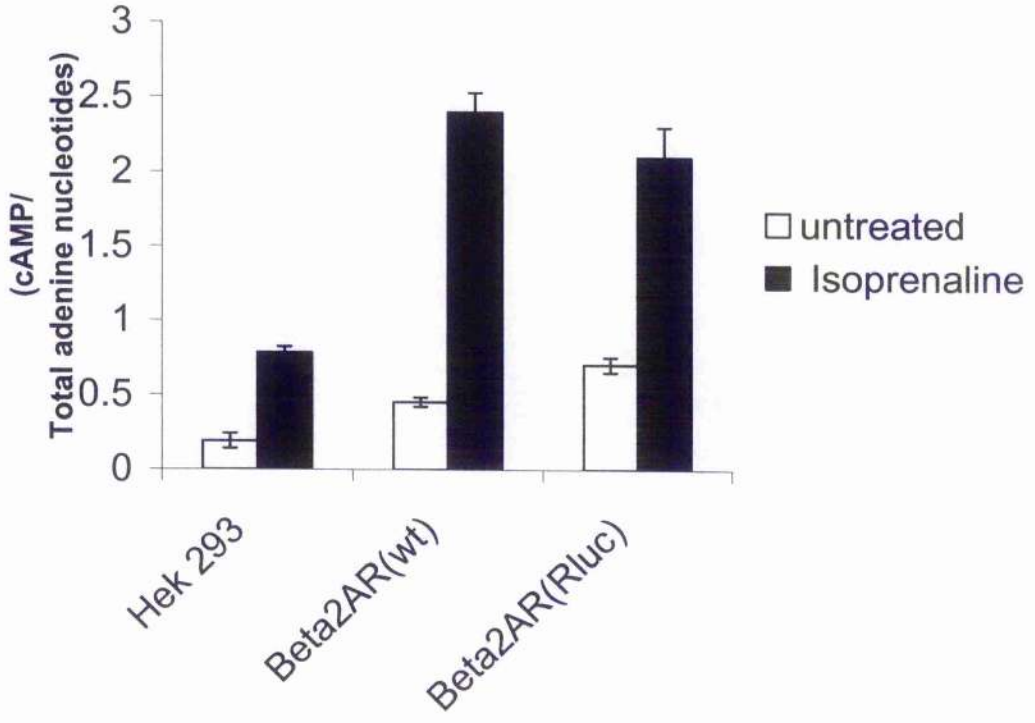
(cAMP/
Total adenine nucleotides)
3
2.5
2
1.5
1
0.5
0
Hek 293
Beta2AR(wt)
Beta2AR(Rluc)
untreated
Isoprenaline

Figure 3.5.

Figure 3.6. Competition Radioligand binding studies performed on cell membranes expressing β2-AR-eYFP.

The capacity of various concentrations of isoprenaline and betaxolol to compete with [^{3}H]-DHA in membrane preparations of HEK 293T cells transiently expressing the β2-AR-eYFP construct. Data represents a mean ±S.E.M. from three independent experiments.

(A)

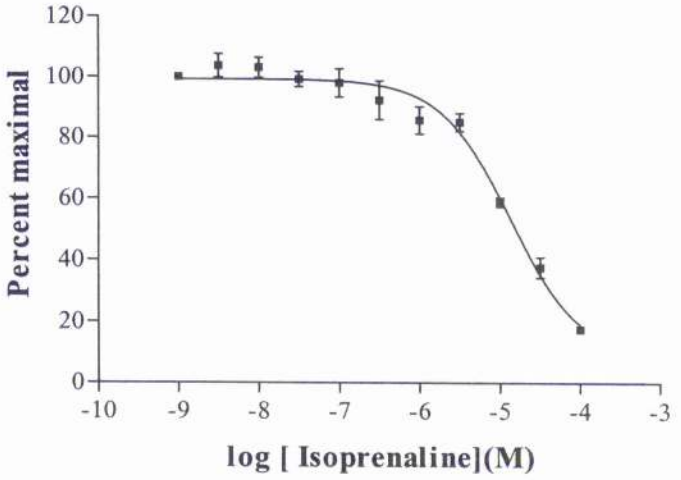
Percent maximal
120
100
80
60
40
20
0
-10
-9
-8
-7
-6
-5
-4
-3
log [Isoprenaline](M)

(B)

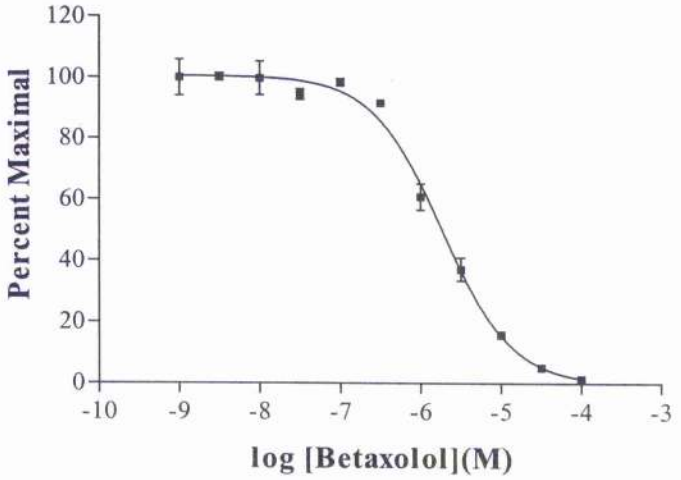
Percent Maximal
120
100
80
60
40
20
0
-10
-9
-8
-7
-6
-5
-4
-3
log [Betaxolol](M)

Figure 3.6.

Figure 3.7. Light emission spectra form BRET positive control: Comparison with light emission spectra obtained from *Renilla* alone.

Emission spectra from HEK 293T cells transiently transfected with either (A) positive control vector or (B) β2-AR-Rluc, following addition of 5μM coelenterazine. The results are from a single transfection, representative of at least three such experiments performed.

(A)

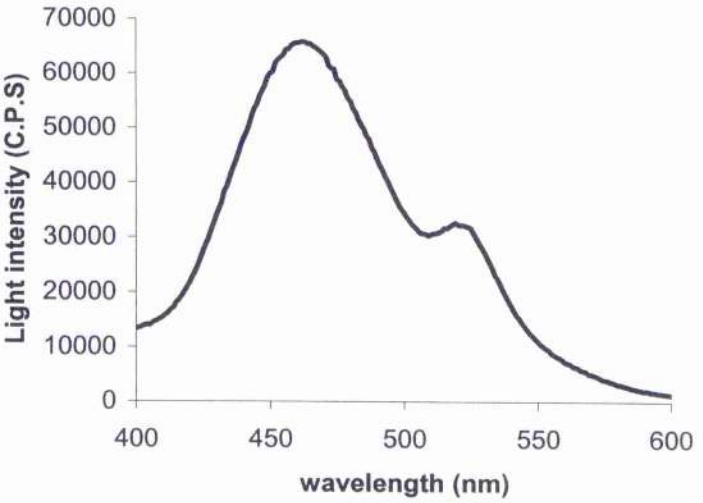
70000
60000
50000
40000
30000
20000
10000
0
Light intensity (C.P.S)
400
450
500
550
600
wavelength (nm)

(B)

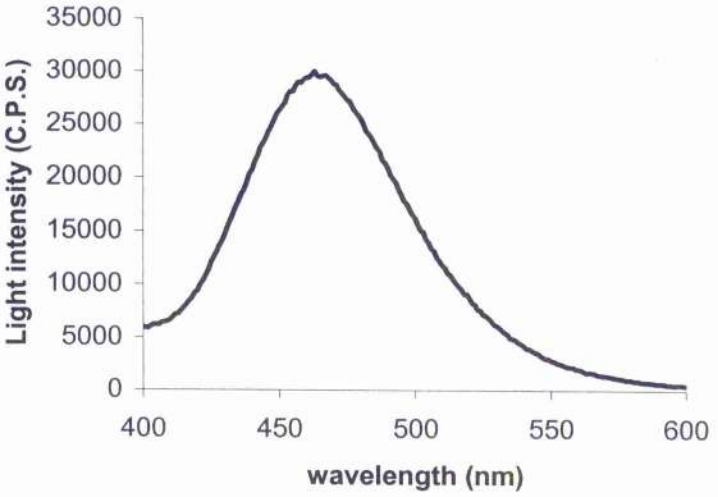
35000
30000
25000
20000
15000
10000
5000
0
Light intensity (C.P.S.)
400
450
500
550
600
wavelength (nm)

Figure 3.7

Figure 3.8. BRET based detection of constitutive β2-AR homo-dimerization in intact cells.

(A) Light emission spectra were obtained from HEK 293T cells transiently transfected with positive control vector (black), a co transfection of β2-AR-Rluc and β2-AR-eYFP (green) and a mixed pool of cells expressing either β2-AR-Rluc or β2-AR-eYFP in separate cells (red). **(B)** Energy transfer values were quantitated, by measuring the area under the normalized light emission spectra between 500nm and 550nm for the above transfections. The data represnt means ± S.E.M for three independent experiments.

(A)

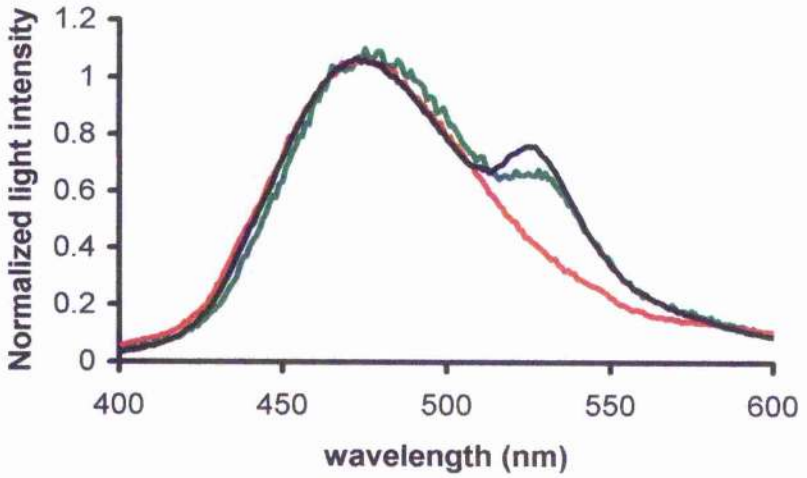
Normalized light intensity
1.2
1
0.8
0.6
0.4
0.2
0
400
450
500
550
600
wavelength (nm)

(B)

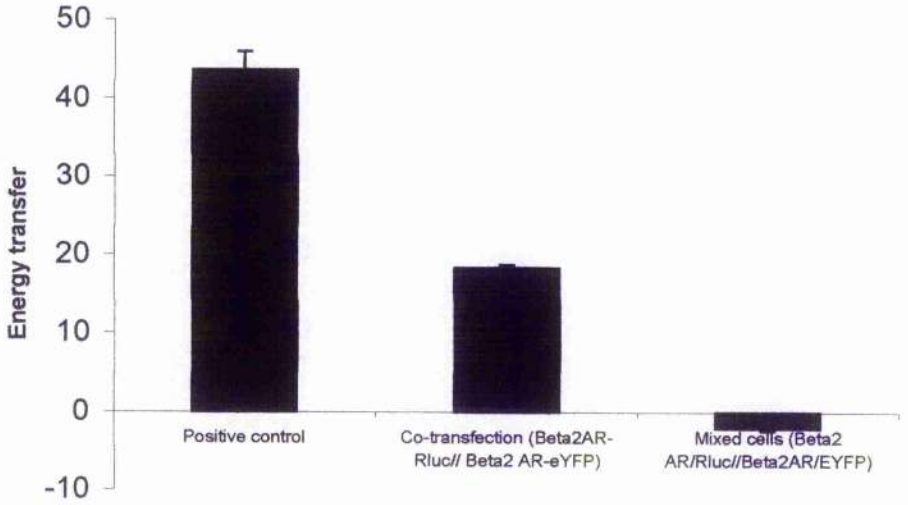
Energy transfer
50
40
30
20
10
0
-10
Positive control
Co-transfection (Beta2AR-Rluc// Beta2 AR-eYFP)
Mixed cells (Beta2 AR/Rluc//Beta2AR/EYFP)

Figure 3.8.

Figure 3.9. Absence of ligand induced regulation of BRET based detection of β2-adrenoceptor homodimerization.

The amount of light emitted from both *Renilla* luciferase or eYFP was quantitated using filters of fixed bandwidth on a Victor^2 multiwell plate reader. Readings were taken from wells containing HEK 293T cells, either transfected with positive control vector, co-transfected with β2-AR-Rluc and β2-AR-eYFP or containing a mixed pool of cells expressing both β2-AR-Rluc and β2-AR-eYFP in separate cells. Data represents means ± S.E.M. of three independent experiments.

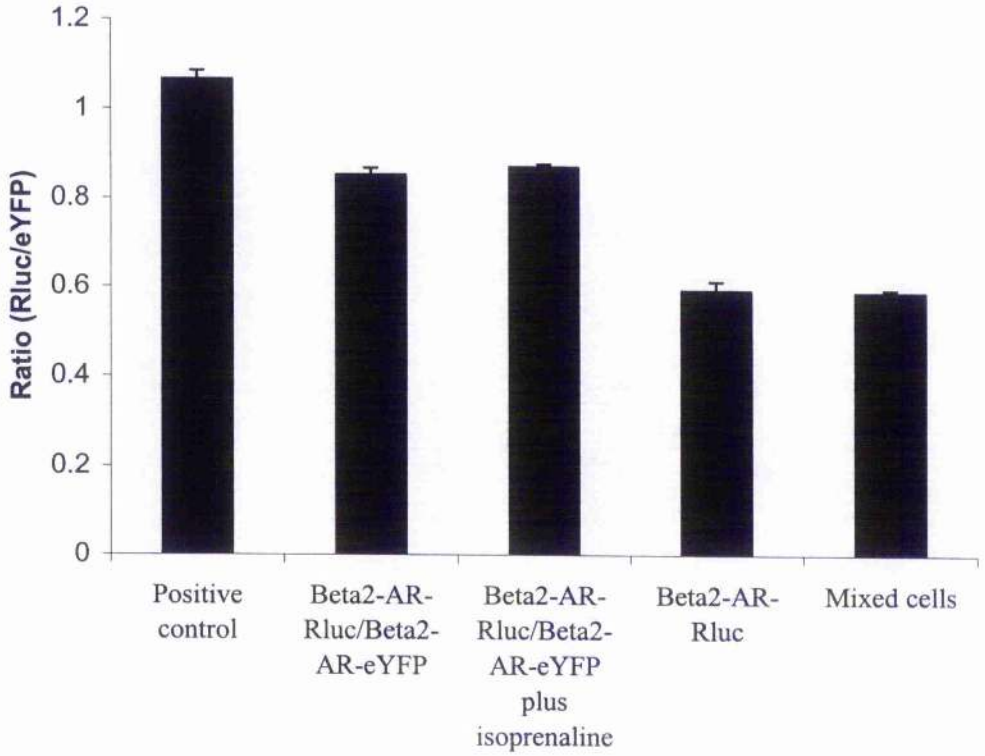
1.2
1
0.8
0.6
0.4
0.2
0
Ratio (Rluc/eYFP)
Positive control
Beta2-AR-Rluc/Beta2-AR-eYFP
Beta2-AR-Rluc/Beta2-AR-eYFP plus isoprenaline
Beta2-AR-Rluc
Mixed cells

Figure 3.9.

Figure 3.10. Expression levels of δ-opioid-Rluc and δ-opioid-eYFP constructs expressed in HEK 293T cells.

Radioligand binding, using a single concentration of [^{3}H]-diprenorphine (5nM), was used to determine the expression levels of either δ-opioid-Rluc or δ-opioid-eYFP transiently expressed in HEK 293T cells. Data represent the results of a single transfection from two such experiments performed, both of which gave similar results.

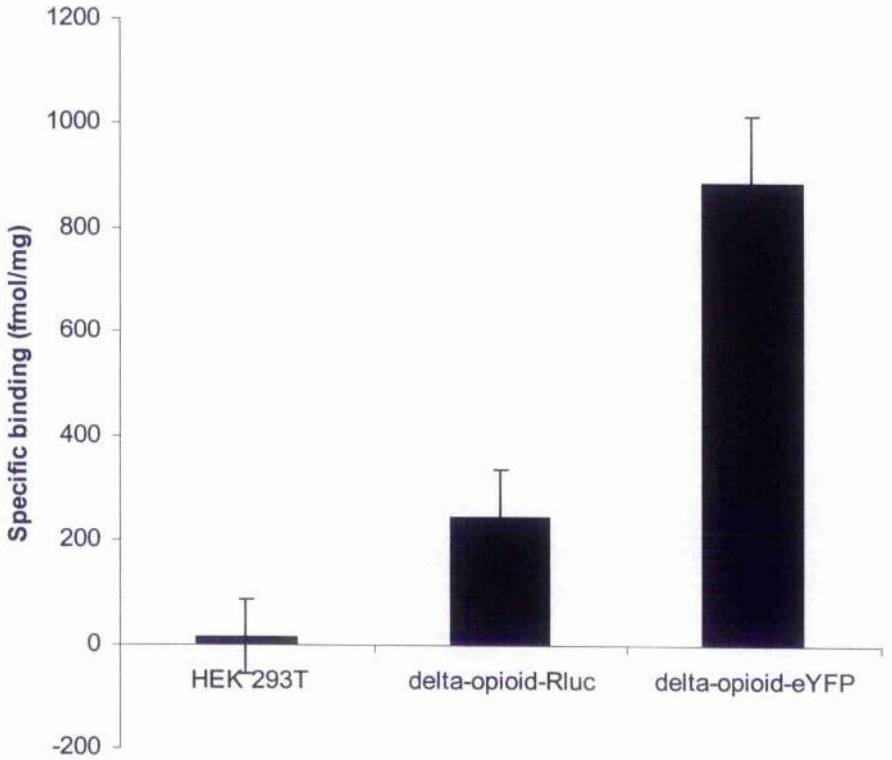
1200
1000
800
600
400
200
0
-200
Specific binding (fmol/mg)
HEK 293T
delta-opioid-Rluc
delta-opioid-eYFP

Figure 3.10.

Figure 3.11. BRET based detection of constitutive homodimerization of the δ-opioid receptor in HEK 293T: Ligands do not effect the dimerization status.

(A) The light emission spectrum from HEK 293T cells transiently co-expressing both δ-opioid-Rluc and δ-opioid-eYFP, was obtained (dark bluc). After a ten-minute pre-incubation at room temperature of either the δ-opioid agonist DADLE (10μM) or the δ-opioid inverse agonist ICI 174 864 (10μM), light emission spectra were re-obtained (red and green spectra respectively). Background is represented by HEK 293T cells expressing δ-opioid-Rluc alone (light blue). **(B)** The light emission spectrum obtained from HEK 293T cells transiently co-expressing both β2-AR-Rluc and δ-opioid-eYFP (red) was obtained. Also included for comparison are the traces obtained from cells co-expressing δ-opioid-Rluc and δ-opioid-eYFP (dark blue) as well as from the positive control vector (black) and δ-opioid-Rluc alone (light blue). **(C)** The area under the normalized emission spectra, obtained from the same types of transfection as those detailed above, were determined as detailed in section 2.6.9. Data represent means ± S.E.M. of four independent experiments.

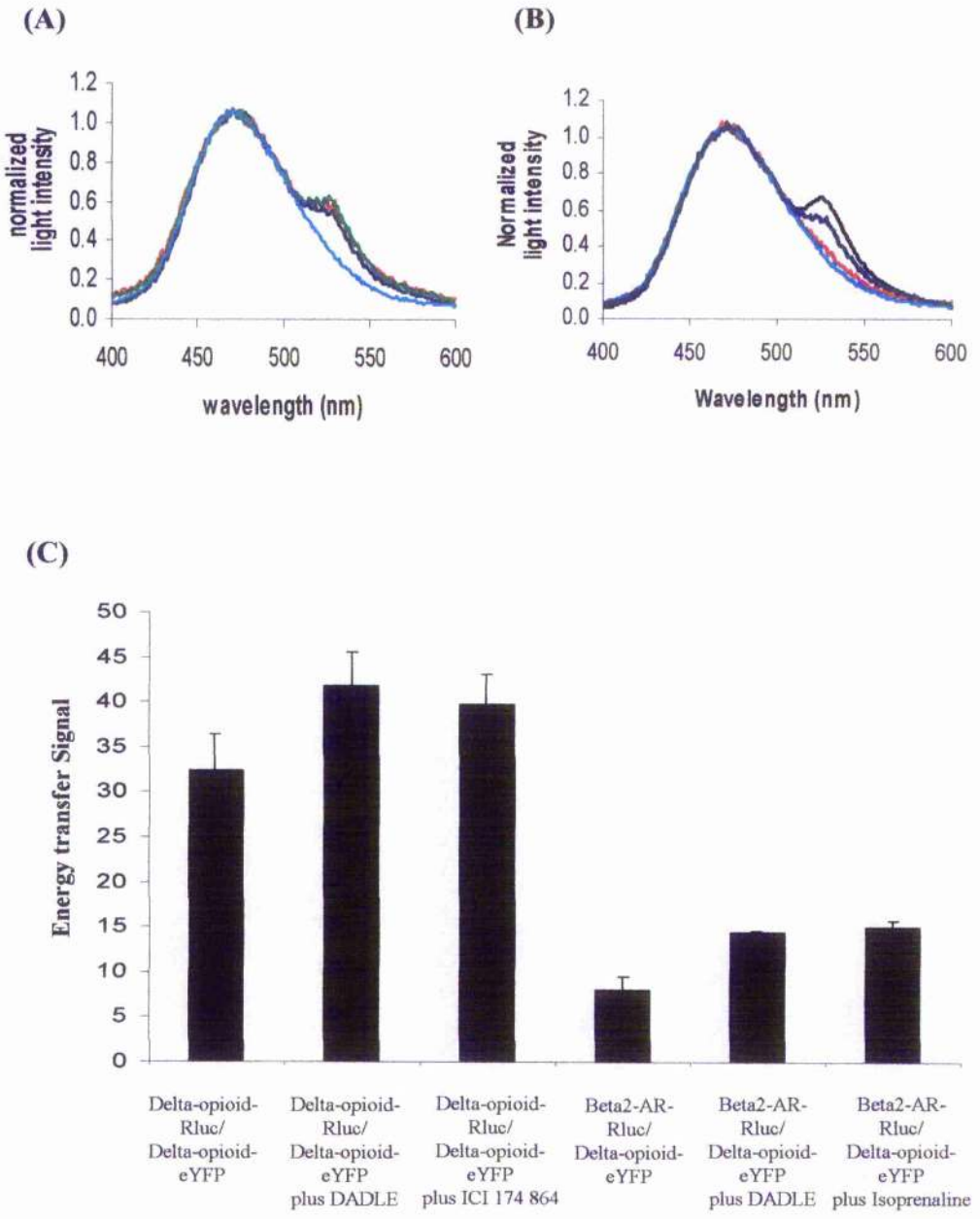
(A)
normalized light intensity
1.2
1.0
0.8
0.6
0.4
0.2
0.0
400
450
500
550
600
wavelength (nm)
(B)
Normalized light intensity
1.2
1.0
0.8
0.6
0.4
0.2
0.0
400
450
500
550
600
Wavelength (nm)
(C)
Energy transfer Signal
50
45
40
35
30
25
20
15
10
5
0
Delta-opioid-Rluc/ Delta-opioid-eYFP
Delta-opioid-Rluc/ Delta-opioid-eYFP plus DADLE
Delta-opioid-Rluc/ Delta-opioid-eYFP plus ICI 174 864
Beta2-AR-Rluc/ Delta-opioid-eYFP
Beta2-AR-Rluc/ Delta-opioid-eYFP plus DADLE
Beta2-AR-Rluc/ Delta-opioid-eYFP plus Isoprenaline

Figure 3.11.

Figure 3.12. Typical data obtained from FACS analysis of cell co-transfected with either (A) δ-opioid-Rluc and δ-opioid-eYFP, (B) β2-AR-Rluc and δ-opioid-eYFP or (C) untransfected cells.

Shown are the plots for forward scatter and side scatter from a representative of four such readings obtained for both co-transfection types. The encircled (gated) area represents the proportion of cells, which were chosen for fluorescence analysis. Also shown are histogram plots of fluorescence intensity readings (FL1-H) from cells within the gated region. The marker M1 denotes the boundary region within which cells were defined as being fluorescent. This was determined using the histogram plot for untransfected cells. The mean fluorescence within this M1 region was recorded for each transfection type.

(A)

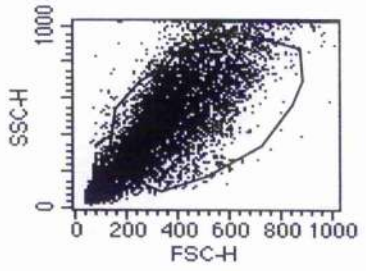

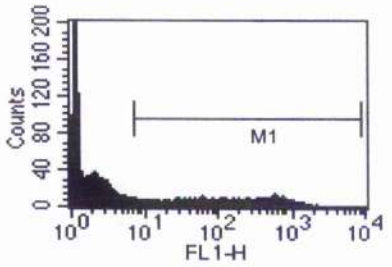

(B)

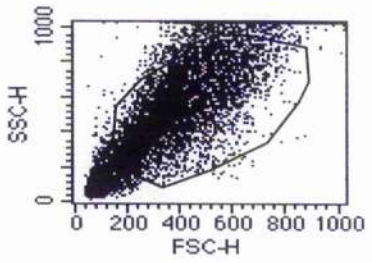

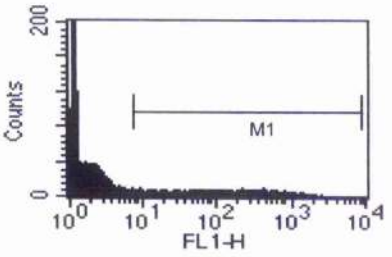

(C)

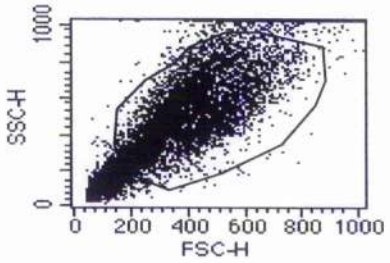

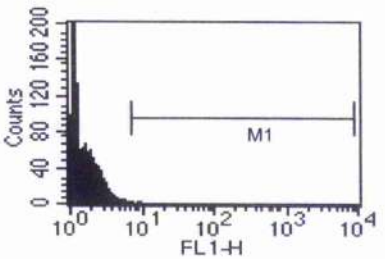

Figure 3.12.

Figure 3.13. Introduction of an untagged version of the δ-opioid into a transfection mix of both δ-opioid Bret partners results in a reduction of the energy transfer signal.

HEK 293T cells were transiently transfected with cDNA for both δ-opioid-Rluc and δ-opioid-eYFP, at a ratio that was deemed optimal for detection of energy transfer. Varying amounts of cDNA for the wild type δ-opioid receptor was included in the transfection mix. The light emission spectra for these transfected cells were determined and the results quantitated by measuring the area under the normalized light emission spectra as detailed in section 2.6.9. The data represent means ± S.E.M. of three independent experiments.

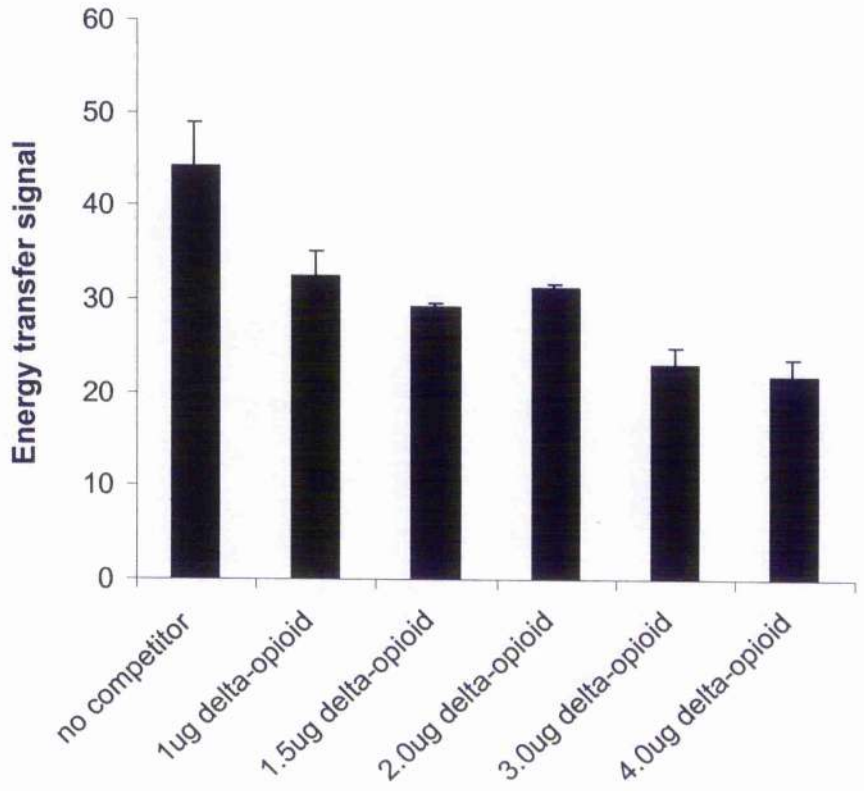
Energy transfer signal
60
50
40
30
20
10
0
no competitor
1ug delta-opioid
1.5ug delta-opioid
2.0ug delta-opioid
3.0ug delta-opioid
4.0ug delta-opioid

Figure 3.13.

Figure 3.14. Introduction of blank pcDNA3 vector into a transfection mix of both δ-opioid BRET partners did not result in a reduction of the energy transfer signal.

HEK 293T cells were transiently transfected with cDNAs for both δ-opioid-Rluc and δ-opioid-eYFP, at ratios that were deemed optimal for detection of energy transfer. Varying amounts of DNA for the pcDNA3 vector was included in the transfection mix. The light emission spectra for these transfected cells were determined and the results quantitated by measuring the area under the normalized light emission spectra as detailed in section 2.6.9. The data represent the results of two such experiments performed.

(A)

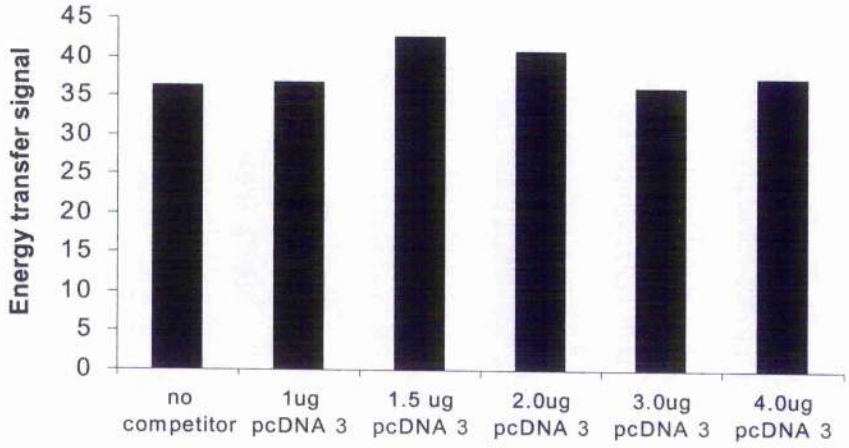

(B)

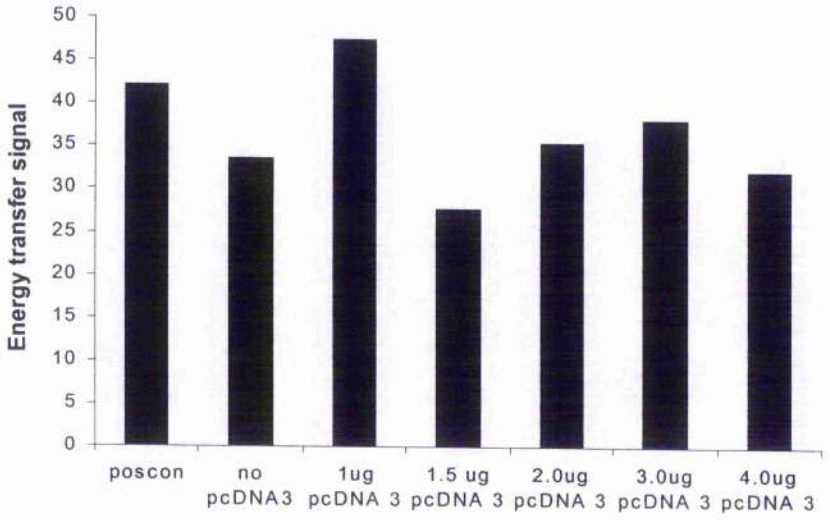

Figure 3.14.

Figure 3.15. Expression levels of κ-opioid-Rluc and κ-opioid-eYFP expressed in HEK 293T cells.

Radioligand binding, using a single concentration of [^{3}H]-diprenorphine (5nM), was used to determine the expression levels of either κ-opioid-Rluc or κ-opioid-eYFP transiently expressed in HEK 293T cells. Data represent means ± S.E.M. of three independent experiments.

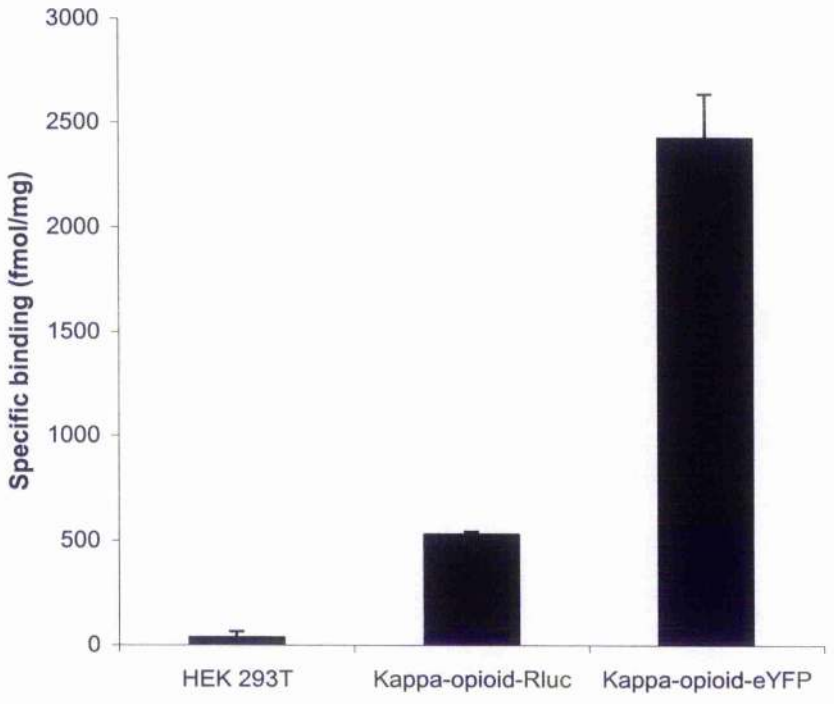
3000
2500
2000
1500
1000
500
0
Specific binding (fmol/mg)
HEK 293T
Kappa-opioid-Rluc
Kappa-opioid-eYFP

Figure 3.15.

Figure 3.16. BRET based detection of κ-opioid receptor homodimerization in HEK 293T cells: Ligands do not affect the dimerization status of this interaction over a thirty-minute time course.

HEK 293T cells were transiently co-transfected with an optimised ratio of cDNA for both κ-opioid-Rluc and κ-opioid-eYFP. The light emission spectrum was obtained both before and after the addition of either the κ-opioid agonist ICI 199 441 or the κ-opioid antagonist GNTI (both at 10μM), and energy transfer was quantified by measuring the area under the trace of the normalized emission spectra between 500nm and 550nm. The emission spectrum was examined at time points 9, 18 and 28 minutes following addition of the test compound. Cells were maintained at 37°C throughout the experiment. Data represent means ± S.E.M. of three individual experiments.

(A)

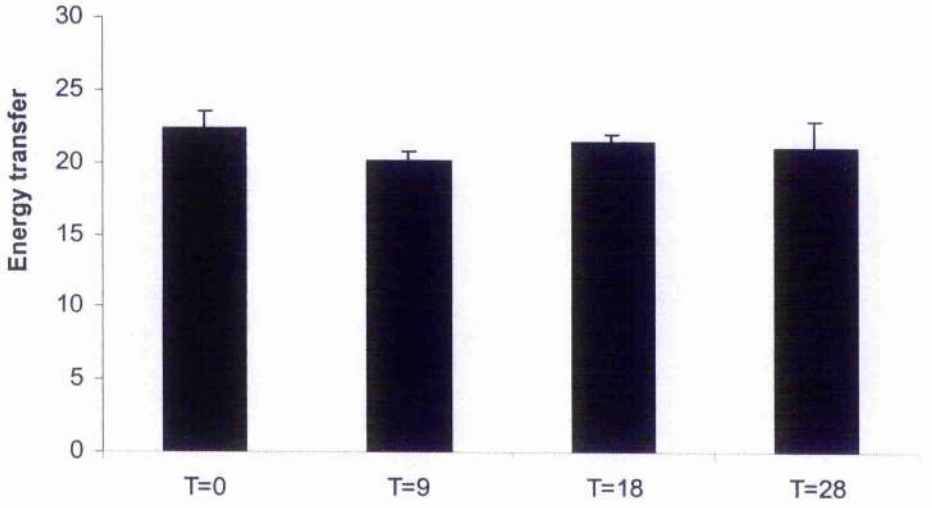

(B)

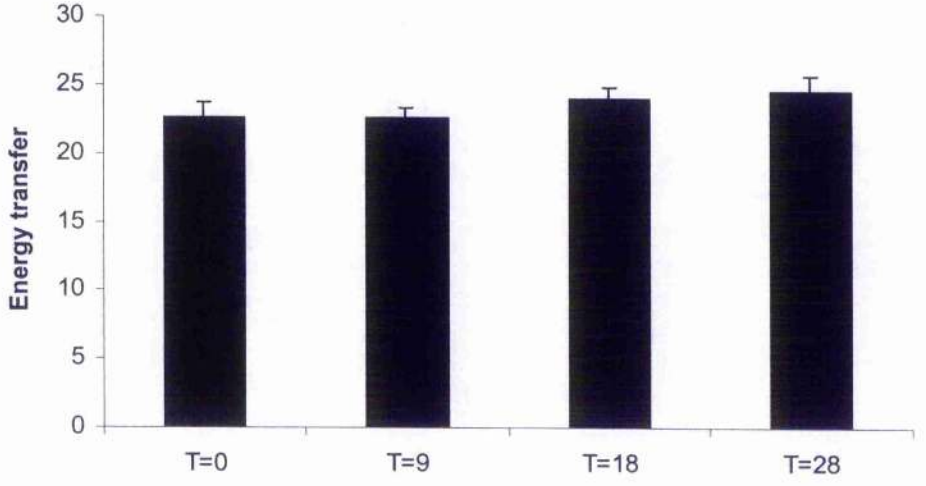

Figure 3.16.

Figure 3.17. Correlation of receptor number against fluorescence from κ-opioid-eYFP.

(A). Membrane preparations from cells transiently transfected with κ-opioid-eYFP were subject to serial dilution then assayed for fluorescence on a Victor^2 multiplate well reader. Parallel binding studies with [^{3}H]-diprenorphine (5nM) on equivalent dilutions of the same membrane preparations determined the amount of receptor (fmol) at each dilution point. The values were highly correlated (r^2=0.973). Data represent the combined results of two independent experiments with error bars representing the S.E.M. between triplicate well readings. **(B).** HEK 293T cells transiently transfected with κ-opioid-eYFP were subject to FACS analysis to determine the mean fluorescence of the cells. The fluorescence of a fixed quantity of the same cells was obtained, using the Victor^2 multiplate well reader, to obtain a parallel set of readings for this instrument. The two sets of values were then correlated (r^2=0.960). Conversion of the x-axis to receptors per cell was achieved using the data from graph (A) as described in section 2.6.8. The results represent the combined data of three such experiments performed.

(A)

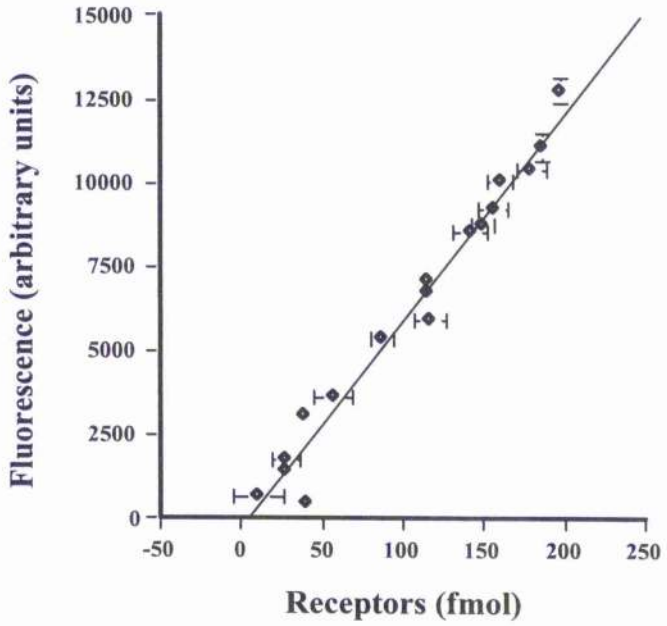

(B)

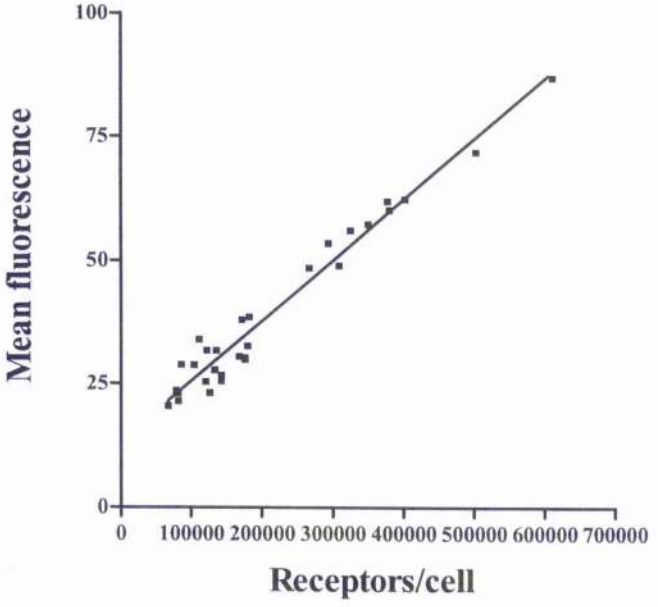

Figure 3.17.

Figure 3.18. Correlation of Receptor number against *Renilla* bioluminescence from β2-AR-Rluc.

Membrane preparations from HEK 293T cells, transiently transfected with β2-AR-Rluc, were subject to serial dilution. The light emission spectrum upon addition of coelenterazine was obtained and the average value of light intensity for the peak centred on 460nm determined in each case. Parallel binding studies with [^{3}H]-DHA (2nM) on equivalent dilutions of the same membrane preparations determined the amount of receptor (fmol) at each dilution point. Both sets of results were then correlated (r^2=0.994). The data is representative of three similar experiments performed. The error bars for triplicate wells used in the radioligand binding assay are too small to be observed.

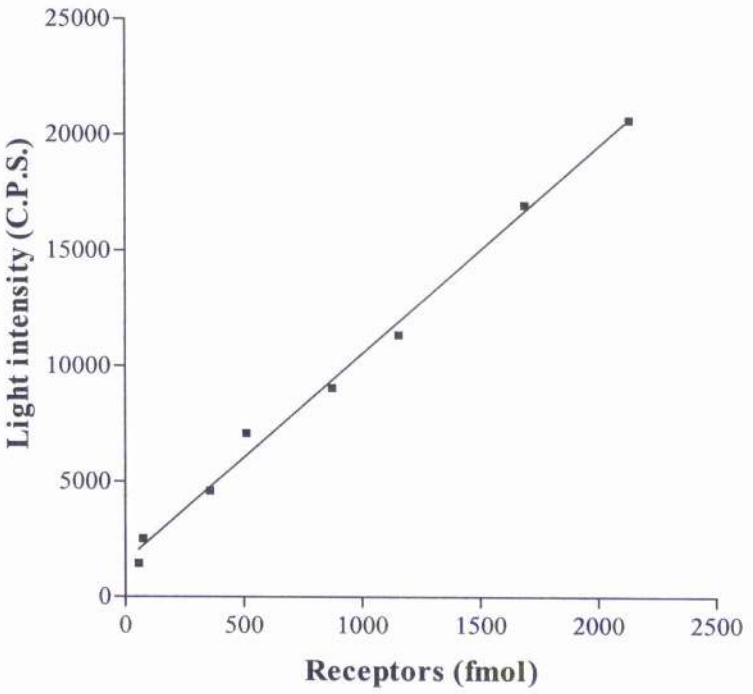
25000
20000
15000
10000
5000
0
Light intensity (C.P.S.)
0
500
1000
1500
2000
2500
Receptors (fmol)

Figure 3.18.

Figure 3.19. For κ-opioid receptor homodimerization, the presence of only 100,000 acceptor tagged receptors/cell is required in order to obtain significant levels of energy transfer.

(A) HEK 293T cells were transiently transfected with a range of cDNA ratios in a co-transfection of κ-opioid-Rluc and κ-opioid-eYFP. The light emission spectra obtained from these transfections were used to determine energy transfer levels by measuring the area under the normalized light emission spectra between 500nm and 550nm. Mean fluorescence values obtained from FACS analysis of the same cells were used to determine the number of receptors/cell using the graph in Figure 3.17B. The two sets of results were then correlated (r^2=0.90). Results represent the pooled data from three individual experiments. **(B)** From the light emission spectra, the average light intensity from the peak centred on 460nm was determined. This value was converted to a donor receptor concentration using the graph of Figure 3.18 These results were then plotted against the energy transfer levels (r^2=0.10).

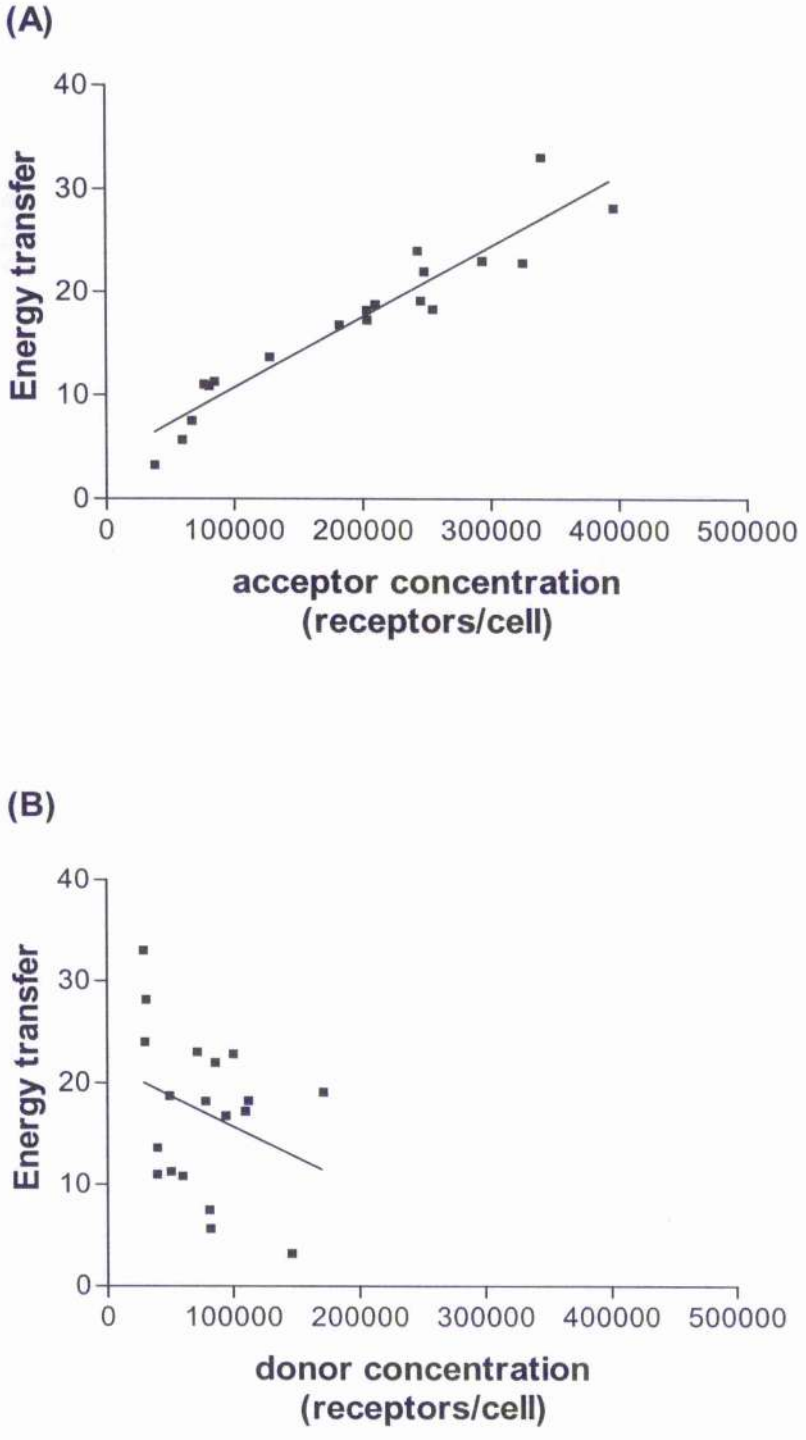
(A)
Energy transfer
40
30
20
10
0
0
100000
200000
300000
400000
500000
acceptor concentration
(receptors/cell)
(B)
Energy transfer
40
30
20
10
0
0
100000
200000
300000
400000
500000
donor concentration
(receptors/cell)

Figure 3.19.

Figure 3.20. For heterodimerization between the TRHr and κ-opioid receptors, the presence of at least 300,000 acceptor tagged receptors/cell is required in order to obtain significant levels of energy transfer.

(A) HEK293T cells were transiently transfected with a range of cDNA ratios in a co-transfection of κ-opioid-Rluc and TRHr-eYFP. The light emission spectra obtained from these transfections were used to determine energy transfer levels by measuring the area under the normalized light emission spectra between 500nm and 550nm. Mean fluorescence values obtained from FACS analysis of the same cells were used to determine the number of receptors/cell using the graph in Figure 3.17B. The two sets of results were then correlated (r^2=0.68). Results represent the pooled data from two individual experiments. **(B)** From the light emission spectra, the average light intensity from the peak centred on 460nm was determined. This value was converted to a donor receptor concentration using the graph of Figure 3.18 These results were then plotted against the energy transfer levels (r^2=0.33).

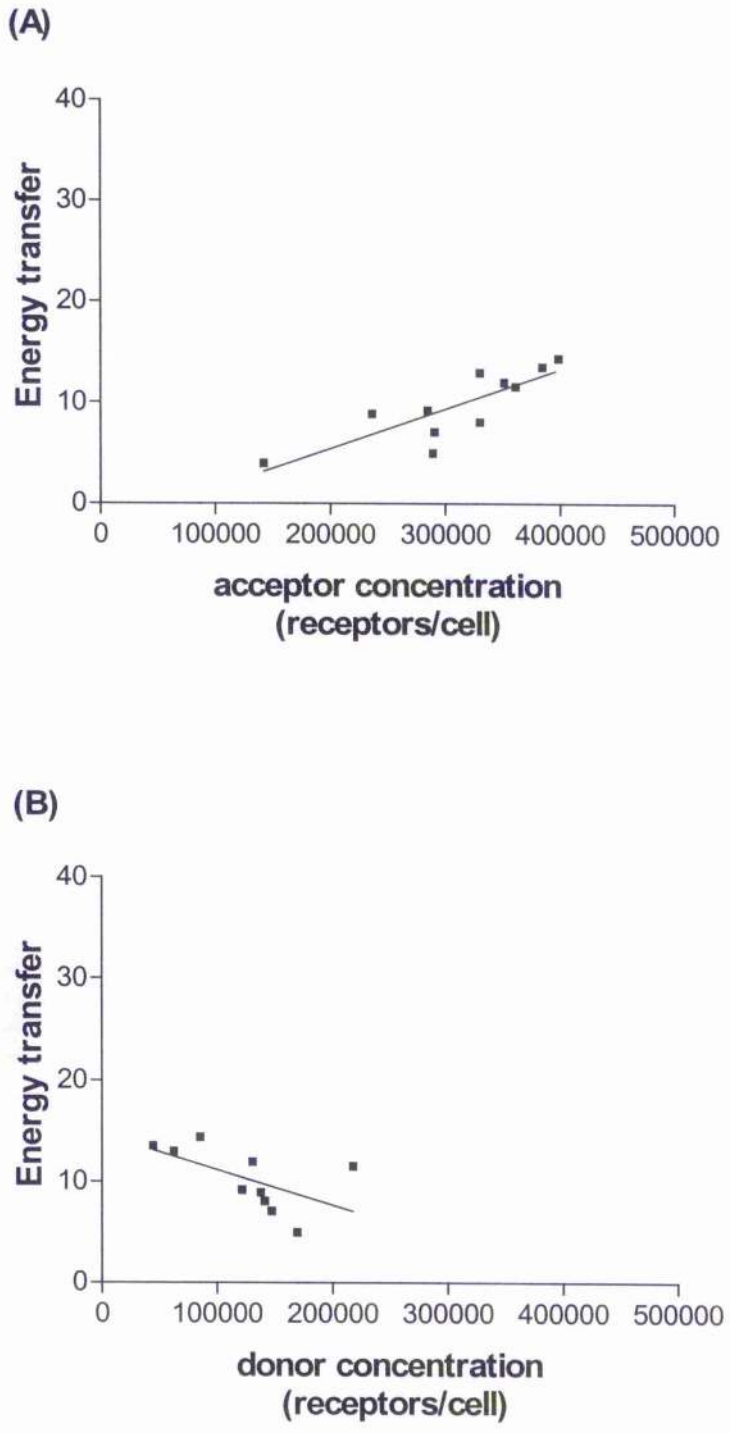
(A)
Energy transfer
40
30
20
10
0
0
100000
200000
300000
400000
500000
acceptor concentration
(receptors/cell)
(B)
Energy transfer
40
30
20
10
0
0
100000
200000
300000
400000
500000
donor concentration
(receptors/cell)

Figure 3.20.

Figure 3.21. The light emission spectra obtained from BRET studies showing a variety of energy transfer levels.

Shows typical emission spectra obtained from HEK 293T cells co-transfected with Rluc and eYFP κ-opioid tagged receptors and their corresponding levels of energy transfer as determined by measuring the area under the normalized light emission spectra between 500nm and 550nm. From such studies it was decided that energy transfer levels above 10 units could be convincingly resolved from the background trace.

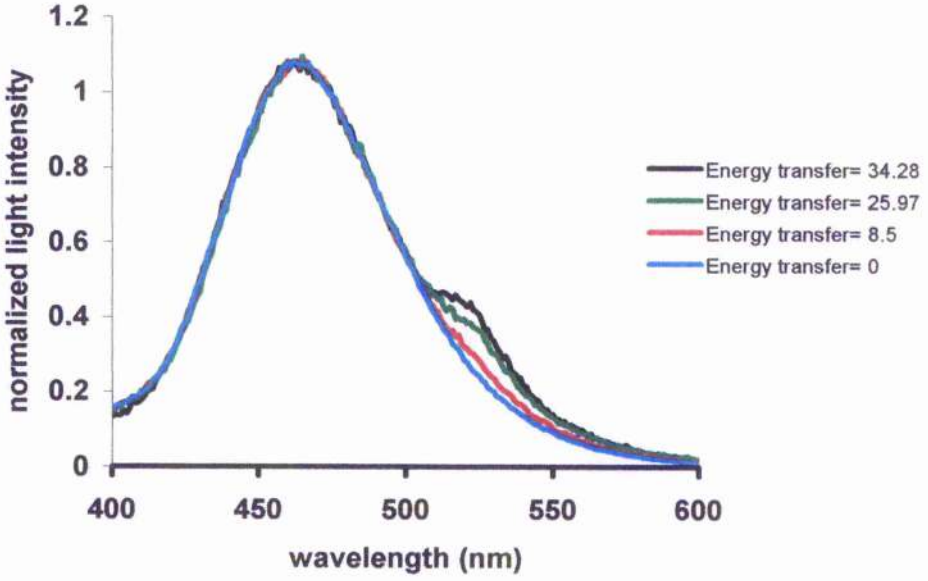
1.2
1
0.8
0.6
0.4
0.2
0
normalized light intensity
400
450
500
550
600
wavelength (nm)
Energy transfer= 34.28
Energy transfer= 25.97
Energy transfer= 8.5
Energy transfer= 0

Figure 3.21.

Figure 3.22. Cellular localization of both κ-opioid-eYFP and TRHr-eYFP constructs expressed in HEK 293T cells.

Images taken using scanning confocal microscopy show that **(A)** the κ-opioid-eYFP construct targeted predominantly to the plasma membrane when expressed transiently in HEK 293T cells. **(B)** When expressed transiently in HEK 293T cells, the TRHr-eYFP construct targeted predominantly to the plasma membrane. The results are representative of three such experiments performed.

(A)

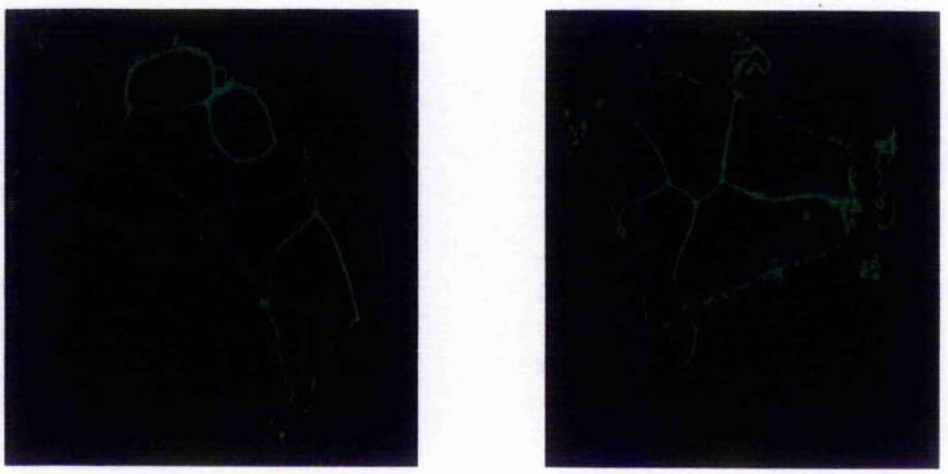

(B)

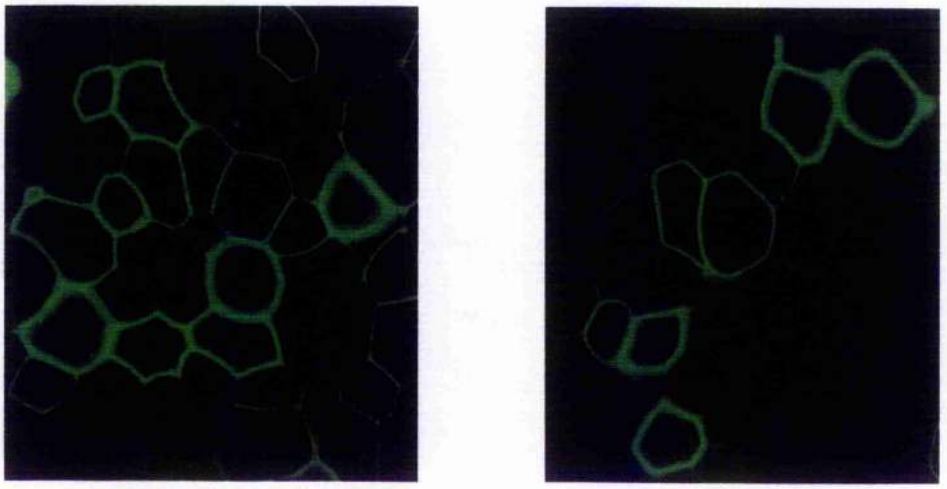

Figure 3.22.

Figure 3.23. Altering the magnitude of the light emission spectra from *Renilla* luciferase did not result in any alteration in the shape of the graph upon normalization of the data.

(A) The light emission spectra from dilutions of membrane preparations of HEK 293T cells, transiently expressing the β2-AR-Rluc construct were obtained. **(B)** Normalization of these traces revealed a near perfect overlap for all such spectra analysed. **(C)** Measurement of the area under the normalized light emission spectra (from (B)) between 500nm and 550nm showed that there was no alteration in the normalized readings due to different magnitudes of signal. Data shown are representative of three such experiments performed.

(A)

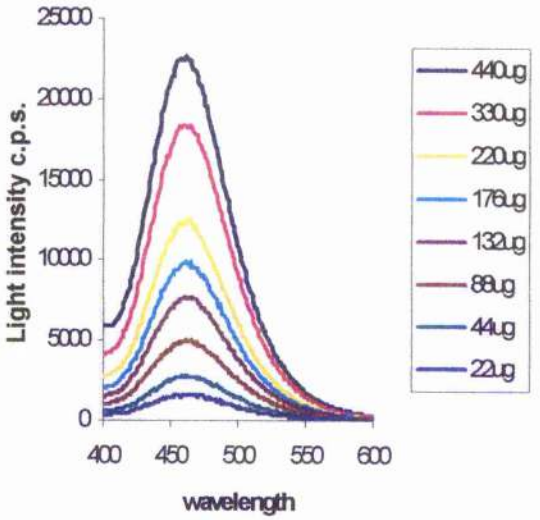

(B)

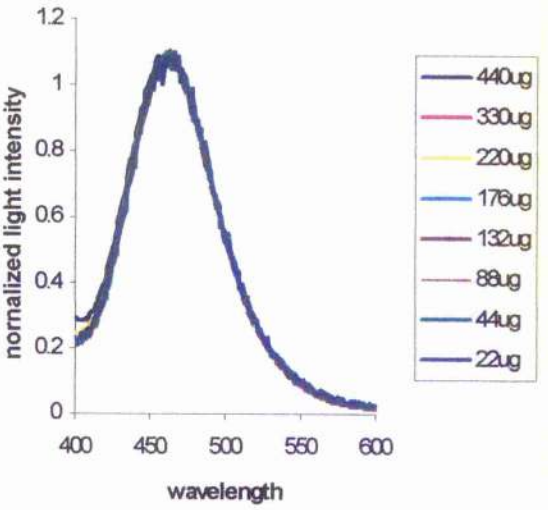

(C)

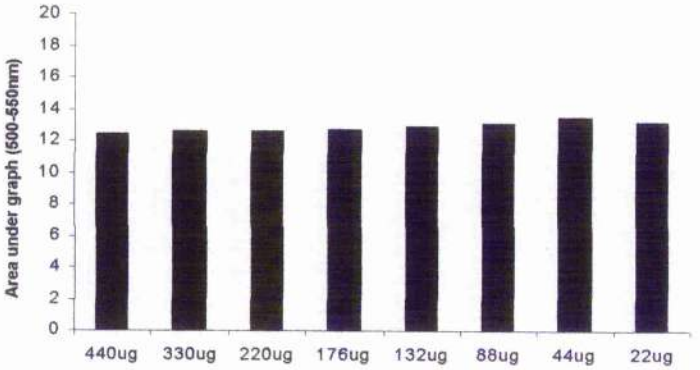

Figure 3.23.

To ensure that the graph area between 500nm and 550nm did not alter upon normalization of traces of different magnitudes the area under the trace obtained from the emission spectrum of a series of membrane dilutions expressing β2-AR-Rluc alone was determined. The peak centred on 460nm ranged in magnitude for these traces, from between 1000 (c.p.s.) to 22,000 (c.p.s.), covering the whole range of values which were obtained in the BRET experiments (Figure 3.23a). Normalization of the peak centred on 460nm revealed a near perfect overlay for all of the traces (Figure 3.23b). The area under the graph between 500nm and 550nm was also unchanging (Figure 3.23c). There is no subtraction for background in Figure 3.23c, so that all of these values represent zero energy transfer. This data would lead us to conclude that even small deviations (i.e. greater than or equal to 10 units), obtained in BRET experiments, would be of significance, provided a good overlay was obtained between the background (Rluc alone) emission spectra and the emission spectrum showing energy transfer.

3.3 Discussion

In this study, bioluminescence resonance energy transfer was used to investigate interactions between various types of G-protein coupled receptors. The results obtained with the β2-AR indicated that this receptor was constitutively dimerized and that addition of ligand did not alter the extent of energy transfer. Previous studies, which were based on co-immunoprecipitation experiments, had suggested that the β2-AR existed as a homodimer when expressed in insect Sf9 cells and also, to a lesser extent, in mammalian CHW cells (Herbert *et al.*, 1996). Further evidence for interactions between β2-ARs was provided by functional rescue experiments, where the β2-AR was seen to be capable of exerting a dominant positive effect on a

constitutively desensitised mutant version of the β2-AR, when co-expressed in insect Sf9 cells (Herbert *et al.*, 1998). In the former study, it was found that a peptide derived from the amino acid sequence of β2-AR transmembrane domain VI was capable of disrupting homodimerization and that this effect could be inhibited by the presence of agonist ligand, presumably by exerting a stabilising effect upon the homomeric complex. The same group have also used BRET to corroborate their previous findings and were successful, both in confirming that the β2-AR is constitutively homodimerized and that the amount of energy transfer observed could by increased upon addition of agonist, an effect which could be blocked by the antagonist propranolol (Angers *et al.*, 2000). With respect to these ligand-induced increases in energy transfer this author was unable to replicate the above-mentioned results. Addition of the agonist isoprenaline was not found to induce a statistically significant increase in energy transfer levels given a ten-minute preincubation time prior to the assay. It should be noted however, that the increases in energy transfer detected by Angers and co-workers (Angers *et al.*, 2000) were extremely small and it is possible they were beyond the limits of resolution for the equipment used in our experiments. Experiments using BRET to detect the homomeric interactions of the thyrotropin releasing hormone receptor, (Kroeger *et al.*, 2001) produced similar results to those of studies focusing on the β2-AR (Angers *et al.*, 2000). In such studies, the TRH receptor was seen to be constitutively homodimerised in the absence of ligand. Addition of TRH resulted in a reproducible, statistically significant increase in the strength of the energy transfer signal, though the magnitude of this increase was still very small in comparison with the constitutive signal.

A problem associated with the detection of ligand-induced alterations in the extent of dimerization between GPCR types is that over expression of receptors, which possess

a certain affinity for one another, may drive any dynamic equilibrium between monomeric and dimeric states towards the associated form. This is implied by the law of mass action which states that the rate of a reaction is proportional to the product of the concentrations of the reactants. If such an equilibrium were to be influenced by the presence of agonist, but the concentrations of the reactants (receptors) were sufficiently high as to force that reaction almost to completion, it would be difficult to detect alterations in energy transfer upon addition of the agonist. Another difficulty is that such extremely small alterations in energy transfer could be due to a reorientation of the donor and acceptor tagged molecules, induced by the presence of agonist ligand in the receptor-binding pocket. This could alter the angle of orientation between the donor and acceptor molecules, which would change the efficiency of the energy transfer process (by Equations 1 and 3, Section 3.1.2).

Other receptor types investigated in the course of conducting the experiments detailed herein, like the β2-AR, similarly failed to produce ligand-induced alterations in the extent of homodimerization. This was the case in examining homomeric interactions with the δ-opioid receptor as well as homomeric interactions of the κ-opioid receptor, where even in a time course of up to thirty minutes following addition of agonist, no changes in the levels of energy transfer were observed. The former result was not consistent with previous studies involving the δ-opioid receptor (Cvejic and Devi, 1997) where upon addition of certain types of agonist (athough not all), dimer complexes of the δ-opioid receptor were seen to be destabilized and that this process preceded receptor internalisation. However, these experiments (Cvejic and Devi, 1997) required the addition of an external cross-linking reagent in order to obtain a stable receptor complex in the presence of the detergent sodium dodecyl sulfate. It is possible that certain ligands may have interfered with this process, perhaps by

masking or sequestering lysine residues important in cross-linking. In contrast, the BRET technique requires no such external manipulations and therefore, perhaps, provides a more genuine result. Credence to this assertion is provided by results obtained from time resolved FRET based assays on living cells, which did not reveal any alterations in the extent of homodimerization between δ-opioid receptors in the presence of agonist (McVey *et al.*, 2001). The FRET based experiments presented by McVey and co-workers (McVey *et al.*, 2001) had certain advantages over the BRET method described herein. Principle of these advantages was that the receptors were tagged with acceptor and donor fluorophores by use of fluorescent antibodies that bound to the amino-terminus of the respective receptors protruding from the extracellular face of the cell. Since these antibodies could not traverse the plasma membrane, only receptors successfully delivered to the plasma membrane were thus tagged and consequently all of the receptors, involved in energy transfer events, must have been accessible to external ligand. This is not the case with BRET where the donor or acceptor tagged receptors may be present at any location within the cell depending on the trafficking properties of the receptor. Hence it may be the case that not all donor or acceptor tagged receptors present in co-transfected cells will be accessible to external ligand provided that it is not sufficiently hydrophobic so as to traverse the cell plasma membrane. Also, it remains difficult to assess to what degree the energy transfer signal is the result of interactions between mature receptor or between immature receptors not yet exported from the endoplasmic reticulum and /or the Golgi apparatus.

Another possible reason as to why it was not possible to detect statistically significant increases and/or decreases in energy transfer upon agonist/antagonist treatment may lie in the fact that the GPCRs do not necessarily exist in equilibrium between

monomers and dimers. Obviously the existence of higher oligomeric states would complicate things. If the GPCRs existed in equilibrium between dimers and tetramers (say) then even if the presence of agonist drove the GPCRs towards the tetrameric state this change would not be detectable with the BRET system described herein. However, it is beyond the scope of these studies to address such issues directly.

As a means of confirming that the energy transfer signals between Rluc and eYFP tagged δ-opioid receptors were due to intermolecular interactions, it was demonstrated that by introducing increasing quantities of untagged δ-opioid receptor into the co-transfection mixture the levels of energy transfer between these two chimeric receptors could be substantially attenuated and that this was not a result of altering the conditions of transfection. This technique may provide a useful method for determining whether any given (untagged) GPCR is capable of interacting with the δ-opioid receptor by measuring the extent to which it is able to disrupt homomeric interactions between the BRET partners with a resultant loss in energy transfer signal. This method circumvents the need to construct more chimeric receptors tagged with Rluc and eYFP and in future studies a wide range of untagged GPCRs may be utilized in this fashion. The technique may also prove useful in elucidating those domains of the receptor that are involved in intermolecular interactions. For instance, since previous studies on the δ-opioid receptor have implicated a role for the carboxyl terminal tail in mediating intermolecular interactions between the homo-dimers (Cvejic and Devi, 1997), it would be interesting to see if a mutated version of the δ-opioid receptor which had a truncation in the carboxyl terminal tail domain was as efficient at disrupting the tagged δ-opioid BRET partners as the full length receptor. This approach might have certain advantages over constructing a truncated δ-opioid receptor modified with either the Rluc or eYFP because it removes the theoretical

possibility that by changing the length of the tail of a chimeric receptor construct, you are potentially altering the distance (R) between the centres of reaction of the donor and acceptor fluorophores.

An experiment intended to assess the extent to which energy transfer signals could be observed between the β2-AR and the δ-opioid receptor was initially designed as a control since it was anticipated that there would be only a small chance of these two receptor types having a significant affinity for each other owing to the low sequence homology between the two. The results did not indicate any significant constitutive interaction between these two receptor pairs. However, addition of either isoprenaline or DADLE caused a statistically significant increase in the energy transfer signal. This might indicate that the presence of either agonist increases the mutual affinity of these two receptor types, thus bringing them into closer proximity. Interactions between the β2-AR and the δ-opioid receptor have been confirmed in a recent study (Jordan *et al.*, 2001), wherein by making use of co-immunoprecipitation techniques they demonstrated that such interactions, athough not capable of altering the ligand binding or G-protein coupling affinities of associated receptors, were capable of altering their trafficking properties. In these experiments it was found that β2-ARs were internalised upon addition of the opioid agonist etorphine when co-expressed with δ-opioid receptors and that this response was not observed in cells expressing β2-AR alone. It can be envisaged that the efficiency of this co-internalization process would be considerably enhanced by an increase in the affinity of the δ-opioid receptors for β2-AR upon binding agonist.

The results presented herein, show that certain types of GPCR are in close spatial proximity when co-expressed within HEK 293T cells and that this therefore leads us to suspect that they possess the close physical intimacy such as would result from

intermolecular interactions. This evidence should not be regarded in isolation however, since there is now a wealth of studies all of which direct our attention to the fact that GPCRs exist as, or are capable of forming dimeric complexes. The range of GPCRs that have been subject to these studies are multitudinous and now include all the major classes of GPCR (class A, class B and class C). Examples are seen in receptors as diverse as the B2 bradykinin receptor, in which involvement of the N-terminus in receptor association was indicated (Said *et al.*, 1999) and in the chemokine receptor for MCP-1 (CCR2), where interactions seem to be largely modulated by the presence of agonist (Rodriguez-Frade *et al.*,1999). Instances of heterodimerization within this family are also common, of which the somatostatin receptors provide particularly illuminating examples. For instance, for the somatostatin receptor subtypes sst_1 and sst_5, heteromeric interactions are reported to result in an increase in agonist potency and efficacy and a change in agonist-mediated endocytosis (Rochville *et al.*, 2000). This is in contrast to interactions between somatostatin subtypes sst_{2A} and sst_3 (Pfieffer *et al.*, 2001) which result in a decrease in agonist potency and efficacy as well as a change in agonist mediated-endocytosis. Another member of the group of type A family receptors, which has been shown to exhibit dimerization, is the gonadotropin releasing hormone receptor (GnRHr). In a FRET based study on this receptor it was found that addition of the agonist buserelin promoted receptor microaggregation (Cornea *et al.*, 2000); this study was extended to show that the increased levels of FRET induced upon addition of agonist were not a consequence of receptor clustering into lipid vesicles but were instead due to a physical intimacy between the receptor molecules, imparted by a gain in mutual affinity. The experimental evidence for this was that the presence of cytocholasin D, a microfilament destabilising agent, did not alter the ability of buserilin to enhance

energy transfer. Type B family GPCRs are represented by interactions between the calcitonin receptor and one TM receptor activity modifying proteins (RAMPs), where the RAMP acts as a chaperone protein to the GPCR, accompanying the receptor as it passes through the cellular trafficking machinery of the E.R. and Golgi apparatus. The maturation process of the receptor is governed by the type of RAMP which is co-expressed with the calcitonin receptor. RAMPs 1and 3, when co-expressed with human calcitonin receptor, generate a receptor with a higher affinity for amylin than when this gene product is expressed with RAMP2 (Christopoulos *et al.*, 1999). Interactions between type C family GPCRs include heteromeric assemblies of subtypes of the γ-amino butyric acidB ($GABA_B$) receptor, where successful cell-surface expression of a fully functional receptor complex requires the presence of both $GABA_{B(R1)}$ and $GABA_{B(R2)}$ subtypes (Jones., *et al.* 1998; Kaupmann., *et al.*, 1998; White *et al.*, 1998; Kuner *et al.*, 1999; Sullivan *et al.*, 2000). Interactions between unrelated receptors belonging to different families have also been described. For instance, the adenosine A1 receptor (family A) has been shown to associate with metabotrobic glutamate receptor 1α (family C), by co-immunoprecipitation of co-expressed receptors in HEK 293T cells as well as endogenously expressed receptors in rat cerebellar synaptosomes (Ciruela., *et al* 2000). A more comprehensive and inclusive discussion of the diverse range of studies concerning the phenomenon of dimerization of GPCRs is provided in Chapter 1.

It had been seen, through the course of this investigation that certain receptors, when tagged with molecules that serve as appropriate donor and acceptor moieties, were capable of producing significant levels of energy transfer when co-expressed within mammalian cells and assayed for BRET (e.g. β2-AR-Rluc and β2-AR-eYFP; δ-opioid-Rluc and δ-opioid-eYFP; κ-opioid-Rluc and κ-opioid-eYFP). These findings

suggested that when co-expressed these respective pairings were in close spatial proximity such as would be expected if the molecules were capable of interacting with one another. Other receptor pairings (e.g. β2-AR-Rluc and δ-opioid-eYFP) did not produce large quantities of energy transfer, so no evidence could be but forward in support of these receptors being able to interact. To further explore the differing propensities of the various types of GPCR to either homo- or hetero-dimerize, it was thought desirable that some system should be established whereby, through consideration of the quantities of donor and acceptor tagged receptors present in the cells, the relative affinity of a particular GPCR tagged with *Renilla* luciferase for other GPCRs tagged with eYFP might be established. It was reasoned that through deliberately maintaining low levels of the *Renilla* luciferase tagged receptor in co-transfections with an eYFP tagged receptor construct, the amount of energy transfer could be monitored as a function of the eYFP tagged receptor concentration. It was anticipated that in such analyses a saturation point would eventually be reached, this point being where practically all of the Rluc tagged receptors would be partnered with eYFP tagged receptors. Through the comparison of the acceptor tagged receptor concentrations at which the system became saturated, it would be possible to draw conclusions about the relative affinities that any donor/acceptor tagged receptor pairing might have for one another, this was of course provided that the donor concentrations could be maintained at comparably low and unvarying levels in the respective analyses.

When such studies were attempted with Rluc and eYFP modified versions of the κ-opioid receptor, it was found that upon introducing increasing levels of κ-opioid-eYFP to a relatively unvarying amount of κ-opioid-Rluc a linear increase in the amounts of energy transfer could be observed (Figure 3.19). A saturation point was

not reached however and since the widest range of cDNA ratios possible were employed in the transfection stages of the experiment there was no way in which this could be achieved short of recourse to an alternative transfection method. In similar experiments, this time employing κ-opioid-Rluc and TRHr-eYFP as the donor/acceptor partners there was no convincing evidence to suggest that significant levels of energy transfer had been achieved (Figure 3.20) even though this parameter was tracked over a similar range of acceptor concentrations as was used in the previous experiment employing κ-opioid-Rluc and κ-opioid-eYFP as the donor/acceptor partners. In both of the experiments the donor tagged receptor concentrations were maintained at similar levels and these were comparatively low compared the acceptor concentrations tested. Despite the obvious differences between the ability of these two pairings to produce energy transfer events, the results presented, though suggestive, do not amount to a rigorous demonstration of an ability for κ-opioid receptor to form a homomeric complex in preference to a heteromeric complex with another distinct and distantly related receptor type.

It is however informative to consider the relationship between the amount of energy transfer and the proportion of the receptor molecules which were acceptors, in the light of a simplified model for GPCR dimerization. For such a model the simplifying assumption will be made that at the super endogenous levels of expression achieved in the experiments detailed above, any equilibrium that exists between donor and acceptor tagged receptors will reduce to a set of conditions where all the receptors are part of a dimeric complex, hence the only equilibrium which need be considered is: $[AA] + [DD] \leftrightarrow 2[AD]$, where [AA] and [DD] represent the concentrations of acceptor tagged receptor homo-dimers and donor tagged receptor homo-dimers respectively and [AD] represents the concentration of a heteromeric complex

consisting of both donor and acceptor tagged receptors. A second simplifying assumption is that all energy transfer signals are generated through the interaction of receptors as opposed to random collisions at the receptor surface densities achieved. Given these assumptions, it is expected that the proportion of donor tagged receptors in the heteromeric complex will determine the extent of energy transfer, since only these will contribute to energy transfer. Now let the proportion of receptor that are acceptors be defined as the acceptor fraction, where: acceptor fraction= (acceptors (receptors/cell)/acceptors (receptors/cell) + donors (receptors/cell)). If looking at homodimerization, then it is logical to assume that there is no bias between the formation of [DD] and [AD], and the proportion of donors in the heteromeric complex will be determined solely through the probability of A and D or D and D interacting with one another. It is evident, given no bias, that the relative concentrations of A and D respectively (represented here by the acceptor fraction) will determine this probability. Following this line of reasoning it is logical that in the case of homodimerization, saturation will only occur when there is an excess of acceptor tagged receptor over donor tagged receptor such that the acceptor fraction is approaching unity. In the case of heterodimerization, if there is strong bias in favour of the heterodimer then the equilibrium will lie well to the right and the associations between A and D will not be determined by random chance alone. In this case it might be expected that saturation would occur well before the proportion of acceptors approached unity, for example, if the bias were strong enough saturation might occur when the proportion of A:D was equal (0.5:0.5). On the other hand, if there was a strong bias against the formation of the heterodimer the equilibrium would lie well to the left and it might be expected that no significant levels of energy transfer would be observed even as the proportion of acceptors tended towards unity.

By plotting the acceptor fraction against the obtained energy transfer values for the κ-opioid-Rluc/κ-opioid-eYFP pairing, it can be seen that energy transfer increases with the acceptor fraction in a relationship that is best described as being linear (r^2=0.8) (Figure 3.24A). As predicted for homodimerization, the highest readings are those that cluster close to the point of unity on the x-axis. From the simplified model of dimerization it would be expected that these are about the highest readings which we might reasonable expect to obtain, since at this point virtually all of the donor molecules must be incorporated into the [AD] complex. In contrast to this when examining heteromeric interactions between κ-opioid-Rluc and TRHr-eYFP, even as the acceptor fraction tends towards unity there is still no evidence that significant levels of energy transfer are being achieved and this is under conditions where, if κ-opioidRluc and TRHr-eYFP had at least an equal affinity for one another it would be expected that the greatest levels of energy transfer achievable would almost have been reached (Figure 3.24B). One explanation for this anomaly, from considering the simple model for dimerization, is that in the case of the κ-opioid-Rluc/TRHr-eYFP pairing there is a very strong bias against the formation of the heterodimer and that even in the presence of a large excess in the proportion of acceptor tagged receptors it is still not possible to detect any significant energy transfer events. Hence one likely interpetation of this data is that κ-opioid-Rluc has a greater tendancy to interact with itself than with the more distantly related TRH receptor.

One alternative explanation for the anomaly between the data generated for the two donor/acceptor tagged receptor pairings tested is that TRHr-eYFP and κ-opioid-eYFP were not predominantly localized within the same compartments of the cell and that this imposed an artificial bias on the ability of κ-opioid-Rluc to interact with κ-opioid-eYFP. However, confocal analysis demonstrated that this was manifestly not the case,

Figure 3.24. Re-evaluation of the data for κ-opioid receptor homodimerization and heterodimerization of the κ-opioid receptor and TRHr receptor through consideration of these results in the light of a simplified dimerization model

(A) The data from Figure 3.19 was taken and the values obtained for the concentrations of both κ-opioid- Rluc and κ-opioid-eYFP (receptors/cell) were used to calculate the acceptor fraction defined as: acceptor fraction= (acceptors (receptors/cell)/ acceptors (receptors/cell) + (donors (receptors/cell)). This new parameter was then plotted against the values of energy transfer to yield the shown correlation graph (r^2=0.8). **(B)** The data from Figure 3.20 was taken and the values obtained for the concentrations of both κ-opioid-Rluc and TRHr-eYFP (receptors/cell) were used to calculate the acceptor fraction. This new parameter was the plotted against the values of energy transfer to yield the shown correlation graph (r^2=0.576).

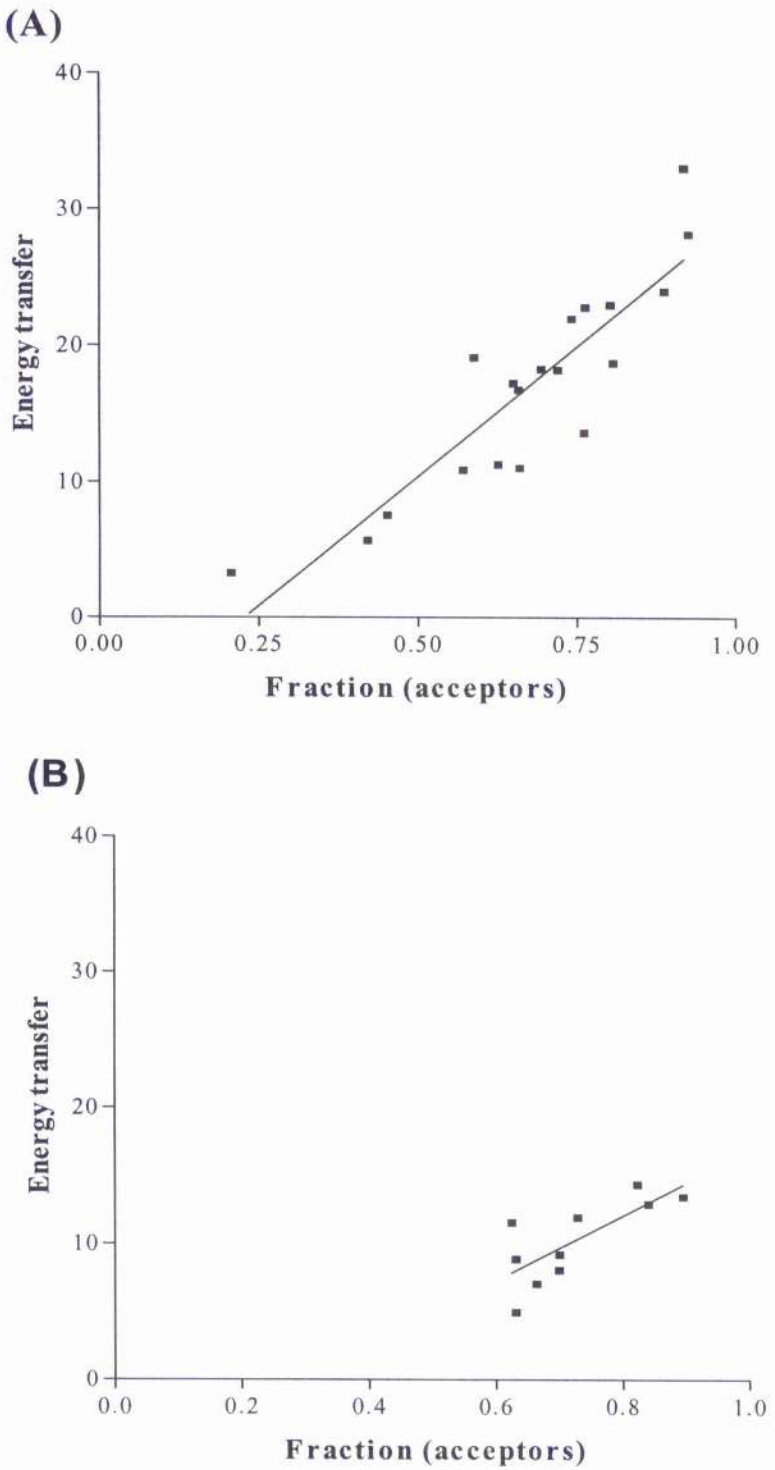
(A)
40
30
20
10
0
Energy transfer
0.00
0.25
0.50
0.75
1.00
Fraction (acceptors)
(B)
40
30
20
10
0
Energy transfer
0.0
0.2
0.4
0.6
0.8
1.0
Fraction (acceptors)

Figure 3.24.

with both TRHr-eYFP and κ-opioid-eYFP being equally capable of targeting successfully to the plasma membrane of the cell. It is therefore logical to assume that when either of these two eYFP tagged receptors were co-expressed with κ-opioid-Rluc there would be no spatial restrictions imposed upon the capacity of either of the pairings to interact.

A third way by which the anomaly between the data generated for the two donor/acceptor tagged receptor pairings may be explained is through the κ-opioid-Rluc/ TRHr-eYFP heterodimer being so orientated as for the efficiency of energy transfer between the two molecules to be effectively zero. It should be mentioned here that there is quite a large difference in the sizes of the carboxyl terminal tails of the TRHr and κ-opioid receptor, with TRHr possessing 91 amino acids immediately downstream of the NPXXY motif that marks the end of the seventh transmembrane helix contrasting with only 50 amino acids in the case of the κ-opioid. However it is not necessarily to be supposed that this carboxyl terminus is simply "dangling" underneath the receptor: it may well interact with other domains of the receptor, such as the intracellular loops and thus be incorporated into part of the receptors overall tertiary structure. It is also evident that many GPCRs are modified at the carboxyl terminus with lipid modifications as palmitic acid and that these are used to anchor the carboxyl terminus to the plasma membrane. The presence of such modifications upon the carboxyl terminal tails of TRHr and κ-opioid receptor would significantly alter the distance of the carboxyl-terminally attached Rluc/eYFP molecule from the periphery of the plasma membrane. Without detailed information concerning the tertiary structure of these two GPCRs it is not easy to determine what influence the discrepancy in the size of the TRHr and κ-opioid receptor carboxyl terminal tails

would have on the relative spatial differences between Rluc and eYFP in either the κ-opioid-Rluc/ κ-opioid-eYFP or the κ-opioid-Rluc/TRHr-eYFP pairings.

3.4. Conclusion

It was demonstrated that constitutive homodimerization could be observed for the β2-AR, the δ-opioid receptor and the κ-opioid receptor, using a biophysical technique called bioluminescence resonance energy transfer. For these receptor types, no ligand induced alterations in the strength of the energy transfer signal could be detected, indicating that the R* conformation of the receptor does not favour dimerization, as has been reported for other receptor types. It would seem rather, that these receptors arrive at the plasma membrane preformed as dimeric complexes, perhaps serving as mutual chaperone proteins, as is the case with the $GABA_B$ receptor, to facilitate in the correct trafficking of the receptor complex to the cell surface and to yield a fully functional receptor unit. When heteromeric interactions between the β2-AR-Rluc and the δ-opioid-eYFP receptors were examined, no strong energy transfer signals could be detected upon performance of the BRET assay so that no evidence that these two distinct and unrelated GPCRs interacted could therefore be obtained. However, upon addition of either the β2-AR agonist isoprenaline or the δ-opioid agonist DADLE, a reproducible, statistically significant increase in the levels of energy transfer could be obtained, suggesting that the presence of either of these two ligands was capable of enhancing the mutual affinity of these two receptor types. To try and elucidate whether or not a given GPCR would have differing affinities for interaction with distinct types of other GPCRs, a method was devised where increases in energy transfer could be monitored by varying the concentration of the acceptor tagged receptor, while maintaining the donor tagged receptor at a relatively unvarying level.

This method was applied to both homo-dimers between the κ-opioid receptors and heterodimers between κ-opioid-receptor and TRHr. The inability to achieve saturation over the range of acceptor concentrations tested in either of the two pairings tested meant that definite conclusions regarding the relative affinities could not be established. However, when the levels of energy transfer were plotted against the acceptor fraction, it could be seen that the data obtained for the κ-opioid-Rluc/ κ-opioid-eYFP pairing was not incompatible with a proposed, simplified dimer model. In the case of the κ-opioid-Rluc/ TRHr-eYFP pairing no significant levels of energy transfer were discernable even when the concentration of acceptor was in great excess of that of the donor. A lower affinity of TRHr for the κ-opioid receptor would be a likely explanation for the observed differences between the two sets of data. It was also possible that the differences could be attributed to very low energy transfer efficiency between a hypothetical κ-opioid-Rluc and TRHr-eYFP heteromer owing to an unfavourable orientation between the BRET partners and/or the discrepancy in the size of the receptors' carboxyl terminal tails.

It is unlikely that BRET-based detection of receptor dimerization would provide a useful basis on which an assay-screening programme for the detection of ligands with an affinity for a particular receptor could be established for industrial purposes. This is principally because, although homodimerization and heterodimerization occurs between certain GPCR types, in not all cases is the degree of interaction influenced by the presence of an externally binding ligand.

Chapter 4

Second Results Chapter

4.1. Introduction

4.1.1. $BRET_2$: a variant of bioluminescence resonance energy transfer

In recent years, resonance energy transfer techniques have become increasingly popular as a means of detecting intermolecular interactions and they are being used by an increasing number of researchers to investigate the phenomenon of dimerization of GPCRs. Such applications of energy transfer to this field of research are diverse with regards to the particular methodology employed, whether it relies on traditional FRET experiments between well characterized fluorophores such as rhodamine and fluorescein; on time resolved FRET experiments or on activation of the donor molecule via bioluminescence with subsequent energy transfer to a mutant GFP.

As a result of the rapid expansion in such applications of resonance energy transfer techniques, a variant of BRET has been developed by Packard, specifically designed to offer considerable advantages over preceding methods employing bioluminescence. This variant system, called $BRET_2$, differs from traditional BRET in two ways: it employs a modified version of h-coelenterazine, known as DeepblueC, to act as a donor for electronic excitation energy and it utilizes a mutant version of GFP (GFP_2) to function as an energy acceptor. These modifications to traditional BRET (hereafter known as $BRET_1$) result in a donor/acceptor pairing which has emission peaks centred on 395nm and 510nm respectively (see manufacturer's web site: http://www.packardbioscience.com). This broad spectral resolution (approximately 115nm) between the donor and acceptor has been shown to offer a substantial

improvement in the GFP signal to background noise when conducting energy transfer experiments using positive controls for both $BRET_1$ and $BRET_2$ systems (see manufacturer's web site: http://www.packardbioscience.com). It should also be mentioned that transition from using $BRET_1$ to $BRET_2$ is greatly facilitated by the fact that DeepBlueC, like h-coelenterazine, acts as a substrate for *Renilla* luciferase, so that Rluc tagged receptor constructs used in previous experiments may be easily incorporated into the $BRET_2$ methodology.

In the previous chapter it was shown that a number of postulates might reasonably be formed concerning the dimerization of GPCRs: that they were capable of both homo and hetero-dimerization; that particular types were constitutively associated when co-expressed within mammalian cells and that receptors which shared a high degree of sequence homology possessed a greater propensity for mutual interaction. It was also established that resonance energy transfer was a novel and effective method for examining the interactions between these molecules. The experiments presented in the first half of the results section of this Chapter make use of $BRET_2$ to both confirm and extend these studies, particularly in determining whether or not agonists and/or antagonists are capable of inducing alterations in the extent of dimerization, since a high degree of sensitivity is required to detect such changes if they are only small in their extent.

4.1.2. Interaction of GPCRs with intracellular molecules involved in the desensitisation process: a possible alternative to GPCR dimerization as a means of identifying ligand activated receptors

The investigation into the phenomenon of dimerization of GPCRs was, to a certain extent, initiated in the hope that such studies would provide novel methods of

screening compounds for ligand binding affinity and that this would lead to the development of an assay that would be applicable to industrial usage in identifying ligands for orphan GPCRs. A different approach, which may prove useful in this respect (that of ligand screening) focuses more on the downstream processes which occur rapidly (typically within a few seconds to minutes) upon agonist activation of GPCRs, a sequence of events known as desensitisation. The process of receptor desensitisation is traditionally seen as resulting in termination or attenuation of receptor signalling. It may be achieved by two different, though similar, patterns of events known as homologous and heterologous desensitisation. The former involves a process mediated by two distinct protein types: G-protein coupled receptor kinases (GRKs) which act to phosphorylate G-protein coupled receptors (Inglese *et al.*, 1993) and β-arrestin molecules, which are recruited from a cytoplasmic pool following receptor phosphorylation (Wilson and Appleby, 1993). A brief account of the mechanism of homologous desensitisation is as follows. To begin with, an agonist binds to and stabilizes the active conformation of a receptor; this is followed by a rapid recruitment of a GRK from the cytosol to the plasma membrane (Barak *et al.*, 1999), probably mediated via the interaction of free βγ subunits of heterotrimeric G-proteins made available by receptor activation (Daaka *et al.*, 1996). Once localized to the plasma membrane, the activated receptor acts as a substrate for the GRK. Consequently, within regions of its carboxyl terminal tail and intracellular loops, the receptor is phosphorylated on serine and threonine residues. This increases the affinity of the receptor for β-arrestin and promotes translocation of β-arrestin from the cytoplasm. Direct physical contact between β-arrestin and the receptor prevents any continuation of receptor-G-protein interactions thus attenuating further signalling events. Only receptors occupied by agonists may serve as substrate for the GRK and

since this will be specifically the activated receptors which initiated desensitisation, the process is strictly homologous. In heterologous desensitisation, phosphorylation of the GPCR is mediated by second messenger dependent kinases such as PKA and PKC. These kinases do not exhibit specificity with regards to the GPCR at the plasma membrane: hence a mechanism is established whereby crosstalk between different receptor pathways can lead to phosphorylation of a substrate receptor without the need for agonist occupancy, priming it for an attenuated response to any subsequent challenges with agonist.

The receptor-β-arrestin interactions that mediate the homologous desensitisation process are particularly attractive as targets for developing an assay that would be capable of detecting agonist affinity for a particular GPCR type. This is because, generally, in the large number of studies involving arrestins and particularly in one study involving more than 15 different types of receptor (Barak *et al.*, 1997), GPCRs have been found to almost universally utilize the β-arrestin pathway in mediated the short term attenuation of signalling.

In the experiments involving β-arrestin presented in the second section of this Chapter, β-arrestin molecules modified with GFP derived from the organism, *Aequoria victoria* or novel fluorescent proteins (NFPs) derived from the organisms *Anemio majano*, *Amenio sulcata* and *Zoanthus Sp*, have been used to examine the relative affinities of β-arrestin-1 and β-arrestin-2 for the chemokine receptor CCR2 using confocal microscopy techniques. The NFPs are part of a new generation of fluorescent proteins that consist of nine separate cDNAs. Upon expression in mammalian cells they fluoresce at distinct wavelengths in response to excitation with light of a suitable wavelength and offer a greater diversity of colours than the GFP range, where mutagenesis of the original GFP cDNA is used to obtain variants with

altered light emission characteristics. Some of the NFPs possess overlapping light excitation and emission spectra: for instance between cyan-NFP and yellow NFP, as well as between yellow NFP and red NFP. This potentially enables them to be used in FRET based experiments designed to examine protein/protein interactions such as those which occur in the process of desensitization, following on from receptor activation. Red NFP should also be useful in studies concerning the co-localization of cellular proteins, as it emits light at a wavelength which is easily distinguishable from that emitted by cyan, yellow or green fluorescent protein variants. Existing studies that attempt to co-localize receptors with intracellular molecules such as β-arrestin tend to make use of a GFP tagged arrestin and an antibody to label the receptor which is usually conjugated to a fluorescent dye such as Rhodamine B or Texas red (for an example see, Groark *et al.*, 1999). An advantage of conducting such experiments with both receptor and intracellular molecule directly fused to either one of two easily distinguishable fluorescent proteins is that the experiments can be conducted on live cells, in real time and do not require any of the fixing processes which are necessary in similar experiments using antibodies.

CCR2, a receptor for the C-C chemokine monocyte chemoattractant protein 1 (MCP-1), was chosen for this study because previous reports had indicated that it utilized the β-arrestin pathway in mediating a rapid attenuation in the generation of second messenger molecules, demonstrated in studies where phosphorylation of the receptors carboxyl terminal tail was accompanied by a rapid desensitisation of calcium mobilization (Aragay *et al.*, 1998). Both GRK2 and β-arrestin have been implicated in this process, forming a macromolecular complex with the receptor shortly after MCP-1 binding (Aragay *et al.*, 1998). This desensitisation pathway may be important in

mediating an on-off mechanism for delivering signals essential for migration across a chemotactic gradient.

The results presented in the subsequent part of this chapter represent the first analysis of β-arrestin interactions with CCR2 using confocal microscopy techniques and at the same time, they provide the groundwork whereby a FRET based assay might be developed for the detection of agonist activation of GPCRs.

4.2. Results

To confirm that $BRET_2$ would be a suitable technique for exending and corroborating the findings detailed in Chapter 3, a positive control vector was constructed which directly fused the cDNA for *Renilla* luciferase with that of the mutant GFP, GFP_2 (as described in section 2.4.4). The light emission spectrum aquired from HEK 293T cells transiently transfected with this positive control vector had two distinct emission peaks visible, one centred on 395nm corresponding to light emitted via the enzymatic action of *Renilla* luciferase on DeepBlueC and the other centred on 510nm corresponding to light emitted as a result of energy transfer to GFP_2 (Figure 4.1A). As was anticipated, the peak centred on 395nm did not exhibit any substantial overlap with the second peak centred on 510nm. This contrasted with the light emission spectrum from the $BRET_1$ positive control vector consisting of a fusion between *Renilla* luciferase and eYFP. The light emission spectrum obtained from HEK 293T cells transiently expressing the $BRET_1$ positive control vector following addition of coelenterazine was obtained previously and is shown again here (Figure 4.1B) to provide a direct comparison between $BRET_1$ and $BRET_2$. The resolution of the two peaks can clearly be seen as being improved in the case of the $BRET_2$. It was also observed however, that the intensity of light emitted from the $BRET_2$ positive control vector was rather weak. This was unlikely to be attributed to low expression levels of

the chimeric protein since addition of coelenterazine to the same cells produced a light emission spectrum which was comparable in intensity to that obtained from transfections with the $BRET_1$ positive control (results not shown). It is more likely that the weak levels of light emission were due to a low quantum yield of the donor molecule, where the number of photons emitted per number of molecules of DeepBlueC converted to the excited electronic state would be low when compared to coelenterazine. Another possibility is that the turnover number of *Renilla* luciferase when using DeepBlueC as a substrate is markedly decreased, but without a more thorough analysis which is beyond the scope of the experiments presented here it is impossible to distinguish between these two hypotheses. Nonetheless, it was decided that given the superior resolution between the donor and acceptor emission peaks, $BRET_2$ would provide a more sensitive means of detecting energy transfer, although detection of the weak light signals emitted from the system would require a high degree of sensitivity on the part of the photo-detection apparatus used in order to adequately detect the signal. Given this set of conditions, it was decided that all $BRET_2$ experiments would henceforth be carried out using optical multiwell plate readers utilizing fixed bandwidth filters, since such devices were more sensitive than more conventional fluorimeters.

$BRET_2$ technology was initially applied to the δ-opioid receptor, principally because this receptor had already been thoroughly investigated previously using $BRET_1$ (see Chapter 3) and it would therefore be of interest to compare results obtained using $BRET_2$, as applied to this receptor, with those obtained formerly. To achieve this, GFP_2 was fused to the carboxyl terminal tail of the δ-opioid receptor (as described in section 2.4.7). To confirm that the δ-opioid-GFP_2 construct was capable of being expressed and targeted appropriately to the plasma membrane the cDNA was

transiently transfected into HEK 293T cells and visualized under a confocal microscope (Figure 4.2). The results confirmed that the construct was capable of reaching the plasma membrane, however unlike κ-opioid-eYFP and TRH-eYFP there were a large number of cells exhibiting a substantial intracellular pool of receptors, apparently retained in the E.R./Golgi apparatus. This intracellular retention of the δ-opioid-GFP_2 is less likely to be due to the carboxyl-terminal tail modification of the receptor as to being a consequence of the maturation process of the receptor itself. This opinion is supported by a recent study were examination of the kinetics of δ-opioid-receptor transport through various intracellular compartments (Petaja-Repo *et al.*, 2000) showed that there was a low overall efficiency of receptor maturation, with less than 50% of the precursor protein being processed to a fully glycosylated receptor and which suggested that only a fraction of the synthesised receptors attained the properly folded conformation that allowed exit from the E.R.

Having established previously that energy transfer levels observed between BRET partners were largely dependent upon the concentration of the acceptor tagged molecules, the receptor number in HEK 293T cells transiently transfected with the cDNA for δ-opioid-GFP_2 was correlated with arbitrary fluorescence as determined using a fluorimeter. This was performed in a manner similar to the experiments described in Chapter 3 using κ-opioid-eYFP. As expected, the correlation graph showed a linear relationship between the two sets of values, allowing the value of receptor number/cell to be conveniently estimated in $BRET_2$ experiments by measuring the fluorescence intensity exhibited upon excitation of a known number of cells (Figure 4.3). Typical receptor expression levels for membranes transfected with δ-opioid-GFP_2 cDNA were (2470 fmol/mg ± 150, n=2), which was significantly

greater than the expression levels obtained in radioligand binding experiments on the δ-opioid-Rluc construct (250 ± 90 fmol/mg).

$BRET_2$ was then applied to reinvestigate homo-dimerization of the δ-opioid receptor. Co-transfection of δ-opioid-GFP_2 and δ-opioid-Rluc into HEK293T cells resulted in a robust enegy transfer signal upon addition of DeepBlueC (Figure 4.4), the magnitude of which was comparable to that obtained for the $BRET_2$ positive control vector. The energy transfer signal generated, in terms of signal to noise, was a substantial improvement over $BRET_1$. The $BRET_2$ positive control exhibited an approximately 4-fold increase in (GFP_2/Rluc) ratio as compared to the ratio obtained from cells expressing the δ-opioid-Rluc alone whereas the $BRET_1$ positive control exhibited only a twofold increase above the ratio (eYFP/Rluc) obtained from HEK 293T cells expressing the β2-AR-Rluc construct alone (see Chapter 3, Figure 3.9). Despite these advantages, it was still not possible to detect any agonist or antagonist induced alterations in the extent of energy transfer when the transfected cells were exposed to a 10 minute pre-incubation of either DADLE or ICI 176 864 (both 10μM) (Figure 4.4). The result reaffirmed the findings of Chapter 3 which indicated that external ligands were incapable of altering the dimerization status of the δ-opioid receptor. Independent monitoring of fluorescence, obtained from the co-transfected HEK 293T cells used in the $BRET_2$ experiments detailed above, revealed that there were approximately 114,000±5000 GFP_2 tagged receptors/cell.

Since previously with traditional BRET it had been shown that a small degree of energy transfer could be observed upon co-expressing the β2-AR-Rluc with δ-opioid-eYFP, it was decided that this result should be re-evaluated using $BRET_2$. HEK 293T cells were co-transfected with both β2-AR-Rluc with δ-opioid-GFP_2 and the light emission spectrum obtained upon addition of DeepBlueC acquired. Energy transfer

levels between these two constructs were lower than those observed between δ-opioid-Rluc and δ-opioid-GFP_2, about 2/3 as great as that observed with the positive control vector (Figure 4.5), despite expressing a greater number of acceptor tagged receptors/cell (152,000± 12,000). The energy transfer signal generated between β2-AR-Rluc and δ-opioid-eYFP was however substantially greater than that which was obtained in experiments which used $BRET_1$ to determine the spatial proximity between these two receptor types. Using $BRET_2$, the strength of this signal seemed to be unaffected by the presence of either the δ-opioid receptor agonist DADLE or the β2-AR agonist isoprenaline. Equally, the concerted action of both agonists together produced no detectable changes (Figure 4.5). These results were somewhat contradictory to those obtained in Chapter 3, where no significant amount of energy transfer was observed between β2-AR-Rluc and δ-opioid-eYFP and it was found that addition of agonist for either receptor type was capable of inducing modest increases in the amount of energy transfer observed. However the results obtained using $BRET_2$ were consistent with a study of these two receptor types, based on co-immunoprecipitation data, where they were found to be constitutively heterodimerized when co-expressed in HEK 293T cells (Jordan *et al.*, 2001). In these studies the effects of ligand occupancy upon the strength of the heteromeric complex were not investigated. Given that the results obtained using $BRET_1$ for energy transfer between this receptor pairing were at or near to the limits of resolution for the detection of interactions and considering the added sensitivity which the $BRET_2$ system confers, it is possible that the $BRET_2$ results are more reliably accurate and that the results obtained with $BRET_1$ were, to a certain extent, artefactual.

Heterodimerization between the δ-opioid receptor and the κ-opioid receptor was investigated next using the $BRET_2$ system. The cDNAs for κ-opioid-Rluc and δ-

opioid-eYFP were co-transfected into HEK 293T cells and the ratio of (GFP_2/Rluc) upon addition of DeepBlueC was determined. A significant degree of energy transfer was detected between the two constructs, this being approximately 80% as strong as that observed with the $BRET_2$ positive control vector (Figure 4.6). Again, neither the addition of agonists or antagonists directed against the δ-opioid receptor (DADLE and ICI 174 864) or the κ-opioid-receptor (ICI 199 441 and GNTI) were capable of affecting the extent of energy transfer and the concerted action of the two agonists together proved similarly ineffective in producing any changes (Figure 4.6). This reinforced the findings obtained in Chapter 3, that these two receptor types were capable of heterodimerization and was in agreement with other previous studies (Jordan and Devi, 1999).

Having firmly established that there was no possibility of detecting alterations in energy transfer signals associated with agonist regulated changes in the dimerization status of opioid receptors, attention was turned to the downstream processes of desensitisation to see if these would provide more suitable targets for the detection of receptor activation.

To begin this study, the cDNA for β-arrestin2 was ligated upstream of the cDNA for the fluorescent proteins, cyan NFP and red NFP. The cDNA for β-arrestin2-cyan NFP was transiently transfected into CHO-K cells stably expressing CCR2, the chemokine receptor for MCP-1. This receptor was chosen as it had been previously reported that it utilized the β-arrestin pathway to mediate desensitisation of receptor signalling, a process strongly influenced by the expression levels of GRK2 (Aragay *et al.*, 1998). Upon visualization of the transfected cells using confocal microscopy, the cyan NFP was clearly visible and was localized exclusively to the cytoplasm of the cell (Figure 4.7.) This was in-keeping with previous observations made with GFP modified

versions of the molecule, where β-arrestin2 was seen to be present in the cytoplasm but excluded from the nucleus of the cell (Barak *et al.*, 1997). Following addition of MCP-1 (1μM), a translocation of the β-arrestin2-cyan NFP from the cytosol to the plasma membrane occurred within a space of 2 to 4 minutes (Figure 4.7). Within 20 minutes, a distinct punctate pattern could be seen to have formed within the cells indicative of a sustained interaction between the internalised receptors and the β-arrestin2-cyan NFP molecule (Figure 4.7). The formation of this pattern persisted within the cell and 30 minutes following agonist exposure the punctate pattern was strongly visible in all cells within the field of view (Figure 4.7). This clearly showed that addition of cyan-NFP to the carboxyl terminal tail of β-arrestin2 did not significantly affect the molecule's ability to target to appropriate cellular locations upon expression in mammalian cells. Nor did it affect the ability of β-arrestin2 to migrate to the plasma membrane in response to receptor activation by an external agonist or its capacity to form part of the macromolecular complex which facilitates the process of receptor desensitisation.

The experiment was then repeated, this time by transiently transfecting the CCR2 stable cell line with the cDNA for the β-arrestin2-red NFP. As was the case with β-arrestin2-cyan NFP the cellular distribution of the β-arrestin2-red NFP construct was seen to be exclusively cytoplasmic when viewed under a confocal microscope (Figure 4.8). Addition of MCP-1 produced a rapid recruitment of the β-arrestin2-red NFP from the cytoplasm as a response to receptor activation with practically all of the cytoplasmic pool having migrated to the plasma membrane within 6 minutes (Figure 4.8). Within 24 minutes a clearly defined punctate pattern could be observed to have formed at the periphery of the cell membrane, indicative of the presence of β-arrestin2-red NFP within endocytic vesicles which could be seen to have migrated

towards sites further inside the cell at later time points (Figure 4.8,G and H) as sequestration proceeded. These observations showed that β-arrestin2 was unaffected as a result of the addition of red NFP to its carboxyl terminal tail.

To extend this study it was decided that similar experiments should be performed to investigate the pattern of β-arrestin1 recruitment in the same CCR2 stable cell line. To achieve this, a β-arrestin1-GFP fusion protein was used, as this had been previously shown to recruit to the plasma membrane in cells stably expressing the TRH receptor-1 upon addition of agonist (Groarke *et al.*, 1999). The cDNA for β-arrestin1-GFP was transiently transfected into the CCR2 stable cell line and then visualized using a confocal microscope. The β-arrestin1-GFP was present both in the cytoplasm and the nucleus of the cell (Figure 4.9 (A)); this was consistent with previous observations in experiments using the same construct (Groarke *et al.*, 1999). Upon addition of the agonist MCP-1 (1μM) there was a distinct translocation of β-arrestin1-GFP from the cytoplasm of the cell to the plasma membrane after about 12 minutes had elapsed, while the nuclear pool of β-arrestin1-GFP remained intact (Figure 4.9). This was considerably slower than the response observed using the β-arrestin2-NFP constructs indicating that the activated CCR2 receptor might have a higher affinity for β-arrestin2 than for β-arrestin1. As was the case with β-arrestin2, β-arrestin1-GFP did not remain localized with an even distribution at the plasma membrane, but instead remained closely associated with the endocytic vesicles containing internalised CCR2 receptor. This is clearly demonstrated by examination of Figure 4.9(H), where the punctate distribution of β-arrestin1-GFP can clearly be seen to have migrated from the cell periphery to more distant sites located within the cell 30 minutes after addition of agonist.

The observations made with the β-arrestin2-cyan NFP and β-arrestin2-red NFP were unlikely to be artefacts coincidently caused by the conditions under which the cells were maintained throughout the course of the experiments. In support of this contention, the CHO-K1 cell line stable expressing CCR2 was transiently transfected with the cDNAs for either β-arrestin2-cyan NFP or β-arrestin2-red NFP. The cells were then set up as previously for viewing under the confocal microscope and were this time challenged with IL-8, a peptide agonist with affinity for CXC-chemokine receptors (types 1 and 2) and which does not have any significant affinity for CCR2. Addition of IL-8 (1μM) did not cause any redistribution of cytoplasmic β-arrestin2-cyan NFP or β-arrestin2-red NFP to the plasma membrane even when monitored up to 30 minutes following exposure to the peptide (Figure 4.10).

To demonstrate that receptor activation was an absolute requirement for the initiation of arrestin-translocation, the response of β-arrestin2-cyan NFP, transiently transfected into the CHO-K cell line stably expressing CCR2, to the CCR2 antagonist GW5906723X (10μM) was monitored using a confocal microscope. It can be seen that exposure to this antagonist compound had no effect on the cytoplasmic distribution of the β-arrestin2-cyan NFP and even after 30 minutes there was no sign of the formation of a punctate pattern such as that which was observed following similar treatments with the agonist MCP-1 (Figure 4.11).

To show that the presence of this antagonist in the extracellular medium was capable of blocking activation of the desensitisation pathway, the CCR2 stable cell line was transiently transfected with β-arrestin2-cyan NFP and then exposed to a 30 minute pre-incubation with GW5906223X (10μM), after which examination of the cells under the confocal microscope did not reveal any signs of a punctate redistribution in the cellular location of β-arrestin2-cyan NFP (Figure 4.12 (A)). Maintaining the cells

in the presence of the antagonist, a further treatment of MCP-1 (1μM) was added to the extracellular medium, following which there was no rapid mobilization of β-arrestin2-cyan NFP to the plasma membrane in contrast to experiments conducted in the absence of any antagonist. After a further 30 minutes had elapsed the cells were again examined and images were obtained, revealing that some of the cells within the field of vision displayed a limited redistribution in the cellular location of β-arrestin2-cyan NFP, although it required close inspection to discern this and it was not especially pronounced (Figure 4.12 (B)). The result suggests that although the presence of antagonist attenuated the efficacy of MCP-1 in mobilizing the intracellular components of the desensitisation pathway through competition with the agonist for receptor binding sites, a small amount of receptor activation still continued to occur.

Attention was next turned towards whether or not these observations might be quantified in a FRET based assay system which would be amenable to a high throughput ligand screening process. To this end the cDNA for the CCR2 receptor was ligated upstream of the cDNA for yellow NFP to create a CCR2-yellow NFP fusion protein. This was then transiently transfected into CHO-K1 and HEK 293T cells and then examined under a confocal microscope. Unfortunately the construct seemed to be impaired in its ability to reach the plasma membrane. This problem was best demonstrated in a co-transfection of CCR2-yellow NFP and β-arrestin2-red NFP in CHO-K cells. Here, excitation of either of the fluorophores, whose respective cellular locations were revealed through use of appropriate filters, showed that the CCR2-yellow NFP was localized entirely within the cellular compartments of the cytoplasm and the nuclear membrane, with the boundaries of the cell being delineated by the cellular distribution of β-arrestin2-red NFP (Figure 4.13). In addition to this,

the cellular distribution of CCR2-yelllow was seen to be somewhat globular, indicative of a certain involuntary aggregation of the chimeric receptor construct. Since the CCR2-yellow NFP seemed incapable of targeting to the plasma membrane it was deemed unsuitable as an exploratory tool for the continuance of these studies, being both inaccessible to agonists present in the extracellular environment and in the wrong location to engage with intracellular components of the desensitisation machinery.

Despite these reverses, the results which showed that β-arrestin2 recruited to the plasma membrane more rapidly than β-arrestin1, hence potentially indicating a higher affinity, were interesting and it was decided that this should be investigated more thoroughly. To achieve this, the CCR2 stable cell line was transiently co-transfected with both β-arrestin1-GFP and β-arrestin2-red NFP and the response of each construct within the same cells to receptor activation with MCP-1 (1μM) was determined. Acquisition of images both before and after the MCP-1 treatment revealed that after 30 minutes had elapsed the β-arrestin2-red NFP had redistributed to a punctate pattern indicating sequestration of this construct at the endocytic vesicles containing internalised receptor (Figure 4.14). In contrast β-arrestin1-GFP displayed no such redistribution in the pattern of localization in cells where it was co-expressed with β-arrestin2-red NFP (Figure 4.14), consistent with the previous observation that the kinetics of β-arrestin1 recruitment were substantially slower than those of β-arrestin2 upon activation of CCR2. This result indicates that in cells co-expressing β-arrestin2-red NFP and β-arrestin1-GFP, a higher affinity for the activated CCR2 receptor promotes the translocation of β-arrestin2-red NFP from the cytosol in preference to β-arrestin1-GFP. Once sequestered at the endocytic vesicles through interaction with

components of the clatherin mediated internalisation pathway, the β-arrestin2-red NFP prevents any translocation of β-arrestin1-GFP.

To provide evidence that the ability of a β-arrestin2- NFP construct to respond to receptor activation was not only restricted to the CCR2 receptor, the response of β-arrestin2-red NFP to agonist stimulation of the angiotensin II type 1 receptor (AT1AR) was examined. To achieve this, CHO-K cells stably expressing the AT1AR were transiently transfected with β-arrestin2-red NFP. The response of the cells to addition of angiotensin II (10μM) was then monitored using a confocal microscope. Initially there was no clear translocation of β-arrestin2-red NFP from the cytosol to the plasma membrane as was observed in similar experiments with CCR2. However after 30 minutes a clearly defined punctate pattern could be recognized, indicating that β-arrestin2-red NFP had been localized to newly formed endosomes within the cell (Figure 4.15).

Finally, to extend further the number of GPCRs for which the nature and kinetics of β-arrestin recruitment could be evaluated using β-arrestin2 NFP constructs, it was thought desirable that the response of these molecules to ligand activation of endogenously expressed GPCRs within HEK 293T and CHO-K cells should be evaluated. Consequently, naïve CHO-K1 cells were transiently transfected with β-arrestin2-cyan NFP and then examined under a confocal microscope. Neither the addition of ATP to stimulate purinergic receptors nor the addition of calcitonin to activate calcitonin receptors was capable of eliciting an immediate response from the β-arrestin2-cyan NFP. More prolonged exposure to the respective agonists similarly failed to result in a redistribution of the β-arrestin2-cyan NFP from a diffuse cytosolic distribution to a localized punctate pattern (Figure 4.16). In similar experiments naïve HEK 293T cells were transiently transfected with the β-arrestin2-cyan NFP construct;

Figure 4.1. Comparison of the light emission spectra obtained from $BRET_2$ positive control with $BRET_1$ positive control.

(A) The light emission spectrum obtained from HEK 293T cells transiently transfected with the $BRET_2$ positive control vector following addition of DeepBlueC reagent (5μM) **(B)** Shown for comparison is the light emission spectrum obtained from HEK 293T cells transfected with $BRET_1$ positive control vector upon addition of coelenterazine (5μM). Results represent a single transfection from three such experiments performed.

(A)

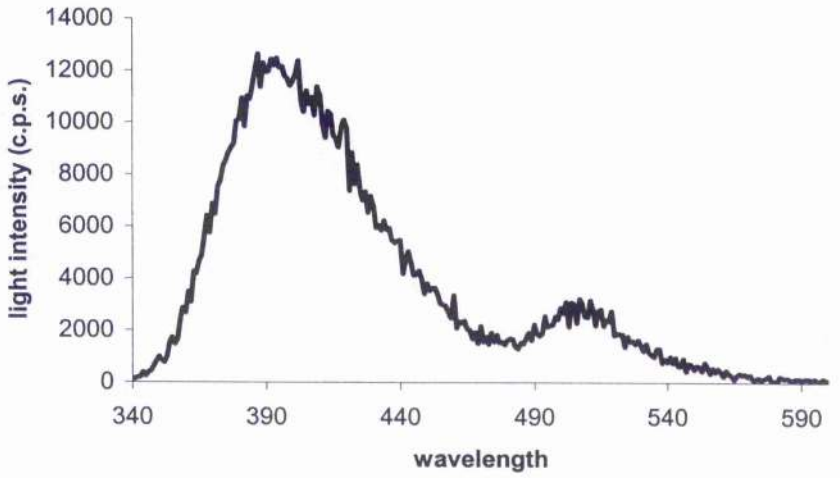
14000
12000
10000
8000
6000
4000
2000
0
light intensity (c.p.s.)
340
390
440
490
540
590
wavelength

(B)

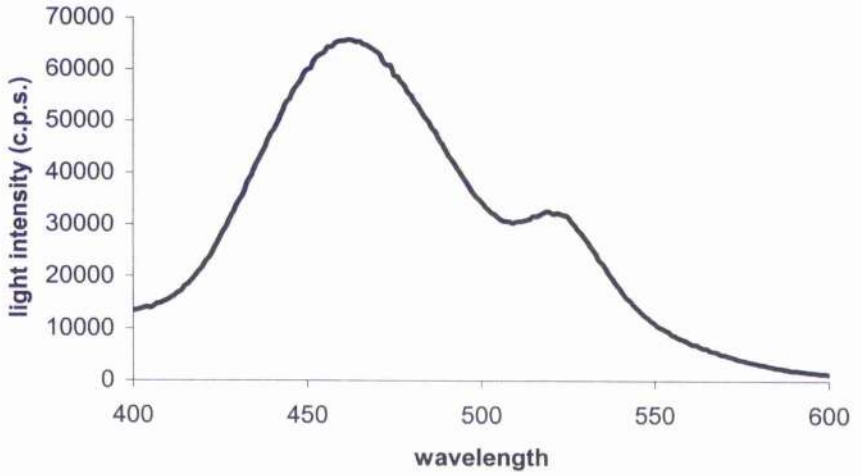
70000
60000
50000
40000
30000
20000
10000
0
light intensity (c.p.s.)
400
450
500
550
600
wavelength

Figure 4.1

Figure 4.2. The cellular location of the δ-opioid-GFP_2 construct when transiently transfected into HEK 293T cells.

Images were generated using scanning confocal microscopy. Results represent typical images obtained from one of two such experiments performed.

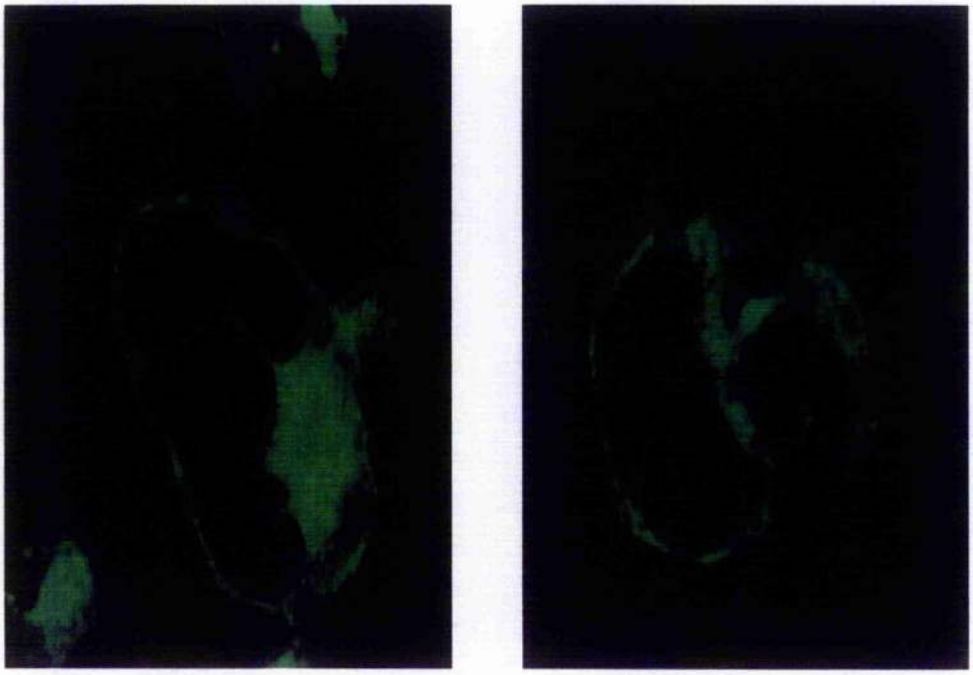

Figure 4.2.

Figure 4.3. Correlation of δ-opioid-GFP_2 receptor number with fluorescence. Membrane preparations from cells transiently transfected with δ-opioid-GFP_2 were subject to serial dilution and each dilution point was then assayed for fluorescence on a Victor^2 multiplate well reader. Parallel binding studies with [^{3}H]-naltrindole (5nM) on equivalent dilutions of the same membrane preparations determined the amount of receptor (fmol) at each dilution point. Data shown is a representative of two such transfections performed with error bars representing the S.E.M. between triplicate well readings. The Y-error bars are too small to be observed.

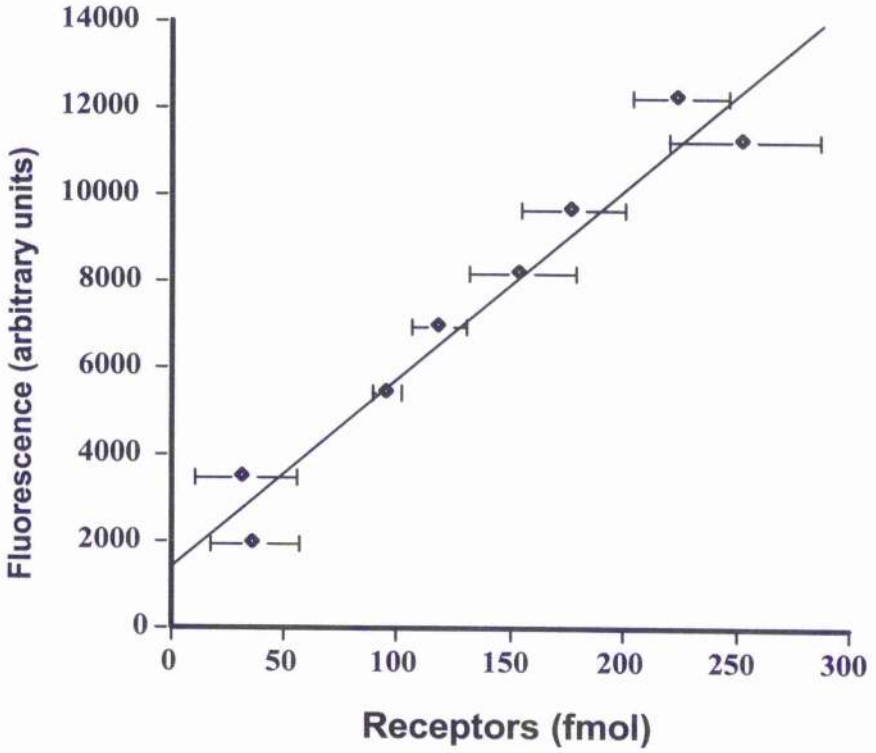
14000
12000
10000
8000
6000
4000
2000
0
Fluorescence (arbitrary units)
0
50
100
150
200
250
300
Receptors (fmol)

Figure 4.3.

Figure 4.4. Detection of δ-opioid receptor homodimerization using $BRET_2$.

The amount of light emitted from both *Renilla* luciferase and GFP_2 was quantitated using filters of fixed bandwidth on a Victor^2 multiwell plate reader. Readings were taken from wells containing HEK 293T cells, either transfected with the positive control vector $pBRET_2$+, with both δ-opioid-Rluc and δ-opioid-GFP_2 constructs, or with δ-opioid-Rluc alone to determine the background ratio of light emission (GFP_2)/Rluc. To see if there were any alterations in the ratio (GFP_2/Rluc) upon addition of agonist or inverse agonist ligands cells co-transfected with both δ-opioid-Rluc and δ-opioid-GFP_2 were subject to a 15 minute pre-incubation period with either DADLE or ICI 174 864 prior to addition of DeepBlueC. The results represent means ± S.E.M. of three independent experiments.

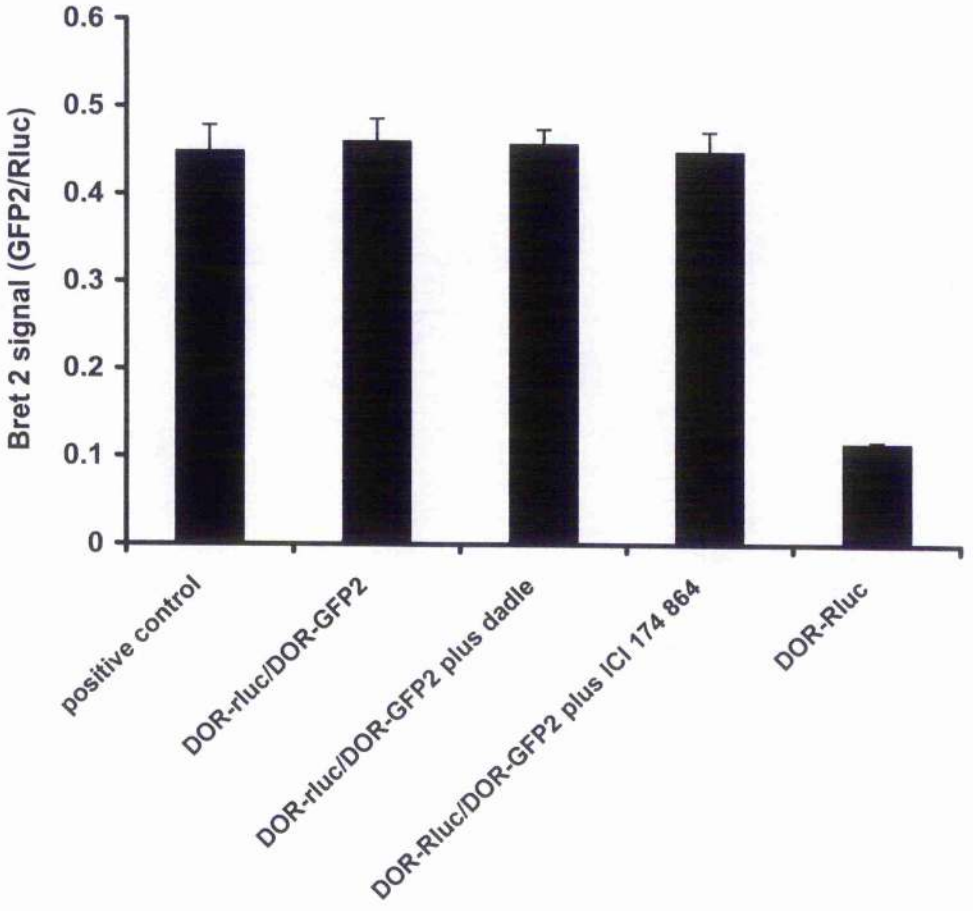
Bret 2 signal (GFP2/Rluc)
0.6
0.5
0.4
0.3
0.2
0.1
0
positive control
DOR-rluc/DOR-GFP2
DOR-rluc/DOR-GFP2 plus dadle
DOR-Rluc/DOR-GFP2 plus ICI 174 864
DOR-Rluc

Figure 4.4.

Figure 4.5. Detection of heterodimerization between the β2-AR and the δ-opioid receptor using $BRET_2$.

The amount of light emitted from both *Renilla* luciferase and GFP_2 was quantitated using filters of fixed bandwidth on a Victor^2 multiwell plate reader. Readings were taken from wells containing HEK 293T cells either transfected with the positive control vector $pBRET_2$+, with both β2-AR-Rluc and δ-opioid-GFP_2 constructs, or with β2-AR-Rluc alone to determine the background ratio of light emission (GFP2)/Rluc. To see if there were any alterations in the ratio (GFP_2/Rluc) upon addition of agonist ligands, cells co-transfected with both β2-AR-Rluc and δ-opioid-GFP_2 were subject to a 15 minute pre-incubation period with either DADLE, isoprenaline, or both DADLE and isoprenaline (each at 10μM) together prior to addition of DeepBlue C. The results represent means ± S.E.M. of three independent experiments.

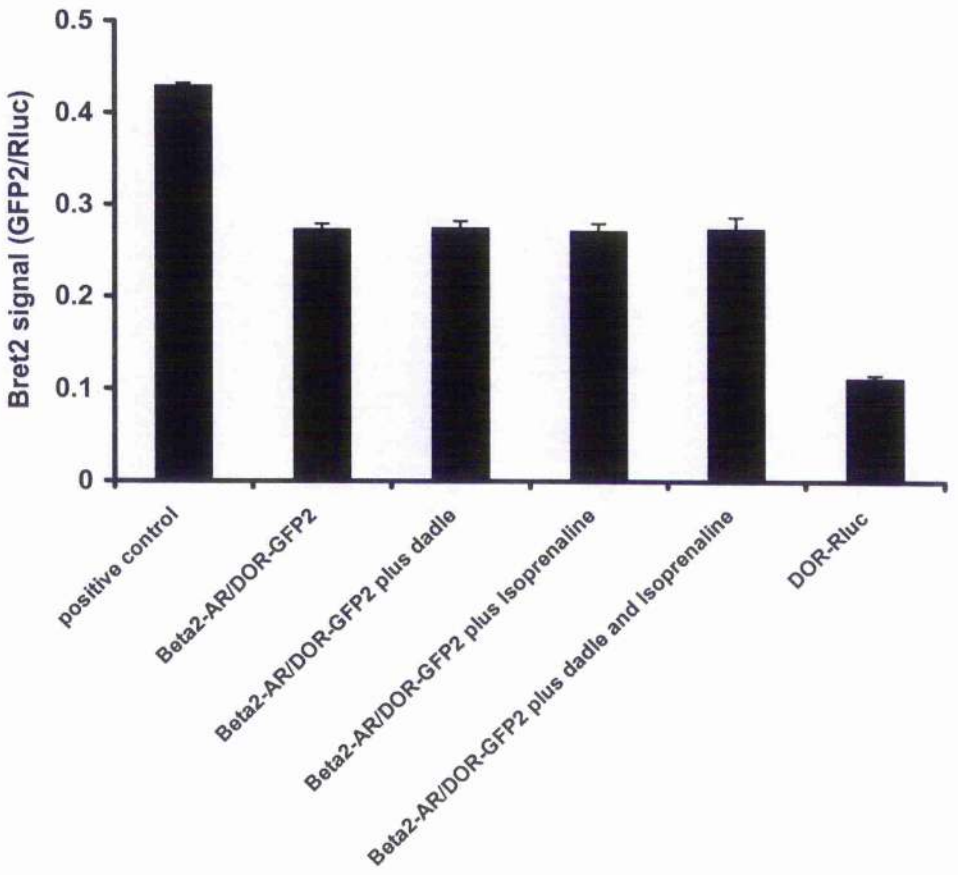
Bret2 signal (GFP2/Rluc)
0.5
0.4
0.3
0.2
0.1
0
positive control
Beta2-AR/DOR-GFP2
Beta2-AR/DOR-GFP2 plus dadle
Beta2-AR/DOR-GFP2 plus Isoprenaline
Beta2-AR/DOR-GFP2 plus dadle and Isoprenaline
DOR-Rluc

Figure 4.5.

Figure 4.6. Detection of heterodimerization between the κ-opioid receptor and the δ-opioid receptor using $BRET_2$.

The amount of light emitted from both *Renilla* luciferase and GFP_2 was quantitated using filters of fixed bandwidth on a Fusion multiwell plate reader. Readings were taken from wells containing HEK 293T cells either transfected with the positive control vector $pBRET_2$+, with both κ-opioid-Rluc and δ-opioid-GFP_2 constructs, or with κ-opioid-Rluc alone to determine the background ratio of light emission (GFP_2)/Rluc. To see if there were any alterations in the ratio (GFP_2/Rluc) upon addition of agonist or antagonist ligands, cells co-transfected with both κ-opioid-Rluc and δ-opioid-GFP_2 were subject to a 15 minute pre-incubation period with either DADLE, ICI 174 864, ICI 199 441, GNTI, or both DADLE and ICI 199441 together (each at 10μM) prior to addition of DeepblueC. The results represent means ± S.E.M. of three independent experiments.

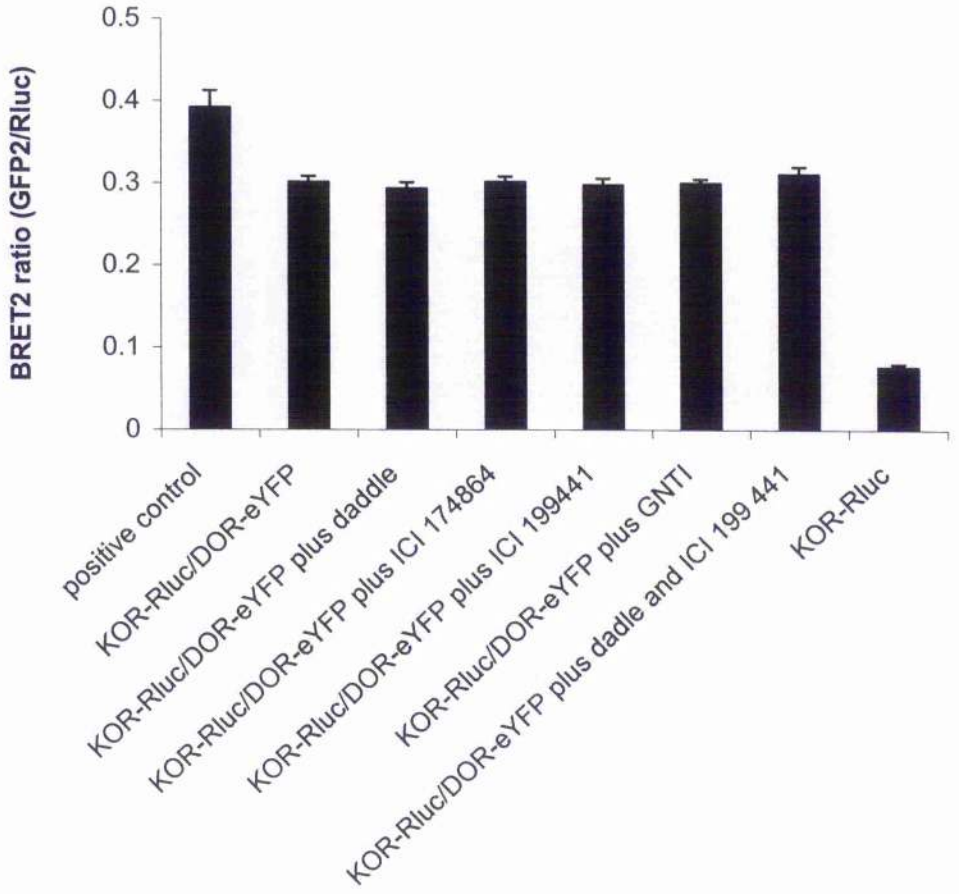
BRET2 ratio (GFP2/Rluc)
0.5
0.4
0.3
0.2
0.1
0
positive control
KOR-Rluc/DOR-eYFP
KOR-Rluc/DOR-eYFP plus daddle
KOR-Rluc/DOR-eYFP plus ICI 174864
KOR-Rluc/DOR-eYFP plus ICI 199441
KOR-Rluc/DOR-eYFP plus GNTI
KOR-Rluc/DOR-eYFP plus dadle and ICI 199 441
KOR-Rluc

Figure 4.6.

Figure 4.7. β-arrestin2-cyan is recruited to the plasma membrane in response to CCR2 activation: it internalises along with the receptor over a thirty-minute time course.

A CHO-K1 cell line stably expressing CCR2 was transiently transfected with the cDNA for the β-arrestin2-cyan NFP construct. The response of the cells following the addition of the CCR2 agonist MCP-1 (1μM) was then monitored using scanning confocal microscopy. **(A)** The cellular location of β-arrestin2-cyan NFP prior to addition of MCP-1. **(B)** Cells 2 minutes after addition of MCP-1. **(C)** Cells 4 minutes after addition of MCP-1. **(D)** Cells 8 minutes after addition of MCP-1. **(E)** Cells 12 minutes after addition of MCP-1. **(F)** Cells 20 minutes after addition of MCP-1. **(G)** Cells 26 minutes after addition of MCP-1. **(H)** Cells 30 minutes after addition of MCP-1. The results shown are of a single transfection, representative of three such performed.

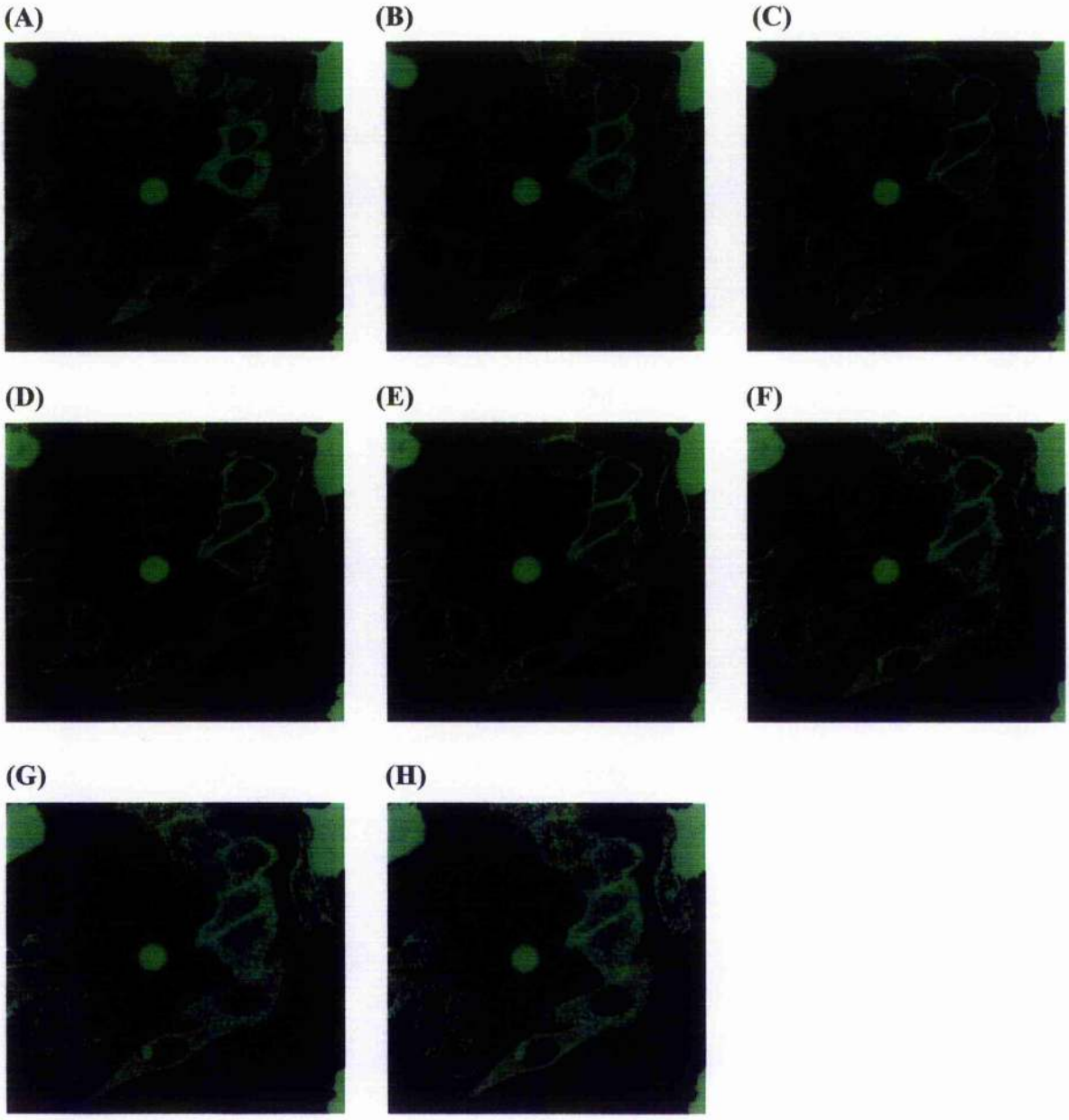

Figure 4.7.

Figure 4.8. β-arrestin2-red is recruited to the plasma membrane in response to CCR2 activation: it internalises along with the receptor over a thirty minute time course.

A CHO-K1 cell line stably expressing CCR2 was transiently transfected with the cDNA for the β-arrestin2-red NFP construct. The response of the cells following the addition of the CCR2 agonist MCP-1 (1μM) was then monitored using scanning confocal microscopy. **(A)** The cellular location of β-arrestin2-red NFP prior to addition of MCP-1. **(B)** Cells 6 minutes after addition of MCP-1. **(C)** Cells 10 minutes after addition of MCP-1. **(D)** Cells 14 minutes after addition of MCP-1. **(E)** Cells 24 minutes after addition of MCP-1. **(F)** Cells 28 minutes after addition of MCP-1. **(G)** Cells 38 minutes after addition of MCP-1. **(H)** Cells 42 minutes after addition of MCP-1. The results shown are of a single transfection representative of two such performed.

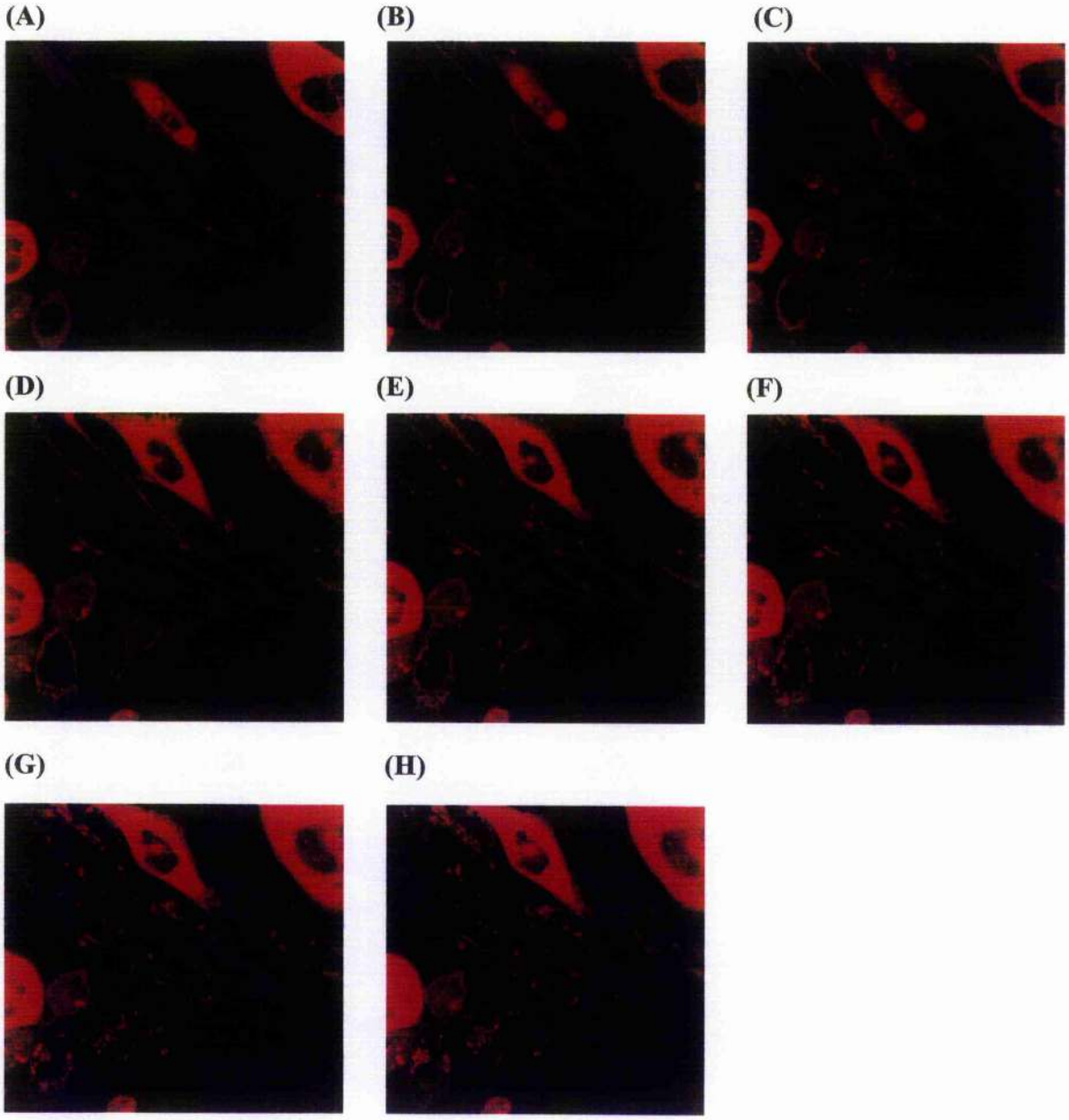

Figure 4.8

Figure 4.9. β-arrestin1-GFP is recruited to the plasma membrane in response to CCR2 activation: it internalises along with the receptor over a thirty minute time course.

A CHO-K1 cell line stably expressing CCR2 was transiently transfected with the cDNA for the β-arrestin1-GFP construct. The response of the cells following the addition of the CCR2 agonist MCP-1 (1μM) was then monitored using scanning confocal microscopy. **(A)** The cellular location of β-arrestin1-GFP prior to addition of MCP-1. **(B)** Cells 6 minutes after addition of MCP-1. **(C)** Cells 8 minutes after addition of MCP-1. **(D)** Cells 12 minutes after addition of MCP-1. **(E)** Cells 16 minutes after addition of MCP-1. **(F)** Cells 20 minutes after addition of MCP-1. **(G)** Cells 26 minutes after addition of MCP-1. **(H)** Cells 30 minutes after addition of MCP-1. The results shown are of a single transfection representative of three such performed.

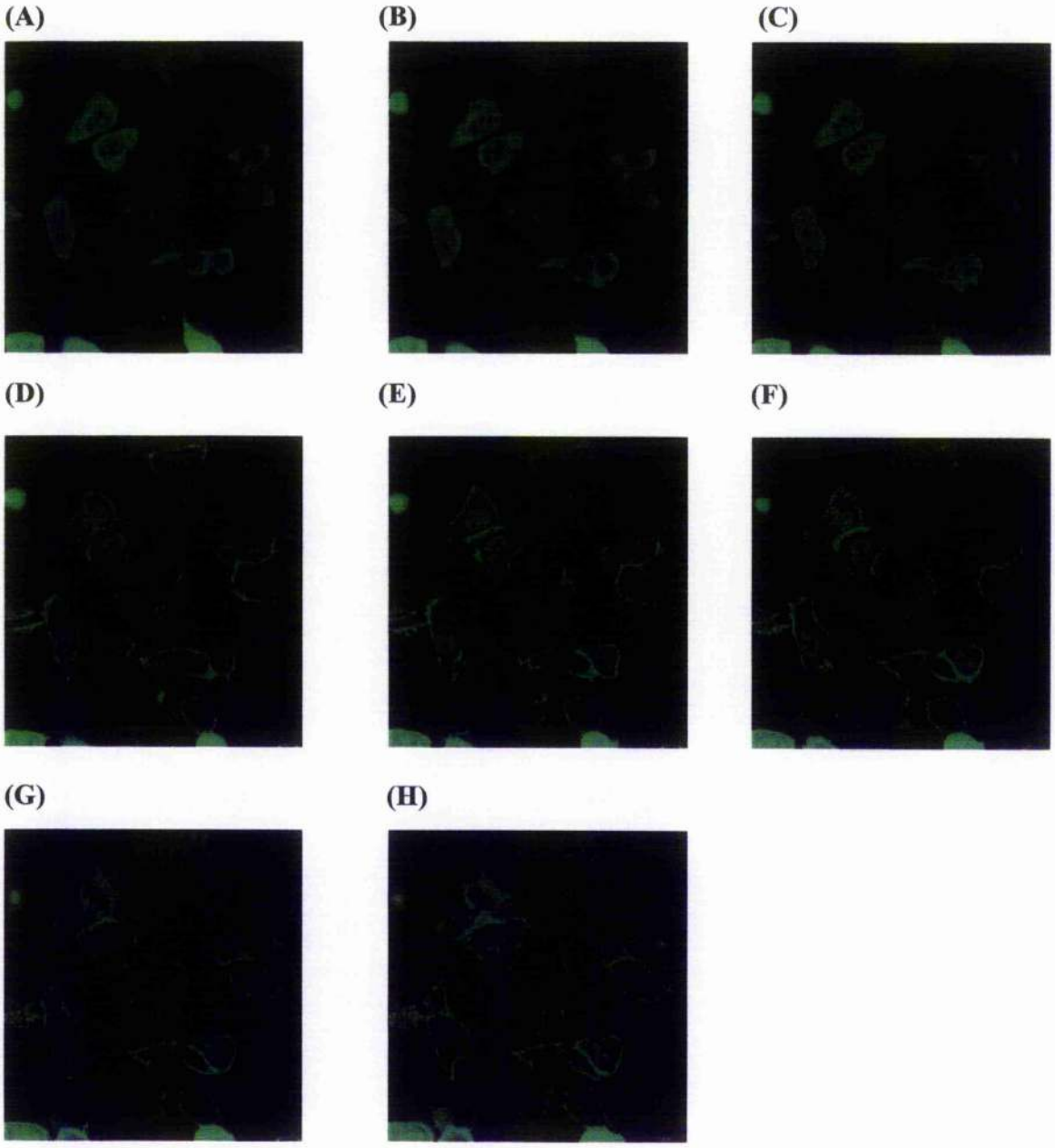

Figure 4.9.

Figure 4.10. β-arrestin2-cyan NFP and β-arrestin2-red NFP are only recruited to the plasma membrane in response to a specific activating agonist.

A CHO-K1 cell line stably expressing CCR2 was transiently transfected with the cDNA for either **(A)** β-arrestin2-cyan NFP or **(B)** β-arrestin2-red NFP and the response of the cells to a chemokine (IL-8) which does not have specificity for the CCR2 was monitored. In each case images were obtained using scanning confocal microscopy. The pictures were taken both before and after the addition of IL-8 (1μM). The results are of a single transfection and are representative of two such experiments performed.

(A)

Before Treatment

30 minutes after treatment

(B)

Before treatment

30 minutes after treatment

Figure 4.10.

Figure 4.11. The presence of an antagonist ligand for CCR2 does not cause translocation of β-arrestin2-cyan NFP transiently expressed in CCR2 stable cell line.

A CHO-K1 cell line stably expressing CCR2 was transiently transfected with β-arrestin2-cyan NFP. The response of the cells following addition of the CCR2 antagonist GW590623X (10μM) was monitored using confocal scanning microscopy. **(A)** The cellular location of β-arrestin2-cyan NFP prior to addition of the compound. **(B)** The cellular location of β-arrestin2-cyan NFP 30 minutes after addition of GW590623X (10μM). The results are of a single transfection and are representative of two such experiments performed.

(A)

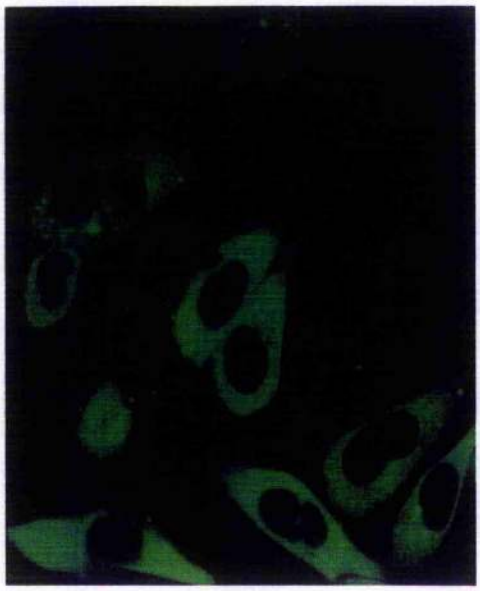

(B)

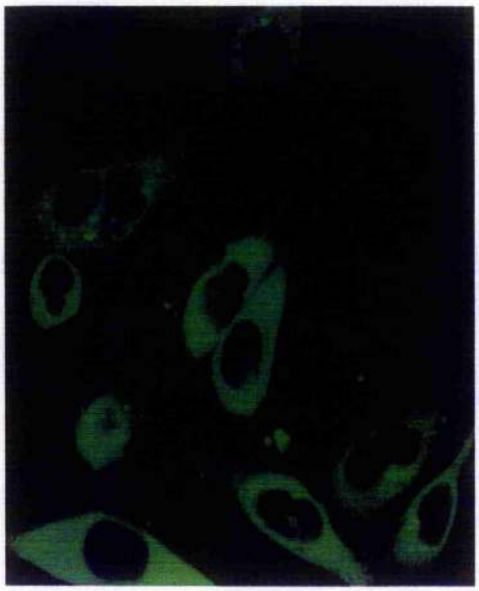

Figure 4.11.

Figure 4.12. The presence of antagonist can effectively block MCP-1 mediated translocation of β-arrestin2-cyan NFP expressed in CCR2 stable cell line.

A CHO-K1 cell line stably expressing CCR2 was transiently transfected with β-arrestin2-cyan NFP. Cells were prepared for confocal scanning microscopy by placing them on a heated stage, as described in section 2.6. **(A)** The cells were given a 30 minutes pre-incubation period with the compound GW590623X (10μM) before obtaining the shown image. **(B)** MCP-1 (1μM) was then added and the cellular location of β-arrestin2-cyan NFP was re-determined after 30 minutes by obtaining the shown image. The results are of a single transfection, and are representative of two such experiments performed.

(A)

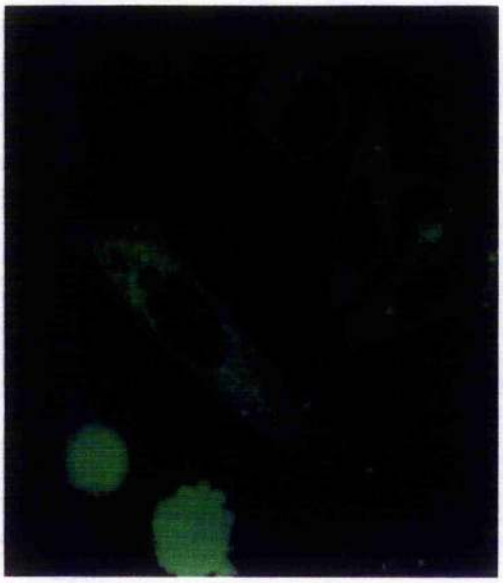

(B)

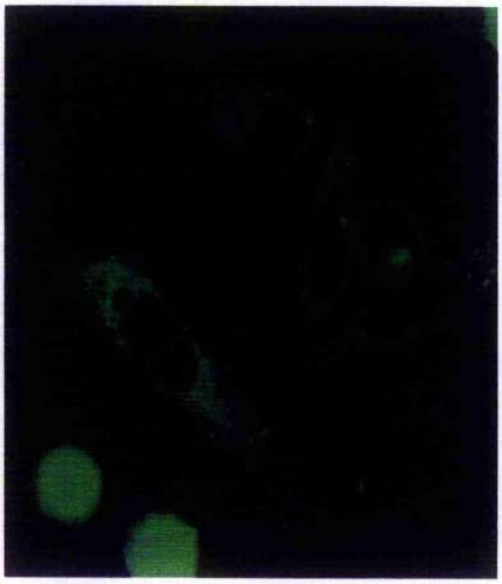

Figure 4.12.

Figure 4.13. Comparison of the cellular locations of CCR2-cyan NFP and β-arrestin2-red NFP when transiently expressed in HEK 293T cells.

HEK 293T cells were transient co-transfected with the cDNAs for both CCR2-cyan NFP and β-arrestin2-red NFP. Images of the respective cellular locations of both constructs within the same cells were then obtained using appropriate excitation wavelengths and emission filters to detect light emitted from either **(A)** CCR2-cyan NFP or **(B)** β-arrestin2-red NFP. The results are a single representative of two such experiments performed.

(A)

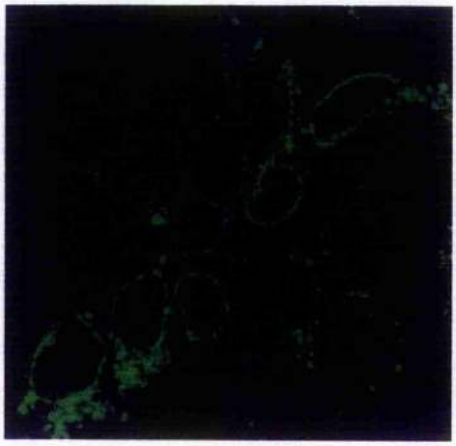

(B)

Figure 4.13.

Figure 4.14. Comparison of the extent of translocation of both β-arrestin2-red NFP and β-arrestin1-GFP expressed within the same cells.

A CHO-K1 cell line stably expressing CCR2 was transiently co-transfected with the cDNA for both β-arrestin2-red NFP and β-arrestin1-GFP. The response of the cells following addition of MCP-1 (1μM) was then monitored using confocal scanning microscopy, switching between green and red filters, in order to visualise light emitted from each fluorescent protein. **(A)** The cellular location of β-arrestin1-GFP both before and 30 minutes after addition of MCP-1. **(B)** The cellular location of β-arrestin2-red NFP both before and 30 minutes after addition of MCP-1. The results are of a single transfection and are representative of two such experiments performed.

(A)

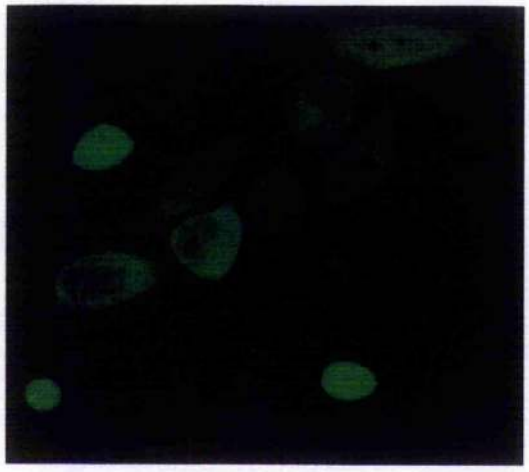

Before treatment

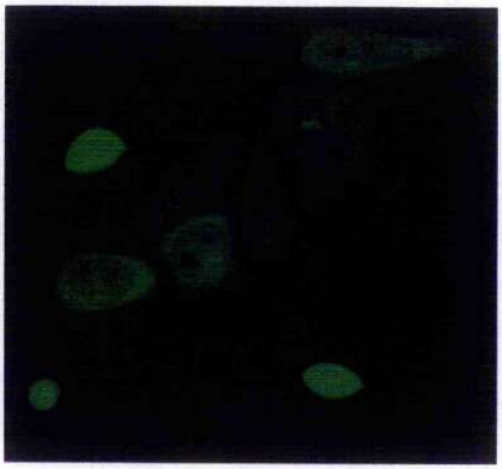

30 minutes after treatment

(B)

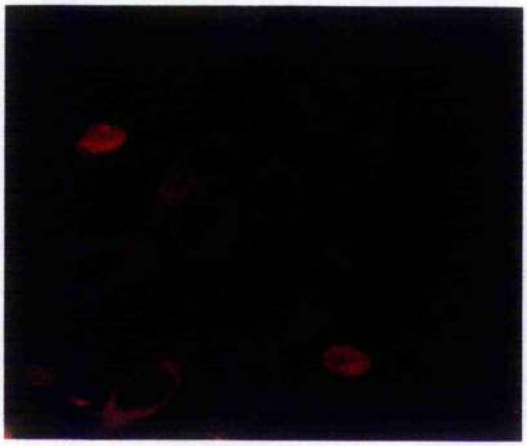

Before treatment

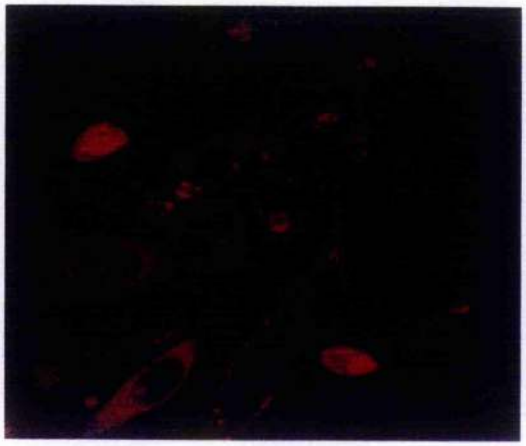

30 minutes after treatment

Figure 4.14.

Figure 4.15. β-arrestin2-red NFP is recruited to the plasma membrane in response to AT1AR activation: it internalises along with the receptor thirty minutes following addition of ligand.

A CHO-K1 cell line stably expressing the AT1AR was transiently transfected with the cDNA for the β-arrestin2-red NFP construct. The response of the cells following addition of angiotensin II (10μM) was then monitored in **(A)** cells prior to addition of angiotensin II and **(B)** cells 30 minutes after the addition of angiotensin. Results are of a single transfection and are representative of two such experiments performed.

(A)

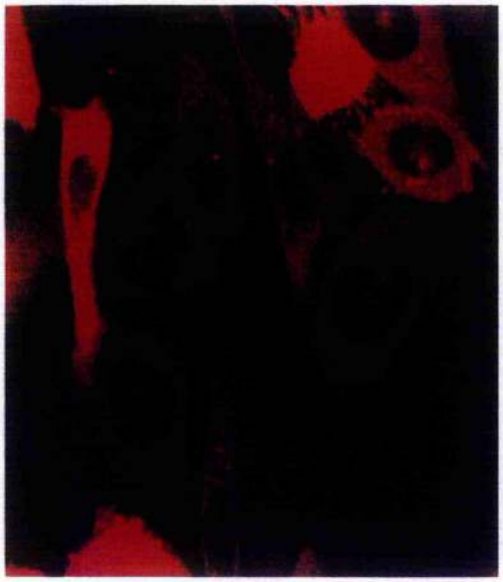

(B)

Figure 4.15.

Figure 4.16. No translocation of β-arrestin2-cyan NFP expressed in CHO-K1 cells could be detected in response to activation of endogenous GPCRs.

CHO-K1 cells were transiently transfected with the cDNA for β-arrestin2-cyan NFP. The response of the cells to either **(A)** ATP (10 μM) or **(B)** calcitonin (10 μM) was then monitored upto 30 minutes after exposure to the compound. The results are a single representative of two such experiments performed.

A)

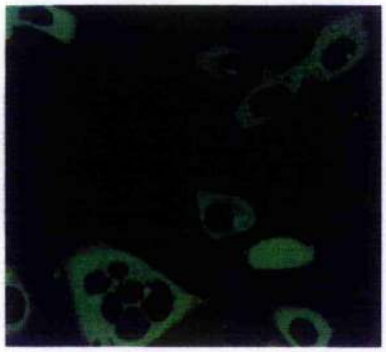

0 minutes

30 minutes

B)

0 minutes

30 minutes

Figure 4.16.

Figure 4.17. No translocation of β-arrestin2-cyan NFP expressed in HEK 293T cells could be detected in response to activation of endogenous GPCRs.

HEK 293T cells were transiently transfected with the cDNA for β-arrestin2-cyan NFP. The response of the cells to either **(A)** Carbachol (100 μM) or **(B)** PGE2 (10 μM) was then monitored up to 30 minutes after exposure to the compound. The results are a single representative of two such experiments performed.

(A)

0 minutes

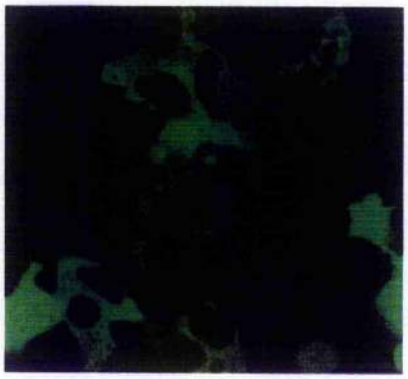

30 minutes (Carbachol)

(B)

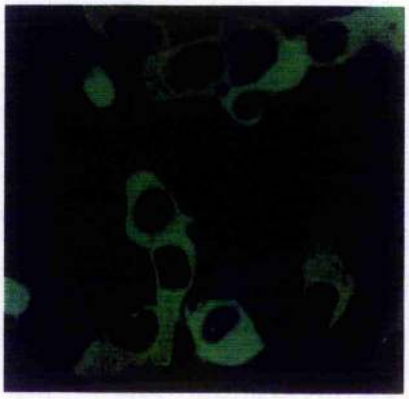

0 minutes

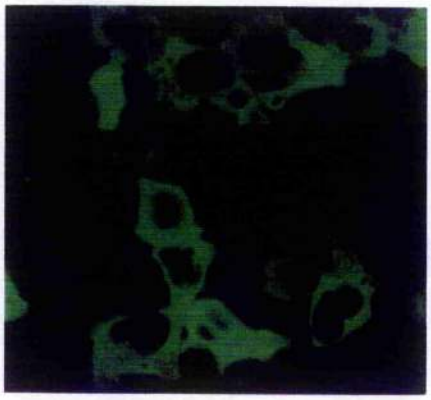

30 minutes

Figure 4.17.

these were then exposed to either carbachol (100μM) or PGE2 (10 μM) while being examined via confocal microscopy. Endogenously expressed M2 and M3 muscarinic receptors and prostaglandin receptors were incapable of inducing an immediate response to agonist such as was seen in the CCR2 stable cell line. Moreover, prolonged exposure of agonist (up to 30 minutes) did not result in the formation of a punctate pattern either at the plasma membrane, or within the cell (Figure 4.17).

4.3 Discussion

4.3.1. Results obtained using $BRET_2$ reinforced previous findings which suggested that the dimerization of opioid receptors was not ligand regulated

There is a rapidly expanding body of evidence which, over the past five years, has established that GPCRs can participate in both homomeric and heteromeric interactions between closely related, and sometimes distantly related, receptor types. Despite this, the role of external ligands in GPCR dimerization remains a contentious one. Many studies report that dimerization of GPCRs is constitutive, with the presence of external ligand increasing the extent of these interactions (Angers *et al.*, 2000; Kroeger *et al.*, 2001). In others, the formation of the dimeric complex seems to be largely agonist dependent (Rochville *et al.*, 2000; Rodriguez-Frade *et al.*, 1999; Cornea *et al.*, 2001). In contrast to these findings, no evidence to support a role for ligand binding in stabilizing the strength of dimeric complexes could be found through the work detailed in the preceding Chapter; this, despite an extensive investigation, utilizing a bioluminescence based energy transfer system.

In this Chapter, it was first verified that by using $BRET_2$ the energy transfer signal (generated with the DeepBlueC/GFP_2 pairing) could be more effectively resolved from background than in $BRET_1$. Experiments conducted using $BRET_2$ confirmed

findings of the previous Chapter that opioid receptor subtypes were able to form both homo and hetero-dimers. Additionally, more compelling evidence was found to support the notion that heteromeric complexes between the delta opioid receptor and the β2-AR could be formed. Yet despite this, in all cases, there was no confirmation that the strength of the dimeric complex could be influenced by the presence of either agonist or antagonist ligands within the receptor-binding pocket.

The findings presented herein would seem to argue, by default, in favour of a role for dimerization which is typified by the GABAb receptor. In this case heterodimerization of two polypepdides (GABAb(R1) and GABAb(R2)) within the endoplasmic reticulum facilitates receptor maturation and delivery to the plasma membrane (Margreta-Metrovic *et al.*, 2000; Kuner *et al.*, 1999) and there is no clear evidence to date which suggests that ligands regulate the interaction of these two receptor subtypes. This view of GPCRs acting as mutual chaperones has been dealt with extensively in Chapter 1; yet, for the purpose of illustration, two further examples may be cited here.

In a study involving the D3 dopamine receptor, co-expression of the wild type receptor with a naturally occurring splice variant lacking transmembrane regions VI and VII blocked successful delivery of the wild type receptor to the plasma membrane. This suggests a role for dimerization in ensuring that correct trafficking is observed as the receptor is processed through the E.R and Golgi apparatus. Any incorrectly folded receptors, or receptors that lack essential determinants in facilitating egress from the said organelles are incapable of targeting properly to the cell plasma membrane (Karpa *et al.*, 2000). Comparable results were obtained in experiments using truncation mutants of the vasopresin V2 receptor where again co-expression of these mutants with the wild type receptor inhibited both receptor

functional activity and delivery to the plasma membrane (Zhu and Wess *et al.*, 1998). From this study, similar functional implications concerning the role of dimerization in facilitating receptor maturation can be drawn.

4.3.2. A FRET assay based on the recruitment of β-arrestin2 to phosphorylated receptors at the plasma membrane would be ideally suited to compound library screening programmes

Having firmly established that, at least in the case of the opioid receptors, the presence of an external ligand in the binding pocket of the receptor was incapable of affecting the extent of dimerization, attention was turned to investigating whether intermolecular interactions between activated receptors and components of the receptor desensitisation pathway might provide a suitable alternative to dimerization for developing an energy transfer based assay capable of detecting ligand binding. The results obtained when examining recruitment of β-arrestin2, modified with either red or cyan fluorescent proteins from various *Anthozoan* species, indicated that the β-arrestin2 was unimpaired in its ability to translocate to the plasma membrane in response to activation of a stably expressed CCR2 receptor in a CHO-K1 cell line. The confocal microscopy techniques used in this study would not of course be suitable as an assay procedure applicable to industrial compound screening programmes since a high throughput assay is required to handle the large number of test compounds used in such circumstances. For this reason, FRET has been proposed as a potentially powerful method for the detection of agonists via activation of the desensitisation pathway. Equally, it may be used to identify antagonists through competitive inhibition of this process, provided at least one agonist for the receptor is known.

Such an assay would require the labelling of both the receptor and the β-arrestin molecules with fluorescent proteins between which energy transfer could occur. Certain fluorescent proteins within the NFP range are excellent candidates for donor/acceptor pairs provided that upon in frame ligation with the aforementioned cellular proteins they yield chimeric molecules that are not impaired in their cellular targeting and functionality. The cyan NFP has been shown to have a maximum emission peak centred on 486nm and the yellow NFP to posses two characteristic emission peaks, one centred on 531nm, and the other (smaller) peak centred on 590nm (personal communication). Similarly the yellow and red NFPs have been shown to exhibit considerable overlap in their respective excitation and emission spectra, with yellow NFP displaying an emission maximum at 540nm and red NFP showing two distinct peaks in its absorbance spectrum, one centred on 571nm, the other centred on 522nm (personal communication). From this information, it is obvious that there is a potential for developing a FRET based assay by monitoring energy transfer between proteins which have been modified with these fluorescent proteins to form cyan NFP/yellow NFP or yellow NFP/red NFP donor/acceptor pairings. In an attempt to exploit this, the CCR2 receptor was modified at the carboxyl terminal tail with yellow NFP. Regrettably, transient transfection of the receptor construct into CHO-K1 cells showed that it was incapable of reaching the plasma membrane and tended to form a globular pattern indicative of retention within intracellular compartments such as the E.R and golgi apparatus. This intracellular retention may have been due to the presence of the NFP on the carboxyl terminal tail of the receptor interfering with the trafficking and maturation steps necessary for correct delivery of the receptor to the plasma membrane. Some receptor types may be more affected by such modifications than others, however, within the time limits

given for these studies it was not possible to construct any further GPCR-NFPs to test this hypothesis and therefore properly evaluate the potentiality of this method for detection of receptor activation in a FRET based format.

If a FRET assay based on this principal could be established it would prove useful in not only identifying new potential ligands for known GPCRs but also provide a powerful method of screening compound libraries for activity at orphan GPCRs. These are new members of the GPCR superfamily of receptors which have been identified either through traditional molecular genetic approaches or through bioinformatic screening of genomic information for structural signatures characteristic of known GPCRs. Identification of ligands for these orphan GPCRs, of which more than 100 have been recognized (Stadel *et al.*, 1997), would result in novel drug discoveries, a significant proportion of which would be useful for treating diseases for which existing therapies are lacking or insufficient.

Arguing in favour of the case for exploiting desensitisation as a means of implementing compound screening programmes in the detection of agonists with affinity for orphan GPCRs, is the fact that it has been demonstrated that GPCRs exhibit considerable redundancy in their ability to couple to the clathrin mediated internalisation pathway. This is illustrated by the AT1AR, a receptor which normally utilizes a pathway which is independent of dynamin and β-arrestin (Zhang *et al.*, 1996) but can be induced to undergo sequestration via clathrin in the presence of over-expressed β-arrestin (Zhang *et al.*, 1999). Present assay systems employed in "fishing" for ligands capable of activating orphan GPCRs usually focus on the ability of the receptor to activate a particular signalling pathway such as stimulation or inhibition of cAMP production or mobilization of intracellular calcium. As it is not always easy to predict accurately the G-protein coupling specificity of an orphan

GPCR from its primary sequence, an assay system which measures the ability of a ligand to engage with a desensitisation pathway almost ubiquitously shared by all GPCRs is of particular interest as a means of compound screening. Such an assay would function simply on the proviso that high levels of β-arrestin were maintained in the cells used.

In addition to high levels of β-arrestin expression, a FRET assay based on the detection of β-arrestin recruitment from the cytosol to phosphorylated receptors at the plasma membrane would probably require high levels of expression of the GPCR under investigation. This is based on the evidence presented herein that diverse GPCR types endogenously expressed in either HEK 293T or CHO-K1 cells, when assessed for their ability to recruit β-arrestin2 cyan NFP to the plasma membrane were unable to elicit a response even after a 30 minute pre-incubation with saturating concentrations of agonists. It is probable that in the studies presented here, the low levels of endogenous GPCR limited the amount of β-arrestin mobilized to the plasma membrane to a level that was undetectable using the confocal microscopy methodologies applied. In support of this it should be noted that, although this approach has been previously used to provide real time analysis of receptor-arrestin interactions (Barak *et al.*, 1999; Zhang *et al.*, 1999; McConaloue., *et al* 1999), there are some studies which report that arrestin recruitment was undetectable when endogenous GPCRs in HEK 293T cells were challenged with agonist and the response of GFP tagged arrestin was subsequently monitored, notably (Mundell and Benovic., 2000).

4.3.3. β-arrestin1 and β-arrestin2 have different affinities for the CCR2 receptor following activation of the desensitisation pathway

An observation of particular interest made during the course of these experiments was that although both β-arrestin2 and β-arrestin1 associated with the endosomes containing the activated CCR2 receptor following receptor sequestration, β-arrestin2 seemed to have a higher affinity for the activated CCR2 receptor than the related protein β-arrestin1, as revealed by examining the kinetics of the respective molecules in singly transfected cells and by observations made in cells co-expressing both arrestin types together. In the latter experiments it was unlikely that these observed differences were due to greater expression levels of β-arrestin2. This is because in all the co-transfected cells CCR2 showed a preference for β-arrestin2 in mediating sequestration and in a transient transfection system we would expect a wide range of expression levels of both constructs within the cells present in the field of vision.

It has been shown in a recent study using confocal microscopy that the pattern of the β-arrestin recruitment process may differ depending upon the type of GPCR that has been stimulated (Oakley *et al.*, 2000). Two classes of GPCR have been identified: class (A) (β2-AR, μ-opioid receptor, endothelin type A receptor, dopamine D1A receptor and the α1b-AR) which bound β-arrestin-2 with higher affinity than β-arrestin-1, did not internalise with β-arrestin as a stable complex and did not interact with visual arrestin and class (B) (angiotensin II type1A receptor, neurotensin receptor 1, vasopressin V2 receptor, TRH receptor and substance P receptor) which bound β-arrestin-1 and β-arrestin-2 with equal affinity, internalised with β-arrestin as a stable complex and were capable of recruiting visual arrestin to the plasma membrane. It has also been suggested in recent studies involving members of both classes of GPCR described above that the duration for which the GPCR- β-arrestin complex persists following receptor sequestration is important in defining the kinetics of resensitization of the receptor (Oakley *et al.*,1999). It was shown that the β2-AR

(class A) was rapidly dephosphorylated and recycled back to the plasma membrane whereas the vassopressin V2 receptor (class B) possessed much slower recycling kinetics, presumably because the prolonged interaction between V2R and β-arrestin inhibits the association of this GPCR with receptor phosphotases present in the acidified endosome. A further proposal in this study was that the observed differences between the two classes of receptor were attributable to the presence of clusters of serine and threonine residues present in the carboxyl terminal tail of the receptor, so that receptors which remained associated with arrestins following ligand activation (such as the vassopresin V2 receptor, neurotensin receptor-1 andangiotensin II type 1A receptor) possessed these clusters whereas receptors which dissociated from arrestins at the plasma membrane (such as β2-AR) did not. This assertion was further backed up in studies where truncation of the carboxyl terminal tail of the substance P receptor (class B) to remove all such serine/threonine clusters, resulted in a receptor which was severely compromised in its ability to recruit a βarrestin2-GFP construct into endocytic vesicles (Oakley et al., 2001).

Examination of the carboxyl terminal domain of the CCR2b receptor (the subtype used in the study herein) reveals the presence of such clusters (Figure 4.18) downstream of the conserved NPXXY motif that marks the end of the seventh transmembrane helix. Shown for comparison are the carboxyl terminal tails of both the AT1AR and β2-AR. Although previous studies have not been precise in exactly what constitutes a serine/threonine cluster, they were typically reported to be located 30-50 amino acids downstream of the NPXXY motif and included three or more serine/threonine residues running together, interspersed by not more than one dissimilar amino acid residue (Oakley *et al.*, 2001). Note the absence of such motifs within the carboxyl terminal tail of the β2-AR. On the basis of this information,

Figure 4.18. Comparison of the carboxyl terminal tails of the CCR2, AT1AR and β2-AR.

Shown are the amino acid compositions of the carboxyl terminal tails of the CCR2, AT1AR and β2-AR downstream of the conserved NPXXY motif (Bold). Clusters of three or more serine/threonine residues together or interspersed by just one dissimilar amino acid residue are underlined.

1) CCR2 -**NPIIY**AFVGEKFRRYLSVFFRKHITKRFCKQCPVFY
RETVDGVTSTNTPSTGEQEVSAGL

2) AT1AR- **NPLFY**GFLGKKFKRYFLQLLKYIPPKAKSHSNLSTK
MSTLSYRPSDNVSSSTKKPAPCFEVE

3) β2-AR - **NPLIY**CRSPDFRIAFQELLCLRRSSLKAYGNGYSSN
GNTGEQSGYHVEQEKENKLLCENLPGTGDPVGHQ
GTVPSDNIDSQGRNCSTNDSLL

Figure 4.18.

CCR2 would have to be classified within the group of receptors that co-internalised with arrestins in a prolonged interaction that would delay dephosphorylation and resensitization of the receptor and its recycling back to the plasma membrane. This was in agreement with the results presented here. However one proposed property of class (B) receptors is that they have equal affinities for both of the major arrestin types (Oakley *et al.*, 1999), though in fairness this was only demonstrated for the AT1AR. Given the findings presented herein, it would seem possible that with regards to affinity for β-arrestin subtypes, the number, position and quality of the serine/threonine clusters or the presence of some yet unidentified motif may be of additional importance in determining a preference for recruitment of either β-arrestin1 or β-arrestin2, whereas the ability to enter into a tightly binding complex with a given arrestin merely requires the presence of such clusters.

Since both β-arrestin1 and β-arrestin2 are ubiquitously expressed in all cell types, though in different proportions (Lohse *et al.*, 1990; Attramadal *et al.*, 1992), there has been a considerable effort to try and determine whether they serve different roles in GPCR signalling or whether they are functionally redundant. In one such study, using embryonic fibroblasts from knockout mice that lack either β-arrestin1 (βarr1-KO), β-arrestin2 (βarr2-KO) or both arrestins (βarr1/2-KO), it was shown that both βarr1-KO and βarr2-KO showed similar impairment in desensitisation of AT1AR and β2-AR when compared to similar experiments in wild type control cells. However, sequestration of β2-AR was impaired only in βarr2-KO whereas it was unaffected in βarr1-KO cells, in contrast to which AT1AR was not compromised in its sequestration when expressed in either βarr1-KO or βarr2-KO alone. In βarr1/2-KO cells both receptors were dramatically impaired in their ability to be internalised (Kohout *et al.*, 2001). This indicates that although in all cells a given receptor may

undergo desensitisation, the ability of some receptor types to be internalised, and hence resensitized, will depend on the relative expression levels of the major arrestins within that cell. This is in contrast to receptors with a high affinity for both β-arrestin1 and β-arrestin2 which will internalise regardless of the cell's arrestin complement.

It is not surprising that the strength of interaction between GPCRs and arrestins are mediated by the presence of serine and threonine residues on the carboxyl terminal tail of the receptor, considering that arrestin recruitment from the cytosol follows on from phosphorylation of the receptor by members of the GRK family of kinases. The binding of β-arrestin to agonist activated GPCRs at the plasma membrane is thought to be mediated by two domains present within the β-arrestin molecule: a large domain within the amino terminus termed the activation recognition domain which engages with the second and third intracellular loops of the receptor (Wu *et al.*, 1997) and a smaller positively charged region within the middle of the molecule which is thought to interact with the phosphorylated carboxyl terminal tail of the receptor called the phosphorylation recognition domain (Kieselbach *et al.*, 1994). It can be envisaged that the presence of clusters of negatively charged phosphate groups present on the serine and threonine residues of class (B) receptors would be sufficient to stabilize the arrestin/receptor complex allowing both to be incorporated into the endocytic vesicle upon receptor internalisation. It is also possible that by engaging the phosphorylated carboxyl terminal tail of the activated receptor, β-arrestin undergoes a conformational change that promotes a high affinity interaction between the two molecules (Vishnivetski *et al.*, 2000). This proposal was advocated in a recent study where truncation of the carboxyl terminal domain of β-arrestin1 resulted in a mutant that remained closely associated with GPCRs lacking serine/threonine clusters following receptor internalisation. This implied that removal of the carboxyl terminus had

uncovered a high affinity-binding site within the β-arrestin molecule, allowing it to interact with GPCRs in the absence of phosphorylation (Oakley *et al.*, 2001).

Enquiry into the nature and mechanisms of the interactions between GPCRs and components of the receptor desensitisation pathway, such as are presented here, might ultimately lead to novel theapeutic targets for the treatment of certain disease processes being uncovered. For instance, a naturally occurring loss of function mutation in the human vasopressin V2 receptor has been identified (Rosenthal *et al.*, 1993), which is associated with familial nephrogenic diabetes insipidus and induces a constitutive arrestin-mediated desensitisation, leading to receptor sequestration even in the absence of agonist. It was found, through subsequent work, that the removal of serine triplets from the carboxyl terminal tail of this mutant receptor rescued it and allowed the receptor to be resensitized and properly localized to the plasma membrane (Barak *et al.*, 2001), suggesting that unregulated desensitisation of GPCRs may be the basis of certain types of disease states and that the desensitisation pathway may provide a possible therapeutic target for intervention in these disease processes.

4.5 Conclusion

In this chapter it was confirmed that the strength of the energy transfer signal generated, relative to background noise, by a variant of traditional BRET, $BRET_2$, was a substantial improvement over its predecessor. This new system was then used to reinforce the observations made in the previous Chapter: that opioid receptors are constitutively associated when transiently co-expressed in mammalian cells and that the strength of the dimeric complex is not influenced by the presence of either agonist or antagonist ligands. Earlier experiments, using $BRET_1$, to investigate interactions between the β2-AR and the δ-opioid receptor were better clarified using $BRET_2$

technology and indicated that these two receptor types do heterodimerize, though, perhaps disappointingly, previous indications of agonist-induced regulation could not be confirmed. Taken together these results support the theory that the role of dimerization is more in facilitating the maturation and cell surface delivery of a fully functional receptor molecule than in facilitating the stabilization of an active conformation of the receptor. These conclusions exclude the general usefulness of dimerization in the detection of ligand induced receptor activation.

Investigation of the desensitisation pathway provided a more attractive alternative to the development of such an assay. The viability of this proposal was been clearly demonstrated through studies using confocal microscopy techniques. Although no actual demonstration has been yet provided, the possibility of adapting the detection of β-arrestin recruitment to a FRET based format could potentially provide industrially based compound library screening programmes with a powerful method for the detection of receptor activation. In addition to this, the studies revealed that a CCR2 receptor, a class B receptor candidate based on the classification system of (Oakley et al., 2000), was capable of forming a high affinity complex with β-arrestin2 with which it remained associated following sequestration. This was in accordance with previous observations made for other class B receptor candidates. However, CCR2 did not display equal affinities for both β-arrestin1 and β-arrestin2, providing a counterexample to the conjecture that all class B receptors possessing serine/threonine clusters on the carboxyl terminal tail would engage the major arrestin types with equal affinity.

Chapter 5

Third results chapter

5.1 Introduction

In recent years, it has been shown that through the process of introducing certain mutations into GPCRs, it is possible to generate mutant receptors that are capable of exhibiting enhanced levels of constitutive activity. This constitutive activity manifests itself through an ability of the mutant GPCR to produce higher levels of second messenger molecules in the absence of an agonist ligand compared to their wild type counterparts when heterologously expressed within the same cell lines. GPCRs thus endowed with these characteristics, generate, in assays designed to measure a functional output, a response that is proportional to the expression levels of the mutant receptor (Samama *et al.*, 1993). Many examples of these mutants have been well characterized and it has been shown that mutations in a diverse range of unrelated receptor regions within a great variety of receptor types can give rise to the phenomenon (Sheer and Cotecchia., 1997; Leurs *et al.*, 1998).

Diverse studies focusing on such constitutively active receptors have provided a wealth of useful information concerning the mechanisms by which GPCRs adopt active conformations in the presence of agonists and about how naturally occurring mutations in GPCRs can form the basis of certain disease processes. They have also illuminated the role of antagonists in GPCR regulation and ligands previously thought of as possessing neutral efficacy have been found to be capable of dampening the basal production of second messenger molecules (Milligan *et al.*, 1995). It is believed that this inhibition is due to the antagonists favouring the enrichment of an inactive

conformation of the receptor and consequently such ligands have come to be known as inverse agonists (Milligan *et al.*, 1995). The phenomenon of inverse agonism is more thoroughly discussed in Chapter 1.

One of the most extensively studied of these constitutively active mutant (CAM) GPCRs is a form of the human β2-AR where a portion of the carboxyl terminal end of the third intracellular loop was replaced by the analogous region from the α_{1b}-adrenoceptor (Samma *et al.*, 1993). This mutant displays all of the phenotypic features nowadays commonly attributed to CAM receptors: it has markedly elevated levels of second messenger molecule production in comparison to the wild type receptor; it produces a basal functional activity which is correlated well with receptor expression levels and it possesses an enhanced affinity for agonists, the rank order of which is dictated by the ligand's intrinsic activity. The prevailing theory which has been offered to explain these findings is that in the case of the CAM β2-AR there is a perturbation in the equilibrium between the inactive (R) and active (R*) states of the receptor; this shifts the equilibrium in favour of the R* conformation and hence leads to an increase in the population of the activated form of the receptor. In all likelihood, this perturbation is brought about through the relaxation of conformational constraints designed to minimize spontaneous coupling to cellular G proteins which in the wild type receptor help to maintain very low levels of constitutive signalling in the absence of any activating ligand (Samma *et al.*, 1993; Lefkowitz *et al.*, 1993).

This theory finds support in experimental observations suggesting that the CAM form of the β2-AR is inherently less stable than the wild type receptor when incubated at 37°C (Gether *et al.*, 1997a). Presumably these findings reflect the fact that when the R* form is adopted, the receptor exists in a high-energy state which is more prone to spontaneous denaturation than the ground state (R) and that the CAM β2-AR, having

an increased proclivity for isomerisation to the R* conformation of the receptor, therefore exhibits a higher rate of degradation than its wild type counterpart. Further evidence comes from studies which have made use of fluorescent dyes that are sensitive to changes in the polarity of their molecular environment to determine whether any structural differences exist between the CAM β2-AR and wild type β2-AR. These have revealed that there do indeed exist distinctions between the two. Specifically observed was an alteration in the conformation of the protein structure within the immediate vicinity of the ligand-binding pocket (Javitch *et al.*, 1997). These differences are accompanied by exaggerated conformational responses of CAM β2-AR to the binding of agonist compounds, suggesting that constitutive activation of the β2-AR confers a higher degree of conformational flexibility to the receptor protein and that this may allow the CAM to more readily undergo transitions between the R and R* states (Gether *et al.*, 1997b).

Aside from the useful structural information that may be gleaned from studies into constitutive activation of GPCRs, investigations within this field have practical implications, applicable to industrially based drug discovery agendas. For instance, it has been recently suggested that through the use of constitutively active GPCRs, ligand-screening programmes designed to identify compounds that possess either positive or negative efficacy might be established. This was demonstrated in a study where *Xenopus laevis* melanophores were transiently transfected with various constitutively active GPCRs. The ability of the mutant receptors to promote the dispersion or aggregation of intracellular melanosomes was then measured through the monitoring of changes in the light transmittance of the cells in both the presence and absence of exogenous ligands. The results suggested that, provided the right expression levels of the mutant receptor could be achieved, such an assay would be

amenable to the detection of ligands for both known and orphan GPCRs (Chen *et al.*, 2000).

In the subsequent section of this chapter the structural instability of the CAM β2-AR is exploited in order to develop a similarly novel, yet more direct, alternative for the screening of potential receptor ligands. To achieve this, the cDNA for the bioluminescent luciferase from the *Anthozoan Renilla reniformis* has been ligated in frame with the cDNA for CAM β2-AR to create a chimeric receptor called CAM β2-AR-Rluc. The construct is modified at its carboxyl terminal tail by the presence of the *Renilla* luciferase enzyme in a similar manner to the wild type β2-AR-Rluc, described in Chapter 3. Through the expediency of in-frame linkage to the *Renilla* luciferase any increase in receptor number, brought about by ligand-mediated stabilization of the receptor construct, should result in an increase in the luminescent output of the enzyme in the presence of its substrate coelenterazine (Figure 5.1). Such a system should prove to be tractable in its application to high throughput compound screening programmes since there are only a very limited number of manipulations required in order to obtain assay readings. It is also seen through the pursuit of these studies that the upregulation observed is most likely to be attributable to a stabilization of the receptor structure that is induced by the presence of the ligand in the binding cavity of the receptor. This conclusion is inferred by a strong correlation between pEC_{50} for receptor upregulation (as measured through luminescence) and pK_i (as determined by competition binding for ligands in the presence of [^{3}H]-DHA).

5.2 Results

The cDNA for a CAM form of the human β2-AR, containing four point mutations within the carboxyl terminal end of its third intracellular loop (previously described in

Figure 5.1. The principal upon which an assay based upon agonist-induced stabilization of a *Renilla* luciferase tagged CAM GPCR might work.

Ligand binding to the CAM receptor favours the formation of a structure that is less liable to spontaneous denaturation. Over a period of 24 hours, in the presence of this ligand, there is an increase in the overall receptor population present within the cells. If the CAM receptor is directly fused to a bioluminescent marker protein (in this case *Renilla* luciferase) in a stoichiometry of 1:1, then this increase in receptor number will be exactly paralleled by an increase in bioluminescence. The increase is readily quantifiable using a sensitive luminometer.

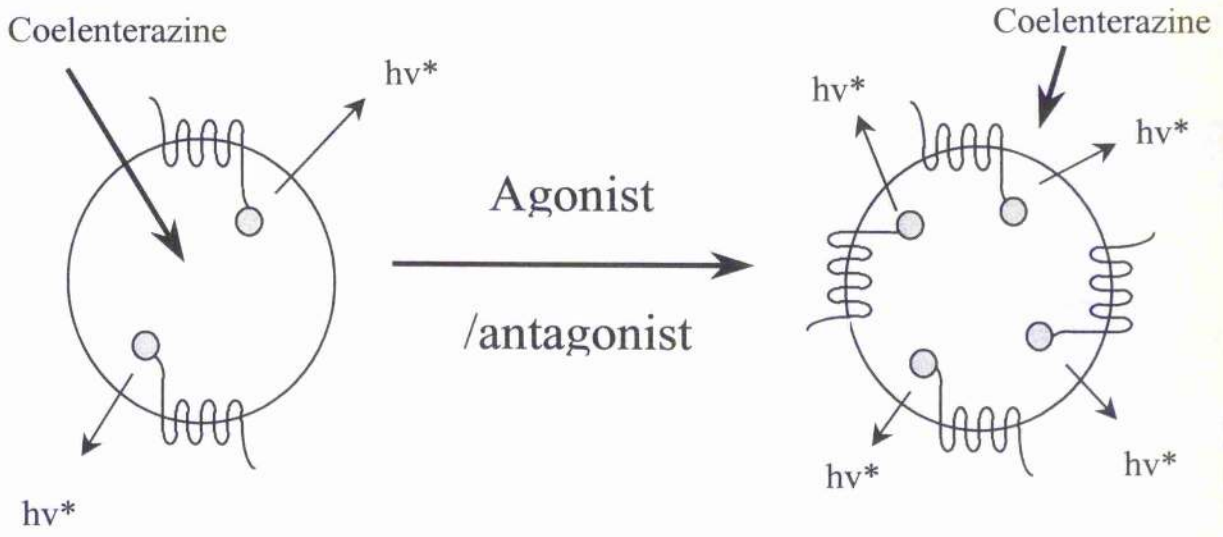
Coelenterazine
hv*
Agonist
/antagonist
hv*
Coelenterazine
hv*
hv*
hv*
hv*

Figure 5.1.

Samama *et al.*, 1993), was ligated in frame with and upstream of the cDNA encoding *Renilla* luciferase (as described in section 2.4.1). To test that this construct (CAM β2-AR-Rluc) was able to form a correctly folded receptor molecule that was capable of binding appropriate ligands, it was transiently transfected into HEK 293 cells and its ability to bind [^{3}H]-DHA in radio-ligand binding studies, using a single concentration of [^{3}H]-DHA (2nM) assessed. Typically, such transfections yielded levels of specific binding that were of the order of 500 to 600 fmol/mg and these were comparable to a version of the CAM β2-AR lacking in the Rluc modification that was assayed simultaneously with the chimera (Figure 5.2). These expression levels were substantially lower than those observed in similar experiments performed on wild type β2-AR and β2-AR-Rluc (see Chapter 3, Figure 3.4) where specific binding was in the range of 1200-1600 fmol/mg of protein. The observations were in accordance with previous work which had shown that the CAM form of the β2-AR expressed less well than the wild type receptor in mammalian cells (MacEwan and Milligan 1996). Saturation binding studies, using a number of concentration points of [^{3}H]-DHA showed that the K_d for CAM β2-AR-Rluc was effectively unaltered through the addition of the *Renilla* luciferase to the carboxyl terminal tail of the receptor (Results shown later).

Similar chimeric constructs were made with the luciferase from the firefly *Photinus pyralis*. Again the cDNA for either CAM or wild type β2-AR was ligated immediately upstream of the cDNA for the luciferase. Following transient transfection within HEK 293 cells, intact cell binding assays were performed to determine whether or not the carboxyl tail modification of the receptor, with this alternative luciferase, prevented successful expression of the receptor construct. It was found that specific binding of [^{3}H]-DHA to the wild type β2-AR was similar to β2-

AR-Pluc (Figure 5.3). However, in the case of the CAM form of the receptor specific binding was not detectable (results not shown). In view of these circumstances it was decided to continue the study by focusing primarily on the CAM β2-AR-Rluc construct with the wild type β2-AR-Pluc used in only a limited number of experiments detailed towards the end of the Results section.

To demonstrate that this CAM β2-AR-Rluc was functionally active and that the carboxyl terminal tail modification of the receptor with *Renilla* luciferase did not interfere with coupling to intracellular G proteins, intact cell adenylyl cyclase assays were performed on cells transiently expressing the chimeric construct. The results of the experiments showed that expression of CAM β2-AR-Rluc within HEK 293 cells had the effect of substantially elevating basal levels of cAMP production, an effect which could be enhanced by the presence of isoprenaline (10μM) (Figure 5.4). These levels of cAMP, measured both in the presence and absence of agonist, were comparable to those seen in similar assays carried out on the unmodified version of the CAM β2-AR, conducted along side those of the chimera (Figure 5.4). In untransfected HEK 293 cells, although basal levels of cAMP were very low, a clear increase could be detected in the presence of isoprenaline, plainly demonstrating the presence of a small population of endogenously expressed β2-AR (Figure 5.4). In contrast to intact cell adenylyl cyclase assays performed on cells transiently transfected with either the Rluc modified or intact wild type β2-AR (Chapter 3, Figure 3.5), basal production of cAMP nucleotides was substantially elevated in the case of CAM-β2-AR-Rluc (Figure 5.4). This was in agreement with the existing notion that constitutively activating mutations produce an elevated basal production of second messenger nucleotides. Taken together, these results indicate that the carboxyl terminal tail modification of CAM β2-AR with *Renilla* luciferase does not interfere

with the ability of the receptor to activate downstream effectors in response to agonists. Nor does the *Renilla* luciferase molecule suppress the CAM characteristics conferred by the presence of the point mutations in intracellular loop 3 of the receptor. To confirm that the modification of CAM β2-AR with *Renilla* luciferase did not affect the ability of the receptor to be upregulated in the sustained presence of inverse agonists, HEK 293 cells were transiently transfected with the cDNA for either CAM β2-AR or CAM β2-AR-Rluc and then exposed to a twenty-four hour incubation with betaxolol (10μM). After this period had elapsed, cells were harvested and the specific binding to membrane preparations of a single concentration of [^{3}H]-DHA was assessed. The outcome was that in the presence of betaxolol both constructs exhibited a three to four fold increase in levels of specific binding (Figure 5.5). This was an observation that was attributable to the presence of the inverse agonist causing a direct increase in the expression levels of the receptor, as was revealed through binding studies on CAM β2-AR-Rluc membranes in which a variety of concentrations of [^{3}H]-DHA were used (Figure 5.6). In these saturation binding experiments, the B_{max} value for receptor expression levels following a twenty-four hour pre-incubation with betaxolol was 2600 fmol/mg; this was in comparison to a B_{max} value of 400 fmol/mg obtained from membranes where the pre-treatment with betaxolol was omitted. Further verification was obtained through experiments where HEK 293 cells transiently expressing CAM β2-AR-Rluc were exposed to varying concentrations of betaxolol for twenty-four hours before the cells were harvested and membranes prepared. Applying the same protein concentration to each assay point, the membranes were monitored both for their ability to bind to antagonist in radioligand assays using a single concentration of [^{3}H]-DHA (2nM) and for their ability to produce light through bioluminescence upon addition of coelenterazine (5μM). Data

collected from both of these assay methods showed that the levels of receptor expression and consequently the bioluminescence of *Renilla* luciferase could be modulated by the concentration of betaxolol used in the pre-incubation step. When the data was normalized to the magnitude of the readings obtained using the highest concentration of betaxolol, it could be seen that the specific binding of [^{3}H]-DHA to the receptor and the values of light emitted via *Renilla* bioluminescence paralleled one another (Figure 5.7). This result is as expected, given the 1:1 stoichiometry that exists between the receptor and the bioluminescent enzyme.

To continue the study, HEK 293 cells stably expressing CAM β2-AR-Rluc were established, a single clone of which was isolated and selected for further examination. Membranes prepared from this clone were subject to saturation binding using multiple concentrations of [^{3}H]-DHA. B_{max} values hence obtained revealed that the receptor was stably expressed at relatively low levels (600 fmol/mg) within the cells and that the K_d for DHA at the CAM β2-AR-Rluc receptor construct was approximately 0.3 ± 0.1nM (Figure 5.8), a value in close agreement with previous observations for other CAM β2-AR constructs (McLean *et al.*, 1999). Cells of this clone were then plated into 96 well plate dishes and then exposed for twenty-four hours to five different antagonist compounds, all of which were known to have affinity for the β2-AR. Subsequent monitoring of the light emitted by *Renilla* luciferase upon addition of coelenterazine (5μM) showed that all five antagonist compounds were capable of inducing an upregulation of CAM β2-AR-Rluc (Figure 5.9) and that typically the degree of upregulation was of the order of two-fold for all compounds tested. The ability of the ligands to upregulate the CAM β2-AR-Rluc did not seem to be related to their efficacy however, since betaxolol and ICI 118 551 (both strong inverse agonists) did not produce a degree of upregulation that was markedly different from that

conferred by propranolol, a ligand of almost neutral efficacy. The EC_{50} values for each compound are shown in Table 5.1. Each of these ligands was able to compete with [^{3}H]-DHA for occupancy of the receptor binding site in membranes prepared from the cell line stably expressing CAM β2-AR-Rluc (Figure 5.10). From this data, the dissociation equilibrium constant K_i (a measure of the binding affinity of a compound for the receptor) was calculated and the values thus obtained revealed that the ligands showed varying affinities for CAM β2-AR-Rluc (Table 5.1). By taking the negative log values for these two sets of results to obtain values of pK_i and pEC_{50}, it could be seen that they correlated well (Figure 5.11) ($r^2 = 0.932$).

Similar sets of experiments were performed using agonist compounds. It was shown that the partial agonists salbutamol and salmeterol, and the full agonist isoprenaline were all capable of giving rise to a degree of upregulation that was comparable in magnitude to that imparted by the antagonist compounds (Figure 5.12). Two of these, isoprenaline and salbutamol, were selected for competition binding studies and were both found to be capable of displacing [^{3}H]-DHA from the receptor binding crevice (Figure 5.13). However, in contrast to values obtained with the antagonist compounds, there was a marked dissimilarity between the EC_{50} and K_i values for isoprenaline (EC_{50}= $3.0\times10^{-6}\pm 3.7\times10^{-7}$, K_i= $2.0\times10^{-8}\pm 4.8\times10^{-9}$) and salbutamol ($EC_{50}$= $1.7\times10^{-6} \pm 2.2\times10^{-7}$, K_i = $8.1\times 10^{-8}\pm 2.9\times10^{-8}$) respectively.

To demonstrate the dependence on the CAM nature of the receptor for upregulation of CAM β2-AR-Rluc, HEK 293 cells were transiently co-transfected with the cDNAs for both CAM β2-AR-Rluc and wild type β2-AR-Pluc. After twenty-four hours the cells were either left untreated or exposed to a saturating concentration of betaxolol (10μM) and then maintained under these conditions at 37°C for a further twenty-four hours. Subsequently, crude membranes were prepared and their protein content

Table 5.1. EC_{50} values for upregulation and K_i values for competition binding obtained in studies with CAM β2-AR-Rluc.

A complete list of all the EC_{50} values obtained from the data for receptor upregulation, as determined through monitoring increases in receptor number via the luciferase assay. Also shown are all the K_i values from the competition binding studies, as were determined through the ability of the test compound to displace [^{3}H]-DHA from receptor binding sites. The results represent means ± S.E.M. of three experiments.

Compound	EC_{50}	K_i
Betaxolol	$1.1x10^{-7} \pm 8.3x10^{-9}$	$6.9x10^{-8} \pm 1.8x10^{-8}$
Propranolol	$3.3x10^{-9} \pm 7.6x10^{-10}$	$6.8x10^{-10} \pm 1.3x10^{-10}$
ICI 118 551	$1.4x10^{-8} \pm 2.7x10^{-9}$	$1.5x10^{-9} \pm 3.2x10^{-10}$
Sotolol	$1.8x10^{-6} \pm 7.2x10^{-7}$	$2.9x10^{-7} \pm 6.0x10^{-8}$
CGP 121 77A	$4.4x10^{-9} \pm 5.1x10^{-10}$	$2.1x10^{-9} \pm 4.2x10^{-10}$

Table 5.1.

evaluated as described in section 2.6.2. The membranes were then monitored in parallel for light output from both *Renilla* and *Photinus* luciferases using the dual luciferase assay system that is described in section 2.6.12. In the presence of betaxolol light output from *Renilla* luciferase was seen to undergo a twofold increase (Figure 5.14) in contrast to the levels of light emitted by *Photinus* which were not elevated above basal levels. This clearly showed that only the version of the β2-AR receptor possessing constitutively activating mutations was capable of being upregulated in the presence of the inverse agonist.

The upregulation effect could only be mediated by antagonists/inverse agonists which had pharmacological specificity for the CAM β2-AR-Rluc. This was shown by transiently transfecting the cDNA for CAM β2-AR-Rluc into a HEK 293 cell line stably expressing a GFP conjugated CAM version of the α_{1b}-adrenoceptor (CAM α_{1b}-AR-GFP) (Stevens *et al.*, 2000). Here, cells were either left untreated, exposed to betaxolol (10μM) or exposed to phentolamine (10μM), a potent inverse agonist that is highly selective for α_1-receptors (Lee *et al.*, 1997). The cells were then maintained in the presence of these compounds for a further 24 hours, after which they were lysed and then treated in such a way as to isolate membranes with the protein content quantified as described in section 2.6.2. Using equal quantities of protein at each assay point, the light output from *Renilla* luciferase upon addition of coelenterazine (5μM) and the resultant fluorescence upon excitation of GFP with an appropriate wavelength of light were then measured in parallel. The results obtained from cell samples that had been exposed to either betaxolol or phentolamine were expressed as percentages of similar readings obtained from the cells that were left untreated during the experiment. In the presence of betaxolol, *Renilla* bioluminescence from CAM β2-AR-Rluc produced a two to threefold increase in the levels of light output (Figure

5.15). The same cells displayed no increases above basal levels of fluorescence however when assayed to quantitate levels of CAM α_{1b}-AR-GFP in an arbitrary manner (Figure 5.15). This effect was antipodal to that seen in cells which had been exposed to phentolamine, where no alterations in the levels of light output from *Renilla* were observed and GFP fluorescence was seen to undergo an approximately threefold increase above basal levels (Figure 5.15). From these results, it can be unambiguously seen that it is only ligands capable of interacting directly with the binding crevice of CAM β2-AR-Rluc that are capable of producing increases in receptor number.

To finish this investigation it was deemed necessary to provide some further confirmatory evidence that the system described herein would lend itself towards the development of a high throughput ligand-screening assay. To this end, the stable cell line expressing CAM β2-AR-Rluc was seeded into 96 well microtiter plates and then exposed for twenty-four hours to a variety of agonist and antagonist compounds, possessing a wide range of pharmacological specificities. Following this pre-incubation period the cells were assayed for luciferase activity in the manner described in section 2.6.12. Generally cells which had been exposed to ligands with a specificity for CAM β2-AR-Rluc tended to produce greater levels of *Renilla* bioluminescence above basal than that observed in cells exposed to compounds that lacked any affinity for adrenergic receptors, as seen in both duplicate runs of this experiment (Figure 5.16). Occasional false positive results made it difficult to interpret whether one or two of the compounds lacking in affinity for β2-AR were capable of inducing upregulation or not (for example DPCPX (Figure 5.16A) and CPA (Figure 5.16B)), however, it is to be anticipated that this could be in some way rectified through the use of triplicate assay points. One of the compounds, melanin-

Figure 5.2. Expression levels of the CAM β2-adrenoceptor and *Renilla* tagged CAM β2-adrenoceptor when expressed in HEK 293T cells.

HEK 293 cells were mock transfected or transiently transfected with the cDNAs for either CAM β2-AR or CAM β2-AR-Rluc. Forty-eight hours later membranes were prepared and the specific binding of [^{3}H]-DHA (2nM) measured. The data are means ± S.E.M. values of triplicate wells taken from a single assay. Two further experiments produced similar results.

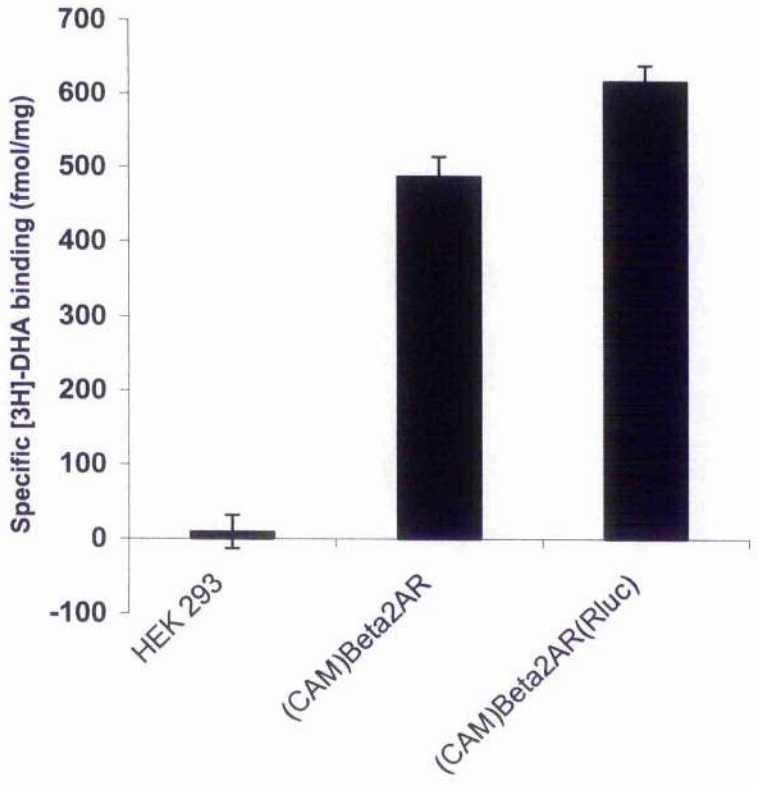
Specific [3H]-DHA binding (fmol/mg)
700
600
500
400
300
200
100
0
-100
HEK 293
(CAM)Beta2AR
(CAM)Beta2AR(Rluc)

Figure 5.2.

Figure 5.3. Expression levels of the wild type β2-adrenoceptor and *Photinus* tagged β2-adrenoceptor when expressed in HEK 293T cells.

HEK 293T cells either mock transfected, transiently transfected with wild type β2-AR or transiently transfected with β2-AR-Pluc were assayed for specific binding of [^{3}H]-DHA via the intact cell methodologies described in section 2.6.3. The experiment is a single representative experiment of three such performed with the error bars representing means ± S.E.M. of triplicate assay points.

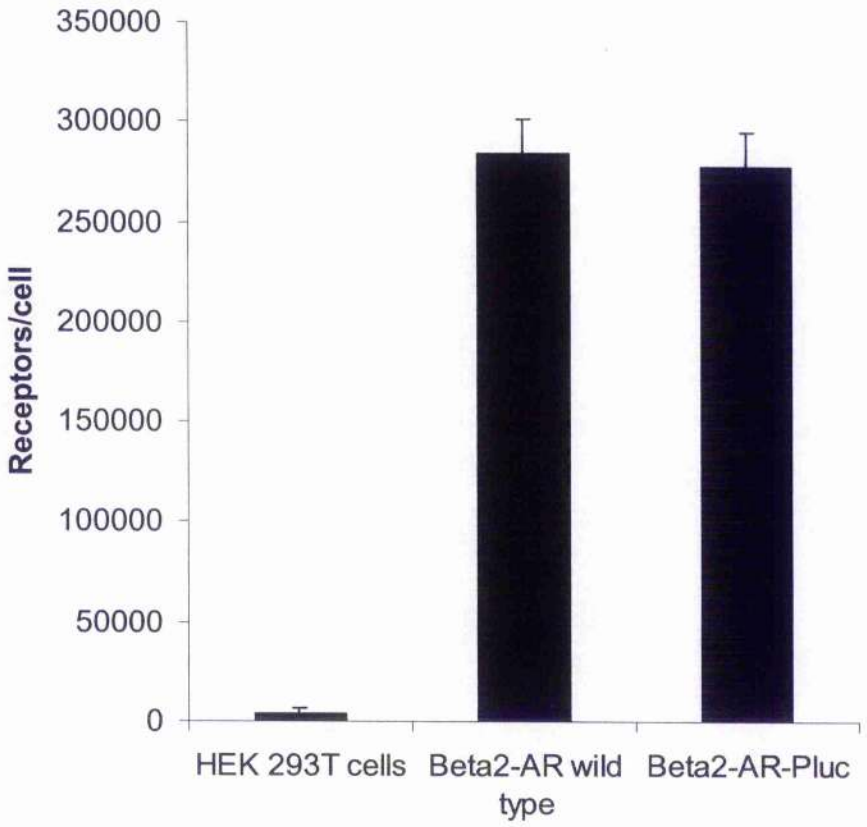
350000
300000
250000
200000
150000
100000
50000
0
Receptors/cell
HEK 293T cells
Beta2-AR wild type
Beta2-AR-Pluc

Figure 5.3

Figure 5.4. Functional coupling of CAM β2-adrenoceptor and *Renilla* tagged CAM β2-adrenoceptor to adenylyl cyclase in HEK 293T cells.

HEK 293 cells were mock transfected or transiently transfected with the cDNA for either CAM β2-AR or CAM β2-AR-Rluc. Twenty-four hours later the cells were labelled with [^{3}H]-adenine. After a further twenty-four hours, cAMP generation was measured (as described in section 2.6.4) in both the presence and absence of the β2-AR agonist isoprenaline (10μM). The data are means ± S.E.M. values of triplicate wells taken from a single assay representative of three such experiments performed.

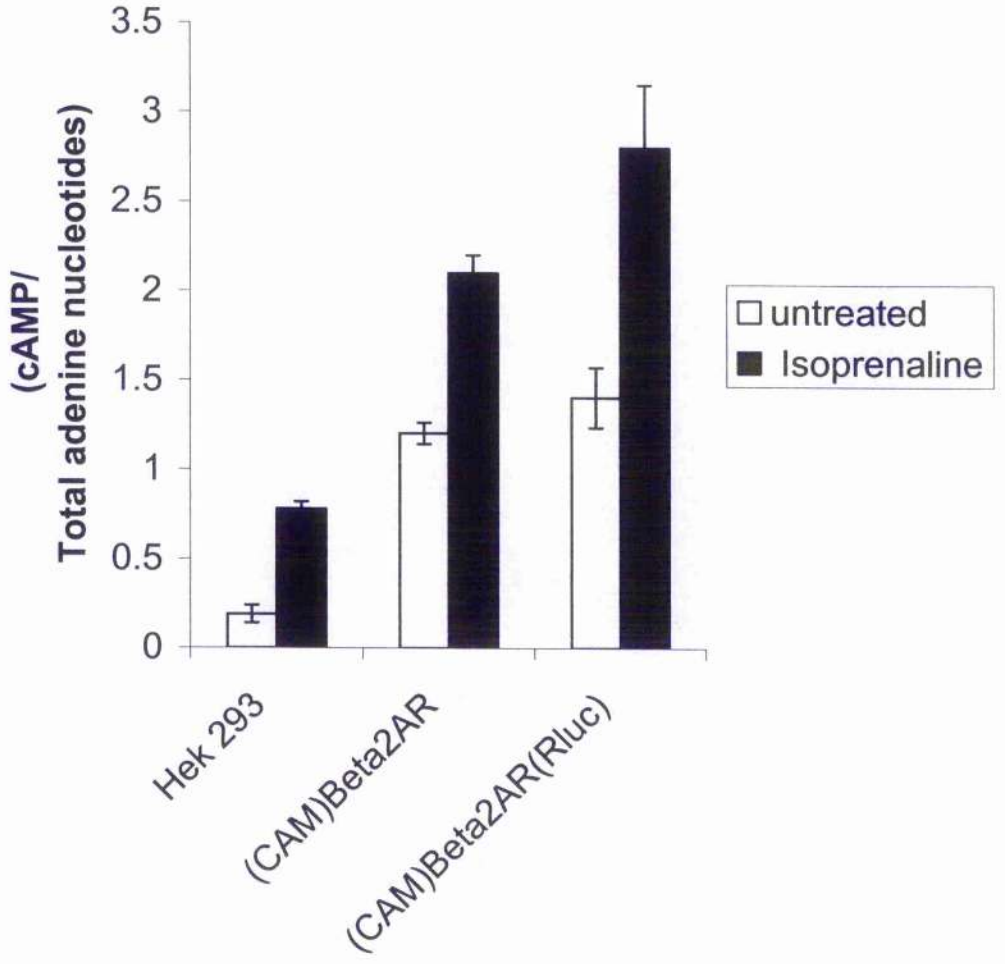
3.5
3
2.5
2
1.5
1
0.5
0
(cAMP/
Total adenine nucleotides)
untreated
Isoprenaline
Hek 293
(CAM)Beta2AR
(CAM)Beta2AR(Rluc)

Figure 5.4.

Figure 5.5. Prolonged treatment with betaxolol upregulates both CAM β2-adrenoceptor and CAM β2-adrenoceptor- Rluc expressed in HEK 293T cells. HEK 293 cells were transiently transfected with the cDNA for either CAM β2-AR or CAM β2-AR-Rluc. Twenty-four hours later the cells were either left untreated or were exposed to betaxolol (10μM). After a further twenty-four hours, membranes were prepared and the specific binding of [^{3}H]-DHA (2nM) was measured. The results are means ± S.E.M. of three independent experiments performed.

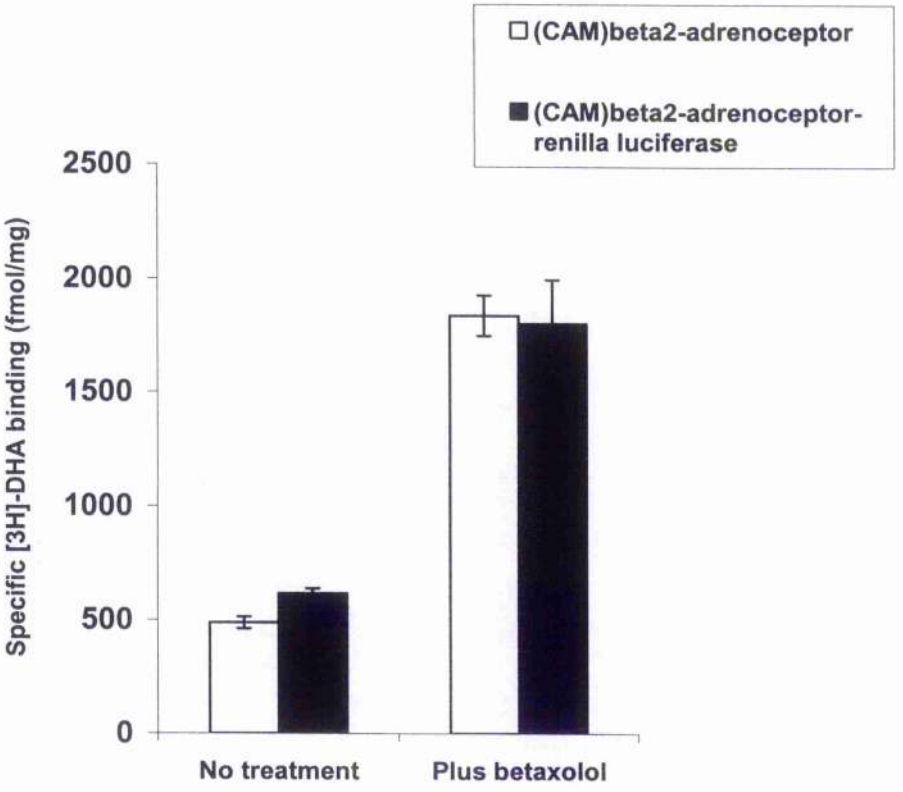
□(CAM)beta2-adrenoceptor
■(CAM)beta2-adrenoceptor-renilla luciferase
Specific [3H]-DHA binding (fmol/mg)
2500
2000
1500
1000
500
0
No treatment
Plus betaxolol

Figure 5.5.

Figure 5.6. Upregulation of CAM β2-adrenoceptor-Rluc in response to prolonged treatment with betaxolol represents a true increase in receptor number.

HEK 293 cells were transiently transfected with the cDNA for CAM β2-AR-Rluc. Twenty-four hours later the cells were either left untreated or were exposed to betaxolol (10μM). After a further twenty-four hours membranes were prepared and the specific binding of a range of [^{3}H]-DHA concentrations measured. The results are a single representative of three independent experiments.

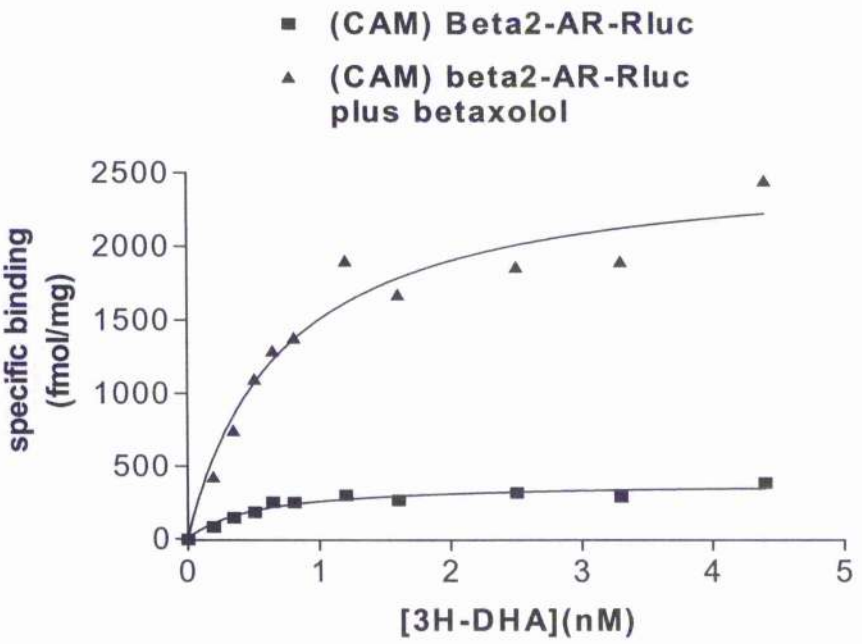
(CAM) Beta2-AR-Rluc
(CAM) beta2-AR-Rluc plus betaxolol
specific binding (fmol/mg)
2500
2000
1500
1000
500
0
0
1
2
3
4
5
[3H-DHA](nM)

Figure 5.6.

Figure 5.7. The increase in receptor number as determined via radioligand binding exactly parallels the increases observed in *Renilla* bioluminescence.

HEK 293 cells were transiently transfected with cDNA to express the CAM β2-AR-Rluc construct. Twenty-four hours later the cells were exposed to varying concentrations of betaxolol. The specific [^{3}H]-DHA (2nM) binding of the receptor and the luminescence from *Renilla* luciferase were then measured in parallel twenty-four hours later. Data are presented as per cent maximal effect with results derived from three independent experiments.

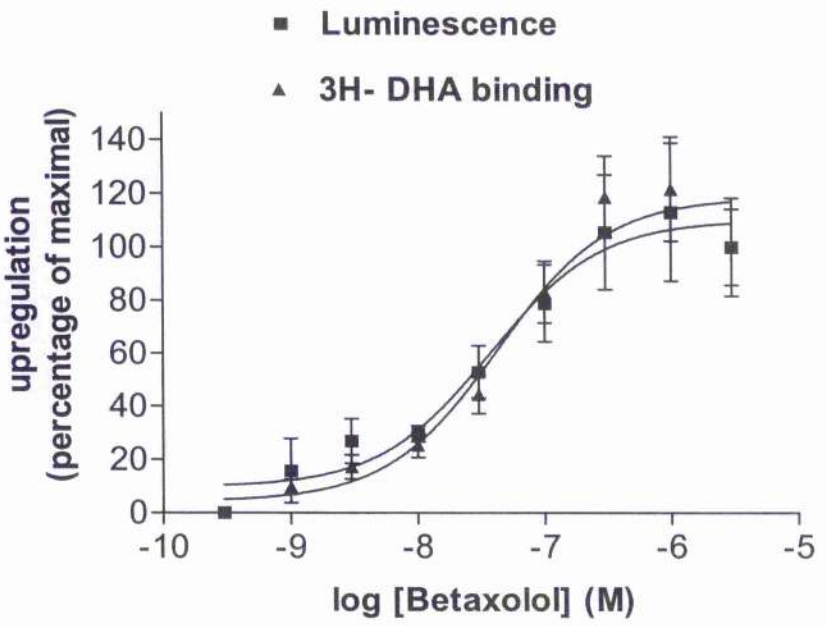
Luminescence
3H- DHA binding
upregulation
(percentage of maximal)
140
120
100
80
60
40
20
0
-10
-9
-8
-7
-6
-5
log [Betaxolol] (M)

Figure 5.7.

Figure 5.8. The K_d for CAM β2-adrenoceptor-Rluc is essentially unaltered by the carboxyl terminal tail modification with *Renilla*.

A HEK 293 cell line stably expressing the CAM β2-AR-Rluc was established from a single clone and membrane preparations were obtained. Specific binding, using a range of [^{3}H]-DHA concentrations, allowed the K_d and B_{max} values for the receptor construct to be determined. Data are from a single transfection representative of three such experiments performed.

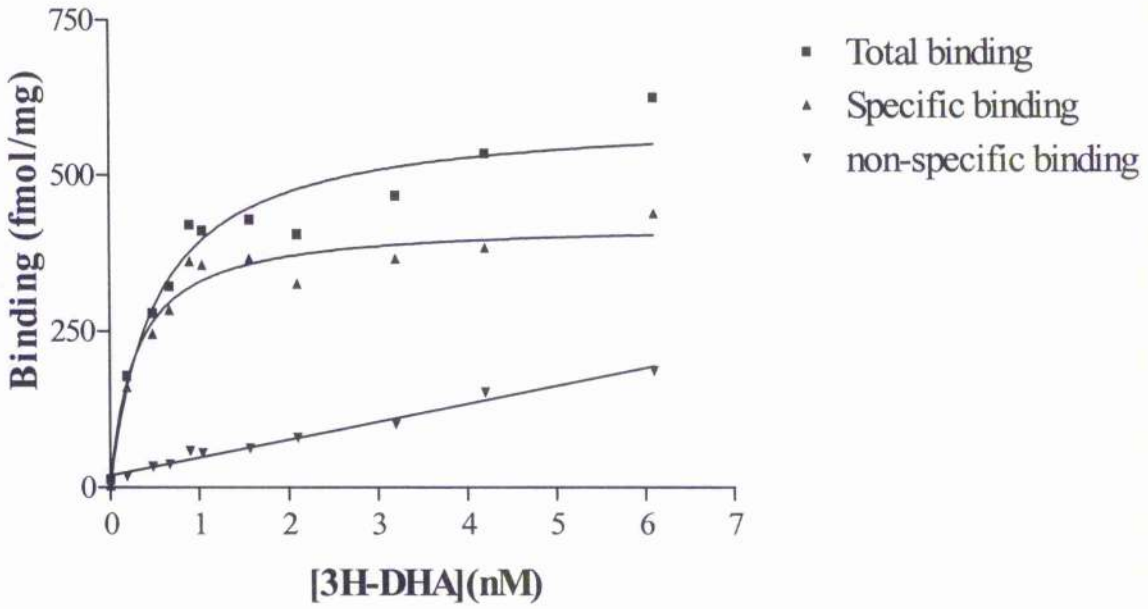
750
500
250
0
Binding (fmol/mg)
0
1
2
3
4
5
6
7
[3H-DHA](nM)
Total binding
Specific binding
non-specific binding

Figure 5.8.

Figure 5.9. The ability of various antagonist compounds to upregulate CAM β2-adrenoceptor-Rluc: EC_{50} values were determined.

Cells of a clone of HEK 293 cells stably expressing CAM β2-AR-Rluc were grown in 96 well microtiter plates and exposed to various concentrations of either **(A)** betaxolol, **(B)** ICI 118 551, **(C)** propranolol, **(D)** CGP 121 77A or **(E)** sotalol for a period of twenty four hours. The light emission from *Renilla* luciferase was then monitored as described in section 2.6.12. The results represent means ± S.E.M. from three experiments.

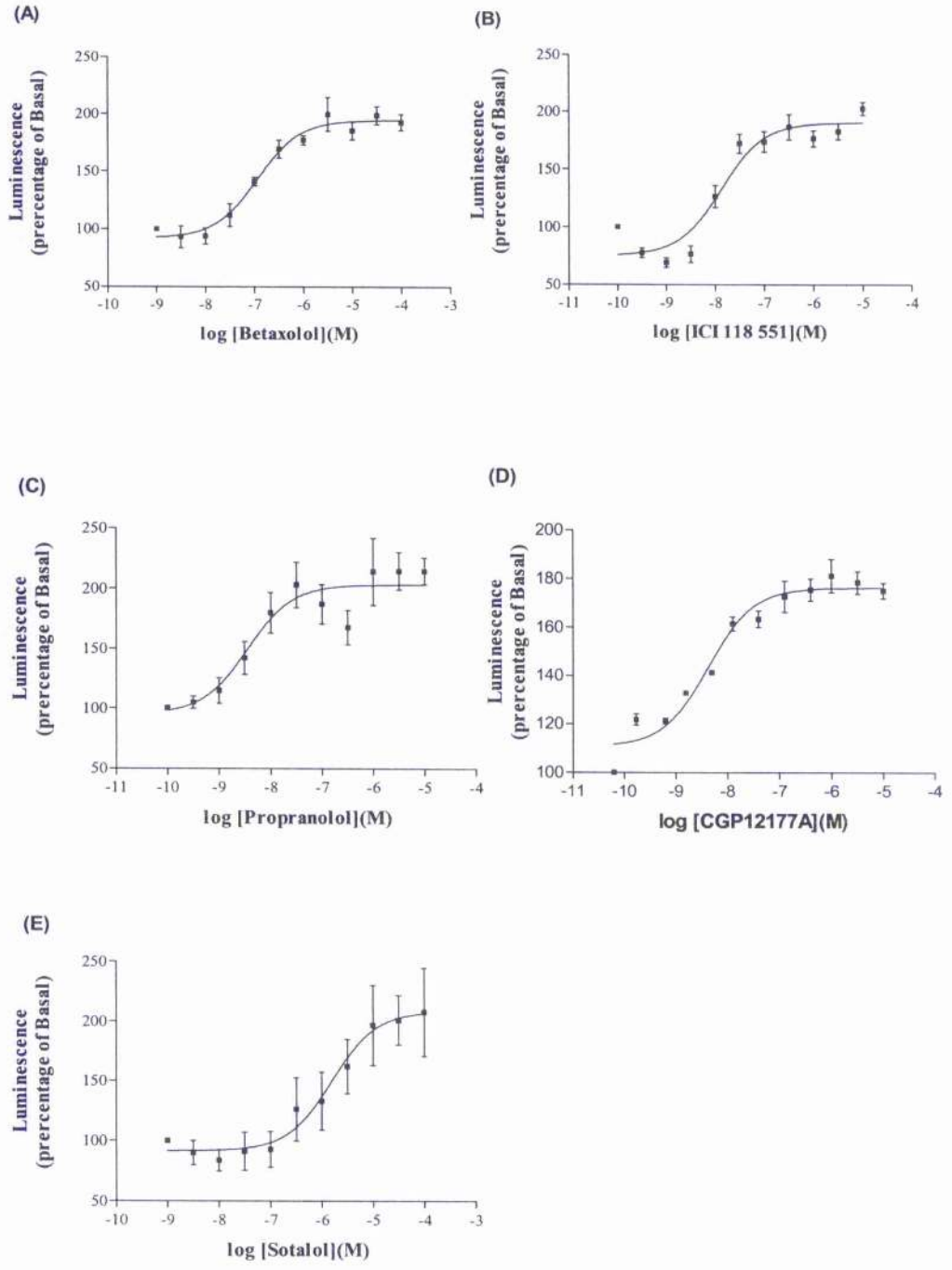
(A)
Luminescence (prercentage of Basal)
log [Betaxolol](M)
(B)
Luminescence (prercentage of Basal)
log [ICI 118 551](M)
(C)
Luminescence (prercentage of Basal)
log [Propranolol](M)
(D)
Luminescence (prercentage of Basal)
log [CGP12177A](M)
(E)
Luminescence (prercentage of Basal)
log [Sotalol](M)

Figure 5.9.

Figure 5.10. The ability of various antagonist compounds to compete with [^{3}H]-DHA for binding to CAM β2-adrenoceptor-Rluc: K_i values were determined.

Membrane preparations from HEK 293 cells stably expressing CAM β2-AR-Rluc were obtained. The capacity for various concentrations of **(A)** betaxolol, **(B)** ICI 118 551, **(C)** propranolol, **(D)** CGP 121 77A or **(E)** sotalol to compete with [^{3}H]-DHA (2nM) for binding to CAM β2-AR-Rluc was assessed. Data represent means ± S.E.M. from three experiments.

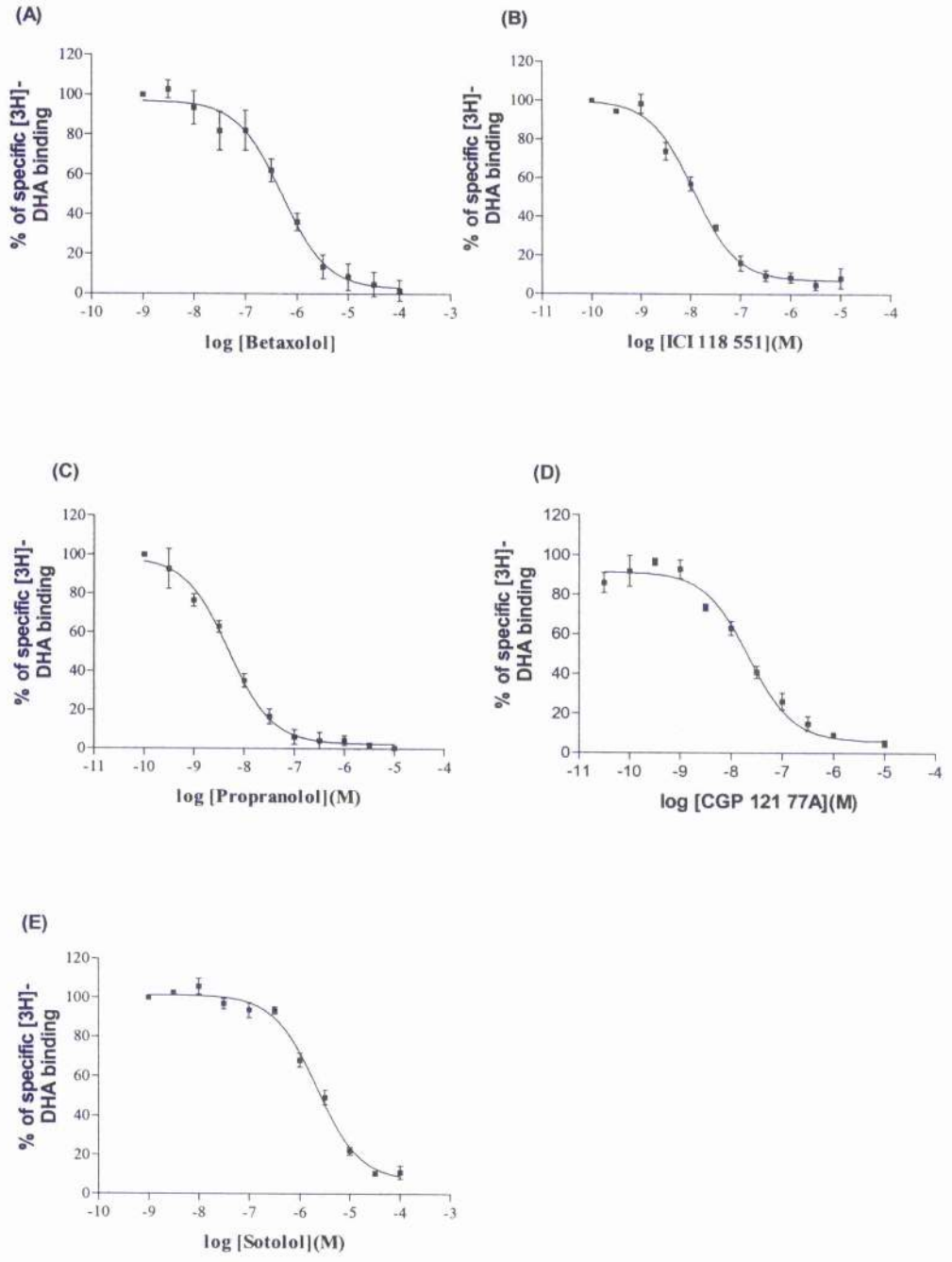
(A)
% of specific [3H]-DHA binding
log [Betaxolol]
(B)
% of specific [3H]-DHA binding
log [ICI 118 551](M)
(C)
% of specific [3H]-DHA binding
log [Propranolol](M)
(D)
% of specific [3H]-DHA binding
log [CGP 121 77A](M)
(E)
% of specific [3H]-DHA binding
log [Sotolol](M)

Figure 5.10.

Figure 5.11. The correlation between the pK_i and pEC_{50} values for a variety of antagonist compounds.

From the data presented in figures 5.9 and 5.10 the pEC_{50} and estimated pK_i values of each compound, **(A)** sotolol, **(B)** betaxolol, **(C)** ICI 118 551, **(D)** CGP 121 77A and **(E)** propranolol were determined. Data represent means ± S.E.M. from three experiments.

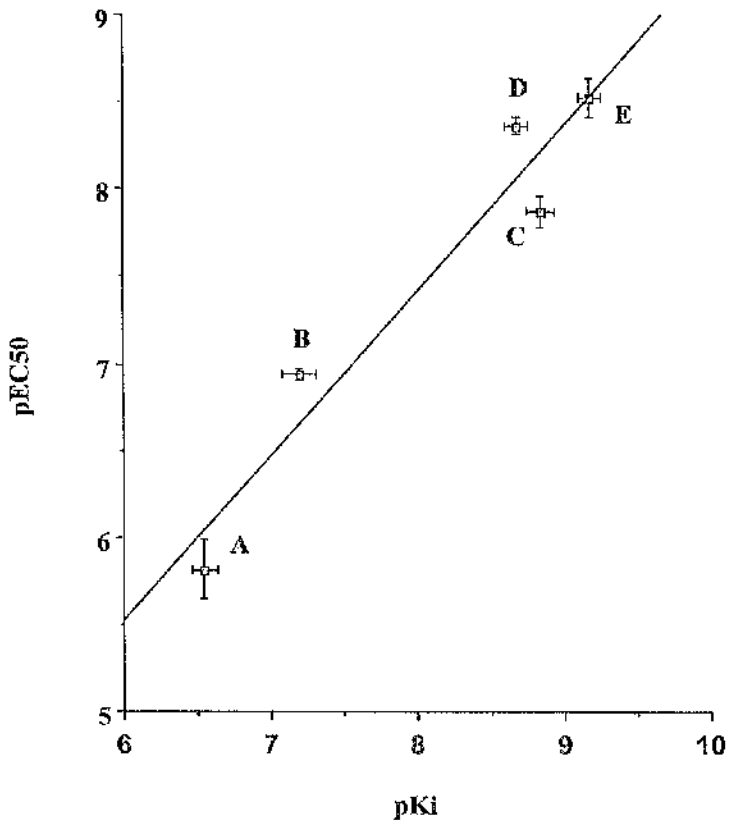

Figure 5.11.

Figure 5.12. The ability of various agonist compounds to upregulate CAM β2-adrenoceptor-Rluc: EC_{50} values were determined.

Cells of a clone of HEK 293 cells stably expressing CAM β2-AR-Rluc were grown in 96 well microtiter plates and exposed to various concentrations of either **(A)** isoprenaline, **(B)** salmeterol or **(C)** salbutamol for a period of twenty four hours. The light emission from *Renilla* luciferase was then monitored as described in section 2.6.12. The results represent means ± S.E.M. from three experiments.

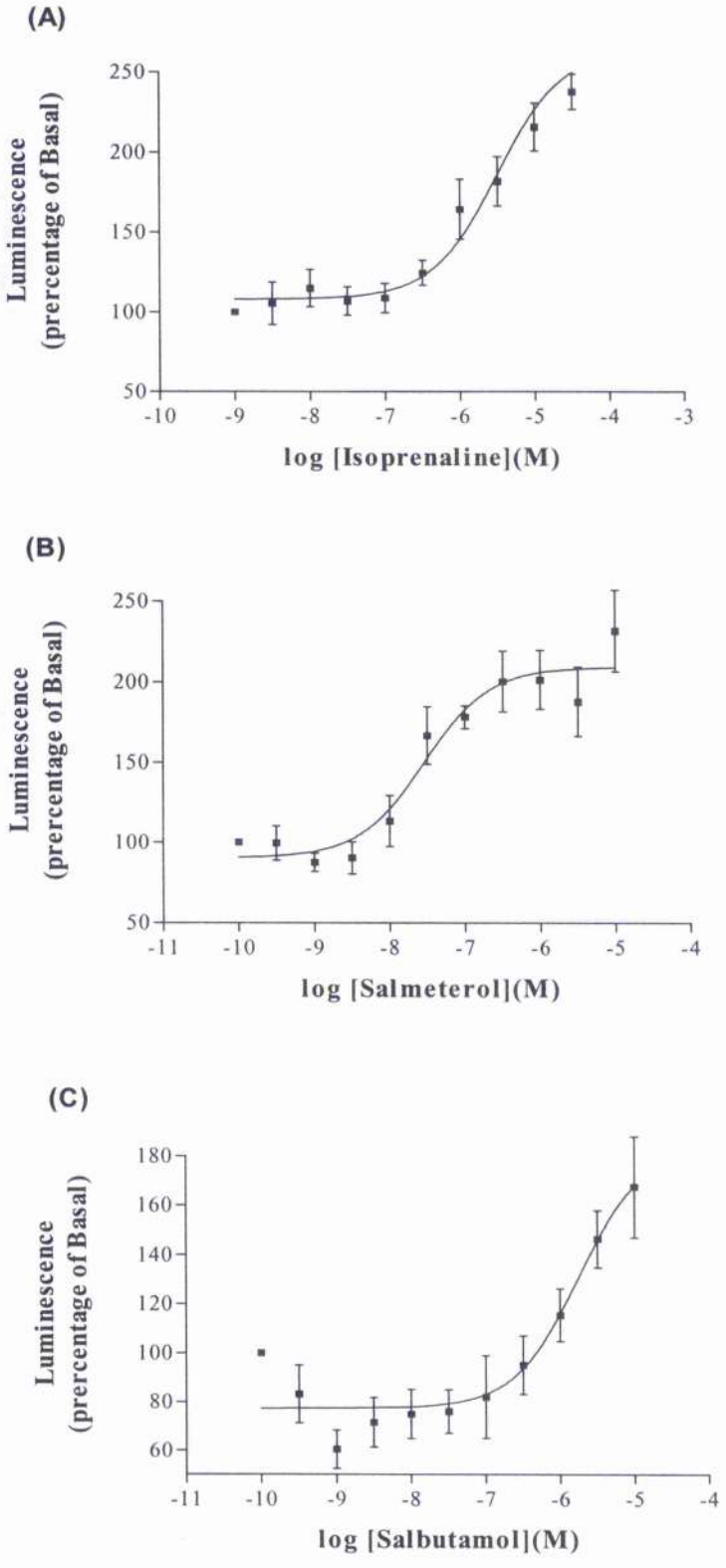
(A)
Luminescence (prercentage of Basal)
250
200
150
100
50
-10
-9
-8
-7
-6
-5
-4
-3
log [Isoprenaline](M)
(B)
Luminescence (prercentage of Basal)
250
200
150
100
50
-11
-10
-9
-8
-7
-6
-5
-4
log [Salmeterol](M)
(C)
Luminescence (prercentage of Basal)
180
160
140
120
100
80
60
-11
-10
-9
-8
-7
-6
-5
-4
log [Salbutamol](M)

Figure 5.12.

Figure 5.13. The ability of various agonist compounds to compete with [3H]-DHA for binding to CAM β2-adrenoceptor-Rluc: K_i values were determined.

Membrane preparations from HEK 293 cells stably expressing CAM β2-AR-Rluc were obtained. The capacity for various concentrations of **(A)** isoprenaline or **(B)** salbutamol to compete with [^{3}H]-DHA (2nM) for binding to CAM β2-AR-Rluc was assessed. Data represent means ± S.E.M. from three experiments.

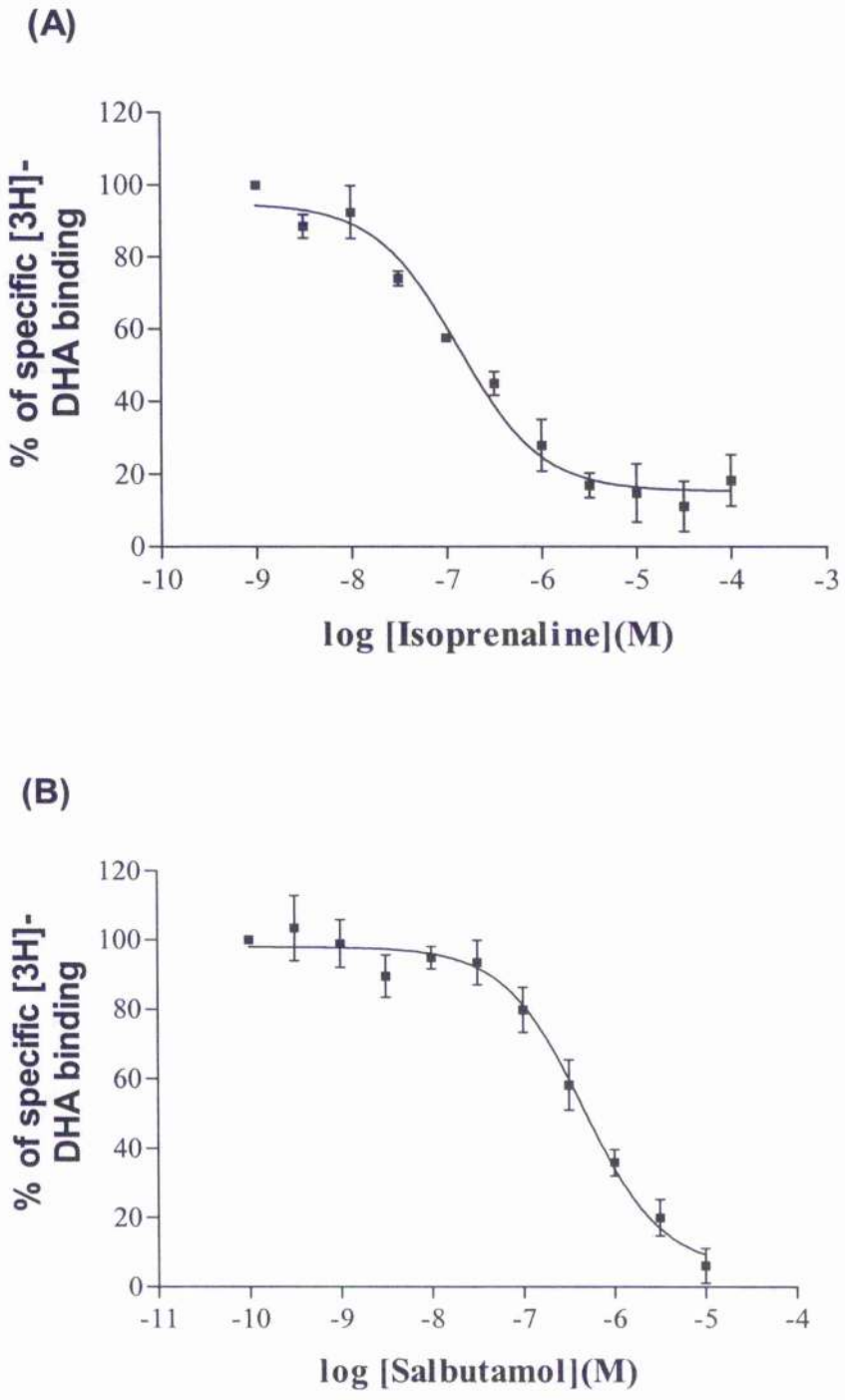
(A)
% of specific [3H]-DHA binding
120
100
80
60
40
20
0
-10
-9
-8
-7
-6
-5
-4
-3
log [Isoprenaline](M)
(B)
% of specific [3H]-DHA binding
120
100
80
60
40
20
0
-11
-10
-9
-8
-7
-6
-5
-4
log [Salbutamol](M)

Figure 5.13.

Figure 5.14. Upregulation of the β2-adrenoceptor requires the constitutively activating mutation.

HEK 293T cells were transiently transfected with a combination of CAM β2-AR-Rluc and wild type β2-AR-Pluc constructs. Cells were then treated twenty-four hours later with or without betaxolol (10μM) for a further twenty-four hours. *Photinus* and *Renilla* luciferase activities were then measured in parallel. Data represent means ± S.E.M. from three experiments.

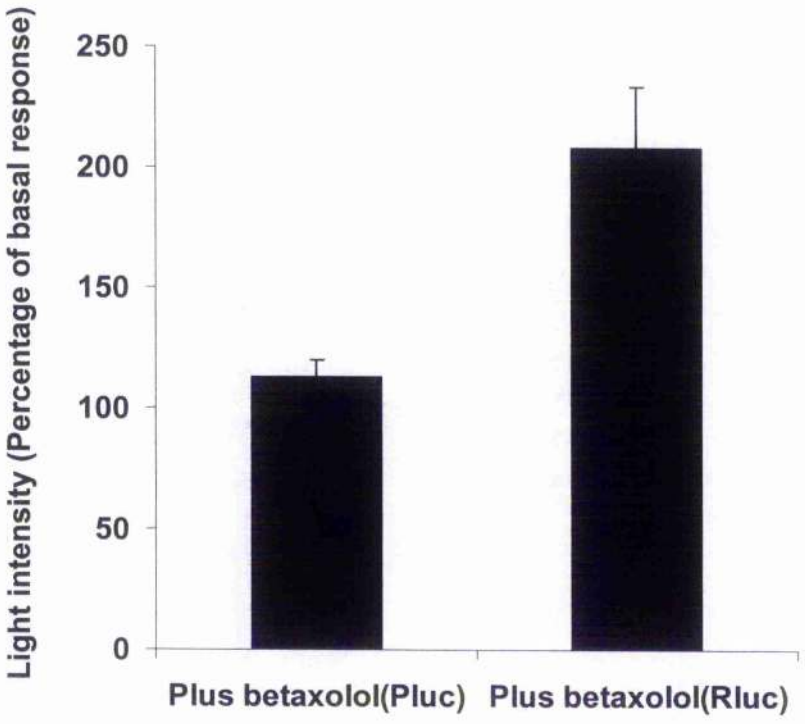
Light intensity (Percentage of basal response)
250
200
150
100
50
0
Plus betaxolol(Pluc)
Plus betaxolol(Rluc)

Figure 5.14

Figure 5.15. CAM β2-adrenoceptor-Rluc is only upregulated by compounds that exhibit pharmacological specificity for the receptor.

A clone of HEK 293T cells stably expressing a CAM α_1-adrenoceptor-GFP construct (Stevens *et al.*, 2000) was transiently transfected for twenty-four hours to express CAM β2-AR-Rluc. The cells were then either exposed to betaxolol (10μM) or to the α_1-adrenoceptor antagonist/inverse agonist phentolamine (each at 10 μM) for twenty-four hours. *Renilla* luciferase activity (as bioluminescence) and GFP fluorescence were then monitored in parallel. Results are presented as per cent of the signals obtained from cells in the absence of any treatment and represent means ± S.E.M. from three experiments.

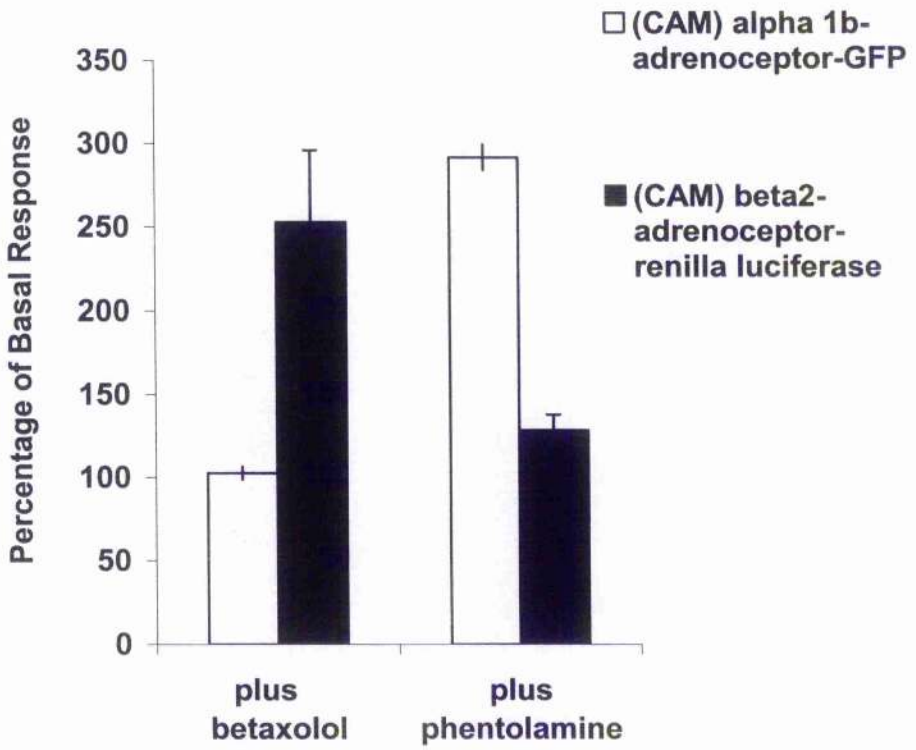
□ (CAM) alpha 1b-adrenoceptor-GFP
■ (CAM) beta2-adrenoceptor-renilla luciferase
Percentage of Basal Response
350
300
250
200
150
100
50
0
plus betaxolol
plus phentolamine

Figure 5.15

Figure 5.16. The upregulation of the CAM β2-adrenoceptor-Rluc could potentially form the basis of an assay for the detection of compounds exhibiting pharmacological specificity for the β2-adrenoceptor.

Cells of a clone of HEK 293 cells stably expressing CAM β2-AR-Rluc were grown in 96 well microtiter plates and then exposed to various test compounds (all at 10μM) for a period of twenty-four hours. The light emission from *Renilla* luciferase was then monitored as described in section 2.6.12. Results are presented as per cent of the signals obtained from cells in the absence of any treatment. The experiment was performed in duplicate with the results from **(A)** and **(B)** (overleaf) representing means ± range obtained from the duplicate wells of each individual test compound.

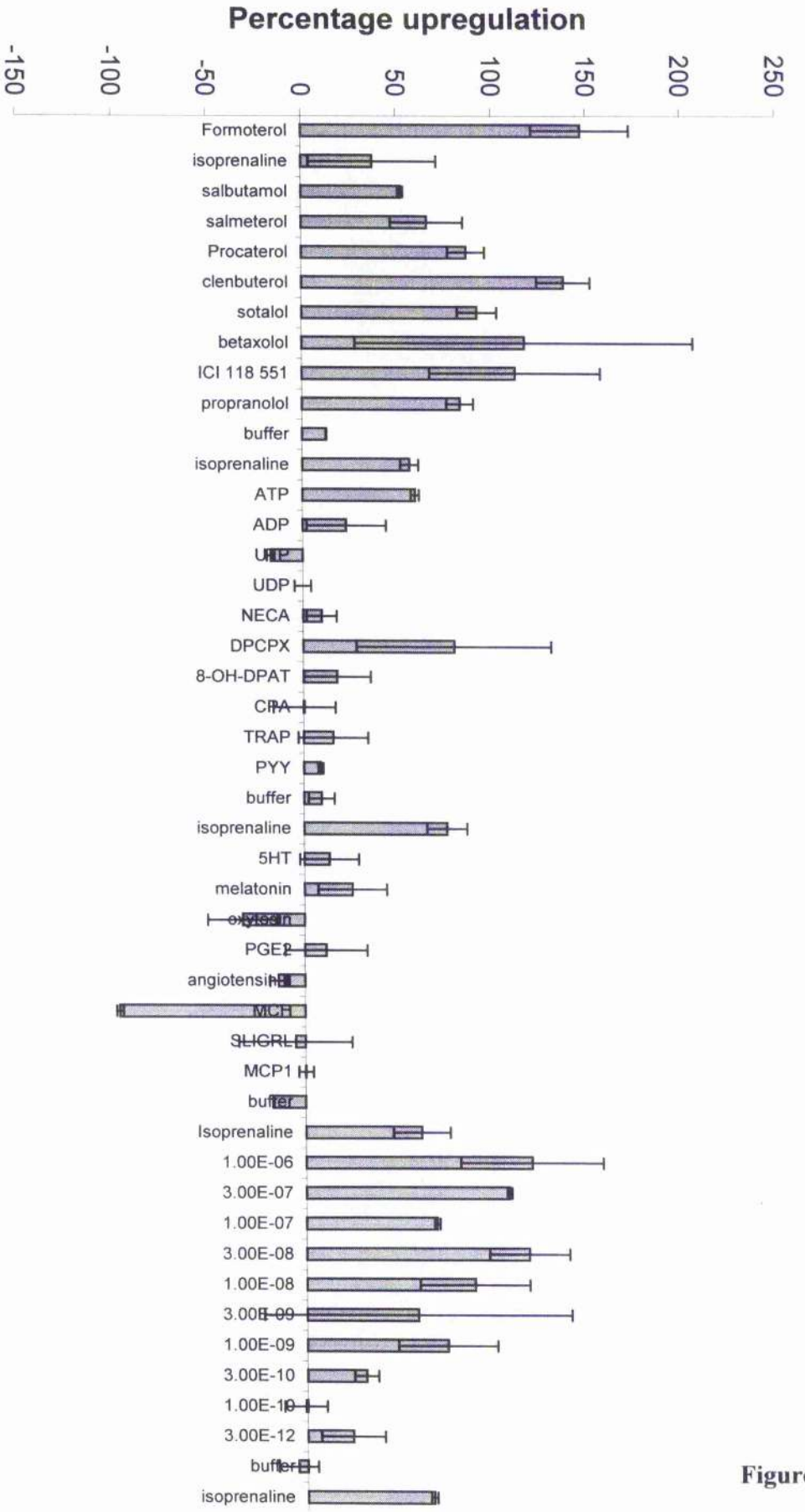
Percentage upregulation
-150
-100
-50
0
50
100
150
200
250
Formoterol
isoprenaline
salbutamol
salmeterol
Procaterol
clenbuterol
sotalol
betaxolol
ICI 118 551
propranolol
buffer
isoprenaline
ATP
ADP
UDP
NECA
DPCPX
8-OH-DPAT
TRAP
PYY
buffer
isoprenaline
5HT
melatonin
PGE2
MCH
MCP1
Isoprenaline
1.00E-06
3.00E-07
1.00E-07
3.00E-08
1.00E-08
1.00E-09
3.00E-10
3.00E-12
isoprenaline

Figure 5.16 (A)

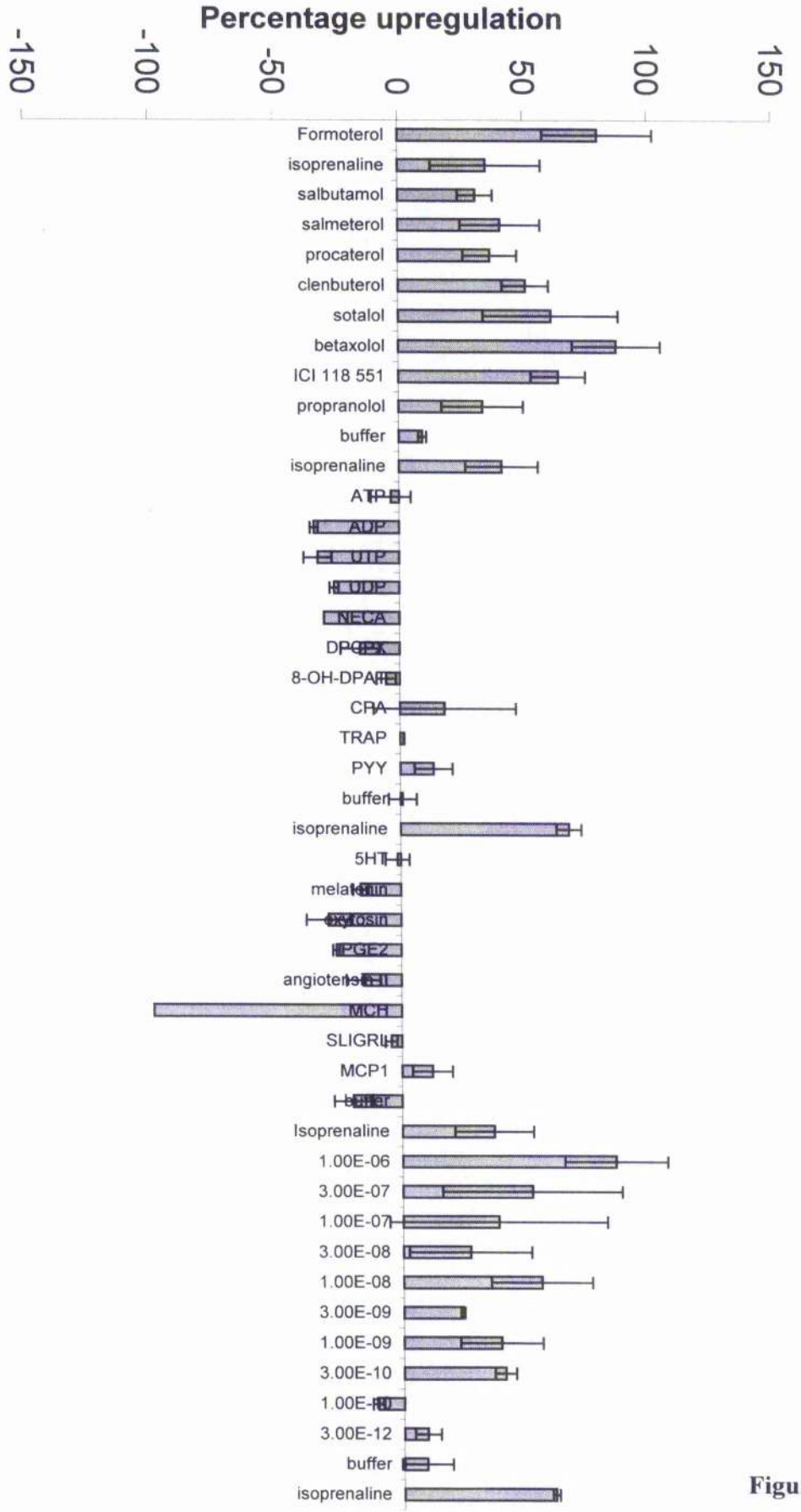
Percentage upregulation
-150
-100
-50
0
50
100
150
Formoterol
isoprenaline
salbutamol
salmeterol
procaterol
clenbuterol
sotalol
betaxolol
ICI 118 551
propranolol
buffer
isoprenaline
ATP
ADP
UTP
UDP
NECA
DPCPX
8-OH-DPAT
CPA
TRAP
PYY
buffer
isoprenaline
5HT
melatonin
oxytocin
PGE2
angiotensin II
MCH
SLIGRL
MCP1
buffer
Isoprenaline
1.00E-06
3.00E-07
1.00E-07
3.00E-08
1.00E-08
3.00E-09
1.00E-09
3.00E-10
1.00E-10
3.00E-12
buffer
isoprenaline

Figure 5.16 (B)

concentrating hormone (MCH), gave extremely poor levels of *Renilla* bioluminescence in both of the experimental runs presented here. It was observed however, throughout the course of conducting these experiments, that MCH tended to lead to toxic effects which induced cell death in the samples under investigation, though whether this was due to some inherent toxicity of the compound to the cells used or simply due some form of contamination present in the compound preparation was not determined.

5.3 Discussion.

Many CAM forms of GPCRs have been generated through molecular biological manipulations in the past ten years. These CAM mutants have been extensively researched and well characterized and many have been shown to be structurally unstable (MacEwan and Milligan, 1996; Gether *et al.*, 1997b). It has been demonstrated that such structurally unstable receptors can be upregulated following a prolonged exposure to certain antagonist compounds and it has been further shown that this is not accompanied by an increase in the levels of transcription of the receptor mRNA in the cell (MacEwan and Milligan, 1996; McLean *et al.*, 1999; Milligan and Bond, 1997). The observed effects, where exposure to various antagonists produced increases in receptor number, are rather thought to be due to the stabilization of the receptor by forcing it to adopt an inactive conformation. The low energy (R) conformation thereby induced is consequently less likely to spontaneously adopt the active (R*) form of the receptor and therefore may be less prone to spontaneous degradation. CAM GPCRs provide good models for examining the conformationally active state of any particular GPCR: studies range from making use of conformationally sensitive fluorescent dyes to identify the structural alterations that

mediate receptor activation (Javitch et al., 1997; Gether et al., 1997b) to more conventional studies where the effects of antagonist/inverse agonist binding on both receptor number and functional endpoint output are investigated (MacEwan and Milligan, 1996).

In order to quantify the ligand-induced upregulation of CAM β2-AR-Rluc, the enzyme *Renilla* luciferase was used to modify the carboxyl terminal tail of this receptor and thereby provide a bioluminescent marker for receptor upregulation. In this respect the chimera thus constructed resembled similar modifications to receptors made with the 27kDa green fluorescent protein from *Aequorea victoria* which has been utilized in a wide variety of studies in recent years. Through the use of confocal microscopy methodologies, the responses of such tagged receptors to agonist ligands have been monitored in real time and this has provided a wealth of information concerning both the kinetics and mechanisms whereby GPCRs are internalised. These methods have also been applied to the study of GPCRs recycling back to the plasma membrane, a process that accompanies receptor resensitisation. In addition, our understanding of the long-term process of receptor downregulation has been considerably enhanced by such studies (Milligan, 1999; Kallal and Benovic, 2000). Fortuitously, in the vast majority of these investigations there has been little evidence to suggest that such carboxyl terminal tail modifications have any significant effect on receptor-ligand binding affinity or on the ability of the receptor to couple to its cognate G-protein and therefore mediate signalling through the generation of second messenger molecules.

Application of these GFP tagged GPCRs to the detection of CAM receptor upregulation has been attempted in a previous study on the β2-AR where a twenty-four hour pre-treatment with a variety of antagonists/inverse agonists lead to a marked

receptor upregulation, detected through the use of confocal microscopy (McLean *et al.*, 1999). However, when trying to monitor the upregulation of β2-AR-GFP through the use of a fluorimeter, quantitation, though possible, was hampered through poor reproducibility of the results, poor agreement between assay point replicates and a poorly pronounced increase in fluorescence signal above that seen in cells which were exempt from antagonist/inverse agonist treatment (McLean *et al.*, 1999). In response to these earlier attempts, it was reasoned that through the expedient of in-frame ligation of a bioluminescent enzyme on to the carboxyl terminal tail of β2-AR, an assay system more amenable to quantitative analysis might be established. To achieve this objective, the cDNA for β2-AR was fused upstream of the cDNA encoding either the luciferase from the anthozoan coelenterate *Renilla reniformis* or the luciferase derived from the firefly *Photinus pyralis*. When expression levels of the various constructs were examined via transient transfection into HEK 293 cells, it was found that although β2-AR-Rluc, β2-AR-Pluc and CAM β2-AR-Rluc (Figures 5.2 and 5.3) expressed at levels which were comparable to their unmodified counterparts which were assayed alongside them, CAM β2-AR-Pluc failed to expressed at quantities detectable through radioligand binding experiments. The abrogation of successful binding to the CAM β2-AR consequent to the presence of *Photinus* luciferase (in contrast to similar modifications with *Renilla* luciferase on the same receptor which did not affect expression levels) may be a reflection of the fact that the *Photinus* luciferase enzyme is a substantially larger molecule than its *Renilla* equivalent, 61kDa compared to 31kDa for *Renilla* luciferase. This is an assertion that can be understood in terms of the CAM receptor being more inherently unstable than the wild type receptor and therefore less likely to tolerate a large carboxyl terminus modification. The CAM β2-AR-Rluc construct that was chosen for the continuation of the study

was not only successfully expressed as a properly folded receptor that was capable of binding to appropriate ligands. It was also capable of reaching the plasma membrane where, in response to stimulation by agonist compounds, it could couple to its cognate G-protein ($G\alpha_s$) and hence stimulate production of cAMP as revealed through the results of the intact cell adenylyl cyclase assays (Figure 5.4). In this respect it was essentially similar in its behaviour to equivalent constructs made between β2-AR and GFP that have been characterised in a number of studies (Barak *et al.*, 1997; Kallal *et al.*, 1998; McLean *et al.*, 1999). In the intact cell adenylyl cyclase assays described herein it was observed that both the β2-AR-Rluc (Chapter 3, Figure 3.5) and CAM β2-AR-Rluc (Figure 5.4) constructs were capable of elevating basal levels of cAMP production, perhaps indicating that the wild type β2-AR possessed a degree of constitutive activity in itself and that this only became apparent when expression levels within the cells were highly elevated. This viewpoint is borne out by the observation that small levels of endogenous receptor (too small to be effectively quantified in radioligand binding assays) did not give rise to any significant levels of basal second messenger production, even though a clear elevation in cAMP levels could be detected from these untransfected cells in the presence of agonist. Agonist independent cAMP levels produced by the wild type β2-AR-Rluc were, however, not nearly so great as those produced by CAM β2-AR-Rluc, especially when it is kept in mind that the expression levels for CAM β2-AR-Rluc were significantly lower than those of β2-AR-Rluc (Figure 5.2 and Chapter 3, Figure 3.4).

In previous investigations, making use of confocal microscopy techniques, it was shown that the β2-AR was capable of being upregulated in the presence of a twenty-four hour pre-incubation with various antagonist/inverse agonist compounds and, as was mentioned previously, this increase in fluorescence was not particularly amenable

to quantification using a fluorimeter (McLean *et al.*,1999). In contrast to this, treatment of a stable cell line stably expressing CAM β2-AR-Rluc with similar antagonist/ inverse agonist compounds lead to a degree of receptor upregulation that was easily quantifiable via the luciferase assay described in section 2.6.12 (Figure 5.9). The results were highly reproducible, with only modest standard errors generated when the results of triplicate experiments were combined. With this degree of reproducibility; given that the assay is carried out in a 96 well microtiter plate format and given that these assay plates can be rapidly processed, it can be anticipated that the assay system should provide a reliable alternative to existing means of high throughput screening for the detection of ligands for both known and orphan GPCRs. When the pEC_{50} values for upregulation obtained from these experiments were compared to the pK_i values acquired from competition radioligand binding experiments, it was found that there was a strong correlation between the two sets of data (Figure 5.11). This result would seem to indicate, at least in the case of the antagonist compounds, that the observed upregulation was mediated primarily through the stabilization of the receptor molecule via the presence of the antagonist in the receptor-binding pocket. As mentioned previously, the increases in receptor number were not attributable to increases in the levels of receptor mRNA, since previous studies focusing upon upregulation of similar CAM mutants of the β2-AR did not detect any modulation in the transcription of these molecules in response to a sustained treatment with betaxolol (MacEwan and Milligan, 1996). The inference of these results is that, rather than through increased rates of protein synthesis, the upregulation is caused primarily through a decrease in the rate of degradation of the CAM β2-AR brought about by a shift in the equilibrium of the receptor towards that

of the less thermally labile (R) conformation of the receptor, a consequence of ligand occupancy of the receptor binding site.

To demonstrate that the upregulation of the CAM β2-AR-Rluc construct was solely attributable to the constitutively active nature of the receptor, an experiment was devised whereby the light output from both CAM β2-AR-Rluc and β2-AR-Pluc could be monitored following exposure to the inverse agonist betaxolol. It was perhaps not surprising that only the CAM version of the β2-AR was capable of producing increases in light intensity when bioluminescence from both *Renilla* and *Photinus* luciferases were monitored together, an observation which suggested that ligand-induced receptor upregulation was entirely dependent on the destabilized nature of CAM β2-AR-Rluc (Figure 5.14). It has recently been demonstrated that a GFP tagged, CAM version of α_{1b}-adrenoceptor (which had a small segment of its third intracellular loop replaced by a corresponding region of the β2-AR) was capable of being upregulated in a manner analogous to CAM β2-AR (Stevens *et al.*, 2000). Therefore, to establish that the upregulation of CAM β2-AR-Rluc could only be accomplished through the use of ligands with a pharmacological specificity for β2-AR, a cell line stably expressing the aforementioned CAM α_{1b}-adrenoceptor was transiently transfected with the cDNA for CAM β2-AR and then exposed to a receptor saturating concentration of either betaxolol or the potent α_{1b}-adrenoceptor inverse agonist phentolamine. The results obtained from these experiments showed that the respective CAM receptors could only undergo upregulation in the presence of a ligand which possessed specificity for that particular receptor type, i.e. betaxolol only induced upregulation of CAM β2-AR-Rluc construct and likewise phentolamine only induced upregulation of CAM α_{1b}-adrenoceptor (Figure 5.15). For the purposes of adapting this assay procedure to high throughput screening procedures the result is an

ideal one, since only ligands which are capable of binding to the receptor of interest will induce an increase in receptor number as detected through the monitoring of light levels emitted via *Renilla* luciferase.

A surprising result obtained in the course of these experiments was that CAM β2-AR-Rluc was capable of undergoing a robust upregulation in response to agonists possessing both partial and full intrinsic activities (Figure 5.12). This was not perhaps to have been expected, considering the traditional view that in the sustained presence of a receptor activating agonist there is a gradual redirection of internalised receptor molecules away from the recycling endosomes towards lyzosomes where proteolytic degradation of the receptor can occur. In consequence, it is rather to be expected that a receptor will undergo a downregulation in the sustained presence of agonists. The only previous findings that could be said to pre-figure these results were those obtained through the transient transfection of a CAM β2-AR into insect Sf-9 cells, where a forty-eight hour exposure to either the inverse agonist ICI 118 551 or the agonist isoprenaline caused a greater than two-fold increase in the levels of receptor expression (Gether *et al.*, 1996a). In the same study, incubation of both purified wild type and CAM β2-AR receptor at 37°C, showed that the CAM β2-AR had a four-fold faster rate of denaturation when compared to its wild type counterpart. This was an effect that could be substantially reversed through the incubation of the CAM β2-AR with either the inverse agonist ICI 118 551 or the agonist isoprenaline. Hence the researchers postulated that their observed results could be explained thus: that the binding of any ligand to the CAM β2-AR had a stabilizing effect upon the receptor and that this therefore produced an decrease in its turnover number, ultimately translating as an increase in receptor expression levels.

A further factor that may influence the expression levels of CAM β2-AR-Rluc upon prolonged exposure to agonist compounds is the carboxyl terminal tail modification with *Renilla* luciferase itself. This particular concern arises from a study which showed that modification of the carboxyl terminal tail of β2-AR with GFP resulted in an impairment in the ability of HEK 293 cells to destroy this receptor type (McLean and Milligan., 2000). This may have been a consequence of the relatively high half-life of the GFP molecule: carboxyl terminal tail modification of β2-AR with the GFP would have had a stabilizing effect on the receptor, extending the receptor's own intrinsic half-life. However, it is also possible that the GFP modification could have interfered with the intracellular trafficking of β2-AR. Any alteration in the ability of the receptor to be redirected from the recycling endosome to the lyzosome would result in a change in its susceptibility to cellular degradation. To distinguish between these two hypotheses it would be necessary to compare the half-lives of both the β2-AR and β2-AR-GFP molecules *in vitro*, as purified receptors.

It is therefore possible that a similar modification to the CAM β2-AR with *Renilla* luciferase would result, upon expression in the HEK 293 cells, in a chimeric receptor that was less prone to cellular destruction, although this idea must remain conjecture at the moment. It should be stressed though that even if such consequences arise through the carboxyl terminal tail modification of β2-AR with *Renilla* luciferase, it in no way detracts from the suitability of the assay for screening compounds for pharmacological selectivity.

In considering the various possibilities concerning the fate of carboxyl tail modified, CAM GPCRs in response to their exposure to agonist ligands, it may be best to regard the effect on receptor number in response to agonists as being dictated by an equilibrium between the ability of the cell to target the receptors for destruction in the

lyzosomes with a propensity for the agonist compound to extend the lifetime of the receptor. Given this, it would be expected that since there is an extremely large number of mutations that can give rise to receptor activation, it might also be the case that that not all of these CAM receptors will be equally destabilised and that they might therefore vary in their ability to be upregulated in response to agonist compounds.

Lending their support to these suppositions, are investigations centred have centred upon the histamine H_2 receptor. In a study that examined the effects of various amino acid substitutions in a conserved DRY motif (located at the boundary of transmembrane helix three and the second intracellular loop) of the histamine H_2 receptor, a number of mutants with enhanced basal production of second messenger molecules were obtained (Alewijnse *et al.*, 2000). These were all expressed at considerably lower levels than the wild type receptor, with one mutant expressed at levels which were too low to facilitate characterization. The wild type H_2 histamine receptor underwent upregulation in response to the inverse agonist ranitidine but was slightly downregulated in response to the agonist histamine. In contrast to this the mutant receptors were upregulated in response to either agonist or antagonist with the degree of upregulation being most pronounced (10 fold) for the mutant that exhibited the lowest levels of basal expression and hence, presumably, was the most destabilized. It can be appreciated that since the receptor was expressed at such low levels to begin with, any stabilization of the receptor construct leading to increases in receptor number will automatically translate as a substantial (percent) increase in expression levels.

It can therefore be seen that not all CAM GPCRs are destabilised to the same extent, nor are they upregulated to the same degree in response to prolonged exposure to

ligands. Further evidence supporting the notion that not all GPCRs with constitutively activating mutations are equal comes from a recent study where three CAM mutants of the α_{1b}-arenoceptor were analysed (Stevens *et al.*, 2000). It was shown that the three mutants each exhibited a different degree of constitutive activation. Only one of these was capable of being upregulated via exposure to a variety of antagonist/inverse agonist compounds and interestingly it was this mutant that displayed the highest degree of constitutive activation. The other two mutants that were less constitutively active were not upregulated in response to the same compounds.

A study on the related α_{1A}-adrenoceptor extends this view to show that CAM receptors may exhibit dissimilarities in their ability to upregulate depending on the type of antagonist used in the pre-incubation step (Zhu et al., 2000). The experimental evidence for this came from observations that a CAM mutant of the α_{1A}-adrenoceptor displayed a marked upregulation when challenged with a sustained treatment of the inverse agonist prazosin whereas a similar treatment with the neutral antagonist KMD-3213 failed to elicit any like effect. Although the researchers did not forward any explanation to account for these discrepancies it is perhaps not too unreasonable to assume, in this particular case, that the upregulation may have been a result of the reduction in basal signalling levels which would in turn lead to an attenuation in the steady-state levels of desensitisation/internalisation of the receptor. Such effects might be expected to lead to an increase in receptor number. Arguing against this viewpoint however was the observation that BMY7378, a ligand of similar efficacy to KMD 3213, did produce a robust upregulation. This was a result that can only suggest that our understanding of CAM GPCR upregulation is incomplete. Comparing the response of the CAM α_{1A}-adrenoceptor in this study (Zhu et al., 2000) with those of the other CAM GPCR responses to antagonists/agonists, cited above, it is evident that

not all constitutively activating mutations lead to identical responses to such ligands and that the degree of inherent instability of the receptor may be of primary importance in dictating whether or not an agonist/antagonist will be capable of mediating upregulation in a specific CAM GPCR type.

One other investigation which merits mention here, being of relevance to the general discussion, is a study where three consecutive point mutations were introduced into separate regions of the α_{1b}-adrenoceptor and it was shown that these mutations acted in a synergistic manner with regards to their effect on basal receptor activation and agonist binding affinity (Hwa *et al.*, 1997). The results showed that there was a direct correlation between agonist binding affinity and basal constitutive activity. This observation is explicable through consideration of the extended ternary complex model for receptor activation in that the perturbation of the equilibrium existing between (R) and (R*) conformations of the receptor in favour of (R*), in the CAM form of the receptor, leads to an enhanced affinity for agonists. From this, it might be anticipated that increased constitutive activity can be predicted by examining the increases in agonist binding affinity to the CAM receptor over that of wild type. A number of recent studies have shown that this is not always the case however, since although all CAM receptors are more structurally unstable than their wild type counterparts, some destabilizing mutations also have the effect of impairing the receptor in its ability to couple to G-proteins. Such receptors do not exhibit enhanced basal functional activity; indeed, it is usually abolished.

These digressions should not deflect our attention from the fact that the results presented herein provide a framework in which an assay based on the detection of receptor upregulation in response to stabilizing pharmacological compounds may be further developed. It was shown that the assay system described, which made use of

the bioluminescent marker enzyme *Renilla* luciferase, was capable of accurately monitoring receptor upregulation in response to sustained exposure of either antagonist or agonist compounds. The potential of this assay system as a method for screening compounds for pharmacological specificity to the β2-AR was assessed by challenging cells stably expressing CAM β2-AR-Rluc with a variety of compounds, some of which had specificity for β2-AR, some of which did not. It was seen that ligands with specificity for β2-AR mediated a 50-100% increase in luciferase output in comparison to other compounds, lacking such specificity, which did not mediate upregulation (Figure 5.16). It was also noted that the assay was somewhat compromised by the generation of one or two false positive results, however, it is to be anticipated that such shortcomings may be somewhat ameliorated through the use of a larger number of replicate wells in the assay system. Further developments in bioluminescence technology may also be of potential use in the future for improving the existing assay methodology. For instance *Gaussia* luciferase, an enzyme for which coelenterazine acts as a substrate, has recently been cloned and is reported to be considerably brighter than *Renilla* luciferase in addition to being a significantly smaller molecule. Use of *Gaussia* luciferase might therefore allow the assay to be more sensitive for the detection of slight increases in receptor number and given the smaller size of Gaussia luciferase (185 amino acids) it is to be expected that GPCR-Gaussia luciferase chimeric constructs will be less likely to be affected with regards to their trafficking properties.

5.4 Conclusion.

In this chapter it has been shown that a chimeric construct consisting of a fusion between a constitutively active mutant of the β2-AR and the enzyme *Renilla*

luciferase was not impaired in its ability to couple to G-protein. As such, this construct (CAM β2-AR-Rluc) generated elevated levels of cAMP nucleotides as compared to the wild type β2-AR when transiently expressed in HEK 293 cells and this was in accordance with previous studies focusing on similar CAM β2-AR receptors. The upregulation of this construct by various β2-AR ligands could be monitored by quantitating the light emitted via *Renilla* bioluminescence upon addition of the enzyme substrate coelenterazine.

The pEC_{50} values from the upregulation of CAM β2-AR-Rluc in response to twenty-four hour exposure to various β2-AR antagonists showed a high degree of correlation with the pK_i values obtained from competition binding studies conducted using the same compounds. These findings suggested that in the case of upregulation by antagonists, it was the presence of the ligand in the binding pocket of the receptor that was primarily responsible for the observed increases in receptor number. When taking into account the substantial amount of research carried out previously on this constitutively active β2-AR, the underlying mechanism of this process could best be explained by the ligand stabilizing the more inherently labile CAM form of the receptor and hence increasing the half life of the receptor. It was also noted that agonist compounds were similarly capable of occasioning a marked degree of receptor upregulation, however, the values of EC_{50} obtained from these experiments were not especially comparable to K_i values obtained for these same compounds in competition binding studies. These observations suggested that there were other mechanisms at work, other than the stabilizing presence of the ligand in the receptor binding crevice, which influenced the observed agonist-mediated upregulation effects. It was shown that upregulation of CAM β2-AR-Rluc was critically dependent upon the constitutively active nature of the receptor construct and that this process was

highly selective, only being engendered through the interaction of pharmacologically specific ligands with the CAM receptor construct. This selectivity was affirmed when HEK 293 cells stably expressing CAM β2-AR-Rluc were exposed to a twenty-four hour pre-treatment with a variety of pharmacological compounds and only those ligands that had specificity for β2-AR were seen to be capable of inducing the upregulation effect.

The upregulation assay, using *Renilla* luciferase as a bioluminescent marker protein, described herein, displays a variety of attractive features which, considered together, suggest that the system would be ideally suited to compound screening programmes attempting to identify new agonist/antogonist compounds for both well characterized and orphan GPCRs. The principal virtues of this assay system are a high degree of pharmacological specificity and an ability to detect ligands endowed with either a positive or negative efficacy, though it should be stressed that because not all CAM GPCRs are seen to be equally destabilized this may not be the case for all such receptors modified with *Renilla* luciferase. These advantages are combined with an assay procedure that is rapid, requires very few manipulations and is readily applicable to a 96 well plate format such as is required for the high throughput demands of industrial screening. Thus a novel and effective method for detecting ligands with a pharmacological specificity for a given receptor has been established, the realization of which was the ultimate purpose of this whole research project.

Chapter 6.

Final discussion

In the introduction to this thesis, the large amount of experimental evidence suggesting that GPCRs were capable of forming dimeric or higher order oligomeric complexes was discussed in some detail. Through consideration of these studies, it was seen that although there was ample evidence to suggest that GPCRs were capable of interacting, there was no single consensus of opinion as to what the ultimate function and biological relevance of these interactions was and instead there were a number of hypotheses presented. However, upon consideration of the discussion of Chapter 1 (Section 1.5) the possible functions of GPCR dimerization may be reasonably categorized into three main areas. These are: 1) that the binding of agonist to the GPCR influences the dimerization status of the receptor and that this in some way facilitates the process of receptor activation; 2) That the interaction of different GPCR types generates receptor units that exhibit a distinct pharmacology and that this contributes to the diversity of receptor subtypes observed *in vivo*; 3) The interaction between different types and splice variants of GPCRs facilitates in regulating the export of the receptor from the endoplasmic reticulum to the surface of the cell. These options are not mutually exclusive. Ligand binding may increase the quantity of heterodimers within a cell and this complex may then possess a pharmacology distinct from the homodimer. Alternatively, two receptors may be tightly associated within the endoplasmic reticulum and serve as mutual chaperones in targeting to the plasma membrane, where once arrived, the sustained interaction would serve to influence the pharmacological profile of the receptor. Option 3 is not so easily reconciled with option 1 however, since it would be supposed that if GPCRs required a tight

constitutive association, mediated either through covalent association or coiled-coil interactions, in order to reach the plasma membrane then it would also be logical to assume that this would persist at the cell surface and it would therefore be unlikely that the presence of ligand would be capable of promoting the dimeric state of the GPCR. It is possible that different classes of GPCR may utilize the process of dimerization in order to achieve different ends. For the class C receptor $GABA_B$ it seems quite likely that dimerization is essential for receptor function. For class A receptors ligand regulation of dimerization may play a more important role in merely promoting receptor activation as opposed to export from the intracellular compartments, though it must be stated that within the class A GPCR family there has been a wide variety of reports concerning the role of ligand regulation some of which have been conflicting.

From the perspective of the results presented herein, the role of GPCR dimerization would seem to be more likely associated with options 2) and 3) rather than 1) since no clear evidence that the presence of ligands in the receptor binding cleft promoted GPCR dimerization could be obtained. This was despite applying two separate variants of bioluminescence resonance energy transfer to address the issue of ligand regulated dimerization. It was seen that ligand occupancy had no effect on δ-opioid receptor homo-dimerization, homo-dimerization of the β2-AR or homo-dimerization of the κ-opioid receptor using $BRET_1$. Using the more sensitive $BRET_2$ technique it was further demonstrated that heterodimerization between the β2-AR and the δ-opioid receptor was not modulated by ligand occupancy, despite earlier indications that this might be the case using $BRET_1$. It was demonstrated using $BRET_2$ that heterodimers between the δ-opioid receptor and the κ-opioid receptor were unaffected by ligand occupancy. The strength of these studies lies in their use of the biophysical technique

BRET. BRET is superior to previous biochemical approaches such as co-immunoprecipitation where non-specific aggregates between proteins possessing highly hydrophobic domains can lead to a non-specific carry over of proteins as a result of the precipitation process. Now that it has been established that GPCR dimerization is a real phenomenon, further work will involve trying to elucidate the domains of the receptors that are responsible for mediating these interactions. This could potentially be achieved through the generation of truncation mutants and /or site directed mutagenesis of the relevant receptors. The ability of these mutants to influence observed energy transfer levels, as well as their ability to effect the pharmacological profile and/or trafficking of the receptors would further extend our knowledge of the role that dimerization plays in regulating the biology of GPCRs.

The experiments where $BRET_1$ was used to determine the effect of receptor density upon the extent of energy transfer, conducted using the transient transfection method, revealed that at a low concentration of acceptor tagged receptors homomeric interactions between the κ-opioid receptor were more favoured than heteromeric interactions between this receptor and the TRHr. One likely interpretation of these results was that the κ-opioid receptor had a greater propensity for self-self interactions than for interactions with more distantly related GPCRs. The experiments also demonstrated the importance of considering the concentrations of the donor and acceptor tagged moieties present in the cells when conducting these types of energy transfer studies. The transient nature of the expression system used in the experiments and the fact that saturating concentrations of acceptor tagged receptors were not achieved made the results somewhat inconclusive however. Future work will need to address this issue by stably expressing the donor tagged receptor with an inducible plasmid with the cDNA for an acceptor tagged receptor integrated into its expression

cassette. Through the introduction of increasing levels of an inducer molecule, progressively higher levels of acceptor tagged receptor protein should be achieved. In this type of system all of the cells would express the receptors at equal concentrations and it would thus be superior to the transient system where there is cell-to-cell variation in the expression levels of the constructs. Another advantage would be that the stably expressed donor tagged receptor would be more relatively invariant in its expression levels as the acceptor concentration increased. Also since there would be no independent pools of cells that only expressed either the donor or the acceptor tagged receptor alone, saturating conditions would be more likely to be achieved. It is clear from the results of Chapter 3 of this thesis that the further development of more quantitative approaches to defining GPCR interactions will lead towards a more complete understanding of how these molecules exist in their native state and also shed light on the relative affinities of interaction between distinct receptor types.

Given that there were no ligand induced alterations in the dimerization status of the receptor pairings tested in the studies presented herein and considering that there are numerous other reports of GPCRs being unaffected by the presence of ligands in the binding pocket of the receptor, it would seem that BRET or FRET based detection of GPCR dimerization would be of limited use for industrial ligand screening programs. It was demonstrated herein that β-arrestin recruitment to the plasma membrane in response to agonist activation of the receptor would be a far more attractive proposition for the establishment of such a FRET/BRET based screening assay since arrestin recruitment is almost ubiquitously utilized by GPCRs in initiating the desensitisation pathway. $BRET_1$ has already been applied to this end, where it was demonstrated that upon co-expression of a β2-AR fused to *Renilla* luciferase along with a β-arrestin fused to eYFP that a dose dependent increase in the level of energy

transfer could be detected following the addition of the agonist isoprenaline (Angers *et al.*, 2000). This system could be easily adapted to a $BRET_2$ format, replacing the eYFP with GFP_2 and substituting coelenterazine with the Deepblue C molecule. This would impart an added sensitivity to the system, perhaps allowing for the detection of ligands that have a low potency and which only cause the GPCR to engage with the downstream desensitisation machinery to a limited degree. Alternatively, a FRET based assay might be developed based on the detection of energy transfer between the novel fluorescent proteins that were employed in the confocal studies of Chapter 4. This might offer an advantage over $BRET_2$ in that there would not be any problems associated with low light output from the donor molecule that sometimes makes signal detection with $BRET_2$ difficult.

A final method that might be successfully applied to compound screening programmes is that of monitoring light output from a *Renilla* tagged CAM GPCR both in the presence and absence of a prolonged exposure to a specific ligand. It was seen in Chapter 5, that such exposures to either antagonist or agonist ligands were capable of inducing an effective upregulation in the receptor number and that this was conveniently detectable from measurement of the luciferase light output on a luminometer. This method of ligand detection might be applicable to other types of GPCR provided that point mutations can be introduced to these receptors in order to impart a sufficient degree of structural instability which could then be subsequently stabilized through the presence of ligand. The large number of positions in which point mutations have been observed to produce receptors where the amount of second messenger production was substantially elevated tends to suggest that such receptors would be reasonably easy to produce. Further work relating to this assay system should involve taking a variety of GPCRs known to possess constitutive activity and

to then modify these at the carboxyl terminal tail with the *Renilla* luciferase enzyme to see if the assay method is equally applicable, and if so to what extent, to all constitutively active GPCRs. Finally, since it was seen with the CAM β2-AR-Rluc that all types of ligand, even full agonists, were capable of inducing upregulation, it would seem advisable to analyse this construct in parallel with the unmodified CAM β2-AR to see to what extent, if any, this construct was impaired in its ability to internalise in response to the presence of agonist ligands. If there is any attenuation in the capacity of the construct to internalise, this may affect the capacity of the cells to downregulate the construct in response to prolonged exposures to agonists.

This concludes the work presented in this thesis, in which much was learned concerning the dimerization of GPCRs. Also the potential of a number of novel methods for the detection of ligand binding were explored; these methods may be of potential future benefit to the pharmaceutical industry where there is currently a high demand for new and effective means for screening compound libraries in order to identify new ligands for both known and orphan GPCRs. Such searches may eventually lead to the development of new drugs that will be of clinical value in the treatment of a diverse range of disease processes.

FINIS

References

AbdaAlla, S., Lother, H., and Quitterer, U. (2000) *Nature* **407**, 94-97

AbdAlla, S., Zaki, E., Lother, E., and Quitteterer, U. (1999) *J. Biol. Chem.* **274**, 26079-26084

Acharya, S., and Karnik, S.S. (1996) *J. Biol. Chem.* **271**, 25409-25411

Alberty, R.A., and Silby, R.J. (1997) in *Physical Chemistry*, John Wiley & Sons, Inc. 2nd edit., pp689-709

Alewijnse, A.E., Smit, M.J., Hoffmann, M., Verzijl, D., Timmerman, H., Leurs, R. (1998) *J. Neurochem.* **71**, 799-807

Alewijnse, A.E., Timmerman, H., Jacobs, E.H., Smit, M.J., Roovers, E., Cotecchia, S., and Leurs, R. (2000) *Mol. Pharmacol.* **57**, 890-898

Allen, L.F., Lefkowitz, R.J., Caron, M.G., and Cotecchia, S. (1991) *Proc. Natl. Acad. Sci. U.S.A.* **88**, 11354-11358

Anborgh, P.H., Dale, L., Seachrist, J., and Ferguson, S.S.G. (2000) *Mol. Endocrinol.* **14**, 2040-2053

Angers, S., Salahpour, A., Joly, E., Chelski, D., Dennis, M., and Bouvier, M. (2000) *Proc. Natl. Acad. Sci. U.S.A.* **97**, 3684-3689

Aragay, A.M., Mellado, M., Frade, J.M.R., Martini, A.M., Jimenez-Sainz, M.C., Martinez-A, C., and Mayor Jr, F. (1998) *Proc. Natl. Acad. Sci.* **95**, 2985-2990

Aramori, I., Ferguson, S.S.G., Bieniasz, P.D., Zhang, J., Cullen, B.R. and Caron, M.G. (1997) *EMBO J.* **16**, 4606-4616

Arshavski, V.Y., and Bownds, M.D. (1992) *Nature* **357**, 416-417

Attramadal, H., Arriza, J.L., Aoki, C., Dawson, T.M., Codina, J., Kwatra, M.M., Snyder, S.H., Caron, M.G., Lefkowitz, R.J. (1992) *J. Biol. Chem.* **267**, 17882-17890

Audiger, Y., Attali, B., Mazsarguil, H., and Cros, J. (1982) *Life Sci.* **31**, 1287-1290

Baird, B., and Holowka, D. (1988) in *Spectroscopic Membrane Probes*, ed. Loew, L.M., CRC press, Boca Raton, pp 93-116

Barak, L.S., Ferguson, S.G., Zhang, J., and Caron, M.G. (1997) *J. Biol. Chem.* **272**, 27497-27500

Barak, L.S., Ferguson, S.S.G., Zhang, J., Martenson, C., Meyer, T., and Caron, M.G. (1997) *Mol. Pharmacol.* **51**, 177-184

Barak, L.S., Oakley, R.H., Laporte, S.A., and Caron, M.G. (2001) *Proc. Natl. Acad. Sci.* **98**, 93-98

Barak, L.S., Warabi, K., Feng, X., Caron, M.G., and Kwatra, M.M. (1999) *J. Biol. Chem.* **274**, 7565-7569

Barlic, J., Khandakar, L.S., Mahon, M.H., Andrews, J., DeVries, M.E., Negrou, E., Mitchell, G.B., Rahimpour, R., Ferguson, S.S.G., and Kelvin, D.J. (1999) *J. Biol. Chem.* **269**, 2790-2795

Berman, D.M., Wilkie, T.M., and Gilman, A.G. (1996) *Cell* **86**, 445-452

Biddlecome, G.H., Berstein, G., and Ross, E.M. (1996) *J. Biol. Chem.* **271**, 7999-8007

Bouvier, M., Hausdorff, W.P., De Blasi, A., O'Dowd, B.F., Kobilka, B.K., Caron, M. G., and Lefkowitz, R.J. (1988) *Nature* **333**, 370-373

Cardullo, R.A., Agrawal, S., Flores, C., Zameknic, P., and Woolf, D.E. (1988) *Proc. Natl. Acad. Sci. U.S.A.* **85**, 8790-8794

Chen, G., Way, J., Armour, S., Watson, C., Queen, K., Jayawickreme, C.K., Chen, W.J., and Kenakin, T. (2000) *Mol. Pharmacol.* **57**, 125-134

Cheng, Z-J, and Miller, L.J. (2001) *J. Biol. Chem.* **276**, 48040-48047

Christopoulos, G., Perry, K.J., Morfis, M., Tilakaratne, N., Gao, Y., Fraser, N.J., Main, M.J., Foord, S.M., and Sexton, P.M. (1999) *Mol. Pharmacol.* **56**, 235-242

Chuang, T.T., Levine, H III., and DeBlasi, A. (1996) *J. Biol. Chem.* **270**, 18660-18665

Circuela, F., Escriche, M., Burgueno, J., Angulo, E., Casado, V., Soloviev, M.M., Canela, E.I., Mallol, J., Chan, W-Y., Lluis, C., McIlhinney, R.A.J., and Franco, R. (2001) *J. Biol. Chem.* **276**, 18345-18351

Coge, F., Guenin, S-P., Renouard-Try, A., Rique, H., Ouvry, C., Fabry, N., Beauverger, P., Nicolas, J-P., Galizzi, J-P., Boutin, J.A., and Canet, E. (1999) *Biochem. J.* **343**, 231-239

Cohen, G.B., Yang, T., Robinson, P.R., and Oprian, D.D. (1993) *Biochemistry* **32**, 6111-6115

Conn, P.J., and Pin, J.P. (1997) *Annu. Rev. Pharmacol. Toxicol.* **37**, 205-237

Cormier, M. J., Hori, K., and Anderson, J.M. (1974) *Biochem. Biophys. Acta.* **364**, 137-164

Cornea, A., Janovick, J-A., Maya-Nunez, G., and Conn, P.M. (2001) *J. Biol. Chem.* **276**, 2153-2158

Costantino, G., Macchiarulo, A., and Pellicciari, R. (1999) *J. Med. Chem.* **42**, 5390-5401

Cotecchia, S., Exum, S., Caron, M.G., and Lefkowitz, R.J. (1990) *Proc. Natl. Acad. Sci.* **87**, 2896-2900

Craft, C.M., Whitmore, D.H., and Wiechmann, A.F. (1994) *J. Biol. Chem.* **269**, 4613-4619

Cvejic, S., and Devi, L. (1997) *J. Biol. Chem.* **272**, 26959-26964

Daaka, Y., Pitcher, J. A., Richardson, M., Stoffel, R.H., Robishaw, J.D., and Lefkowitz, R.J. (1997) *Proc. Natl. Acad. Sci.* **94**, 2180-2185

Davies, A., Schertler G.F., Gowen, B.E., and Saibil, H.R. (1996) *J. Struct. Biol.* **177,** 36- 44

De Rooji, J., Zwartkruis, F.J.T., Verheijen, M.H.G., Cool, R.H., Nijman, S.M.B., Wittinghofer, A. and Bos, J.L. (1998) *Nature* **396**, 474-477

Diviani et al., (1996) *J. Biol. Chem.* **271**, 5049-5055

Drmota, T., Gould, G. W., and Milligan, G. (1998) *J. Biol. Chem.* **273**, 24000-24008

Egan, T., and North, R. (1981) *Science* **214**, 923-924

Farahbakhsh, Z.T., Ridge, K.D., Khorana, H.G., and Hubbell, W.L. (1995) *Biochemistry* **34**, 8812-8819

Farrens, D.L., Altenbach, C., Yang, K., Hubbell, W.L., and Khorana, H.G. (1996) *Science* **274**, 768-770

Ferguson, G., Watterson, K.R., and Palmer, T.M. (2000) *Mol. Pharmacol.* **57**, 546-552

Ferguson, S.G. (2001) *Pharm. Rev.* **53**, 1-24

Ferguson, S.S.G., Downey, W.E., Colapietro, A-M., Barak, L.S., Menard, L., and Caron, M.G. *Science* **271**, 363-366

Fields, H., Emson, P., Leigh, B., Gilbert, R., and Iverson, L. (1980) *Nature* **284**, 551-353

Forster, T. (1966) In *Modern Quantum Chemistry*, New York: Academic, ed. Sinanoglu, O., Section III B, pp93-137

Franke, R.R., Sakmar, T.P., Graham, R.M., and Korana, H.G. (1992) *J. Biol. Chem.* **267**, 14767-14774

Freedman et al., (1995) *J. Biol. Chem.* **270**, 17953-17961

Fukushima, Y., Asano, T., Siatoh, T., Anai, M., Funaki, M., Ogihara, T., Katigiri, H., Matsuhashi, N., Yazaki, Y., and Sugano, K. (1997) *FEBS Lett.* **409**, 283-286

Fung, B.K.K. and Stryer, L. (1978) *Biochemistry*, **17**, 5241-5248

George, S.R., Fan, T., Xie, Z., Tse, R., Tam, V., Varghese, G., and O'Dowd, B.F. (2000) *J. Biol. Chem.* **275**, 26128-26135

Gether, U., Ballesteros, J., Seifert, R., Sanders-Bush, E., Weinstein, H., and Kobilka, B.K. (1997a) *J. Biol. Chem.* **272**, 2587-2590

Gether, U., Lin, S., Ghanouni, P., Ballesteros, J.A., Weinstein, H., and Kobilka, B.K. (1997b) *EMBO J.* **16**, 6737-6747

Goodman, O.B. Jr., Krupnick, J.G., Santini, F., Gurevich, V.V., Penn, R.B., Gagnon, A.W., Keen, J.H., and Benovic, J.L. (1996) *Nature* **383**, 447-450

Gordon, Y.K. Ng., O'Dowd, B.F., Lee, S.P., Chung, H.T., Brann, M.R., Seeman, P., and George, S.R. (1996) *Biochem. Biophys. Res. Comm.* **227**, 200-204

Groark, D. A. Wison, S., Krasel, C., and Milligan, G. (1999) *J. Biol. Chem.* **274**, 23263-23269

Guangyu, W., Krupnick, J.G., Benovic, J.L., Lanier, S.M. (1997) *J. Biol. Chem.* **272**, 17836-17842

Guervich, V.V., Dion, S.B., Onorato, J.J., Ptasienski, J., Kim, C.M., Sterne-Marr, R., Hosey, M.M., and Benovic, J.L. (1995) *J. Biol. Chem.* **270**, 720-731

Han, G.-M., and Hampson, D.R. (1999) *J. Biol. Chem.* **274**, 10008-10013

Haylett, D.G. (1996)in *Textbook of Receptor Pharmacology*. CRC press, pp121-149.

Hazum, E., Chang, K., and Cuatrecasus, P. (1979) *Nature*, **282**, 626-628

Herbert, T., Loisel, T.P., Adam, L., Bither, N., Onge, S., and Bouvier, M. (1998) *Biochem. J.* **330**, 287-293

Herbert, T.E., Moffett, S., Morello, J-P., Loisel, T.P., Bichet, D.G., Barret, C., and Bouvier, M. (1996) *J. Biol. Chem.* **271**, 16384-16392

Hill-Eubanks, D., Burstein, E.S., Spalding, T.A., Brauner-Osborne, H., and Brann, M.R. (1996) *J. Biol. Chem.* **271**, 3058-3065

Hirsch, J.A., Shubert, C., Gurevich, V.V., and Sigler, P.B. (1999) *Cell* **97**, 257-269

Högger, P., Shockley, M.S., Lameh, J., and Sadee, W. (1995) *J. Biol. Chem.* **270**, 7405-7410

Hwa, J., Gaivin, R., Porter, J.E., and Perez, D.M. (1997) *Biochemistry* **36**, 633-639

Inglese, J., Freedman, N.J., Koch, W.J., and Lefkowitz, R.J. (1993) *J. Biol. Chem.* **268**, 23735-23738

Innamortari, G., Sadeghi, H.M., Tran, N.T., and Birnbaumer, M. (1998) *Proc. Natl. Acad. Sci. U.S.A.* **95**, 2222-2226

Itokawa, M., Toru, M., Ito, K., Tsuga, H., Kameyama, K., Haga, T., Arinami, T., and Hamaguchi, H. (1996) *Mol. Pharmacol.* **49**, 560-566

Javitch, J. A., Fu, D., Liapakis, G., and Chen, J. (1997) *J. Biol. Chem.* **272**, 18546-18549

Jiang, Q., Takemori, A., Sultana, M., Portoghese, P., Bowen, W., Mosberg, H., and Porreca, F. (1991) *J. Pharmacol. Exp. Ther.* **257**, 1069-1075

Jones, K.A., Borowski, B., Tamm, J.A., Craig, D.A., Durkin, M.M., Dai, M., Yao, W-J., Johnson, M., Gunwaldsen, C., Huang, L-Y., Tang, C., Shen, Q., Salon, J.A., Morse, K., Laz, T., Smith, K.E., Nagarathnam, S.A., Noble, T.A., Gerald, B., and Gerald, C. (1998) *Nature* **396**, 674-678

Jones, P.J., Curtis, C.A.M., and Hulme, E.C. (1995) Eur. J. Pharmacol. 288, 251-257

Jordan, B., and Devi, L. (1999) *Nature* **399**, 697-700

Jordan, B.A., Trapaidze, N., Gomes, I., Nivarthi, R., and Devi, L.A. (2001) *Proc. Natl. Acad. Sci. U.S.A.* **98**, 343-348

Kallal, L., and Benovic, J.L. (2000) *Trends Pharmacol. Sci.* **21**, 175-180

Kallal, L., Gagnon, A.W., Penn, R.B., and Benovic, J.L. (1998) *J. Biol. Chem.* **273**, 322-328

Karpa, K. D., Lin, R., Kabbani, N., and Levenson, R. (2000) *Mol. Pharmacol.* **58**, 677-683

Kaupmann, K., Malitschek, B., Heldt, J., Froestl, W., Beck, P., Mosbacher, I., Bischoff, S., Kulik, A., Shigemoto, R., Karschin, A., and Bettler, B. (1998) *Nature* **396**, 683-686

Kawasaki, H., Springett, G.M., Mochizuki, N., Toki, S., Nakaya, M., Matsuda, M., Housman, D.E. and Graybiel, A.M. (1998) *Science* **282**, 2275-2279

Kieselbach, T., Irrgang, K.D., and Ruppel, H. (1994) *Eur. J. Biochem.* **226**, 87-97

Kleinfeld, A. (1988) in *Spectroscopic Membrane Probes*, ed. Loew, L.M., CRC press, Boca Raton, pp 63-92

Kohout, T.A., Lin, F-T., Perry, S.J., Conner, D.A., and lefkowitz, R.J. (2001) *Proc. Natl. Acad. Sci.* **98**, 1601-1606

Konig, B., Arendt, A., McDowell, J.H., Kahlert, M., Hargrave, P.A., and Hofmann, K.P. (1989) *Proc. Nat. Acad. Sci. U.S.A.* **86**, 6878-6882

Koppel, D.E., Fleming, P.J., and Strittmater, P. (1979) *Biochemistry* **18**, 5450-5464

Kroeger, K.M., Hanyaloglu, A.C., Seeber, R.M., Miles, R.M., and Eidne, K.A. (2001) *J.Biol. Chem.* **276**, 14092-14099

Kundel, M.T., and Peralta, E.G. (1993) *EMBO J.* **12**, 3809-3815

Kuner, R., Kohr, G., Grunewald, S., Eisenhardt, G., Bach, A., and Kornau, H-C. (1999) *Science* **283**, 74-77

Kunishima, N., Shimada, Y., Tsuji, Y., Sato, T., Yamomoto, M., Kumasaka, T., Nakashima, S., Jingami, H., and Morikawa, K. (2000) *Nature* **407**, 971-977

Laporte, S.A., Oakley, R.H., Holt, J.A., Barak, L.S., and Caron, M.G. (2000) *J. Biol. Chem.* **275**, 23120-23126

Latif, R., Graves, P., and Davies, T.F. (2001) *J. Biol. Chem.* **276**, 45217-45224

Lee, C., Ji, I., Ryu, K., Song, P. Y., Conn, M., and Ji, T. H. (2002) *J. Biol. Chem.* Papers in Press.

Lefkowitz, R.J., Cotecchia, S., Samama, P., and Costa, T. (1993) *Trends Pharmacol. Sci.* **14**, 303-307

Leurs, R., Smit, M.J., Alewijnse, A.E., and Timmerman, H. (1998) *Trends Biochem. Sci.* **23**, 418-422

Lohse, M.J., Andexinger, S., Pitcher, J., Trukawinski, S., Codina, J., Faure, J-P, Caron, M.G., Lefkowitz, R.J. (1992) *J. Biol. Chem.* **267**, 8558-8564

Lohse, M.J., Benovic, J.L., Codina, J., Caron, M.J., and Lefkowitz, R.J. (1990) *Science* **248**, 1547-1550

MacEwan, D.J., and Milligan, G. (1996) *Mol. Pharmacol.* **130**, 1825-1832

MacEwan, D.J., Kim, G-D., and Milligan, G. (1995) *Mol. Pharmacol.* **48**, 316-325

Maggio, R., Barbier, P., Colleli, A., Salvadori, F., Demontis, G., and Corsina, G. (1999) *J. Pharmacol. Exp. Ther.* **291**, 251-257

Maggio, R., Vogel, Z., and Wess, J. (1993) *Proc. Natl. Acad. Sci. U.S.A.* **90**, 3103-3107

Mahajan, N.P., Linder, K., Berry, G., Gordon, G.W., Heim, R., and Hermann, B. (1998) *Nat. Biotechnol.* **16**, 547-552

Maniatis, T., J. Sambrook., and Fritch, E.F. in *Molecular cloning, a laboratory manual*, 2nd ed. cold spring harbour laboratory press, ed. Nolan, C. (1989), Vol 3, appendix E.5.

Margreta-Mitrovich, M., Jan, Y. N., and Jan, L.Y. (2001) *Proc. Natl. Acad. Sci. U.S.A.* **98**, 14643-14648

Margreta-Mitrovich, M., Jan, Y.N., and Jan, L.Y. (2000) *Neuron* **27**, 97-106

Mattia, A., Vanderah, T., Mosberg, H., and Porrcea, F. (1991) *J. Pharmacol. Exp. Ther.* **258**, 583-587

McConalogue, K., Dery, O., Lovett, M., Wong, H., Walsh, J.H., Grady, E.F., and Bunnett, N.W. (1999) *J. Biol. Chem.* **274**, 16257-16268

McLatchie, L.M., Fraser, N.J., Main, M.J., Wise, A., Brown, J., Thomson, N., Solari, R., Lee, M.G., and Foord, S.M. (1998) *Nature* **393**, 333

McLean, A.J., and Milligan, G. (2000) *Br. J. Pharmacol.* **130**, 1825-1832

McLean, A.J., Bevan, N., Rees, S., and Milligan, G. (1999) *Mol. Pharmacol.* **56**, 1182-1191

McLoughlin, D.J., and Strange, P.G. (2000) *J. Neurochem.* **74**, 347-357

McPherson, M.J., and Moller, S.G. in *PCR*, Bios scientific publishers, ed. Bosher, A. (2000), pp23-66

McVey, M., Ramsay, D., Kellett, E., Rees, S., Wilson, S., Pope, A.J., and Milligan, G. (2001) *J. Biol. Chem.* **276**, 14092-14099

Mellado, M., Rodriguez-Frade, J.M., Vila-Coro, A.J., Fernandez, S., De Ana, A.M., Jones, D.R., Toran, J.L., and Martinez-A, C. (2001) *EMBO J.* **20**, 2497-2507

Menard, L., Ferguson, S.S.G., Zhang, J., Lin, F., Lefkowitz, R.J., Caron, M.G., Barak, L.S. (1997) *Mol. Pharmacol.* **51**, 800-808

Milligan, G. (1999) *Br. J. Pharmacol.* **128**, 501-510

Milligan, G., and Bond, R.A. (1997) *Trends Pharmacol. Sci.* **18**, 468-474

Milligan, G., Bond, R.A., and Lee. M. (1995) *Trends Pharmacol. Sci.* **16**, 10-13

Mundell, S.J., and Benovic, J.L. (2000) *J. Biol. Chem.* **275**, 12900-12908

Munich, G., Dees, C., Hekman, M., and Palm, D. (1991) *Eur. J. Biochem.* **198**, 357-364

Nakata, H., Kameyama, K., Haga, K., and Haga, T. (1994) *Eur. J. Biochem.* **220**, 29-36

Nimchinsky, E.A., Hof, P.R., Janssen, W.G.M., Morrison, J.H., and Schmauss, C. (1997) *J. Biol. Chem.* **272**, 29229-29237

Nock, B., Rajpara, A., O'Connor, L., and Cicero, T. (1988) *Life Sci.* **42**, 2403-2412

O'Hara, P.J., Sheppard, P.O., Thogerson, H., Venezia, D., Haldeman, B.A., McGrane, V., Houmed, K.M., Thomsen, C., Gilbert, T.L., and Mulvihill, E.R. (1993) *Neuron* **11**, 41-52

Oakley, R.H., Laporte, S.A., Holt, J.A., Barak, L.S., and Caron, M.G. (1999) *J. Biol. Chem.* **274**, 32248-32257

Oakley, R.H., Laporte, S.A., Holt, J.A., Barak, L.S., and Caron, M.G. (2001) *J. Biol. Chem.* **276**, 19452-19460

Oakley, R.H., Laporte, S.A., Holt, J.A., Caron, M.G., Barak, L.S. (2000) *J. Biol. Chem.* **275**, 17201-17210

Okamoto, T., and Nishimoto, I. (1992) *J.Biol. Chem.* **267**, 8342-8346

Ozaki, N., Shibasaka, T., Kashima, Y., Miki, T.K.T., Ueno, H., Sunaga, Y., Yano, H., Maatsuura, Y., Iwanagi, T., Takai, Y. and Seino, S. (2000) *Nat. Cell. Biol.* **2**, 805-811

Palczewski, K., Kumasaka, T., Hori, T., Behnke, C.A., Motoshima, H., Fox, B.A., Le Trong, I., Teller, D.C., Okada, T., Stenkamp, R.E., Yamomoto, M., and Miyano, M. (2000) *Science* **289**, 739-745

Pei, G., Samama, P., Lohse, M., Wang, M., Codina, J., Lefkowitz, J. (1994), *Proc. Natl. Acad. Sci. U.S.A.* **91**, 2699-2702

Petaja-Repo, U.E., Hogue, M., Laperriere, A., Walker, P., and Bouvier, M. (2000) *J. Biol. Chem.* **275**, 13727-13736

Pfieffer, M. Koch, T., Schroder, H., Klutzney, M., Kirscht, S., Kreienkamp, H-J., Hollt, V., and Schultz, S. (2001) *J.Biol. Chem.* **276**, 14027-14036

Pippig, S., Andexinger, S., Daniel, K., Puzicha, M., Caron, M.G., Lefkowitz, R.J. and Lohse, M.J. (1993) *J. Biol. Chem.* **268**, 3201-3208

Pitcher, J.A., Tesmer, J.J., Freeman, J.L., Capel, W.D., Stone, W.C., and Lefkowitz, R.J. (1999) *J. Biol. Chem.* **274**, 34531-34534

Pitcher, J.A., Touhara, K., Payne, E.S., and Lefkowitz, R.J. (1995) *J. Biol. Chem.* **270**, 11707-11710

Ramsay, D., Kellett, E., McVey, M., Rees, S. and Milligan, G. (2002) *Biochem. J.* **365**, 429-440

Ray, K., and Hauschild, B.C. (2000) *J. Biol. Chem.* **275**, 34245-24251

Rochville, M., Lange, D.C., Kumar, U., Sasi, R., Patel, R.C., and Patel, Y.C. (2000) *J. Biol. Chem.* **275**, 7862-7869

Rodriguez-Frade, J.M., Vila-Coro, A.J., De Ana, A.M., Albar, J. P., Martinez-A, C., and Mellado, M. (1999) *Proc. Nalt. Acad. Sci.* **96**, 3628-3633

Rosenthal, W., Antaramian, A., Gilbert, S., and Birnbaumer, M. (1993) *J. Biol. Chem.* **268**, 13030-13033

Rothman, R., and Westfall, T. (1981) *Eur. J. Pharmacol.* **72**, 365-368

Rothman, R., and Westfall, T. (1981) *Mol. Pharmacol.* **21**, 548-557

Sack, J.S., Saper, M.A., and Quiocho, F.A. (1989) *J. Mol. Biol.* **206**, 171-191

Sakmar, T.P. (1998) *Prog. Nucleic Acid Res. Mol. Biol.* **59**, 1-34

Samama, P., Cotecchia, S., Costa, T., and Lefkowitz, R.J. (1993) *J. Biol. Chem.* **268**, 4625-4636

Samama, P., Pei, G., Costa, T., Cotechia, S., and Lefkowitz, R.J. (1994) *Mol. Pharmacol.* **45**, 390-394

Saravese, T.M., and Fraser, C.M. (1992) *Biochem J.* **283**, 1-19

Schwartz, T.W., Gether, U., Schambye, H.T., Hjorth, S.A. (1995) *Curr. Pharm. Design* **1**, 325-342

Schwartz, W. (1996) in *Textbook of Receptor Pharmacology*. CRC press, pp 65-84.

Sheer, A., and Cotecchia, S. (1997) *J. Recept. Signal Transduct. Res.* **17**, 57-73

Sheer, A., Fanelli, F., Costa, T., De Benedetti, P.G., and Cotechia, S. (1996) *EMBO J.* **15**, 3566-3578

Shih, M., and Malbon, C.C. (1994) *Proc. Natl. Acad. Sci. U.S.A.* **91**, 12193-12197

Smit, M.J., Leurs, R., Alewijnse, A.E., Blauw, J., V-N Amerongen, G.P., V-D Vrede, Y., Roovers, E., Timmerman, H. (1996) Proc. Natl. Acad. Sci. U.S.A. 93, 6802-6807

Smith, W.C., Milam, A.H., Dugger, D., Arendt, A., Hargrave, P.A., and Palczewski, K. (1994) *J. Biol. Chem.* **273**, 17749-17755

Sofflel, R.H., Inglese, J., Macrae, A.D., Lefkowitz, R.J., and Premont, R.T. (1998) *Biochemistry* **37**, 16053-16059

Stadel, J.M., Wilson, S., and Bergsma, D.J. (1997) *Trends Pharmacol. Sci.* **18**, 230-237

Stevens, P. A., Bevan, N., Rees, S., and Milligan, G. (2000) *Mol. Pharmacol.* **58**, 438-448

Strader, C. D., Candelmore, M.R., Hill, W.S., Sigal, I.S., and Dixon, R.A.F. (1989) *J. Biol. Chem.* **264**, 13572-13578

Strader, C.D., Fong, T.M., Tota, M.R., Underwood, D., and Dixon, R.A.F. (1994) *Annu. Rev. Biochem.* **63**, 101-132

Strader, C.D., Graffney, T., Sugg, E.E., Candelore, M.R., Keys, R., Patchett, A.A., and Dixon, R.A.F. (1991) *J. Biol. Chem.* **266**, 5-8

Strange, P.G. (2002) *Trends Pharmacol. Sci.* **23**, 89-95

Takahishi, K., Tsuchida, K., Tanabe, Y., Masu, M., and Nakanishi, S. (1993) *J. Biol. Chem.* **268**, 19341-19345

Tota, R.T., and Strader, C.D. (1991) *J. Biol. Chem.* **265**, 16891-16897

Tsuji, Y., Shimada, Y., Takeshita, T., Kajimura, N., Nomura, S., Sekiyama, N., Otoma, J., Usukuru, J., Nakanishi, S., and Jingami, H. (2000) *J. Biol. Chem.* **36**, 28144-28151

Tsutsumi, M., Zhou, W., Millar, R.P., Mellon, P.L., Roberts, J.L., Flanagan, C.A., Dong, K., Gillo, B., and Sealfon, S.C. (1992) *Mol. Endocrinol.* **6**, 1163-1169

Unger, V.M., and Schertler G.F. (1995) *Biophys. J.* **68**, 1776-1786

Unger, V.M., Hargrave, P.A., Baldwin, J.M., and Schertler, G.F. (1997) *Nature* **389**, 203-206

Vanessa, N., Walthuis R.M.F., de Tand, M-F., Janoueix-Lerosey, I., Bos, J.L. and de Gunzburg, J. (1999) *J. Biol. Chem.* **274**, 8737-8745

Vaught, J., and Takemori, A. (1979) *J. Pharmacol. Exp. Ther.* **208**, 86-94

Vila-Coro, A.J., Mellado, M., Martin de Ana, A., Lucas, P., del Real, G., Martinez-A, C., and Rodriguez-Frade, J.M. (2000) *Proc. Natl. Acad. Sci. U.S.A.* **97**, 3388-3393

Vishnivetski, S.A., Schubert, C., Climaco, G.C., Gurevich, Y.V., Velez, M.G., and Gurevich, V.V. (2000) *J. Biol. Chem.* **275**, 41049-41057

Volger, O., Nolte, B., Voss, M., Schmidt, M., Jakobs, K. H., and van Koppen, C.J. (1999) *J. Biol. Chem.* **274**, 12333-12338

Von Heijne, G. (1990) *J. Membr. Biol.* **115**, 195-201

Wade, S.M., Lan, K-L., Moore, D.J., and Neubig, R.R. (2001) *Mol. Pharmacol.* **59**, 532-542

Ward, W.W. and Cormier, M.J. (1979) *J. Biol. Chem.* **254**, 781-788

Weiland, K. Zuurmond, H.M., Krasel, C., Ijzerman, A.P., and Lohse, M.J. (1996) *Proc. Nat. Acad. Sci. U.S.A.* **93**, 9276-9281

Weiss, J.M., Morgan, P.H. Lutz, M.W., and Kenakin, T.P. (1996) *J. Theor. Biol.* **178**, 151-167

White, J. H., Wise, A., Main, M.J., Green, A., Fraser, N., Disney. G., Barnes, A. A., Emson, P., Foord, S.M., and Marshall, F.H. (1998) *Nature* **396**, 697-682

Wilson, C.J. and Applebury, M.L. (1993) *Curr. Biol.* **3**, 683-686

Wong, Y.G. (1994) *Methods Enzymol.* **238**, 81-94

Wu, G., Krupnick, J.G., Benovic, J.L., and Lanier, S.M. (1997) *J.Biol. Chem.* **272**, 17836-17842

Wurch, T., Matsumoto, A., and Pauwels, P.J. (2001) *FEBS Lett.* **507**, 109-113

Xu, Y., piston, D.W., and Johnson, C.H. (1999) *Proc. Natl. Acad. Sci. U.S.A.* **96**, 151-156

Zhang, J., Barak, L.S., Anborgh, P.H., Laporte, S.A., Caron, M.G., and Ferguson, S.S.G. (1999) *J. Biol. Chem.* **272**, 27005-27014

Zhang, J., Barak, L.S., Anborgh, P.H., Laporte, S.A., Caron, M.G., and Ferguson, S.S.G. (1999) *J. Biol. Chem.* **274**, 10999-11006

Zhang, J., Ferguson, S.S.G., Barak, L.S., Menard, L., and Caron, M.G. (1996) *J. Biol Chem.* **271**, 18302-18305

Zhang, J., Ferguson, S.S.G., Barak, L.S., Menard, L., and Caron, M.G. (1996) *J. Biol. Chem.* **31**, 18302-18305

Zhu, J., Taniguchi, T., Takaugi, R., Suzuki, F., Tanaka, T., and Muramatsu, I. (2000) *Br. J. Pharmacol.* **131**, 546-552

Zhu, S.Z., Wang, S.Z., Hu, J., and El-Fakahany, E.E. (1994) *Mol. Pharmacol.* **45**, 517-523

Zhu, X., and Wess, J. (1998) *Biochemistry* **37**, 15773-15784

Zhukovski, E.A., Robinson, P.R., and Oprian, D.D. (1992) *Biochemistry* **31**, 10400-10405

Zieglgansberger, W., French, E., Mercuri, N., Peleyo, F., and Williams, J. (1982) *Life Sci.* **31**, 2343-2346

Zimprich, A., Simon, T., and Hollt, V. (1995), *FEBS Lett.* **359**, 142-146

Zukin, R., Eghbali, M., Oliver, D., Unterwald, E., and Tempel, A. (1988) *Proc. Natl. Acad. Sci. U.S.A.* **85**, 4061-4065